Patrick Luig

A consistent Eulerian rate model for shape memory alloys

RUHR-UNIVERSITÄT BOCHUM

INSTITUT FÜR MECHANIK
RUHR-UNIVERSITÄT BOCHUM

Patrick Luig

A consistent Eulerian rate model for shape memory alloys

Summary

In this treatise, a constitutive theory for pseudoelastic shape memory alloys is proposed. The model is derived within a Eulerian framework of finite deformations. Specifically, a hypoelastic formulation is adopted on the basis of the Kirchhoff stress (weighted Cauchy stress), the stretching tensor, and the logarithmic rate. The material model is consistently formulated within a thermodynamic framework of solid state phase transformations. In this context, a non-convex Helmholtz free energy function is introduced, which includes phase specific energies as well as an energy for phase interactions. Internal variables reflect, in average, the microstructure of the material. They particularly comprise the scalar-valued overall martensitic mass fraction and the tensorial average orientation of the martensite variants. Evolution equations are proposed for both variables accounting for a proportional and for a non-proportional loading path. In addition, in order to describe the thermomechanically coupled material behavior, a rate equation for the temperature is derived from the first law of thermodynamics. The constitutive model is successfully implemented into the finite element method. A calibration to experimental measurements and a subsequent validation show the appropriateness of the constitutive assumptions. The treatise closes with a fully thermomechanically coupled simulation of a shape memory structure at finite deformations.

Zusammenfassung

In dieser Arbeit wird ein konstitutives Modell zur Beschreibung pseudoelastischer Formgedächtnislegierungen vorgestellt. Das Modell wird in einem Eulerschen Rahmen finiter Formänderungen formuliert. Insbesondere wird ein hypoelastischer Ansatz verwendet, der auf der Kirchhoff Spannung (gewichtete Cauchy Spannung), dem Streckgeschwindigkeitstensor und der logarithmischen Rate basiert. Das Materialmodell ist in einem thermodynamisch konsistenten Rahmen zur Beschreibung von Festkörper-Phasentransformationen eingebettet. In diesem Zuge wird eine nicht-konvexe Helmholtz Energie eingeführt, die neben den phasenspezifischen Energien einen Anteil zur Erfassung von Phaseninteraktionen enthält. Die Mikrostruktur wird durch interne Variablen beschrieben, die den mittleren Massenanteil des Martensit sowie die mittlere Orientierung der Martensitvarianten umfassen. Für beide Größen werden Evolutionsgleichungen für proportionale und nicht-proportionale Lastpfade vorgestellt. Außerdem wird zur Erfassung des thermomechanisch gekoppelten Materialverhaltens aus dem ersten Hauptsatz der Thermodynamik eine Rategleichung für die Temperatur hergeleitet. Das Materialmodell ist in die Finite-Elemente-Methode implementiert. Die Eignung der konstitutiven Annahmen wird durch eine Kalibrierung an experimentelle Ergebnisse und eine Validierung gezeigt. Die Arbeit schließt mit einer thermomechanisch gekoppelten Simulation einer Formgedächtnisstruktur unter finiten Formänderungen.

Vorwort

Die vorliegende Arbeit entstand während meiner Tätigkeit als wissenschaftlicher Mitarbeiter am Lehrstuhl für Technische Mechanik der Ruhr-Universität Bochum. Sie wurde im Rahmen des Sonderforschungsbereiches 459 *Formgedächtnistechnik* von der Deutschen Forschungsgemeinschaft gefördert und von der Fakultät für Maschinenbau der Ruhr-Universität Bochum als Dissertation angenommen.

Mein besonderer Dank gilt meinem Lehrer Herrn Prof. Dr.-Ing. Otto T. Bruhns für die Anregung und die Unterstützung dieser Arbeit. Ich danke ihm für sein Vertrauen und die mir gewährten Freiräume bei der Gestaltung meiner Forschungsarbeit, die meine wissenschaftliche Qualifikation sehr stark geprägt haben. Herrn Prof. Dr.-Ing. Peter Haupt danke ich für die Übernahme des Koreferates sowie für die zügige und sorgfältige Durchsicht des Manuskriptes.

Bei allen Mitarbeitern des Lehrstuhls für Technische Mechanik bedanke ich mich für die angenehme Arbeitsatmosphäre. Besonders hervorheben möchte ich die Herren Prof. Dr. Heng Xiao, Prof. Dr.-Ing. Jörn Mosler, Dr.-Ing. Albert Meyers, Dr.-Ing. Claus Oberste-Brandenburg und Dr.-Ing. Christian Grabe, die mir in zahlreichen konstruktiven Diskussionen und Gesprächen wertvolle Impulse für meine Arbeit gaben. Auch bedanke ich mich bei Frau M. Sc. Lidija Stanković und den Herren Dr.-Ing. Stefan Reichling, M. Sc. Zoran Stanković, Dipl.-Ing. Alexander Arnold und Dipl.-Ing. Nikolaus Bleier für die gute Zusammenarbeit und die schöne gemeinsame Zeit.

Mein Dank gilt gleichfalls den Herren Dipl.-Ing. Daniel Christ, Dr.-Ing. Harald Kruggel-Emden, Dipl.-Ing. Tim Sadek, Dr.-Ing. Dipl.-Wirtsch.-Ing. Christoph Müller, Dr.-Ing. Adam Knopik und Dipl.-Ing. Sven Langbein. Neben den unzähligen fachlichen Gesprächen werden mir auch die vielen außerdienstlichen Aktivitäten in guter Erinnerung bleiben.

Schließlich danke ich meiner Familie für ihre Unterstützung und ihren Rückhalt während der letzten Jahre.

Bochum, im Juni 2008   Patrick Luig

Contents

List of Figures

List of Tables

Glossary

Scalars (Latin characters)

a_1, a_2	Parameters of functions k^β
A	Coherency coefficient
A_1, A_2	Parameters of function A
A^s	Austenite start temperature
A^f	Austenite finish temperature
b_1, b_2	Parameters of functions k^β
B	Open set of particles defining a body
c_1, c_2	Parameters of functions k^β
c	Specific heat
da	Area element in the current configuration
dA	Area element in the reference configuration
dm	Mass element
dv	Volume element in the current configuration
dV	Volume element in the reference configuration
E	Young's modulus
f^β	Phase transformation functions
g	Specific Gibbs free energy
h	Specific enthalpy
J	Jacobian determinant
k^β	Phenomenological functions prescribing π^ξ
k	Thermal conductivity
m	Mass
M^s	Martensite start temperature
M^f	Martensite finish temperature
p	Specific power
P	Power
P	Particle
q_{gen}	Generated heat per unit mass
Q	Heat power
r	Heat source per unit mass
r	Reorientation function
s	Specific entropy
s_1, s_2, s_3	Eigenvalues of tensor s
t_1, t_2, t_3	Eigenvalues of tensor t
t	Time
u	Specific internal energy

Scalars (Greek characters)

α	Thermal expansion coefficient
α	Eulerian scalar

α_0	Lagrangian scalar
$\Delta u_0, \Delta s_0$	Internal energy and entropy differences of the unloaded phases
ε	Nominal (linearized) tensile strain
γ	Nominal (linearized) shear strain
γ'	Scaled nominal (linearized) shear strain
η	Degree of mechanical interactions between the phases
Θ	Absolute temperature
Θ_0	Reference temperature
ϑ	Deviation between stress direction and martensite orientation
λ	Lamé constant
μ	Lamé constant
ν	Poisson's ratio
ξ	Overall mass fraction of martensite
π^ξ	Thermodynamic driving force for phase transformations
ρ_0	Density in the reference configuration
ρ	Density in the current configuration
σ	Nominal (linearized) tensile stress
τ	Nominal (linearized) shear stress
τ'	Scaled nominal (linearized) shear stress
τ_0	Average distortion of the martensite
τ_{eq}	Equivalent Kirchhoff stress
ψ	Specific Helmholtz free energy

Vectors (Latin characters)

b	Body force per unit mass
c	Rigid body translation of the observer
dx	Line element in the current configuration
dX	Line element in the reference configuration
da	Area element in the current configuration
dA	Area element in the reference configuration
n	Unit vector in the current configuration
N	Unit vector in the reference configuration
q	Heat flux
v	Velocity
x	Position in the current configuration
X	Position in the reference configuration

Vectors (Greek characters)

$\boldsymbol{\alpha}$	Eulerian vector
$\boldsymbol{\alpha}_0$	Lagrangian vector
$\boldsymbol{\varphi}$	Motion

Second-order tensors (Latin characters)

$\mathbf{A}$	Eulerian tensor
$\mathbf{A}_0$	Lagrangian tensor
$\mathbf{B}$	Left Cauchy-Green tensor
$\mathbf{C}$	Right Cauchy-Green tensor
$\mathbf{D}$	Stretching tensor
$\mathbf{e}$	Almansi-Eulerian strain tensor
$\mathbf{E}$	Green-Lagrangian strain tensor
$\mathbf{f}$	Relative deformation gradient
$\mathbf{F}$	Deformation gradient
$\mathbf{h}$	Hencky strain tensor in the current configuration
$\mathbf{H}$	Hencky strain tensor in the reference configuration
$\mathbf{I}$	Identity tensor
$\mathbf{L}$	Velocity gradient
$\mathbf{P}$	First Piola-Kirchhoff stress tensor
$\mathbf{Q}$	Orthogonal tensor
$\mathbf{r}$	Relative rotation tensor
$\mathbf{R}$	Rotation tensor
$\mathbf{s}$	Stress direction
$\mathbf{S}$	Second Piola-Kirchhoff stress tensor
$\mathbf{S}_1, \mathbf{S}_2, \mathbf{S}_3$	Eigenprojections of $\mathbf{s}$
$\mathbf{T}_1, \mathbf{T}_2, \mathbf{T}_3$	Eigenprojections of $\mathbf{t}$
$\mathbf{t}$	Average orientation of the martensite variants
$\mathbf{U}$	Right stretch tensor
$\mathbf{V}$	Left stretch tensor
$\mathbf{W}$	Vorticity tensor

Second-order tensors (Greek characters)

$\boldsymbol{\alpha}$	Tensor of thermal expansion coefficients
$\boldsymbol{\varepsilon}$	Nominal (linearized) strain tensor
$\boldsymbol{\pi}^t$	Thermodynamic driving force for reorientations
$\boldsymbol{\sigma}$	Cauchy stress tensor
$\boldsymbol{\sigma}$	Nominal (linearized) stress tensor
$\boldsymbol{\tau}$	Kirchhoff stress tensor
$\boldsymbol{\Omega}$	Spin tensor
$\boldsymbol{\Xi}, \boldsymbol{\zeta}$	General sets of internal variables

Fourth-order tensors (Latin characters)

$\mathbb{C}$	Elasticity tensor
$\mathbb{D}$	Elastic compliance tensor
$\mathbb{I}$	Identity tensor
$\mathbb{O}$	Zero tensor

Other symbols

$\mathcal{B}_t$	Current configuration
$\mathcal{B}_0$	Reference configuration
$\mathcal{R}_t$	Domain of $\mathcal{B}_t$
$\mathcal{R}_0$	Domain of $\mathcal{B}_0$
$\partial\mathcal{B}_t$	Surface of $\mathcal{B}_t$
$\partial\mathcal{B}_0$	Surface of $\mathcal{B}_0$
$\partial\mathcal{R}_t$	Surface of $\mathcal{R}_t$
$\mathcal{E}$	Euclidean point space
$\mathbb{R}$	Set of real numbers
$\mathcal{O}$	Observer

Operators

$\cdot$	Single contraction or scalar product
$:$	Double contraction
$\star$	Rayleigh product
$\times$	Vector product
$\otimes$	Dyadic product
Δ	Increment
∇	Gradient in $\mathcal{B}_t$
$|(\cdot)|$	Norm of $(\cdot)$
$\mathrm{tr}\,(\cdot)$	Trace of $(\cdot)$
$(\cdot)^{\mathrm{T}}$	Transpose of $(\cdot)$
$(\cdot)^{-1}$	Inverse of $(\cdot)$
$(\cdot)'$	Deviator of $(\cdot)$
$(\cdot)'$	Derivative of $(\cdot)$
$\dot{(\cdot)}$	Material time rate of $(\cdot)$
$\overset{\diamond}{(\cdot)}$	Arbitrary objective time rate of $(\cdot)$
$\overset{\circ}{(\cdot)}$	Arbitrary objective corotational time rate of $(\cdot)$
$\overset{\circ}{(\cdot)}{}^{\mathrm{Log}}$	Logarithmic time rate of $(\cdot)$

Superscripts

$(\cdot)^{\mathrm{A}}$	Austenitic
$(\cdot)^{\mathrm{A}\rightarrow\mathrm{M}}$	Related to austenite-martensite transformations
$(\cdot)^{\mathrm{el}}$	Elastic
$(\cdot)^{\mathrm{in}}$	Inelastic
$(\cdot)^{\mathrm{irr}}$	Irreversible

$(\cdot)^{Log}$	Logarithmic
$(\cdot)^{M}$	Martensitic
$(\cdot)^{M \rightarrow A}$	Related to martensite-austenite transformations
$(\cdot)^{pt}$	Phase transformational
$(\cdot)^{rev}$	Reversible
$(\cdot)^{ro}$	Reorientational
$(\cdot)^{tr}$	Transformational
$(\cdot)^{\beta}$	β is place holder for A $\rightarrow$ M or M $\rightarrow$ A
$(\cdot)^{\gamma}$	γ is place holder for A or M
$(\cdot)^{\xi}$	Related to phase transformations
$(\cdot)^{\tau}$	Related to stress
$(\cdot)^{t}$	Related to reorientations
$(\cdot)^{*}$	Quantity $(\cdot)$ after a change of frame

Subscripts

$(\cdot)_{con}$	Convective
$(\cdot)_{e}$	External
$(\cdot)_{gen}$	Generated
$(\cdot)_{i}$	Internal
$(\cdot)_{loc}$	Local
$(\cdot)_{n}$	Beginning of increment n
$(\cdot)_{n+1}$	Beginning of increment $n+1$

1 Introduction

In the past decades, the development of multifunctional materials considerably enhanced the efficiency of engineering applications and promoted many innovative solutions for technical problems. Among these materials, shape memory alloys are in the focus of this treatise. They show remarkable thermomechanical properties which result in three effects referred to as *pseudoelastic effect, one-way shape memory effect*, and *two-way shape memory effect*. The pseudoelastic effect is characterized by large apparently elastic deformations during mechanical loadings, which are, in fact, inelastic as they lead to a hysteretic material behavior and, thus, to an energy dissipation. Large apparently plastic deformations at the end of a deformation process are addressed by the one-way shape memory effect. These deformations can, however, be fully reversed upon heating. The two-way shape memory effect refers to switching deformation states of the material upon heating and cooling. This means that a predefined deformation behavior can be regulated by controlling the temperature.

The unique feature of shape memory alloys may be ascribed to a material memory with regard to an initial deformation state which originates in the crystallographic material structure. This memory is principally governed by two factors, i.e., a phase transformation between two solid phases termed *martensite* and *austenite*, which is related to *thermoelastic martensitic transformations*, and a low crystallographic symmetry of the martensite compared to the austenite. Due to the latter, different martensite variants can be constructed from one austenite variant. In this context, an application of an external thermomechanical load leads to a selection of preferred martensite variants and, in consequence, to an observable pseudoelastic or pseudoplastic deformation. As the original crystallographic structure can be reconstructed from a reverse transformation into the austenite, this deformation can be fully reversed.

Shape memory alloys are employed by various engineering structures. The pseudoelastic effect is, for instance, used by flexible guide wires for minimally invasive surgeries, flexible antennas for cellular phones, or flexible eyeglass frames. The efficiency of dental therapies can be increased by pseudoelastic orthodontic arch wires. They adjust the teeth by a constant force which is realized during the pseudoelastic effect. Pseudoelastic endovascular stents are used to expand the cross section areas of constricted blood vessels to ensure a sufficient blood flow. The volumetric, fine wired structures are restrained on catheters by compression and are guided to the stenosis, at which they are expanded. An endovascular NiTi stent system during the expansion process is depicted in Figure 1.1 (a). A similar procedure is employed for endovascular instruments during minimally invasive surgeries. They access regions within the body through the major blood vessels, such that the size of the surgeries can locally be restricted. This results in a reduced trauma and a
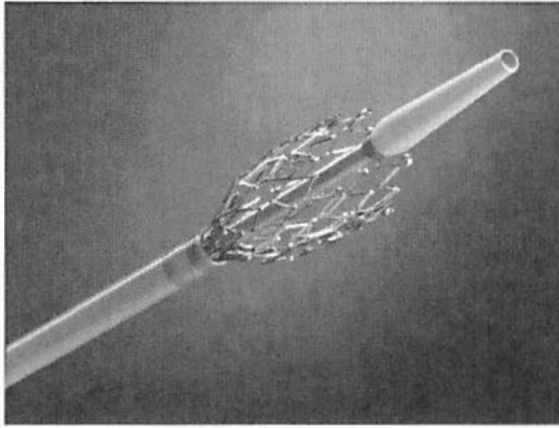
(a) Self-expandable NiTi stent system   (b) NiTi tube coupling (courtesy of
     (courtesy of ev3 Inc., USA)   Memory-Metalle GmbH, Germany)
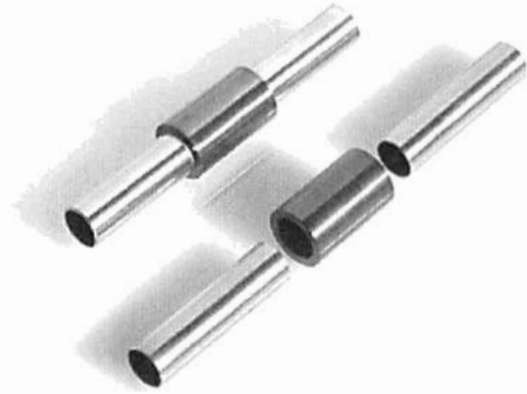
Figure 1.1: NiTi applications

shorter recovery time. Examples for these instruments are pseudoelastic re-
trievers which are used to remove intravascular clots. The retriever system
consists of a microcatheter, through which a tapered NiTi wire is advanced.
After passing through the clot, the wire is expanded, such that the clot can
be drawn into the catheter. Lightweight couplings for hydraulic tubes shown
in Figure 1.1 (b) or foot staples for foot surgeries are two typical applications
for the one-way shape memory effect. Foot staples connect the fracture zones
of toes by a well-defined clamping force. The two-way shape memory effect is
commonly used for actuators, as distinct deformations states can externally be
controlled by a given temperature. In this vein, the actuators may additionally
operate as sensors in order to reduce the complexity of an actor-sensor system.
Nowadays, numerical simulations are well-established in the product develop-
ment to predict the functionality and reliability of the new products in an early
development stage. In this context, a constitutive theory for shape memory
alloys is derived in this treatise. The model is embedded within a Eulerian
framework to account for the large deformations exhibited by shape memory
structures. Specifically, a hypoelastic formulation is adopted on the basis of
the Kirchhoff stress (weighted Cauchy stress), the stretching tensor, and the
logarithmic rate. Certainly, the local strains arising from the observed shape
memory effects may be regarded as moderate, such that a geometrically linear
kinematical framework may be employed. This pragmatical approach proves
to be reasonable if the investigation of fundamental effects of the material is
preferably in the focus of the material modeling. Nevertheless, as it can be ob-
served during the expansion process of the endovascular NiTi stent considered
above, these strains may lead to severe structural deformations, such that a
finite deformation framework is mandatory for realistic simulations.

The material model is consistently formulated within a thermodynamic framework of solid state transformations between the two phases austenite and martensite. Of fundamental importance in this context is the introduction of a non-convex Helmholtz free energy function, which comprises the phase specific energies of the two phases as well as an energy for phase interactions. The Helmholtz free energy is written in terms of stress, temperature, and internal variables. The dependence on the stress should not be regarded as contradiction to the classical formulation, as the purely elastic component of the total strain, which is commonly taken as an independent variable, can be considered as redundant to the total stress. The determination of the elastic strain, however, is cumbersome within a framework of finite deformations. The internal variables reflect, in average, the microstructure of the material. They particularly comprise the scalar-valued overall martensitic mass fraction and the tensorial average orientation of the martensite variants. Special attention of this treatise lays on the pseudoelastic effect. On the grounds of the introduced general internal variables, however, the model can be extended to the additionally observed one-way and two-way shape memory effects. An evolution equation for the mass fraction of martensite is derived from the Clausius-Duhem inequality, whereas the proposed evolution equation for the average orientation of the martensite variants is based on a thorough analysis of the material response determined during biaxial experimental tests. In this context, focus is on reorienting martensite variants during non-proportional loadings. Finally, on exploiting the first law of thermodynamics, a rate equation for the temperature is derived to account for the thermomechanically coupled material behavior.

In regard of the significance of numerical simulations, the material model is implemented into the finite element method. A calibration and a validation with experimental measurements show the appropriateness of the constitutive assumptions. The applicability of the material model is then demonstrated on the basis of a fully thermomechanically coupled simulation of a shape memory structure at finite deformations.

Throughout this treatise, the considerations are restricted to NiTi alloys due to their elevated technical relevance. Indeed, among different shape memory alloys such as Cu-based or Fe-based alloys, NiTi is the most attractive. The reason for this stems from the superior properties of NiTi with regard to recoverable strains, transformation stresses, fatigue, and biocompatibility.

1.1 State of the art review

Numerous modeling approaches for shape memory alloys have been established in the past decades which may principally be classified into three groups, i.e., micromechanical models, models based on statistical mechanics, and phenomenological models. Some of these are briefly reviewed in the following.

1.1.1 Micromechanical models

Micromechanical models for shape memory alloys conceptually predict the material response on the basis of a microstructure approximation. For this purpose, a wide class of approaches employ the concept of a representative volume element in defining macroscopic quantities as volumetric averages of corresponding microscopic quantities (see Patoor et al. (2006)). Within the scope of this concept, microscopic internal variables are introduced accounting for the volume fractions of distinct martensite variants. They are linked to corresponding microscopic phase transformation strains. The thermomechanical state of the material is characterized by a microscopic Helmholtz free energy in terms of microscopic stresses and strains. On the basis of its volumetric average, evolution equations for the internal variables are then formulated. Averaging this energy over the representative volume element exhibits, however, an interaction term which particularly arises from a local stress field. In regard of an approximation of this interaction energy, various concepts have been proposed which may be ascribed to single-variant and multi-variant concepts. Within the single-variant concepts, only a single active martensite variant is taken into account, as it may be observed during simple tension tests of single crystals (e.g., see Lu & Weng (1997) and Vivet & Lexcellent (1998)). Contrarily, multi-variant concepts consider the interaction of simultaneously activated variants (e.g., see Patoor et al. (1996), Huang & Brinson (1998), Siredey et al. (1999), Gall & Sehitoglu (1999), Gao et al. (2000), Huang et al. (2000), Niclaeys et al. (2002), Jung et al. (2004), and Wang et al. (2008)). Alternatively to the preceding approaches, Govindjee et al. (2003) propose a multi-well approach in which the martensite and austenite variants are characterized by distinct Helmholtz free energy functions (see Ball & James (1987)). The energy of the phase mixture, thus, represents a highly non-convex energy functional. Hall & Govindjee (2002) and Hackl & Heinen (2008), for instance, compute the volume fractions of the martensite variants by minimizing the relaxed energy functional. Contrarily, Govindjee & Miehe (2001) and Stein & Sager (2008) quantify the martensitic volume fractions from the postulate of the maximum dissipation. In both approaches, the highly non-convex energy functional is subjected to a convexification to ensure uniqueness of the solution.

1.1.2 Models based on statistical mechanics

Models for shape memory alloys based on statistical mechanics adopt principles of statistical physics to describe the transformation between different austenite and martensite variants. The underlying approach may be attributed to the works of Achenbach & Müller (1985), Müller (1985a), and Achenbach (1989) (see also Müller (2001)). A key issue therein is the decomposition of the body of interest into mesoscopic lattice particles which describe the structural behavior in a statistical mean. On restricting to a one-dimensional description,

it is assumed that the particles can obtain three different configurations, i.e., two for martensite (e.g., one for tension and one for compression) and one for austenite. These configurations are characterized by distinct potential energy minima, i.e., by distinct potential wells, which are separated by potential barriers. On the grounds of thermal activation processes, it is further supposed that the particles fluctuate about their equilibrium states. In this regard, depending on the thermomechanical load, the particles can overcome the potential barriers and can, thus, change their configurations. This furnishes processes of phase transformation and reorientation of the austenite and martensite variants. The transformation ability of the particles depends, however, on certain transformation probabilities, which are determined from principles of statistical physics. They are employed to derive rate equations for the average phase fractions of the austenite and martensite variants.

Seelecke (1997, 2002) and Seelecke & Müller (2004) successfully apply the foregoing concept to simulations of shape memory structures. Seelecke (1997, 2002) analyzes torsional vibrations of a shape memory wire and of a thin-walled shape memory tube. The behavior of shape memory actuators is simulated in Seelecke & Müller (2004). The computations in these works are carried out thermomechanically coupled in order to account for the generated heat of the transformation processes. An extension of the model from a single crystalline description to polycrystals is discussed by Heintze & Seelecke (2008). Govindjee & Hall (2000) study the numerical implementation of a model based on statistical mechanics in conjunction with a mixture theory.

The concept of statistical mechanics for shape memory alloys is in its current formulation restricted to one-dimensional models. As it is shown by Seelecke et al. (2005) and Kim & Seelecke (2007) for ferroelectric single crystals, an extension to higher dimensions seems, however, to be possible.

1.1.3 Phenomenological models

Phenomenological models for shape memory alloys concentrate on the prediction of the macroscopic material behavior. Several modeling approaches have been established, ranging from purely descriptive models which adopt the theory of plasticity as basic framework to multiphase models addressing the mechanism of solid state transformations.

Plasticity based concepts can be found in Bertram (1982), Graesser & Cozzarelli (1994), Delobelle & Lexcellent (1996), and Trochu & Qian (1997). For instance, Bertram (1982) defines two temperature-dependent yield functions to model the phase transformation strain during forward and reverse transformations, whereas a viscoplastic framework is adopted by Delobelle & Lexcellent (1996) for the description of the pseudoelastic effect. The latter work is based on a shift of the viscoplastic hysteresis to form a pseudoelastic hysteresis, which is realized by a set of internal variables furnishing a back stress tensor.

Multiphase models formulated on the grounds of solid state transformations commonly define the overall martensitic phase fraction as primitive quantity, which basically represents the material microstructure during phase transformation processes. An early three-dimensional constitutive model for pseudoelasticity based on this concept is proposed by Raniecki et al. (1992). The model extends the one-dimensional thermodynamically founded theory of Müller (1989) and Müller & Xu (1991) for stress-induced phase transitions. It is formulated within a geometrically linear framework on the basis of a non-convex Helmholtz free energy comprising phase specific energies as well as an energy for phase interactions (see Müller (1989)). In this context, solely the scalar-valued martensitic phase fraction is defined as internal variable. The inelastic strain arising from phase transformations is then uniquely determined by the current stress direction and the martensitic phase fraction, i.e., it is postulated that the stress direction and the martensite orientation are parallel throughout the deformation process. A constitutive equation for the martensitic phase fraction is obtained by ensuring thermodynamic consistency in terms of the Clausius-Duhem inequality. In regard of its thermodynamical foundation, the model accounts for the thermomechanically coupled material behavior observed during phase transformations. The approach of Raniecki et al. (1992) promoted many research publications as, e.g., Raniecki & Lexcellent (1994, 1998), Lexcellent et al. (1994a,b, 2000, 2002, 2006), Leclercq & Lexcellent (1996), Müller (2003), Bouvet et al. (2004a), and Ziólkowski (2007). An approach for the description of the asymmetric transformation behavior of shape memory alloys well-known as tension/compression asymmetry can be found in Raniecki & Lexcellent (1998) and Lexcellent et al. (2002, 2006). The derivations are, however, restricted to proportional loadings with constant stress directions. An attempt to cover non-proportional loadings is given in Bouvet et al. (2004a). Approaches to model R-phase activities and the two-way shape memory effect are considered by Lexcellent et al. (1994b, 2000). Müller (2003) and Ziólkowski (2007) reformulate the geometrically linear model within a framework of finite deformations. Both works adopt the Eulerian configuration in terms of the Kirchhoff stress and the Hencky strain. Müller (2003) additionally implements the model into the finite element method and conducts simulations of shape memory structures.

Boyd & Lagoudas (1996a,b) propose an enhancement of the work of Raniecki et al. (1992) by accounting for reorientations of the martensite variants during non-proportional loadings. Their approach is based on a non-convex Gibbs free energy, which is comparable to the Helmholtz free energy considered by Raniecki et al. (1992). The description of martensite reorientations is realized by a split of the inelastic strain rate into transformational and reorientational parts. Two general potentials are then introduced to define rate equations for the martensitic phase fraction and for the reorientational transformation strain. These rate equations, however, depend on Lagrange multipliers, which

have to be determined from a coupled system of equations. In its original formulation, the model is restricted to pseudoelasticity within a geometrically linear framework. An extension to cover the one-way shape memory effect seems possible. In a series of publications, Bo & Lagoudas (1999a,b,c) and Lagoudas & Bo (1999) revise the approach of Boyd & Lagoudas (1996a,b). The modified model conceptually relies on a set of five internal variables in terms of the phase fraction of martensite, a macroscopic transformation strain, a plastic strain, a back stress, and a drag stress. Back stress and drag stress account for internal stress fields arising from microstructural changes during phase transformations, whereas the plastic strain expresses transformation-induced permanent deformations. In contrast to the approach of Boyd & Lagoudas (1996a,b), reorientations of the martensite variants are not accounted for in the revised model. Three-dimensional numerical implementations can be found in Qidwai & Lagoudas (2000a,b), Lagoudas & Entchev (2004), and Entchev & Lagoudas (2004). Among these works, only the implementation of Qidwai & Lagoudas (2000b) considers finite deformations. It is particularly based on an additive decomposition of the Green-Lagrangian strain tensor. The main issue of the authors is to cover the asymmetric transformation behavior of the material. In contrast to Lagoudas & Entchev (2004) and Entchev & Lagoudas (2004), Qidwai & Lagoudas (2000a,b) do not implement plasticity-like effects considered in the original model.

A variety of models employs phase diagrams to obtain relations for the transformation kinetics (e.g., see Brinson (1993), Auricchio (1995), Leclercq & Lexcellent (1996), Lagoudas & Shu (1999), Juhász et al. (2002), Helm (2003), Peultier et al. (2006), Panico & Brinson (2007), and Popov & Lagoudas (2007)). These diagrams distinguish different phase domains in terms of uniaxial critical transformation stresses for forward and reverse transformations plotted against the temperature. Of fundamental importance in this regard is the concept of the additive decomposition of the martensitic phase fraction into oriented and self-accommodated parts. That is, both parts are regarded as distinct phases, such that detwinning of the martensite variants can conceptually be treated as phase transformation process. For instance, Auricchio (1995) adopts this concept for the description of, both, the pseudoelastic effect and the one-way shape memory effect (see also Lubliner & Auricchio (1996), Auricchio & Taylor (1997), and Auricchio et al. (1997)). The authors particularly model the critical transformation stresses by phenomenological functions of Drucker-Prager type. These functions govern, on the one hand, the transformation kinetics of the scalar-valued internal variables for oriented and self-accommodated martensite and, on the other hand, an additionally introduced tensorial internal variable for the direction of the phase transformation strain. The model is implemented into a framework of finite deformations employing a multiplicative decomposition of the deformation gradient. Thermomechanical effects, such as the heat generation arising from phase transitions, are not accounted

for. A significant enhancement of this approach from a thermodynamic point of view is proposed by Juhász et al. (2002). Therein, in contrast to Auricchio (1995), the whole phase transformation strain is introduced as tensorial internal variable. The uniaxial critical phase transformation stresses are represented by linear functions in the temperature. They are formulated in terms of an equivalent stress measure, which accounts for the asymmetric transformation behavior of the material. In line with Raniecki et al. (1992), a Helmholtz free energy function comprising the phase specific thermoelastic energies and an energy for phase interactions characterizes the thermodynamic state of the material. This energy is used to derive a rate equation for the temperature from the first law of thermodynamics. The model of Juhász et al. (2002) is restricted in its current formulation to a geometrically linear framework.

A well-developed constitutive model on the basis of a phase diagram approach, covering the pseudoelastic and the one-way shape memory effect, is proposed by Helm (2001, 2003). In addition to the scalar-valued internal variables expressing the martensitic phase fractions of oriented and self-accommodated variants, tensorial internal variables accounting for the total transformation strain and for the internal stress field are introduced. The phase fraction of oriented martensite variants is particularly set proportional to the transformation strain. A Helmholtz free energy function comparable to the one used by Raniecki et al. (1992) is employed in this model. Therewith, and on ensuring thermodynamic consistency in terms of the Clausius-Duhem inequality, the principle structure of the evolution equations for the internal variables is obtained. Specifically, in deriving an evolution equation for the phase transformation strain, a yield function known from the theory of plasticity is introduced. The evolution equation is then formulated on the basis of a Lagrange multiplier of Perzyna-type (cf. Perzyna (1963)) to describe a possibly viscous material behavior. On exploiting the first law of thermodynamics, the generated heat arising from phase transformation processes is quantified. Numerical implementations of the model and thermomechanically coupled simulations, both restricted to a geometrically linear framework, are addressed in Helm (2007a) and Christ et al. (2004). A rigorous identification of the material parameters with the focus on pseudoelasticity is regarded by Helm (2005). The calibration is carried out on the basis of neural networks. Finite deformations are considered in Helm (2001, 2007b) and Reese & Christ (2008) on employing the concept of the multiplicative decomposition of the deformation gradient. Reese & Christ (2008) additionally present a calibration to biaxial experimental data obtained by Helm (2001), and a thermomechanically coupled simulation of a stent structure.

It should be noted that only a few constitutive models are currently available at a geometrically non-linear framework (see Auricchio (1995), Qidwai & Lagoudas (2000b), Helm (2001), and Müller (2003)), in spite of the strong demand for reliable simulations of shape memory structures.

1.2 Outline

This treatise is structured into seven chapters. The present introductory chapter is followed by a brief survey on some basic properties of NiTi shape memory alloys. Therein, the mechanisms within the crystallographic structure leading to the different shape memory effects as well as the observable macroscopic material response are revisited in detail.

The mechanical foundations of the proposed constitutive model at finite deformations are presented in Chapter 3. The kinematics of a deforming body are thoroughly analyzed with the focus on the notion of local deformations and velocities. On this basis, measures of strain and stress are introduced. An essential property of physical quantities in terms of their transformation behavior during rigid body motions is addressed by the notion of *objectivity*. A physical quantity is specifically said to be objective if it is invariant under a change of frame of the observer. Rigid body motions may strongly affect the time derivatives of physical quantities. To account for this effect, *objective time derivatives* are introduced.

The kinematic and static relations are complemented by thermodynamics in order to ensure a physically consistent framework for the development of general material laws. This is considered in Chapter 4. General balance relations of thermodynamics are derived, and the strain and stress measures introduced in Chapter 3 are related to each other on employing a conjugated work analysis. A key issue of this chapter is the presentation of a general formalism which ensures the development of a thermodynamically consistent material law. In this regard, a general structure of the Helmholtz free energy function is introduced which is written, in contrast to the classical formulation, in terms of the total stress instead of the elastic strain. Even though both quantities may be regarded as redundant to some extent, the determination of the elastic strain during elastic-inelastic finite deformation processes is considered as cumbersome. The chapter is concluded with an analysis of the heat generation during general deformation processes.

The constitutive equations of the proposed material model are considered in Chapter 5. They are consistently formulated within a Eulerian framework on the basis of the Kirchhoff stress tensor, the stretching tensor, and the logarithmic rate. A Helmholtz free energy function is defined to characterize the energetic state of the material. It embodies the phase specific energies of austenite and martensite as well as an energy for the interaction of the single phases. In reflecting the essential structure of solid state phase transformations, a set of internal variables is specified in terms of a scalar-valued variable for the mass fraction of martensite and a tensorial variable related to the average orientation of the martensite variants. These quantities describe, in average, the microstructure of the material. On reviewing the interactions of the single phases, a relation for the phase specific stresses is proposed. The total stretching tensor and the total stress tensor are then specified on the ba-

sis of the principle of local equilibrium. The thermodynamic consistency of the constitutive assumptions is ensured on satisfying the Clausius-Duhem inequality. In this regard, an evolution equation for the mass fraction of martensite is obtained. The derivation of a constitutive equation for the average orientation of the martensite variants relies on a thorough study of experimental biaxial measurements. Finally, the heat generated during processes of deformation is quantified.

Chapter 6 addresses the implementation and validation of the proposed constitutive model. The main objective is to asses its reliability for complex loadings and its applicability for structural simulations. The calibration is carried out within a geometrically linear framework as experimental data are generally given in terms of nominal quantities. In this context, comparisons between numerical and experimental results for biaxial loadings are presented. The material model is then implemented into a framework of finite deformations. A key issue therein is to ensure objectivity of the integration procedure. On this basis, a fully thermomechanically coupled simulation of a shape memory structure is conducted.

This treatise closes in Chapter 7 with a summary of the results and an outlook on future work. The latter particularly comprises a possible extension to cover the one-way shape memory effect.

1.3   Mathematical notations

Throughout this treatise, a *Cartesian coordinate system* is used. Its mutually orthogonal base vectors $\mathbf{e}_i$ possess the property

$$\mathbf{e}_i \cdot \mathbf{e}_j = \delta_{ij} \quad , \tag{1.1}$$

with δ_{ij} denoting the *Kronecker-delta*

$$\delta_{ij} = \left\{ \begin{array}{ll} 1 & \text{if } i = j \\ 0 & \text{otherwise} \end{array} \right. . \tag{1.2}$$

Here and henceforth, the indices such as i and j represent $(1, 2, 3)$ if not otherwise stated. Therewith, the second-order and the fourth-order identity tensors read

$$\mathbf{I} = \delta_{ij}\, \mathbf{e}_i \otimes \mathbf{e}_j \quad \text{and} \quad \mathbb{I} = \delta_{im}\, \delta_{jn}\, \mathbf{e}_i \otimes \mathbf{e}_j \otimes \mathbf{e}_m \otimes \mathbf{e}_n \quad . \tag{1.3}$$

For the two vectors $\mathbf{a}$ and $\mathbf{b}$ and the two second-order tensors $\mathbf{A}$ and $\mathbf{B}$, contraction operators are defined as:

$$\begin{aligned} \mathbf{a} \otimes \mathbf{b} &= a_i b_j\, \mathbf{e}_i \otimes \mathbf{e}_j \\ \mathbf{a} \cdot \mathbf{b} &= a_i b_i \\ \mathbf{A} \cdot \mathbf{B} &= A_{ij} B_{jk}\, \mathbf{e}_i \otimes \mathbf{e}_k \\ \mathbf{A} : \mathbf{B} &= A_{ij} B_{ij} \end{aligned} \tag{1.4}$$

In regard of the second-order tensor $\mathbf{A}$, the quantities $\mathbf{A}^T$, $\mathbf{A}^{-1}$, $\mathrm{tr}\,(\mathbf{A})$, and $\mathbf{A}'$ denote its *transpose*, *inverse*, *trace*, and *deviator*, with the properties:

$$
\begin{aligned}
\mathbf{A}^T &= A_{ij}\,\mathbf{e}_j \otimes \mathbf{e}_i \\
\mathbf{A} \cdot \mathbf{A}^{-1} &= \delta_{ij}\,\mathbf{e}_i \otimes \mathbf{e}_j \\
\mathrm{tr}\,(\mathbf{A}) &= A_{ii} \\
\mathbf{A}' &= \mathbf{A} - \frac{1}{3}\,\mathrm{tr}\,(\mathbf{A})\mathbf{I}
\end{aligned}
\tag{1.5}
$$

The *Euclidean norm* of the vector $\mathbf{a}$ and the *Frobenius norm* of the second-oder tensor $\mathbf{A}$ read

$$
|\mathbf{a}| = \sqrt{\mathbf{a} \cdot \mathbf{a}} \quad \text{and} \quad |\mathbf{A}| = \sqrt{\mathbf{A} : \mathbf{A}} \quad .
\tag{1.6}
$$

Let $\mathbf{Q}$ denote a second-order tensor belonging to the *special orthogonal group*. It then exhibits the following properties

$$
\mathbf{Q} \cdot \mathbf{Q}^T = \mathbf{I} \quad \text{and} \quad \mathrm{tr}\,(\mathbf{Q}) = 1 \quad .
\tag{1.7}
$$

Therewith, the *Rayleigh products* of a vector and a second-oder tensor read:

$$
\begin{aligned}
\mathbf{Q} \star \mathbf{a} &= \mathbf{Q} \cdot \mathbf{a} \\
\mathbf{Q} \star \mathbf{A} &= \mathbf{Q} \cdot \mathbf{A} \cdot \mathbf{Q}^T
\end{aligned}
\tag{1.8}
$$
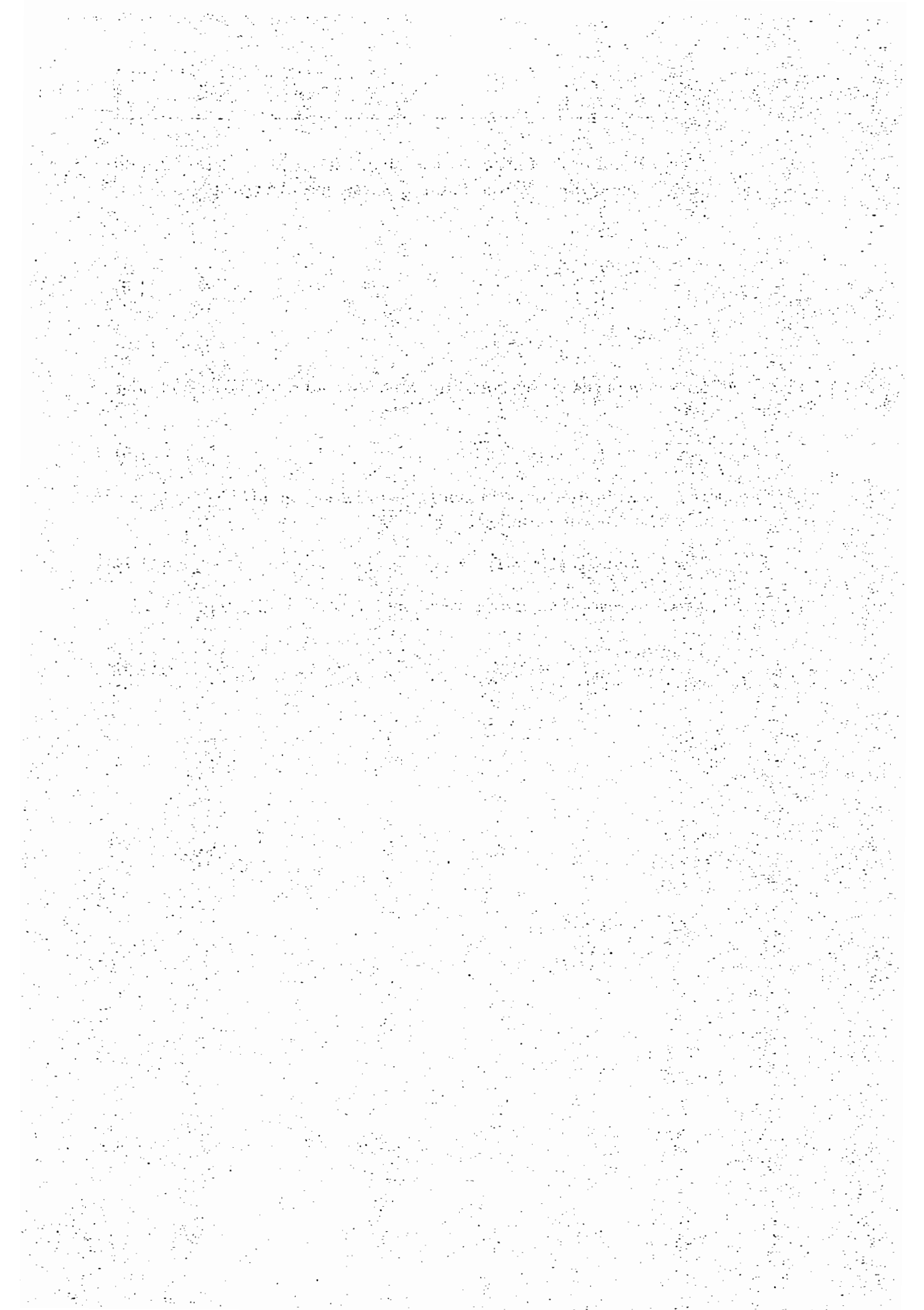
2 Physical phenomena of NiTi shape memory alloys

The unique properties of shape memory alloys can be ascribed to solid state phase transformations, in particular to *thermoelastic martensitic transformations* within the crystallographic structure of the material. They are addressed in the first part of this chapter. The second part is devoted to related thermomechanical characteristics. This chapter is intended as brief introduction to fundamental properties of NiTi shape memory alloys which are essential for the understanding of the constitutive relations proposed in Chapter 5. An elaborated review on this matter can be found in Funakubo (1987), Duerig et al. (1990), Miyazaki (1996), and Otsuka & Wayman (1998c).

2.1 Crystallographic perspective

Martensitic transformations denote particular solid state transformations occurring in a variety of metals and alloys (see Wayman & Duerig (1990)). They are characterized by a *diffusionless*, cooperative movement of the atoms within the crystal lattice of the material and are, thus, referred to as *displacive*. The domains subjected to martensitic transformations are traditionally termed *austenite* and *martensite* in honor of the metallurgists Sir William Chandler Roberts-Austen (1843-1902) and Adolf Martens (1850-1914).[1] These terms identify distinct *phases* within the material with homogeneous physical and chemical properties.[2] A key issue of shape memory alloys is that austenite usually inherits a highly symmetric crystal lattice in contrast to martensite. On this account, a variety of martensite crystals with distinct orientations may be constructed from one austenite crystal. For instance, the austenitic phase of NiTi shape memory alloys shows a body-centered-cubic crystal structure of B2-type and its martensitic counterpart exhibits a monoclinic structure of B19'-type. Both arrangements are schematically depicted in Figure 2.1, according to Otsuka & Ren (1999). In this case, 24 variants are conceivable for martensite, whereas the austenite possesses only one variant.

Martensitic transformations are generally *athermal* (see Wayman & Duerig (1990)), i.e., they only initiate if the current thermal or mechanical load reaches a critical value. As no diffusion of the atoms occurs, the transformation progress is specifically time-independent. Martensitic transformations of shape memory alloys are additionally *thermoelastic*. This essential property expresses an equilibrium between thermal and elastic effects, so that the size of the nucleated martensite crystals depends solely on the current thermal or mechanical load. The interfacial energy as well as the energy due to plastic deformations can particularly be considered as small. In this vein, the original

---

[1] An overview on atomic arrangements undergoing martensitic transformations can be found in Wayman & Duerig (1990).

[2] Note that the crystal structures related to the terms austenite and martensite are generally not unique for different alloys.

B2 austenite   B19' martensite
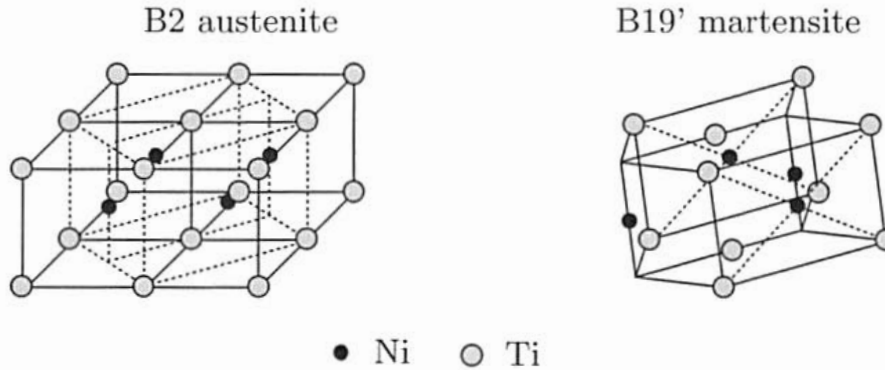
● Ni   ○ Ti

Figure 2.1: Crystal structures of B2 austenite and B19' martensite

austenitic structure before the initiation of the transformation into martensite can be fully recovered. Thermoelastic martensitic transformations are therefore referred to as *crystallographically reversible*.

The deformations arising from martensitic transformations may be subdivided into two components, i.e., *Bain strain* and *lattice invariant shear* (see Otsuka & Ren (1999)). The Bain strain is related to the deformations of the originally austenitic crystal lattice during martensitic transformations on disregarding the surrounding crystal lattice. These deformations generally involve severe volumetric and shear components, so that a reduction of the total deformation is eminent for the martensite in order to accommodate its environment. This reduction is expressed by the lattice invariant shear. In this context, two accommodation modes principally exist, i.e., *slip* and *twinning*, which are schematically depicted in Figure 2.2. During slip, the accommodation of the martensite is realized by plastic deformations of the martensite variants,

austenite

martensite

(a)   (b)
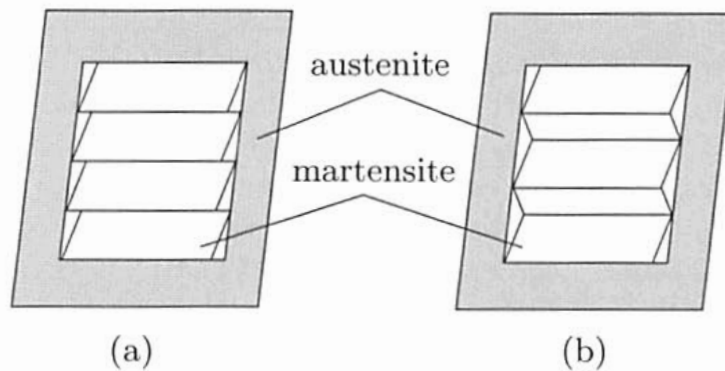
Figure 2.2: Lattice invariant shear: accommodation of a martensitic domain within an austenitic matrix due to (a) slip and (b) twinning (Auricchio (1995))

which induce irreversible damages into the crystal lattice. This, however, is not observable for shape memory alloys, as these alloys are ideally free of permanent deformations during phase transformations. The accommodation mode of shape memory alloys is merely driven by twinning of the martensite variants, i.e., the accommodation proceeds by the formation of twin crystals. The latter particularly possess mobile twin boundaries, which is why they can easily move under an applied stress. In this context, the term *detwinning* expresses the growth of certain martensite variants with favorable orientations to the applied stress direction. This growth proceeds on the expense of unfavorably oriented variants and leads to an observable shear deformation of the crystal lattice. Volume changes during twinning and detwinning processes are specifically negligible. In fact, NiTi shape memory alloys undergoing martensitic transformations exhibit volume changes in the range of 0.34 % (cf. Shimizu & Tadaki (1987)).

As the influences of thermal and mechanical loads on thermoelastic martensitic transformations are comparable, different shape memory effects can be observed. They are schematically summarized in Figure 2.3. The first sketch illustrates the *pseudoplastic effect* in combination with the *one-way shape memory effect*. The initial martensitic structure being in a stress-free state may be obtained from an unstressed austenitic structure by a temperature-induced martensitic transformation. In this case, martensite twins form in this way, that the external shape of the structure remains unaffected by the phase transformation. This effect is referred to as *self-accommodation* of the martensite variants. Then, under an applied stress, detwinning of the martensite variants initiates, which ideally leads to the formation of one favored variant at the conclusion of the detwinning process. The detwinned martensite variants are specifically stable in the unstressed state for the considered low temperature regime, so that an apparently plastic deformation is perceivable on unloading. This property characterizes the memory of shape memory alloys. In particular, due to the crystallographic reversibility of the material structure, the original austenitic structure can be fully restored through a temperature-induced phase transformation upon heating. In this case, the apparently plastic deformation of the martensitic phase vanishes and is therefore referred to as *pseudoplastic*. Then, along with an additional temperature-induced transformation into the self-accommodated martensite, the martensitic structure before the loading-unloading cycle can be recovered. This final step concludes the one-way shape memory effect.

The second sketch in Figure 2.3 depicts the *pseudoplastic effect* in combination with the *two-way shape memory effect*. In contrast to the preceding one-way shape memory effect, the self-accommodation of the martensite variants upon cooling is inhibited by external or internal stresses, so that oriented martensite variants form upon cooling. On this account, the pseudoplastic deformation being existent prior the phase transformation into the austenite is regained

Pseudoplasticity & one-way effect

Loading   Unloading   Heating

Martensite   Martensite   Austenite

Cooling
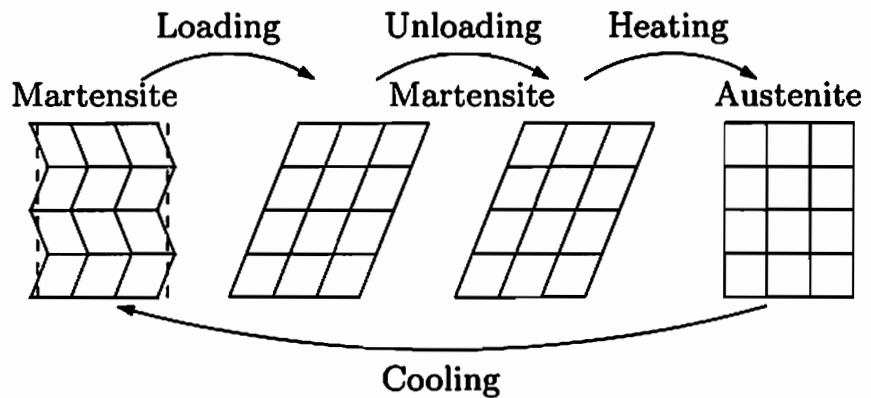
Pseudoplasticity & two-way effect

Loading   Heating

Martensite   Martensite   Austenite

Cooling

Pseudoelasticity

Loading

Austenite   Martensite

Unloading
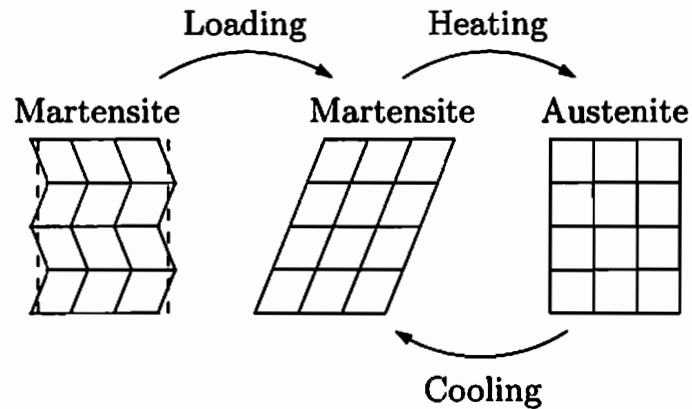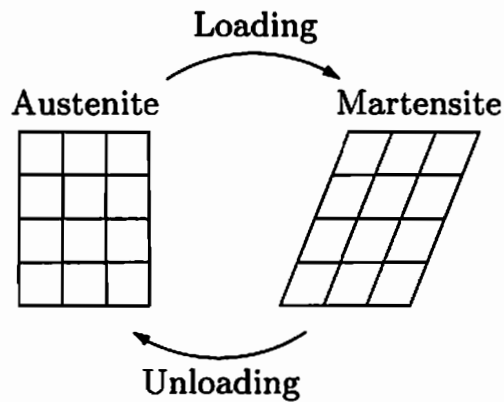
Figure 2.3: Structural changes of shape memory alloys (Helm (2001))

after the phase transformation into the martensite. This leads to well-defined shape changes of the material structure by temperature variations. In regard of the separation between external and internal stresses necessary to induce the two-way shape memory effect, the two categories of the *extrinsic* and the *intrinsic* effects may be distinguished. Both effects, however, provide similar material responses. It also bears emphasis that the internal stresses may be generated by dislocations or precipitates on employing an appropriate thermo-mechanical treatment of the material referred to as *training process*, whereas external stresses may result from external loads.

Apart from a stabilization of the martensite by temperature, martensite can also be stabilized by stress. This is observable for the *pseudoelastic effect*, which is visualized in the third sketch of Figure 2.3.[3] For instance, subjecting an initially austenitic structure to an external stress may trigger a stress-induced martensitic transformation. In this case, oriented martensite variants into the current stress direction are preferably activated, furnishing an observable inelastic deformation of the entire structure. However, as the martensite becomes unstable in the unstressed state for the considered high temperature regime, a reverse phase transformation into the austenite initiates upon unloading, so that the initial crystal lattice of the material reappears. Consequently, the inelastic deformation vanishes in the stress-free state. In this regard, the observable inelastic deformation is referred to as *pseudoelastic*.

Up to this point, the considerations are restricted to a direct transformation from austenite into martensite. Frequently, however, NiTi alloys show an additional premartensitic phase with a trigonal crystal structure which is identified by the rhombohedral *R-phase*.[4] Like the transformation into the B19' martensite, the transformation into the R-phase belongs to thermoelastic martensitic transformation. It usually initiates prior the transformation into the B19' martensite and it, thus, leads to a two-step phase transformation. The lattice distortions arising from B2 to R-phase transformations may, however, be regarded as small compared to the distortions resulting from B2 to B19' transformations. A comprehensive introduction to R-phase activities can be found in Miyazaki & Otsuka (1986) and Otsuka (1990).

2.2   Thermomechanical characteristics

The macroscopic material responses in terms of strain, temperature, and stress resulting from the crystallographic phenomena above are schematically visualized in Figures 2.4 and 2.5. The martensitic start and finish temperatures M_0^s and M_0^f express the initiation and conclusion of temperature-induced martensitic transformations from B2 austenite to B19' martensite upon cooling. The subscript 0 indicates the absence of stress. Accordingly, A_0^s and A_0^f are the corresponding austenitic start and finish temperatures upon heating. At temperatures above M_0^d, NiTi shape memory alloys do not exhibit any shape memory effect. In this case, the material behavior is elastoplastic as depicted

---

[3]The term *pseudoelasticity* as adopted here addresses the strain recovery upon unloading at constant temperature. Note, however, that pseudoelasticity is not uniquely restricted to phase transformations as a pseudoelastic material response can also be observed in the martensitic state during detwinning of the martensite variants (cf. Otsuka & Wayman (1998b) and Hornbogen (1995)). In this regard, the terms *superelasticity* and *rubber-like behavior* are often introduced to distinguish between the *transformation pseudoelasticity* and the *twinning pseudoelasticity*, respectively. Throughout this treatise, the rubber-like behavior is not considered.

[4]The R-phase may occur for near-equiatomic NiTi alloys after a suitable thermomechanical treatment, for ternary NiTiFe and NiTiAl alloys, and for Ni-rich NiTi alloys (cf. Saburi (1998)).
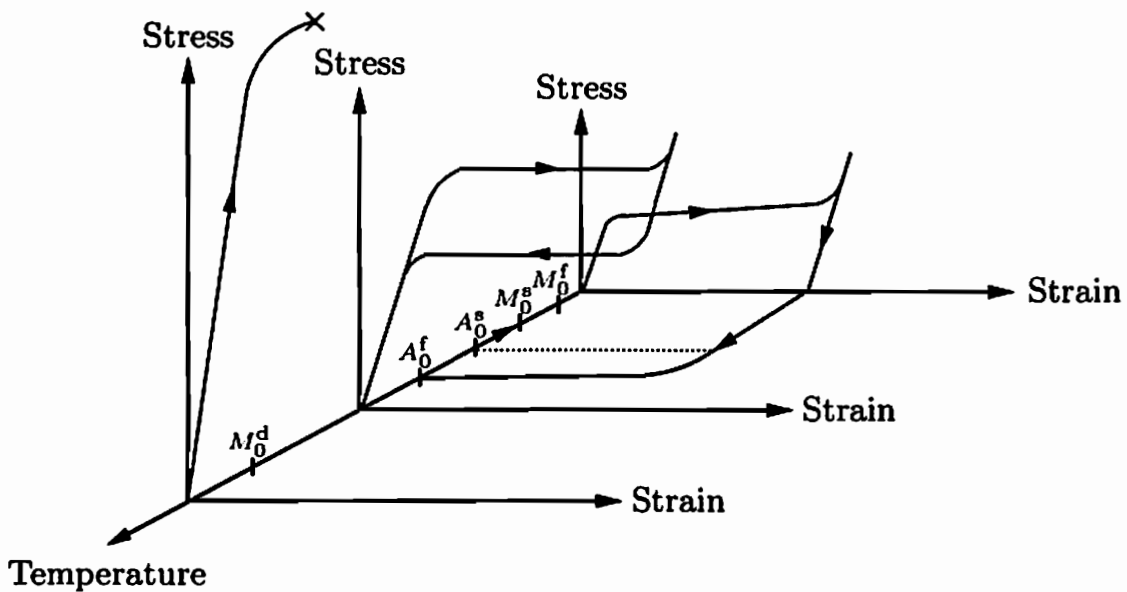
Figure 2.4: Front to rear: elastoplasticity, pseudoelasticity, pseudoplasticity, and one-way shape memory effect (Wayman & Duerig (1990))

in Figure 2.4. The pseudoelastic effect occurs within the temperature range between A_0^f and M_0^d. Therein, stress-induced phase transformations initiate on exceeding a critical stress after a linear elastic loading of the austenite. These transformations result in the formation of oriented martensite variants and, thus, in pseudoelastic deformations. At the end of the phase transformation process, the martensitic material is ideally loaded elastically.[5] Then, after an elastic unloading, phase transformations into austenite initiate, providing an observable hysteretic material behavior and, in addition, disappearing pseudoelastic deformations at zero stress. The pseudoplastic effect can be observed on lowering the temperature below M_0^f in the absence of stress, so that temperature-induced martensitic transformations take place which convert the material from an initially austenitic structure to an initially self-accommodated martensitic structure. Hence, no macroscopic deformations can ideally be observed during this transformation process. Subjecting the material to mechanical loadings then leads at first to elastic deformations of the martensite followed by the formation of oriented martensite variants and, thus, by inelastic deformations. In contrast to the foregoing pseudoelastic effect, however, the martensitic phase is stable in the absence of stress, so that the inelastic deformations persist after an elastic unloading into an unstressed state. In regard of their pseudoplastic property, however, these deformation

---

[5] Note that a complete stress-induced phase transformation into martensite is experimentally not observed for polycrystals (see Miyazaki et al. (1981), Brinson et al. (2004), Schmahl et al. (2004)). Thus, the deformation at the end of the observable plateau of the hysteresis is still affected by phase transformations. The remaining amount of austenite may, however, be regarded as subordinate.

can be fully reversed upon heating the material above the temperature A_0^f, for which the martensitic phase is unstable. Cooling below M_0^f finally concludes the one-way shape memory effect by recovering the self-accommodated martensitic structure before the deformation process. Maximum recoverable strains of NiTi alloys for pseudoelasticity and pseudoplasticity are in the range of 8% (cf. Miyazaki (1996)).

The temperature-strain response during the intrinsic two-way shape memory effect can be reviewed in Figure 2.5. Temperature variations from M_0^f to A_0^f and vice versa induce phase transformations between austenite and martensite. In contrast to the one-way shape memory effect, however, the formation of self-accommodated martensite variants is prevented by internal stresses. The latter enforce the formation of oriented martensite variants, leading to macroscopic deformations. This effect can alternatively be realized by external stresses in the course of the extrinsic two-way shape memory effect. Depending on the specific chemical composition of the NiTi alloy, maximum strains of the two-way shape memory effect are in the range of 4% (cf. Miyazaki (1996)).
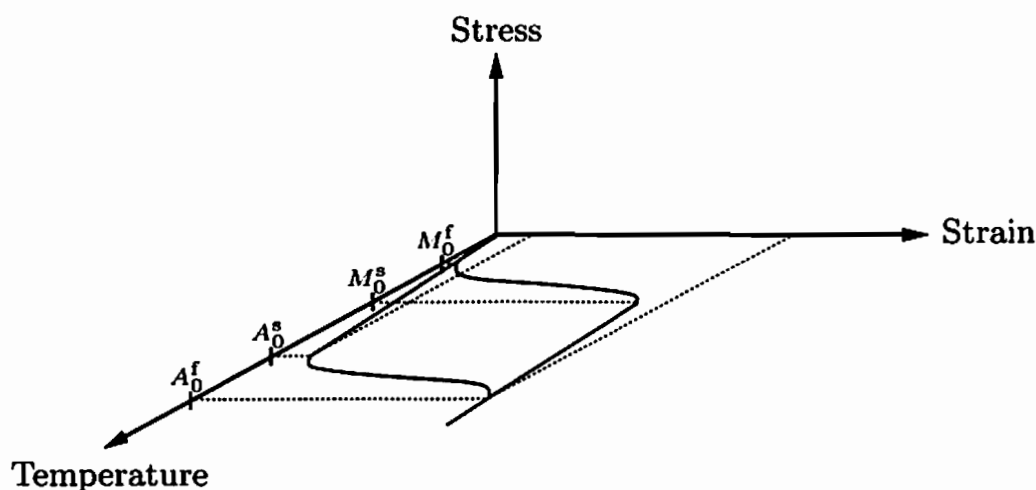
Figure 2.5: Two-way shape memory effect (Hornbogen (1987))

The temperature dependences of the one-way shape memory effect as well as of the pseudoelastic effect are summarized in Figure 2.6 in terms of a phase diagram. A fully developed one-way shape memory effect may be observed for an initially martensitic structure below the temperature A_0^s in conjunction with heating above A_0^f and subsequent cooling below M_0^f, whereas a complete pseudoelastic effect may be realized for an initially austenitic structure above A_0^f. For a thermomechanical loading within the temperature range between A_0^s and A_0^f, both effects overlap, i.e., this range is dominated by partial pseudoelastic and pseudoplastic effects. The straight line starting in M_0^s indicates the critical stresses for the initiation of stress-induced martensitic transformations in accordance to the *Clausius-Clapeyron-like relation* (see Ortín & Planes
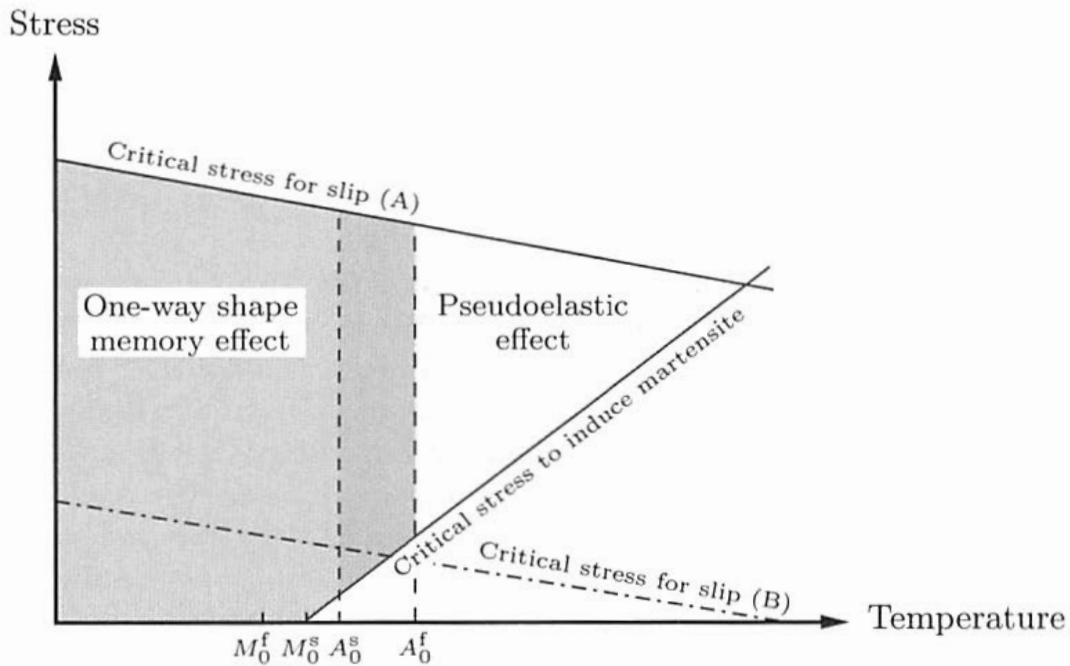
Figure 2.6: Principle structure of a phase diagram for shape memory alloys (Otsuka & Wayman (1998b))

(1989)). In order to avoid plastic deformation and to ensure the complete recovery of the inelastic deformations, the critical stress for slip has to exceed the critical stress for phase transformations throughout the process of deformation. This is indicated by the two lines (A) and (B), i.e., only for line (A) slip occurs after phase transformations on mechanically loading the material above A_0^f.

Processes of phase transformations are thermomechanically involved, i.e., heat is released during the *exothermic* austenite to martensite transformation, while heat is absorbed during the *endothermic* martensite to austenite transformation (cf. Shaw & Kyriakides (1995) and Tobushi et al. (1998)). For an unstressed thermal loading cycle, this effect is usually monitored during a DSC[6] analysis. Due to the severe temperature dependence of the critical transformation stresses, the generation of heat exhibits a strong influence on the mechanical material response.

Sometimes, shape memory alloys show an asymmetric deformation behavior well-known as *tension-compression asymmetry* (e.g., see Jacobus et al. (1996) and Bouvet et al. (2004b)). This effect may be attributed to an asymmetric transformation behavior of the single grains within the material microstructure (cf. Saburi (1998) and Gall & Sehitoglu (1999)). More precisely, as different martensite variants are activated for different loading directions and as each variant exhibits a characteristic deformation behavior, the deformations of the

---

[6] *Differential scanning calorimetry*, e.g., see Pope & Judd (1977)

single crystals show a strong orientation dependence on the mechanical load. Thus, depending on the degree of texture of the polycrystals, this may result in an inherent asymmetric transformation behavior. In particular, for untextured polycrystals in which the grains are randomly oriented, the asymmetric transformation behavior may be neglected.

As mentioned in the preceding section, the deformations resulting from R-phase activities are small compared to the deformations arising from transformations into B19' martensite. In fact, maximum strains from R-phase transformations are in the range of 1 % (cf. Otsuka & Ren (1999)). Due to this, they may often not be perceived within the strain-stress diagram. However, the heat generated during transformations into the R-phase and into B19' martensite is comparable. In this regard, as the critical transformation stresses are strongly temperature-sensitive, R-phase activities may exhibit significant influences on the observable material response. A thorough analysis on this matter can be found in the works of Šittner et al. (2006a,c).
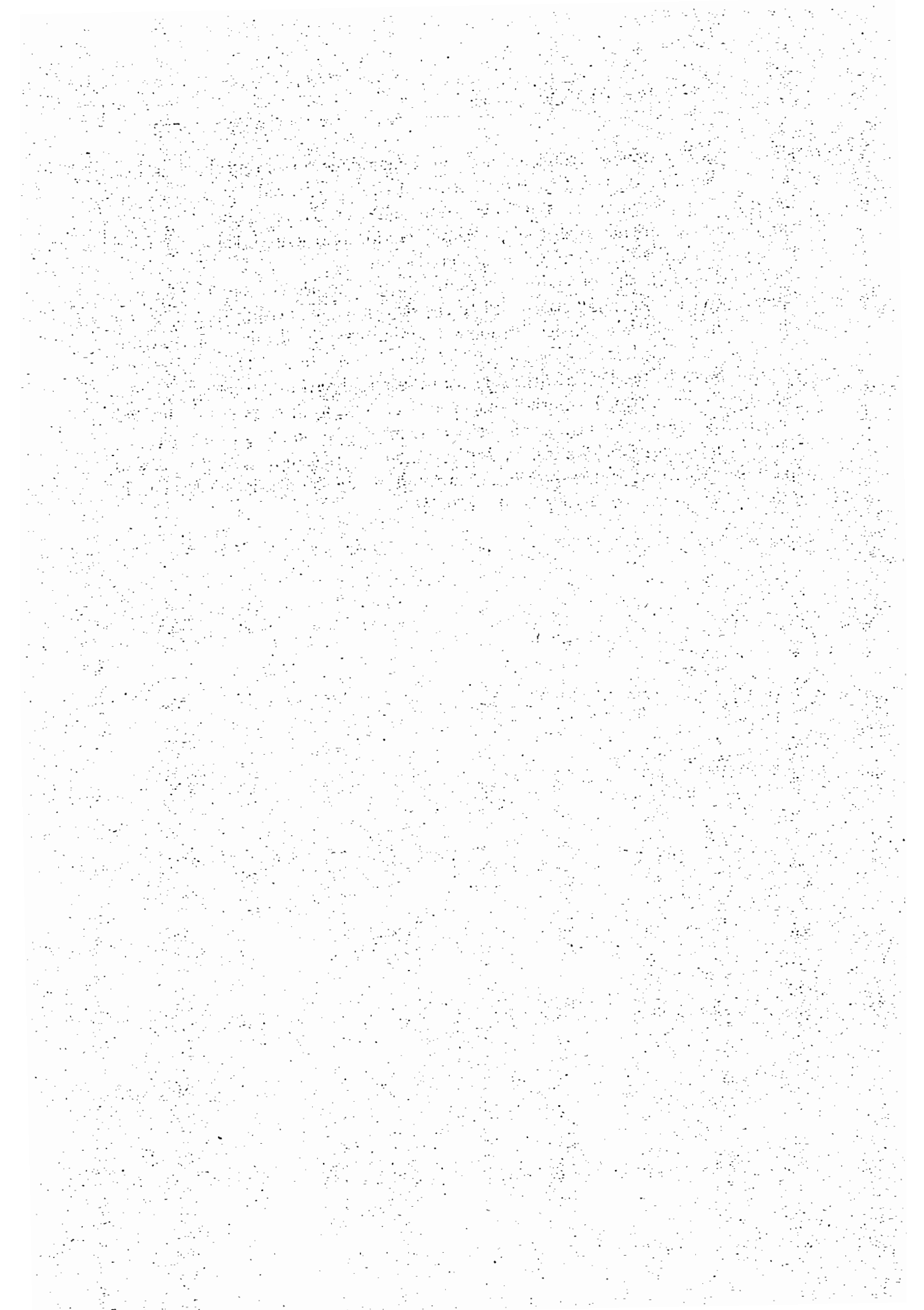
3 Kinematics and statics of a deforming body

This chapter is devoted to fundamental kinematic and static relations of non-linear continuum mechanics which are essential for the constitutive theory derived in Chapter 5. The kinematics of a deforming body are presented in Section 3.1. They particularly address the deformation gradient and the velocity gradient as basic kinematical quantities. On the basis of these variables, the concept of strain as measure for local shape changes is introduced in Section 3.2. Static relations of the deforming body are regarded in Section 3.3 in terms of the stress as measure for the local load. Section 3.4 deals with the notion of objectivity. This essential property conceptually expresses the transformation behavior of physical quantities such as strain or stress under rigid body motions. As these motions may affect the monitoring of the change rate of physical quantities, objective time derivatives are mandatory. They are addressed in Section 3.5. The intention of this chapter is to provide a brief review on some basic principles of continuum mechanics. An elaborated overview can be found in Malvern (1969), Chadwick (1976), Marsden & Hughes (1983), Ogden (1984), Haupt (2000), Belytschko et al. (2000), and Xiao et al. (2006a).

3.1 Deformations of continuous bodies

Continuum mechanics focuses on deformable *bodies* which obey the *continuum hypothesis*, i.e., a particular body of interest is assumed to consist of an open set B of continuously distributed *material points* or *particles* $P \in B$. The current geometric representation $\mathcal{B}_t$ of B within the three-dimensional Euclidean space $\mathcal{E}$ of physical observation is termed *current* or *Eulerian configuration*. As depicted in Figure 3.1, $\mathcal{B}_t$ identifies the region that is occupied by B in $\mathcal{E}$ at time t. Since the current configuration of the body changes throughout the ongoing deformation process, the *current position* x of each particle P may be expressed by the time-dependent one-to-one mapping

$$\mathbf{x} = \chi(P, t) \quad , \tag{3.1}$$

which is supposed to be continuously differentiable.[7] A *physical observer* $\mathcal{O}$ who perceives the deformation process can only quantify x and t if a *frame of reference* is given. In this regard, $\mathcal{O}$ monitors space and time relative to an observer-related basis $\mathbf{e}_i$ with origin o and relative to a referential time t_r, such that the quantities x and t represent a *position vector* and a *time interval*. Specifically, the pair $(\mathbf{x}, t)$ recorded by $\mathcal{O}$ is termed *event*. It may be inferred that the definition of a frame of reference underlies a certain arbitrariness, i.e., different observers may choose different frames of reference. This issue is addressed in Section 3.4.

---

[7]Note that this classical description does not reflect any orientational information of distinct material particles.
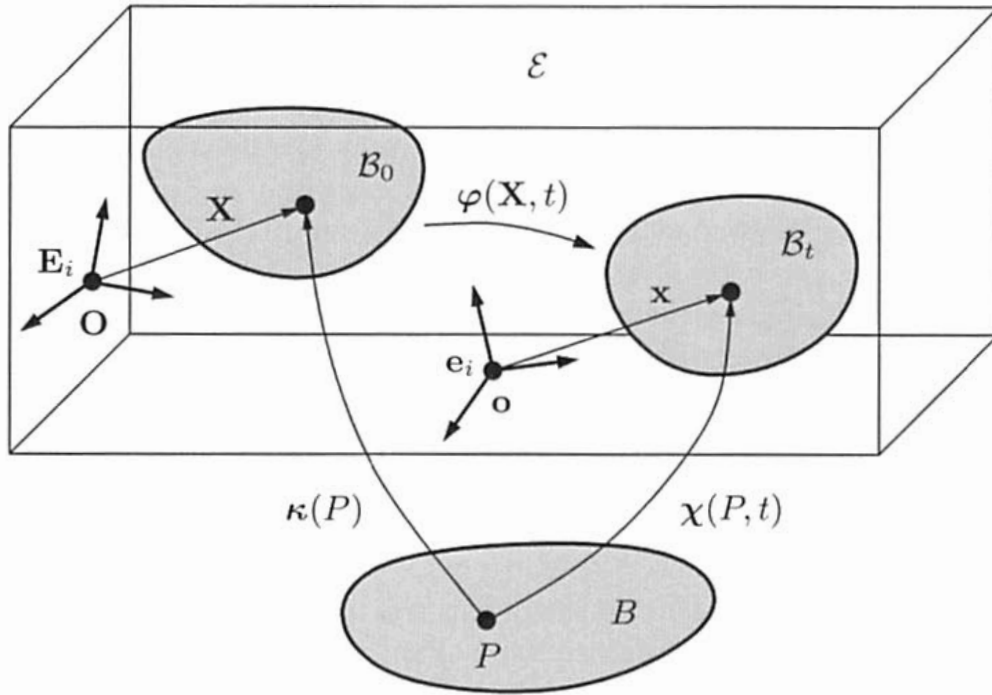
Figure 3.1: Current and reference configurations

In order to allow the observer to identify each particle of the body, it may be helpful to introduce the time-independent referential geometric representation $\mathcal{B}_0$ of B called *reference* or *Lagrangian configuration*. Therein, the *reference position* $\mathbf{X}$ in $\mathcal{E}$ of each particle P of B is expressed by the bijective continuously differentiable mapping

$$\mathbf{X} = \kappa(P) \quad . \tag{3.2}$$

The reference configuration does not need to be a region that was actually occupied by B during its deformation history. However, it is often convenient to define $\mathcal{B}_0$ as the *initial configuration*, i.e., as the current configuration of B at *initial time* $t = 0$, to monitor the relative motion of all particles during a process of deformation starting in $t = 0$. Basis and origin in the reference configuration are denoted by $\mathbf{E}_i$ and $\mathbf{O}$, respectively.

Replacing P in (3.1) by the inverse relation of (3.2) yields the time-dependent one-to-one mapping φ

$$\mathbf{x} = \chi\left(\kappa^{-1}(\mathbf{X}), t\right) = \varphi(\mathbf{X}, t) \quad . \tag{3.3}$$

It describes the relative *deformation* from $\mathcal{B}_0$ to $\mathcal{B}_t$. The term deformation is used here in line with Truesdell & Noll (2004) in a general sense. It includes changes in shape and in position in space of the body. While the former leads to a varying distance of at least a particle subgroup of the body, the latter

reflects a *rigid body motion*. Particularly, in disregarding shape changes, a pure rigid body motion can be expressed by

$$\varphi(\mathbf{X}, t) = \mathbf{Q}(t) \cdot \mathbf{X} + \mathbf{c}(t) \quad . \tag{3.4}$$

The first term on the right-hand side, the product $\mathbf{Q} \cdot \mathbf{X}$, describes a *rigid body rotation*, with $\mathbf{Q}(t)$ denoting a time-dependent proper orthogonal second-order tensor of the special orthogonal group. The second term on the right-hand side, the time-dependent vector $\mathbf{c}(t)$, accounts for a *rigid body translation*.

The two configurations $\mathcal{B}_0$ and $\mathcal{B}_t$ provide separate frameworks in which physical phenomena associated with the deformation of a body may be expressed. The description in the reference configuration $\mathcal{B}_0$ is termed *Lagrangian* or *material description*. Here, the *material coordinates* $\mathbf{X}$ are employed as primitive geometric quantities. The *Eulerian* or *spatial description* is based on the current configuration $\mathcal{B}_t$, i.e., on the *spatial coordinates* $\mathbf{x}$. Thus, depending on the underlying framework, all scalar, vector, or tensor fields ascribed to physical phenomena of the body are functions in $\mathbf{X}$ or $\mathbf{x}$. A tensor is particularly labeled *Lagrangian tensor* if it is completely defined in the referential Lagrangian configuration, while a *Eulerian tensor* is related to the current Eulerian configuration. A two-point second-order tensor defined in, both, the reference as well as the current configuration is named *Lagrangian-Eulerian* or *Eulerian-Lagrangian tensor*.

3.1.1 Deformation gradient

Within the context of the continuum hypothesis, φ is assumed to be continuously differentiable with respect to $\mathbf{X}$. This implies that the local deformations in the vicinity of each particle P of B are sufficiently smooth, so that the neighborhood of all particles is retained. In this regard, the spatial derivative of (3.3)

$$\mathbf{F} = \frac{\partial \varphi(\mathbf{X}, t)}{\partial \mathbf{X}} \quad , \tag{3.5}$$

termed *deformation gradient*, is well-defined. Since φ is a one-to-one mapping between $\mathbf{X}$ and $\mathbf{x}$, the quantity $\mathbf{F}$ is always invertible and, thus, its *Jacobian J* is non-zero

$$J = \det(\mathbf{F}) \neq 0 \quad . \tag{3.6}$$

On stipulating that the frame of reference of the observer is a Cartesian coordinate system, such that

$$\mathbf{x} = x_i \, \mathbf{e}_i \quad \text{and} \quad \mathbf{X} = X_i \, \mathbf{E}_i \quad , \tag{3.7}$$

with $\mathbf{e}_i$ and $\mathbf{E}_i$ being mutually orthogonal unit vectors, the tensor $\mathbf{F}$ takes the form

$$\mathbf{F} = \frac{\partial x_i}{\partial X_j}\,\mathbf{e}_i \otimes \mathbf{E}_j \quad . \tag{3.8}$$

It may be inferred that the deformation gradient is a two-point tensor defined in the Eulerian as well as in the Lagrangian configuration. Consequently, it requires the existence of a reference configuration.

Deformation of line, surface, and volume elements

By virtue of the second-order tensor $\mathbf{F}$, geometrical quantities such as line, surface, and volume elements defined in the current configuration can be transferred into the reference configuration and vice versa. For an infinitesimal line element $d\mathbf{X}$ at position $\mathbf{X}$ in the reference configuration, connecting two generic particles in the neighborhood of $\mathbf{X}$, the corresponding line element $d\mathbf{x}$ in the current configuration can be obtained by the linear mapping

$$d\mathbf{x} = \mathbf{F} \cdot d\mathbf{X} \quad . \tag{3.9}$$

The deformation gradient may, thus, be interpreted as natural measure for the local deformation state of a generic line element. On the basis of this relation, a referential surface element $d\mathbf{A}$ can be transformed to its current representation $d\mathbf{a}$ by *Nanson's formula*

$$d\mathbf{a} = J\,\mathbf{F}^{-T} \cdot d\mathbf{A} \quad . \tag{3.10}$$

The quantities $d\mathbf{A}$ and $d\mathbf{a}$ are defined as

$$d\mathbf{A} = \mathbf{N}\,dA \quad \text{and} \quad d\mathbf{a} = \mathbf{n}\,da \quad , \tag{3.11}$$

with the unit vectors $\mathbf{N}$ and $\mathbf{n}$ being normal to the respective surfaces with infinitesimal areas dA and da. The volume elements dV and dv in the reference and current configuration are related to each other by the Jacobian as

$$dv = J\,dV \quad . \tag{3.12}$$

Evidently, the requirement

$$J > 0 \tag{3.13}$$

must hold true in addition to (3.6) in order to ensure physically reasonable deformation states.

Polar decomposition

The deformation gradient embodies two essential kinematical information for general deformations, i.e., the rigid rotation as well as the stretch of a generic

line element dX. Rigid translations are not account for by F as it may be deduced from relations (3.4) and (3.5). The two kinematical information can uniquely be determined from a right and a left polar decomposition[8] of F

$$F = R \cdot U = V \cdot R \quad , \tag{3.14}$$

which is schematically depicted in Figure 3.2 for a line element dX. The Lagrangian tensor U and the Eulerian tensor V are positive definite symmetric second-order tensors named *right* and *left stretch tensors*. Both describe the stretch of dX in the respective configurations (cf. Malvern (1969)). The proper orthogonal *rotation tensor* R expresses the rigid rotation of dX.[9] Accordingly, F may be regarded as composition of a rigid rotation and a stretch of dX. It should be noted that F equals R for a process of pure rigid rotation, so that $U = V = I$.
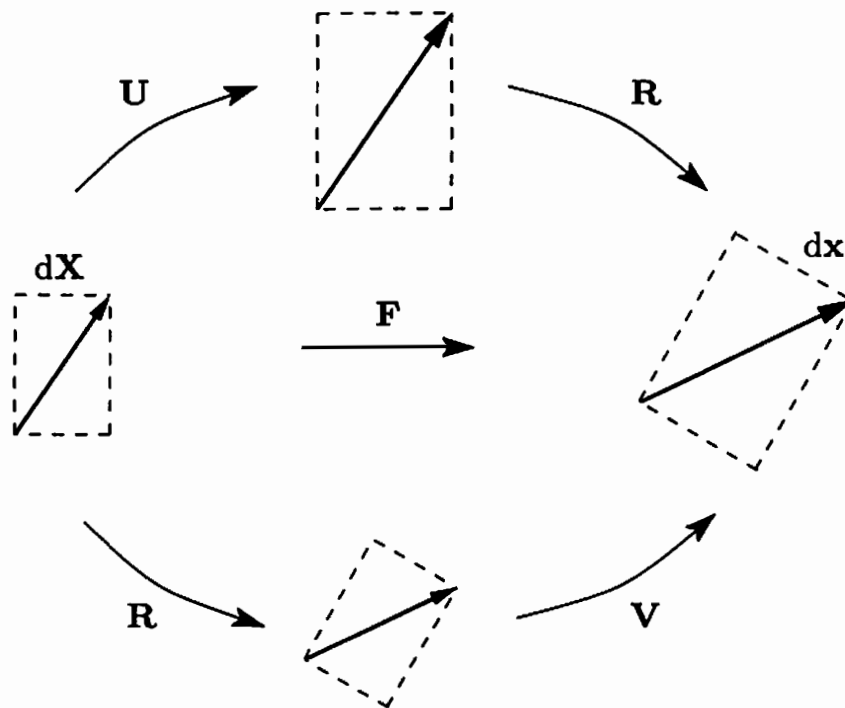
Figure 3.2: Polar decomposition of F and its impact on the deformation of line element dX

Since $R \cdot R^T = R^T \cdot R = I$, the quantities U and V may be determined by virtue of (3.14) from

$$U = \sqrt{F^T \cdot F} \quad \text{and} \quad V = \sqrt{F \cdot F^T} \quad . \tag{3.15}$$

---

[8] The polar decomposition can always be applied to arbitrary second-order tensors T with $\det(T) > 0$ (cf. Gurtin (1981)), which is fulfilled here for F (see equation (3.13)).

[9] In general, the rotation tensors for the left and the right polar decomposition differ, since they are defined in different configurations. According to Ogden (1984), however, they can be regarded as identical.

It may also be deduced from (3.14) that the left stretch tensor $\mathbf{V}$ can be transformed into $\mathbf{U}$ and vice versa by the rotated correspondences

$$\mathbf{U} = \mathbf{R}^T \star \mathbf{V} \quad \text{and} \quad \mathbf{V} = \mathbf{R} \star \mathbf{U} \quad . \tag{3.16}$$

As the computation of $\mathbf{U}$ and $\mathbf{V}$ from $\mathbf{F}$ requires the evaluation of a square root, it may be convenient to introduce the *right* and *left Cauchy-Green tensors* $\mathbf{C}$ and $\mathbf{B}$ as

$$\mathbf{C} = \mathbf{U}^2 = \mathbf{F}^T \cdot \mathbf{F} \quad \text{and} \quad \mathbf{B} = \mathbf{V}^2 = \mathbf{F} \cdot \mathbf{F}^T \quad . \tag{3.17}$$

Similar to the stretch tensors, the following rotated correspondences hold for these quantities

$$\mathbf{C} = \mathbf{R}^T \star \mathbf{B} \quad \text{and} \quad \mathbf{B} = \mathbf{R} \star \mathbf{C} \quad . \tag{3.18}$$

3.1.2 Velocity gradient

The change rate of the current position vector of a generic material particle P during a deformation process is expressed by the *velocity* $\mathbf{v}$. It is defined as

$$\mathbf{v} = \dot{\mathbf{x}} = \frac{d\mathbf{x}}{dt} \quad , \tag{3.19}$$

with the total time derivative $d(\cdot)/dt$ termed *Lagrangian* or *material time derivative*. This time derivative is evaluated for a constant particle P or, alternatively with (3.2), at constant position vector $\mathbf{X}$. The Eulerian second-order tensor $\mathbf{L}$ defined as

$$\mathbf{L} = \frac{\partial \mathbf{v}(\mathbf{x}, t)}{\partial \mathbf{x}} \tag{3.20}$$

is labeled *velocity gradient*. It maps a line element $d\mathbf{x}$ in the current configuration onto its rate $d\dot{\mathbf{x}}$ as

$$d\dot{\mathbf{x}} = \mathbf{L} \cdot d\mathbf{x} \quad . \tag{3.21}$$

In this regard, the velocity gradient may be interpreted as natural measure for the local deformation change rate of a generic line element. It bears emphasis that, in contrast to the deformation gradient, the definition of the velocity gradient does not rely on any reference configuration.

$\mathbf{L}$ provides two essential kinematical information, i.e., the stretch rate as well as the rigid rotation rate of a line element $d\mathbf{x}$ defined in the current configuration. The former is represented by the *stretching tensor* $\mathbf{D}$ and the latter is expressed by the *vorticity tensor* $\mathbf{W}$ (cf. Malvern (1969)). Both quantities are Eulerian second-order tensors. They can be determined on employing an

additive decomposition of $\mathbf{L}$ into a symmetric part $\mathbf{D}$ and skew-symmetric part $\mathbf{W}$ according to

$$\mathbf{L} = \mathbf{D} + \mathbf{W} \quad , \tag{3.22}$$

which are defined as

$$\mathbf{D} = \frac{1}{2}\left(\mathbf{L} + \mathbf{L}^{\mathrm{T}}\right) \quad \text{and} \quad \mathbf{W} = \frac{1}{2}\left(\mathbf{L} - \mathbf{L}^{\mathrm{T}}\right) \quad . \tag{3.23}$$

Note that by virtue of $\mathbf{D}$, a volume element $\mathrm{d}v$ in the current configuration can be mapped onto its rate $(\mathrm{d}v)^{\cdot}$ as

$$(\mathrm{d}v)^{\cdot} = \mathrm{d}v \, \mathrm{tr}\,(\mathbf{D}) \quad . \tag{3.24}$$

3.2 Strain measures

A body B is said to be *strained* in $\mathbf{X}$ if the length of a generic line element $\mathrm{d}\mathbf{X}$ based on $\mathbf{X}$ has changed after a deformation process of B. Strictly speaking, a strained body in $\mathbf{X}$ exhibits a stretched line element $\mathrm{d}\mathbf{X}$. This implies that the stretch tensor $\mathbf{U}$ related to $\mathrm{d}\mathbf{X}$ is not the identity. Accordingly, B is said to be *unstrained* in $\mathbf{X}$ if $\mathbf{U} = \mathbf{I}$. This is, for instance, the case for a pure rigid rotation of $\mathrm{d}\mathbf{X}$, i.e., for $\mathbf{F} = \mathbf{R}$. Although the preceding consideration is based on the Lagrangian configuration, it may also be employed for the Eulerian configuration, i.e., for a line element $\mathrm{d}\mathbf{x}$ at position $\mathbf{x}$, along with the corresponding stretch tensor $\mathbf{V}$. It also bears emphasis that the notion of strain requires the introduction of a reference configuration to allow the observer to monitor the change in length of the line elements. In other words, a strain cannot be determined without a reference configuration.
Based on the stretch tensors $\mathbf{U}$ and $\mathbf{V}$, Hill (1968, 1978) (see also Wang & Truesdell (1973)) introduces general classes of Lagrangian and Eulerian strain tensors $\mathbf{E}^{(m)}$ and $\mathbf{e}^{(m)}$, respectively. This definition, however, proves to be inconvenient, as the computation of the stretch tensors may be regarded as cumbersome. Hence, a modified definition in terms of the right and left Cauchy-Green tensors as, e.g., adopted in Xiao et al. (1998b) is employed here. It reads

$$\mathbf{E}^{(m)} = \sum_{i=1}^{\sigma} g(\chi_i)\,\mathbf{C}_i \quad \text{and} \quad \mathbf{e}^{(m)} = \sum_{i=1}^{\sigma} g(\chi_i)\,\mathbf{B}_i \quad , \tag{3.25}$$

where χ_i designates the σ distinct eigenvalues of either $\mathbf{C}$ or $\mathbf{B}$, and $\mathbf{C}_i$ as well as $\mathbf{B}_i$ are the respective eigenprojections.[10] The scale function $g(\cdot)$ is a sufficiently smooth monotonously increasing function obeying the conditions

$$g(1) = 0 \quad \text{and} \quad g'(1) = \frac{1}{2} \quad , \tag{3.26}$$

---

[10]Due to the rotated correspondences (see equation (3.18)), $\mathbf{C}$ and $\mathbf{B}$ possess equal eigenvalues but different eigenprojections.

with $g'(\cdot)$ denoting the first derivative of $g(\cdot)$. The former condition accounts for the property of strains to vanish in the unstrained state, while the latter ensures the strain tensors to be close to the well-known linearized strain tensor for sufficiently small magnitudes (cf. Wang & Truesdell (1973)). On defining the scale function as

$$g(\chi_i) = \begin{cases} \dfrac{1}{2m}\left(\chi_i^m - 1\right) & \text{for } m \neq 0 \\[2ex] \dfrac{1}{2}\ln\left(\chi_i\right) & \text{for } m = 0 \end{cases} \tag{3.27}$$

(see Doyle & Ericksen (1956) or Seth (1964)), with $m \in \mathbb{R}$, all commonly used Lagrangian and Eulerian strain tensors can be expressed. For instance, selecting $m = 1$ yields the *Green-Lagrangian strain tensor*

$$\mathbf{E} = \frac{1}{2}\sum_{i=1}^{\sigma}\left(\chi_i - 1\right)\mathbf{C}_i = \frac{1}{2}\left(\mathbf{C} - \mathbf{I}\right) \quad, \tag{3.28}$$

and setting $m = -1$ gives the *Almansi-Eulerian strain tensor*

$$\mathbf{e} = \frac{1}{2}\sum_{i=1}^{\sigma}\left(1 - \chi_i^{-1}\right)\mathbf{B}_i = \frac{1}{2}\left(\mathbf{I} - \mathbf{B}^{-1}\right) \quad. \tag{3.29}$$

The very particular case $m = 0$ leads to the *Hencky strain tensors* in the Lagrangian description

$$\mathbf{H} = \frac{1}{2}\sum_{i=1}^{\sigma}\ln\left(\chi_i\right)\mathbf{C}_i = \frac{1}{2}\ln\left(\mathbf{C}\right) \tag{3.30}$$

and in the Eulerian description

$$\mathbf{h} = \frac{1}{2}\sum_{i=1}^{\sigma}\ln\left(\chi_i\right)\mathbf{B}_i = \frac{1}{2}\ln\left(\mathbf{B}\right) \quad. \tag{3.31}$$

A suggestive interpretation for $\mathbf{E}$ as well as $\mathbf{e}$ is given by the difference between the squared lengths of corresponding line elements $d\mathbf{X}$ and $d\mathbf{x}$ in the Lagrangian and Eulerian configurations as

$$|d\mathbf{x}|^2 - |d\mathbf{X}|^2 = d\mathbf{X}\cdot\mathbf{E}\cdot d\mathbf{X} = d\mathbf{x}\cdot\mathbf{e}\cdot d\mathbf{x} \quad. \tag{3.32}$$

The Hencky strain tensors may be interpreted as the well-known *natural strain* into the principal directions of $\mathbf{C}$ or $\mathbf{B}$ (see Hencky (1928, 1929a, 1929b)).

3.3   Stress measures

If a deformable material body as considered in Section 3.1 is exposed to an external mechanical load, internal interactions between adjacent material particles arise throughout the body. They are reflected by the notion of *stress* as measure for the local mechanical load. Stresses may be quantified by virtue of imaginary surfaces passing through the current configuration $\mathcal{B}_t$ of the body B as depicted in Figure 3.3. Therein, $\mathcal{S}_t$ denotes a single surface with unit normal vector n and area a which cuts $\mathcal{B}_t$ into the two parts $\mathcal{B}_{t,1}$ and $\mathcal{B}_{t,2}$, and $\bar{\mathbf{F}}_i$ represents a set of external force vectors (see Section 4.2.2). The internal
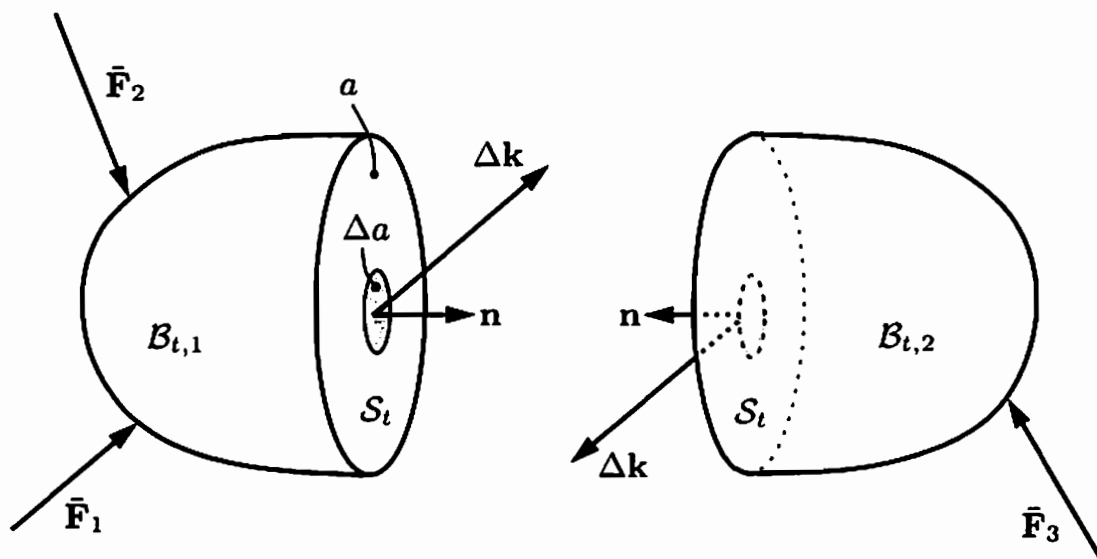
Figure 3.3: Imaginary surface $\mathcal{S}_t$ passing through a body B in its current configuration $\mathcal{B}_t$

force resulting from the transmission of the external load through the uncut body is schematically accounted for by the internal surface force vector $\Delta\mathbf{k}$ assigned to an area element Δa within $\mathcal{S}_t$. Taking the limit

$$\mathbf{t} = \lim_{\Delta a \to 0} \frac{\Delta\mathbf{k}}{\Delta a} = \frac{d\mathbf{k}}{da} \tag{3.33}$$

then yields the *Cauchy stress vector* $\mathbf{t}\,(\mathbf{x}, t, \mathbf{n})$ which identifies a *surface force density*. The explicit dependence of $\mathbf{t}$ on position $\mathbf{x}$, time t, and unit normal n is in accord with *Cauchy's fundamental postulate*. *Cauchy's theorem* particularly relates $\mathbf{t}$ and n by the linear mapping

$$\mathbf{t} = \boldsymbol{\sigma} \cdot \mathbf{n} \quad , \tag{3.34}$$

with the Eulerian second-order tensor $\boldsymbol{\sigma}\,(\mathbf{x}, t)$ termed *Cauchy stress tensor*.[11]
This tensor maps an area element da onto the force vector $d\mathbf{k}$ as

$$d\mathbf{k} = \mathbf{t}\,da = \boldsymbol{\sigma} \cdot d\mathbf{a} \quad . \tag{3.35}$$

Since the derivation of the Cauchy stress tensor is solely based on quantities of the current configuration, it is also referred to as *true stress tensor*. The definition of stress measures is, however, not restricted to the Eulerian configuration, i.e., different measures of stress may be defined for different configurations. For instance, transformation of the surface element $d\mathbf{a}$ used in (3.35) into the reference configuration by virtue of Nanson's formula (3.10) yields the relation

$$d\mathbf{k} = \boldsymbol{\sigma} \cdot d\mathbf{a} = J\boldsymbol{\sigma} \cdot \mathbf{F}^{-T} \cdot d\mathbf{A} = \mathbf{P} \cdot d\mathbf{A} \quad . \tag{3.36}$$

The *first Piola-Kirchhoff stress tensor*

$$\mathbf{P} = J\boldsymbol{\sigma} \cdot \mathbf{F}^{-T} = \boldsymbol{\tau} \cdot \mathbf{F}^{-T} \quad , \tag{3.37}$$

thus, associates the force vector $d\mathbf{k}$ in the current configuration with an area element $d\mathbf{A}$ in the reference configuration. In this sense, $\mathbf{P}$ is a Eulerian-Lagrangian two-point tensor. In (3.37), the *Kirchhoff stress tensor* or *weighted Cauchy stress tensor* $\boldsymbol{\tau}$ is introduced as

$$\boldsymbol{\tau} = J\boldsymbol{\sigma} \quad , \tag{3.38}$$

representing a Eulerian second-order tensor. An additional transformation of the force vector $d\mathbf{k}$ into the reference configuration yields the *second Piola-Kirchhoff stress tensor* $\mathbf{S}$, which maps the Lagrangian area element $d\mathbf{A}$ onto the Lagrangian surface force vector $d\mathbf{K}$ according to

$$d\mathbf{K} = \mathbf{F}^{-1} \cdot d\mathbf{k} = \mathbf{F}^{-1} \cdot \mathbf{P} \cdot d\mathbf{A} = \mathbf{S} \cdot d\mathbf{A} \quad . \tag{3.39}$$

Hence, the Lagrangian second-order tensor $\mathbf{S}$ takes the form

$$\mathbf{S} = \mathbf{F}^{-1} \cdot \mathbf{P} = J\mathbf{F}^{-1} \cdot \boldsymbol{\sigma} \cdot \mathbf{F}^{-T} = \mathbf{F}^{-1} \cdot \boldsymbol{\tau} \cdot \mathbf{F}^{-T} \quad . \tag{3.40}$$

3.4 Objectivity

In Section 3.1, an observer $\mathcal{O}$ is introduced who monitors a deformation process of a material body within the three-dimensional Euclidean space. It is pointed out that position vector $\mathbf{x}$ and time t, both corresponding to the location of a specific particle of the body recorded by $\mathcal{O}$, depend on the arbitrarily chosen frame of reference of the observer, namely basis $\mathbf{e}_i$ with origin $\mathbf{o}$ and referential time t_r. In this sense, a second observer $\mathcal{O}^*$ using a different frame of reference,

---

[11]Sometimes, $\boldsymbol{\sigma}$ is introduced by the relation $\mathbf{t} = \mathbf{n} \cdot \boldsymbol{\sigma}$. The so-defined stress tensor and the stress tensor used in this treatise differ by a transposition.

i.e., basis e_i^* with origin o^* and referential time t_r^*, and being possibly in relative motion to the first observer, records position x^* and time t^* for the same particle. Generally, both measurements do not coincide. The observers should, however, agree about the distances in space and time they record. Strictly speaking, there exist one-to-one mappings between x and x^* as well as between t and t^*, such that the distances in space and time as well as the order in which physical phenomena occur during the process of deformation are invariant. These mappings are referred to as *change of frame* and can be expressed by

$$x^* = Q(t) \cdot x + c(t) \quad \text{and} \quad t^* = t - a \quad . \tag{3.41}$$

The spatial part consists of a relative rotation and a relative translation between the two observers, represented by the time-dependent proper orthogonal tensor $Q(t)$ and the time-dependent vector $c(t)$. The temporal part corresponds to a time shift by the constant quantity $a \in \mathbb{R}$. On comparing relations (3.4) and (3.41), a change of frame for $a = 0$, i.e., at fixed referential time $t_r = t_r^*$, may be interpreted as rigid body motion recorded by one single observer.

The consequences of a change of frame for scalar, vector, and tensor fields are reflected by the notion of *objectivity*. Conceptually, the preceding quantities are said to be objective if they satisfy the transformation rule given by (3.41). Objectivity addresses the transformation behavior as property of physical quantities, in contrast to the *principle of material frame indifference*. The latter states that the mathematical description of physical phenomena must be invariant under a change of frame (see Haupt (2000)), which has to be ensured in the formulation of material laws. The principle of material frame indifference is considered in Section 4.4.

According to Ogden (1984), the objectivity property depends on the configuration in which the physical quantities are defined. Lagrangian scalars α_0, vectors α_0, and second-order tensors A_0 are said to be objective if they are invariant under a change of frame, i.e.,

$$\alpha_0^* = \alpha_0$$
$$\alpha_0^* = \alpha_0 \tag{3.42}$$
$$A_0^* = A_0 \quad .$$

In this regard, the Lagrangian configuration is referred to as *frame indifferent*. Conversely, objective Eulerian scalars α, vectors α, and second-order tensors A transform according to

$$\alpha^* = \alpha$$
$$\alpha^* = Q \cdot \alpha \tag{3.43}$$
$$A^* = Q \star A \quad .$$

Objectivity of the mixed Lagrangian-Eulerian and Eulerian-Lagrangian second-order tensors defined as

$$\tilde{\mathbf{A}} = \boldsymbol{\alpha}_0 \otimes \boldsymbol{\alpha} \quad \text{and} \quad \tilde{\tilde{\mathbf{A}}} = \boldsymbol{\alpha} \otimes \boldsymbol{\alpha}_0 \tag{3.44}$$

finally requires

$$\tilde{\mathbf{A}}^* = \tilde{\mathbf{A}} \cdot \mathbf{Q}^{\mathrm{T}} \quad \text{and} \quad \tilde{\tilde{\mathbf{A}}}^* = \mathbf{Q} \cdot \tilde{\tilde{\mathbf{A}}} \quad . \tag{3.45}$$

Apparently, the Eulerian parts of the two-point tensors are transformed in line with (3.43_2). For instance, from (3.41) follows that line element $\mathrm{d}\mathbf{x}$ becomes under a change of frame

$$\mathrm{d}\mathbf{x}^* = \mathbf{Q} \cdot \mathrm{d}\mathbf{x} \quad , \tag{3.46}$$

whereas the velocity $\mathbf{v} = \dot{\mathbf{x}}$ takes the form

$$\mathbf{v}^* = \mathbf{Q} \cdot \mathbf{v} + \dot{\mathbf{Q}} \cdot \mathbf{x} + \dot{\mathbf{c}} \quad . \tag{3.47}$$

As it may be recognized by comparison with (3.43_2), the Eulerian vectors $\mathrm{d}\mathbf{x}$ and $\mathbf{v}$ are objective and non-objective, respectively. This is not surprising, as the change of frame is length preserving, while the relative motion between the two frames of reference, represented by $\dot{\mathbf{Q}}$ and $\dot{\mathbf{c}}$, affects the perceived velocity. Both results are crucial for the objectivity analysis of the deformation gradient $\mathbf{F}$ and the velocity gradient $\mathbf{L}$ as well as their derived quantities. Substitution of (3.46) in (3.5) shows that the deformation gradient is an objective Eulerian-Lagrangian second-order tensor

$$\mathbf{F}^* = \frac{\partial \mathbf{x}^*}{\partial \mathbf{X}} = \mathbf{Q} \cdot \frac{\partial \mathbf{x}}{\partial \mathbf{X}} = \mathbf{Q} \cdot \mathbf{F} \quad . \tag{3.48}$$

Contrarily, the Eulerian velocity gradient is non-objective as it may be deduced from (3.20) and (3.47) as

$$\mathbf{L}^* = \frac{\partial \mathbf{v}^*}{\partial \mathbf{x}^*} = \mathbf{Q} \star \mathbf{L} + \dot{\mathbf{Q}} \cdot \mathbf{Q}^{\mathrm{T}} \quad . \tag{3.49}$$

Accordingly, the Lagrangian right Cauchy-Green tensor $\mathbf{C}$ is objective

$$\mathbf{C}^* = (\mathbf{F}^*)^{\mathrm{T}} \cdot \mathbf{F}^* = \mathbf{F}^{\mathrm{T}} \cdot \mathbf{F} = \mathbf{C} \quad , \tag{3.50}$$

which also holds true for the Eulerian left Cauchy-Green tensor $\mathbf{B}$

$$\mathbf{B}^* = \mathbf{F}^* \cdot (\mathbf{F}^*)^{\mathrm{T}} = \mathbf{Q} \cdot \mathbf{F} \cdot \mathbf{F}^{\mathrm{T}} \cdot \mathbf{Q}^{\mathrm{T}} = \mathbf{Q} \star \mathbf{B} \quad . \tag{3.51}$$

From this it may be inferred that the stretch tensors $\mathbf{U}$ and $\mathbf{V}$, the strain tensors $\mathbf{E}$ and $\mathbf{e}$, as well as the Hencky strain tensors $\mathbf{H}$ and $\mathbf{h}$ are objective

Lagrangian and Eulerian quantities, respectively. Moreover, although the velocity gradient is non-objective, its symmetric part, i.e., the Eulerian stretching tensor $\mathbf{D}$, is invariant under a change of frame as

$$\mathbf{D}^* = \frac{1}{2}\left(\mathbf{L}^* + \mathbf{L}^{*\mathrm{T}}\right) = \mathbf{Q} \star \mathbf{D} \quad . \tag{3.52}$$

This is conversely not the case for the Eulerian vorticity tensor $\mathbf{W}$

$$\mathbf{W}^* = \frac{1}{2}\left(\mathbf{L}^* - \mathbf{L}^{*\mathrm{T}}\right) = \mathbf{Q} \star \mathbf{W} + \dot{\mathbf{Q}} \cdot \mathbf{Q}^{\mathrm{T}} \quad . \tag{3.53}$$

Hence, $\mathbf{D}$ is objective, while $\mathbf{W}$ is non-objective. With respect to the stress tensors defined in Section 3.3, the stress vector $\mathbf{t}$ and the unit normal vector $\mathbf{n}$ transform under a change of frame according to $\mathbf{t}^* = \mathbf{Q} \cdot \mathbf{t}$ and $\mathbf{n}^* = \mathbf{Q} \cdot \mathbf{n}$. This leads to

$$\mathbf{t}^* = \boldsymbol{\sigma}^* \cdot \mathbf{n}^* = \boldsymbol{\sigma}^* \cdot \mathbf{Q} \cdot \mathbf{n} \overset{!}{=} \mathbf{Q} \cdot \mathbf{t} \quad , \tag{3.54}$$

which can only be fulfilled in general if the Eulerian Cauchy stress tensor is objective, i.e.,

$$\boldsymbol{\sigma}^* = \mathbf{Q} \cdot \boldsymbol{\sigma} \cdot \mathbf{Q}^{\mathrm{T}} \quad . \tag{3.55}$$

Since the scalar-valued Jacobian is invariant under an orthogonal transformation of $\mathbf{F}$, objectivity is also preserved by the Eulerian Kirchhoff stress tensor $\boldsymbol{\tau}$. Therewith, the objectivity proofs for the Eulerian-Lagrangian first Piola-Kirchhoff stress tensor $\mathbf{P}$ and for the Lagrangian second Piola-Kirchhoff stress tensor $\mathbf{S}$ are straightforward as

$$\mathbf{P}^* = \boldsymbol{\tau}^* \cdot \mathbf{F}^{*-\mathrm{T}} = \mathbf{Q} \cdot \boldsymbol{\tau} \cdot \mathbf{Q}^{\mathrm{T}} \cdot \mathbf{Q} \cdot \mathbf{F}^{-\mathrm{T}} = \mathbf{Q} \cdot \mathbf{P} \tag{3.56}$$

and

$$\mathbf{S}^* = \mathbf{F}^{*-1} \cdot \mathbf{P}^* = \mathbf{F}^{-1} \cdot \mathbf{Q}^{\mathrm{T}} \cdot \mathbf{Q} \cdot \mathbf{P} = \mathbf{S} \quad . \tag{3.57}$$

An elaborated analysis of the objectivity properties of Lagrangian and Eulerian quantities can be found in Haupt (2000).

3.5 Objective time derivatives

As Lagrangian second-order tensors are invariant under a change of frame (see equation (3.42_2)), objectivity is identically guaranteed for their material time derivatives, i.e.,

$$\dot{\mathbf{A}}_0^* = \dot{\mathbf{A}}_0 \quad . \tag{3.58}$$

Contrarily, the material time derivatives of objective Eulerian second-order tensors are affected by a change of frame according to

$$\dot{\mathbf{A}}^* = \mathbf{Q} \cdot \dot{\mathbf{A}} \cdot \mathbf{Q}^{\mathrm{T}} + \dot{\mathbf{Q}} \cdot \mathbf{A} \cdot \mathbf{Q}^{\mathrm{T}} + \mathbf{Q} \cdot \mathbf{A} \cdot \dot{\mathbf{Q}}^{\mathrm{T}} \quad . \tag{3.59}$$

Consequently, on preserving objectivity, *objective time derivatives* for objective Eulerian second-order tensors are mandatory. In this regard, a variety of different rates has been established which may be classified into the two categories of *corotational* and *non-corotational* objective rates (cf. Bruhns et al. (2004)). Both categories have in common, that the material rate of the objective Eulerian tensor $\mathbf{A}$ is applied in a *codeforming frame*[12]. Prominent examples are the non-corotational *Oldroyd rate* and the corotational *Green-Naghdi rate* on the basis of the reference configuration and a corotating configuration, respectively.

In line with Xiao et al. (2005, 2006b), a *generalized objective time derivative* comprising corotational as well as non-corotational rates can be derived in a compact way on defining the *generalized codeforming frame* $(\cdot)^+$ through a time-dependent *generalized deformation gradient* $\boldsymbol{\Psi}$. Transformation of line element $\mathrm{d}\mathbf{x}$ then gives

$$\mathrm{d}\mathbf{x}^+ = \boldsymbol{\Psi}(t) \cdot \mathrm{d}\mathbf{x} \quad \text{with} \quad \boldsymbol{\Psi}|_{t=0} = \mathbf{I} \quad , \tag{3.60}$$

and transformation[13] of the tensor $\mathbf{A}$ provides

$$\mathbf{A}^+ = \boldsymbol{\Psi} \cdot \mathbf{A} \cdot \boldsymbol{\Psi}^{\mathrm{T}} \quad . \tag{3.61}$$

$\boldsymbol{\Psi}$ is general in this sense, that it may include rotations and stretches. For instance, $\boldsymbol{\Psi}$ equals $\mathbf{F}^{-1}$ and $\mathbf{R}^{\mathrm{T}}$ for the Oldroyd rate and the Green-Naghdi rate, respectively. It should be noted in this context that $\boldsymbol{\Psi}$ modifies the eigenvalues of $\mathbf{A}$ under a transformation if it is non-orthogonal.

With the codeforming frame on the basis of $\boldsymbol{\Psi}$ at hand, the generalized objective rate of $\mathbf{A}$ may be defined as

$$\overset{\circ}{\mathbf{A}} = \dot{\mathbf{A}} + \boldsymbol{\Gamma}^{\mathrm{T}} \cdot \mathbf{A} + \mathbf{A} \cdot \boldsymbol{\Gamma} \quad , \tag{3.62}$$

with

$$\boldsymbol{\Gamma} = \dot{\boldsymbol{\Psi}}^{\mathrm{T}} \cdot \boldsymbol{\Psi}^{-\mathrm{T}} \quad . \tag{3.63}$$

It can be obtained from the material time derivative of (3.61) as

$$\dot{\mathbf{A}}^+ = \boldsymbol{\Psi} \cdot \dot{\mathbf{A}} \cdot \boldsymbol{\Psi}^{\mathrm{T}} + \dot{\boldsymbol{\Psi}} \cdot \mathbf{A} \cdot \boldsymbol{\Psi}^{\mathrm{T}} + \boldsymbol{\Psi} \cdot \mathbf{A} \cdot \dot{\boldsymbol{\Psi}}^{\mathrm{T}} = \boldsymbol{\Psi} \cdot \overset{\circ}{\mathbf{A}} \cdot \boldsymbol{\Psi}^{\mathrm{T}} \quad . \tag{3.64}$$

Evidently, the generalized objective rate coincides with the material rate in the codeforming frame. For $\boldsymbol{\Psi} = \mathbf{Q}$, it identically satisfies the transformation rule (3.43$_2$) if the objective rate of $\mathbf{A}$ is an objective Eulerian quantity. Integration of (3.64) as it stands, followed by a backward transformation

---

[12]Recall that the term *deformation* includes changes in shape and in position in space.

[13]Formally, this transformation corresponds to a *push-forward* or a *pull back* of *co-* or *contravariant* second-order tensors (e.g., see Ogden (1984)). For the sake of brevity, mixed second-order tensors are not regarded here.

with (3.61) from the codeforming frame, leads to the corresponding *generalized objective time integration* of the objective rate

$$\mathbf{A} = \boldsymbol{\Psi}^{-1} \cdot \int_t \boldsymbol{\Psi} \cdot \overset{\diamond}{\mathbf{A}} \cdot \boldsymbol{\Psi}^T \mathrm{d}t \cdot \boldsymbol{\Psi}^{-T} \quad . \tag{3.65}$$

Analogously to the generalized objective rate, the time integration is applied in the codeforming frame.

3.5.1 Non-corotational rates

The specific choice

$$\boldsymbol{\Gamma} = \mathbf{W} + m\,\mathbf{D} + c\,\mathrm{tr}\,(\mathbf{D})\,\mathbf{I} \tag{3.66}$$

with the two parameters $(c, m) \in \mathbb{R}$ describes a family of infinitely many objective non-corotational rates (cf. Xiao et al. (2005, 2006b) and Hill (1968, 1970, 1978)) which includes well-known rates as particular cases. For instance, the *Oldroyd rate*

$$\overset{\diamond}{\mathbf{A}}{}^{\mathrm{Ol}} = \dot{\mathbf{A}} - \mathbf{L} \cdot \mathbf{A} - \mathbf{A} \cdot \mathbf{L}^T \tag{3.67}$$

(see Oldroyd (1950)) is obtained for $m = -1$ and $c = 0$, setting $m = 1$ and $c = 0$ yields the *Cotter-Rivlin rate*

$$\overset{\diamond}{\mathbf{A}}{}^{\mathrm{CR}} = \dot{\mathbf{A}} + \mathbf{L}^T \cdot \mathbf{A} + \mathbf{A} \cdot \mathbf{L} \tag{3.68}$$

(see Cotter & Rivlin (1955)), and the combination $m = -1$ and $c = 0.5$ leads to the *Truesdell rate*

$$\overset{\diamond}{\mathbf{A}}{}^{\mathrm{Tr}} = \dot{\mathbf{A}} - \mathbf{L} \cdot \mathbf{A} - \mathbf{A} \cdot \mathbf{L}^T + \mathrm{tr}\,(\mathbf{D}) \cdot \mathbf{A} \tag{3.69}$$

(see Truesdell (1953)). All three examples may be attributed to the so-called *Lie-derivative* (cf. Marsden & Hughes (1983)). The Cotter-Rivlin rate of the Almansi-Eulerian strain tensor $\mathbf{e}$ exhibits the unique property that it equals the stretching tensor $\mathbf{D}$

$$\overset{\diamond}{\mathbf{e}}{}^{\mathrm{CR}} = \mathbf{D} \quad . \tag{3.70}$$

In this sense, the stretching tensor may be considered as *rate* of the Almansi-Eulerian strain tensor.
Selection (3.66) implicitly defines the generalized codeforming frame through the initial value problem

$$\boldsymbol{\Gamma} = \dot{\boldsymbol{\Psi}}^T \cdot \boldsymbol{\Psi}^{-T} \quad \text{with} \quad \boldsymbol{\Psi}|_{t=0} = \mathbf{I} \tag{3.71}$$

(see equations (3.63) and (3.60₂)), for which Xiao et al. (2006b) provide an exact solution for the choice $m = \pm 1$ as

$$\boldsymbol{\Psi} = J^c \, \mathbf{R}^T \cdot \mathbf{V}^m \quad . \tag{3.72}$$

This solution includes the examples of the Lie-derivative considered above. It particularly leads to the results $\boldsymbol{\Psi} = \mathbf{F}^{-1}$ for the Oldroyd rate and to $\boldsymbol{\Psi} = \mathbf{F}^T$ for the Cotter-Rivlin rate.

3.5.2   Corotational rates

The selection $\boldsymbol{\Psi} = \mathbf{Q}$ restricts the codeforming frame $(\cdot)^+$ to a corotating frame $(\cdot)^*$ and provides the general form of the *corotational rate* as

$$\overset{\circ}{\mathbf{A}} = \dot{\mathbf{A}} - \boldsymbol{\Omega} \cdot \mathbf{A} + \mathbf{A} \cdot \boldsymbol{\Omega} \quad . \tag{3.73}$$

In line with (3.64), this rate of the objective Eulerian second-order tensor $\mathbf{A}$ corresponds to the material rate of $\mathbf{A}$ in the corotating frame (cf. Xiao et al. (1998a)), i.e.,

$$\dot{\mathbf{A}}^* = \mathbf{Q} \star \overset{\circ}{\mathbf{A}} \quad . \tag{3.74}$$

The tensor $\boldsymbol{\Omega}$ in equation (3.73) identifies the skew-symmetric *spin tensor* defined as

$$\boldsymbol{\Omega} = \dot{\mathbf{Q}}^T \cdot \mathbf{Q} = -\mathbf{Q}^T \cdot \dot{\mathbf{Q}} = -\boldsymbol{\Omega}^T \quad . \tag{3.75}$$

Therewith, the corotating frame may implicitly be defined. This definition is based on a given spin tensor $\boldsymbol{\Omega}$, along with a solution of the initial value problem

$$\dot{\mathbf{Q}} = -\mathbf{Q} \cdot \boldsymbol{\Omega} \quad \text{with} \quad \mathbf{Q}|_{t=0} = \mathbf{I} \tag{3.76}$$

(see equations (3.63) and (3.60₂)). The specification of $\boldsymbol{\Omega}$ is by no means arbitrary, i.e., it has to be ensured that the corotational rate of $\mathbf{A}$ is an objective second-order tensor. A suitable expression for $\boldsymbol{\Omega}$ accounting for this requirement is derived by Xiao et al. (1998a, 1998b). Motivated by the consideration that $\boldsymbol{\Omega}$ is related to the local deformation, the authors state that $\boldsymbol{\Omega}$ depends in a most general form on the deformation gradient $\mathbf{F}$ and on the velocity gradient $\mathbf{L}$, i.e.,

$$\boldsymbol{\Omega} = \boldsymbol{\Omega}(\mathbf{F}, \mathbf{L}) \quad , \tag{3.77}$$

both characterizing the local deformation state as well as its change rate, respectively. In this sense, $\boldsymbol{\Omega}$ is referred to as *material spin tensor* (see Xiao et al. (1997a)). On ensuring objectivity, $\boldsymbol{\Omega}$ then takes the form

$$\boldsymbol{\Omega} = \mathbf{W} + \boldsymbol{\Upsilon}(\mathbf{B}, \mathbf{D}) \quad , \tag{3.78}$$

where Υ denotes an isotropic skew-symmetric tensor-valued function depending on the left Cauchy-Green tensor $\mathbf{B}$ and on the stretching tensor $\mathbf{D}$. Υ is specifically continuous in $\mathbf{B}$. Then, on imposing necessary and reasonable physical constraints, followed by an application of the representation theorem for isotropic skew-symmetric tensor-valued functions given in, e.g., Wang (1970b) thereafter, Xiao et al. (1998a, 1998b) arrive at the expression

$$\Omega = \mathbf{W} + \sum_{i \neq j}^{\sigma} \tilde{h} \left(\frac{\chi_i}{\operatorname{tr}(\mathbf{B})}, \frac{\chi_j}{\operatorname{tr}(\mathbf{B})} \right) \mathbf{B}_i \cdot \mathbf{D} \cdot \mathbf{B}_j \quad . \tag{3.79}$$

The continuous function $\tilde{h}$ of positive real variables is referred to as *spin function*. It owns the property $\tilde{h}(x, y) = -\tilde{h}(y, x)$. Equation (3.79) describes a general family of possible and reasonable material spin tensors for which the corotational rate of a Eulerian tensor $\mathbf{A}$ is an objective quantity. Thus, together with (3.79), the corotational rate defined by (3.74) is objective.
A subclass of (3.79) including all known spin tensors as particular cases is given by

$$\Omega = \mathbf{W} + \sum_{i \neq j}^{\sigma} h \left(\frac{\chi_i}{\chi_j} \right) \mathbf{B}_i \cdot \mathbf{D} \cdot \mathbf{B}_j \quad , \tag{3.80}$$

where the property $h(z^{-1}) = -h(z)$ is assumed for the continuous function h. For instance, setting $h(z) = 0$ yields the *Zaremba-Jaumann rate*

$$\overset{\circ}{\mathbf{A}}{}^{\mathrm{J}} = \dot{\mathbf{A}} - \Omega^{\mathrm{J}} \cdot \mathbf{A} + \mathbf{A} \cdot \Omega^{\mathrm{J}} \quad \text{with} \quad \Omega^{\mathrm{J}} = \mathbf{W} \tag{3.81}$$

(see Zaremba (1903) and Jaumann (1911)). This rate was frequently used in constitutive theories until it turned out to provide an oscillatory stress response for simple shear tests at finite deformations (e.g., see Lehmann (1972), Dienes (1979), and Khan & Huang (1995)). In regard of this deficiency, numerous alternative corotational rates have been established (cf. Xiao et al. (2000)). Among these is the *polar rate* or *Green-Naghdi rate*

$$\overset{\circ}{\mathbf{A}}{}^{\mathrm{R}} = \dot{\mathbf{A}} - \Omega^{\mathrm{R}} \cdot \mathbf{A} + \mathbf{A} \cdot \Omega^{\mathrm{R}} \quad \text{with} \quad \Omega^{\mathrm{R}} = \dot{\mathbf{R}} \cdot \mathbf{R}^{\mathrm{T}} \tag{3.82}$$

(e.g., see Green & Naghdi (1965) and Green & McInnis (1967)), which can be obtained on selecting

$$h(z) = \frac{1 - \sqrt{z}}{1 + \sqrt{z}} \quad . \tag{3.83}$$

By contrast, it may be inferred from equations (3.75) and (3.82$_2$) that the corotating frame of the Green-Naghdi rate is defined by $\mathbf{R}^{\mathrm{T}}$. Special attention in this treatise is on the choice

$$h(z) = \frac{1 + \sqrt{z}}{1 - \sqrt{z}} + \frac{2}{\ln(z)} \tag{3.84}$$

which leads to the *logarithmic rate*

$$\overset{\circ}{\mathbf{A}}{}^{\mathrm{Log}} = \dot{\mathbf{A}} - \mathbf{\Omega}^{\mathrm{Log}} \cdot \mathbf{A} + \mathbf{A} \cdot \mathbf{\Omega}^{\mathrm{Log}} \tag{3.85}$$

defined by the *logarithmic spin tensor* $\mathbf{\Omega}^{\mathrm{Log}}$

$$\mathbf{\Omega}^{\mathrm{Log}} = \mathbf{W} + \sum_{i \neq j}^{\sigma} \left(\frac{1 + (\chi_i/\chi_j)}{1 - (\chi_i/\chi_j)} + \frac{2}{\ln(\chi_i/\chi_j)} \right) \mathbf{B}_i \cdot \mathbf{D} \cdot \mathbf{B}_j \tag{3.86}$$

(see Lehmann et al. (1991), Reinhardt & Dubey (1995, 1996) and Xiao et al. (1997b)). The unique property of this rate is demonstrated by Xiao et al. (1997b) in relating an arbitrary Eulerian strain measure $\mathbf{e}^{(m)}$ defined in (3.25) with the stretching tensor $\mathbf{D}$ by means of a corotational rate. The authors show that a solution of the corresponding linear tensor equation

$$\overset{\circ}{\mathbf{e}}{}^{(m)} = \dot{\mathbf{e}}^{(m)} - \mathbf{\Omega} \cdot \mathbf{e}^{(m)} + \mathbf{e}^{(m)} \cdot \mathbf{\Omega} \overset{!}{=} \mathbf{D} \tag{3.87}$$

only exists if the Eulerian strain measure $\mathbf{e}^{(m)}$ is identical to the Eulerian Hencky strain tensor $\mathbf{h}$

$$\mathbf{e}^{(m)} \overset{!}{=} \mathbf{h} \quad . \tag{3.88}$$

It then turns out that $\mathbf{\Omega}^{\mathrm{Log}}$ is the unique solution of (3.87) for $\mathbf{\Omega}$ (cf. Xiao et al. (1997b, 1998a, 1998b)). Strictly speaking, the logarithmic rate of the Eulerian Hencky strain tensor equals the stretching tensor

$$\overset{\circ}{\mathbf{h}}{}^{\mathrm{Log}} = \dot{\mathbf{h}} - \mathbf{\Omega}^{\mathrm{Log}} \cdot \mathbf{h} + \mathbf{h} \cdot \mathbf{\Omega}^{\mathrm{Log}} = \mathbf{D} \quad , \tag{3.89}$$

and it is only the logarithmic rate among all corotational rates showing this property. The stretching tensor can, thus, be regarded as *rate* of the Eulerian Hencky strain tensor in terms of the logarithmic rate. Note that this result is not in contradiction with (3.70), since both assignments rely on different types of objective rates, i.e., on corotational and non-corotational rates.

The time integration of the corotational rate of an objective Eulerian tensor on the basis of the generalized objective time integration (3.65) requires the evaluation of the corotating frame. This may be achieved by solving the initial value problem (3.76), which particularly takes the form

$$\dot{\mathbf{R}}^{\mathrm{Log}} = -\mathbf{R}^{\mathrm{Log}} \cdot \mathbf{\Omega}^{\mathrm{Log}} \quad \text{with} \quad \mathbf{R}^{\mathrm{Log}}|_{t=0} = \mathbf{I} \tag{3.90}$$

with $\mathbf{R}^{\mathrm{Log}}$ denoting the logarithmic rotation tensor. The *corotational integration* then reads (see Khan & Huang (1995))

$$\mathbf{A} = (\mathbf{R}^{\mathrm{Log}})^{\mathrm{T}} \star \int_t \mathbf{R}^{\mathrm{Log}} \star \overset{\circ}{\mathbf{A}}{}^{\mathrm{Log}} dt \quad . \tag{3.91}$$

4 Continuum thermodynamics

The kinematics and statics of a deforming body regarded in the previous chapter have to be complemented by thermodynamics to provide a physically consistent framework in which general material laws can be formulated. More precisely, quantities are introduced in Chapter 3 describing the mechanical state of continuous material bodies, i.e., the local deformation state as well as the local stress state, which must obey physically reasonable universal rules under given conditions. These rules are imposed by thermodynamics. They are regarded in this chapter, which is organized as follows: In Section 4.1, basic concepts of thermodynamics are considered which are used throughout this treatise and fundamental theories concerning equilibrium and non-equilibrium thermodynamics are discussed. Section 4.2 addresses general balance relations of thermodynamics which have to be obeyed by the material model developed in Chapter 5. This is followed by a conjugated work analysis in Section 4.3 to relate the stress and strain measures with each other which are considered in Chapter 3. In Section 4.4, the formalism of rational thermodynamics ensuring a thermodynamically consistent development of material laws is presented. Focus is on the Eulerian framework in which the constitutive equations are later formulated. The chapter closes with the derivation of a rate equation for the thermomechanical coupling of general deformation processes.

4.1 Introduction

The introduction of a *thermodynamic system* and its *environment* proves eminent in the thermodynamic analysis of physical processes. Geometrically, a thermodynamic system is defined by a region in space named *control volume*. The region outside the control volume is considered as *environment*. Both, thermodynamic system and environment interact with each other, which may be reflected by the following basic classification of thermodynamic systems:

1. *Open systems* may exchange energy and matter with their environment.

2. *Closed systems* may exchange energy but no matter with their environment.

3. *Isolated systems* do not exchange any energy or matter with their environment.

The thermodynamic analysis in classical continuum mechanics is usually concerned with deformable bodies obeying the continuum hypothesis. In this regard, the control volume of the thermodynamic system is often defined as at least a subdomain of the geometric representation in space of the body at

issue. Since any exchange of matter between the system and its environment is ruled out, the type of thermodynamic system is classically restricted to closed systems.

Besides the control volume, *state variables* are major components in the definition of a thermodynamic system (see Kuiken (1994)). They may be interpreted as *thermodynamic coordinates* of the system characterizing its thermodynamic state in terms of the mechanical state as a whole, such as position in space or velocity, and the thermodynamical state, e.g., density, temperature or, stress. State variables can be classified into *extensive* and *intensive* quantities. Conceptually, *extensive* quantities are dependent on and *intensive* quantities are independent of the size of the thermodynamic system (cf. Honig (1999)). For instance, volume or mass represent extensive state variables, whereas stress or temperature are intensive state variables. An extensive quantity divided by the mass of the thermodynamic system is labeled *specific* (see the recommendations of Cohen & Giacomo (1987)). If the magnitudes of the state variables change, the thermodynamic system is said to undergo a *change of state*. Such a change may be induced by interactions between the system and its environment furnishing a *thermodynamic process*, i.e., a thermodynamic process reflects any process for which the state of the thermodynamic system changes significantly (cf. Hudson (1996)). A change of state is well-defined by the initial and final states of the system during a thermodynamic process and is, thus, path-independent. Contrarily, since a specific change of state can be reached by a series of different processes, a thermodynamic process is *path-dependent*. Moreover, although the final state of the system for a given process does generally not coincide with the initial state, the initial state can always be recovered by virtue of additional processes (see Planck (1897)). If the latter lead to a sustainable change within the environment of the system, the given process is termed *irreversible*, otherwise it is referred to as *reversible* (cf. Honig (1999)). Irreversibility is predominant in natural processes, whereas reversibility may be regarded as limiting case for idealized processes (see also Hudson (1996)).

A very particular state of a thermodynamic system represents the *equilibrium state*. A system is conceptually regarded to be in the state of equilibrium if the variation of its state variables is negligible in a suitable time period (cf. Honig (1999)). The equilibrium state is reached by virtue of internal relaxation processes initiating at the end of a given external process (see Baehr (2002)). If the external process proceeds with a velocity much smaller than the velocity of the internal relaxation processes, the resulting change of state can be regarded as a sequence of equilibrium states. In this case, the external process is said to be *quasi-static*. A general process, however, is a sequence of non-equilibrium states (cf. Callen (1960)) and is, thus, named *dynamic*. In this sense, the assumption of a quasi-static change of state may be considered as approximation. It also bears emphasis that reversible processes are quasi-

static, whereas quasi-static processes are not necessarily reversible (cf. Adkins (1983) and Kuiken (1994)). Only if no dissipative effects occur, a quasi-static process is reversible. Moreover, a state of equilibrium is not to be confused with the state the system takes for a stationary process. Although the state of the system within a stationary process remains constant, the system may be far from an equilibrium state. In this context, by interrupting the external process, the system attains an equilibrium by virtue of internal relaxation processes.

In regard of a mathematical treatment of general thermodynamic processes, different thermodynamic frameworks have been established. One of these is the classical theory of *equilibrium thermodynamics* for which the system at issue is supposed to be in a global state of equilibrium (e.g., see Kuiken (1994)). Non-equilibrium processes are only qualitatively regarded, i.e., it is stated that they are irreversible. For natural processes, however, the assumption of a global equilibrium turns out to be too restrictive. In this context, the theory of *thermodynamics of irreversible processes* provides a first approach to *non-equilibrium thermodynamics*, extrapolating classical thermodynamics to irreversibility (e.g., see De Groot & Mazur (1963)). Thermodynamics of irreversible processes conceptually relies on the *principle of local equilibrium*, i.e., it is assumed that the state of the system is locally close to an equilibrium state, so that the relations of classical thermodynamics remain valid (see Kuiken (1994)). In contrast to classical equilibrium thermodynamics, however, the system is not supposed to be globally in a state of equilibrium. With this principle at hand, an evolution equation for the *entropy* as measure for the irreversibility of a given process can be derived. The production of entropy is particularly governed by conjugated thermodynamic forces and fluxes. While the known forces are functions of the current state of the thermodynamic system, the unknown fluxes are defined by phenomenological functions in this manner that the production of entropy vanishes for a global equilibrium state. The principle of local equilibrium may, however, also be too restrictive for a wide class of natural processes (cf. Müller (1985b)), although it can be considered as good assumption for slow processes. In this sense, thermodynamics of irreversible processes may be regarded as a first order theory (cf. Kuiken (1994)). The principle of local equilibrium is removed within the theory of *rational thermodynamics* (e.g., see Truesdell (1969)). This theory is principally based on the postulate of an evolution equation for the production of entropy named *Clausius-Duhem inequality*, which is used to derive equations for the thermodynamic state of the system. The postulation of the Clausius-Duhem inequality relies, however, on the definition of an entropy flux, which is only valid close to equilibrium. Thus, although the removal of the principle of local equilibrium within the theory of rational thermodynamics provides a step into the direction of proper non-equilibrium thermodynamics, this theory still cannot be regarded as general (cf. Müller (1985b)). Improvements of both

preceding non-equilibrium theories are given, for instance, by the theory of *extended irreversible thermodynamics* (see Jou et al. (1993)) and by the theory of *rational extended thermodynamics* (see Müller & Ruggeri (1998)). Compared to the unextended theories, the theoretical complexity of the extensions is significantly increased. In what follows, the theory of rational thermodynamics is assumed to be sufficiently accurate.

4.2 Balance equations

Physical quantities such as mass, momentum, energy, and entropy can be exchanged between a thermodynamic system and its environment across the boundaries of the system and directly into its interior (see Müller (1985b)). This exchange is mathematically reflected by thermodynamical *balance relations*. If a physical quantity cannot be created or destroyed within the thermodynamic system, it is specifically referred to a *conservative*, i.e., a conservative quantity remains constant, if its exchange between the thermodynamic system and the environment is interrupted. In this sense, the balance equations for conservative quantities are named *conservation laws*. This section provides an overview on the balance relations of continuum thermodynamics. A detailed review on this subject can be found in the works of Malvern (1969), Wang & Truesdell (1973), Marsden & Hughes (1983), Ogden (1984), Müller (1985b), Stein & Barthold (1996), Šilhavý (1997), Haupt (2000), and Truesdell & Noll (2004). Throughout this section, all derivations are based on the current configuration $\mathcal{B}_t$ of the body B. The considered thermodynamic system is defined as a subdomain $\mathcal{R}_t$ of $\mathcal{B}_t$, i.e., $\mathcal{R}_t \subseteq \mathcal{B}_t$, with boundary or surface $\partial \mathcal{R}_t$.

4.2.1 Balance of mass

The *total mass* $m(t)$ of the subdomain $\mathcal{R}_t$ can be obtained from

$$m = \int_{\mathcal{R}_t} \rho \, \mathrm{d}v \quad , \tag{4.1}$$

with the *mass density* $\rho\left(\mathbf{x}, t\right) \geq 0$ in the current configuration of the body B. Since m is a conservative quantity and $\mathcal{R}_t$ represents a closed system, such that any external supply of mass is excluded, m remains constant throughout a process of deformation and, thus, its material time derivative vanishes

$$\dot{m} = \frac{\mathrm{d}m}{\mathrm{d}t} = 0 \quad . \tag{4.2}$$

Equation (4.2) represents the global form of the *balance of mass* also known as *continuity equation*. It can be recast into

$$\dot{m} = \int_{\mathcal{R}_t} \left[\dot{\rho} + \rho \operatorname{tr}\left(\mathbf{D}\right) \right] \mathrm{d}v = 0 \tag{4.3}$$

by transforming (4.1) through (3.12) into the time-independent reference configuration, along with the relation

$$\dot{J} = J \operatorname{tr}(\mathbf{D}) \quad . \tag{4.4}$$

The global form of the balance of mass holds true for every chosen subdomain $\mathcal{R}_t \subseteq \mathcal{B}_t$. Thus, on stipulating that the integrand in (4.3) is continuous in $\mathbf{x}$, the local form of the balance of mass becomes

$$\dot{\rho} + \rho \operatorname{tr}(\mathbf{D}) = 0 \quad , \tag{4.5}$$

or, equivalently,

$$(\rho J)^{\cdot} = 0 \quad . \tag{4.6}$$

4.2.2 Balance of linear momentum

The conservative quantity $\mathbf{I}(t)$ of subdomain $\mathcal{R}_t$ defined as

$$\mathbf{I} = \int_{\mathcal{R}_t} \mathbf{v} \, dm = \int_{\mathcal{R}_t} \mathbf{v} \, \rho \, dv \tag{4.7}$$

is referred to as *linear momentum*. Its material time derivative reflects the rate at which the linear state of motion of $\mathcal{R}_t$ changes (see Haupt (2000)). In agreement with the global form of the *balance of linear momentum* termed *Euler's first law of motion*

$$\dot{\mathbf{I}} = \frac{d\mathbf{I}}{dt} = \mathbf{F} \quad , \tag{4.8}$$

this change rate is only affected by the resultant applied force $\mathbf{F}$ the thermodynamic system is exposed to. As indicated in Figure 4.1, the force $\mathbf{F}$ may be attributed to external forces $\bar{\mathbf{F}}_i$ acting on the surface $\partial \mathcal{B}_t$ of the body B and to internal *volume force densities* $\rho \, \mathbf{b}(\mathbf{x}, t)$ acting on each particle P within the volume $\mathcal{B}_t$ of the body B. In particular, with the considerations of Section 3.3 at hand, these applied forces lead to the force densities $\mathbf{t}$ and $\rho \, \mathbf{b}$ acting on the thermodynamic system. In this regard, $\mathbf{F}$ can additively be decomposed as

$$\mathbf{F} = \mathbf{F}_a + \mathbf{F}_v \tag{4.9}$$

into a resultant applied surface force

$$\mathbf{F}_a = \int_{\partial \mathcal{R}_t} \mathbf{t} \, da = \int_{\mathcal{R}_t} \nabla \cdot \boldsymbol{\sigma} \, dv \tag{4.10}$$

expressing the integrated surface force densities **t** and into a resultant applied volume force

$$\mathbf{F_v} = \int\limits_{\mathcal{R}_t} \mathbf{b}\, dm = \int\limits_{\mathcal{R}_t} \mathbf{b}\, \rho\, dv \qquad (4.11)$$

arising from the integrated volume force densities $\rho\, \mathbf{b}$. In relation (4.10), Cauchy's theorem is used and the divergence theorem is applied thereafter. Equations (4.8) and (4.9) reflect the nature of **I** as conservative quantity, i.e., **I** only changes with a supply of linear momentum through the boundaries of $\mathcal{R}_t$ as well as into its interior, expressed by $\mathbf{F_a}$ and $\mathbf{F_v}$. It bears emphasis that surface and volume torque densities are excluded in Figure 4.1. This assumption is sometimes referred to as *Boltzmann's theorem*. Moreover, (4.8)
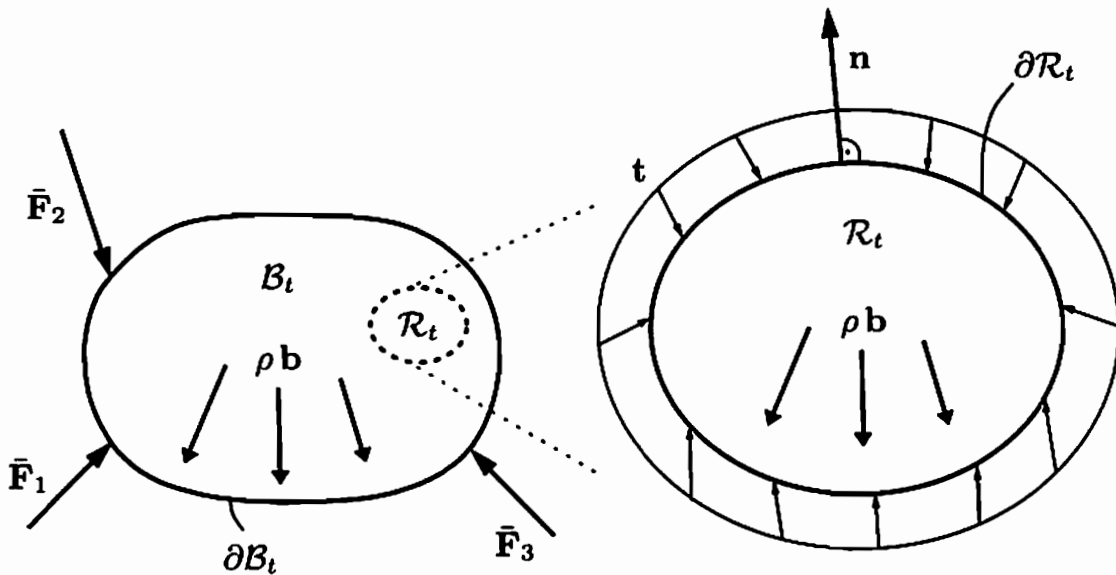

Figure 4.1: Forces acting on the current configuration $\mathcal{B}_t$ of the body B as well as on the (magnified) subdomain $\mathcal{R}_t \subseteq \mathcal{B}_t$

is based on the existence of an *inertial frame of reference*, i.e., on a frame of reference in which **I** is constant for vanishing force **F** (cf. Ogden (1984)).
With equations (4.7) to (4.11), in conjunction with the continuity equation (4.6), the balance of linear momentum takes the form

$$\int\limits_{\mathcal{R}_t} \dot{\mathbf{v}}\, \rho\, dv = \int\limits_{\mathcal{R}_t} [\nabla \cdot \boldsymbol{\sigma} + \rho\, \mathbf{b}]\, dv \quad . \qquad (4.12)$$

On stipulating that this equation is valid for arbitrary subdomains $\mathcal{R}_t \subseteq \mathcal{B}_t$ and that the integrand is continuous in **x**, the local form of the balance of linear momentum named *Cauchy's first law of motion* becomes

$$\dot{\mathbf{v}}\, \rho = \nabla \cdot \boldsymbol{\sigma} + \rho\, \mathbf{b} \quad . \qquad (4.13)$$

4.2.3   Balance of angular momentum

The *angular momentum* $\mathbf{H}^0(t)$ of subdomain $\mathcal{R}_t$ defined as

$$\mathbf{H}^0 = \int\limits_{\mathcal{R}_t} \left(\mathbf{x} - \mathbf{x}^0\right) \times \mathbf{v}\,\rho\,dv \tag{4.14}$$

is a conservative quantity, expressing the rotational state of motion of $\mathcal{R}_t$ about an arbitrary position $\mathbf{x}^0$ within the Euclidean space. According to the global form of the *balance of angular momentum* referred to as *Euler's second law of motion*, the material time derivative of $\mathbf{H}^0$ equals the resultant applied *moment* or *torque* $\mathbf{M}^0$ the domain $\mathcal{R}_t$ is subjected to with respect to $\mathbf{x}^0$

$$\dot{\mathbf{H}}^0 = \frac{d\mathbf{H}^0}{dt} = \mathbf{M}^0 \quad . \tag{4.15}$$

In line with Boltzmann's theorem stated previously, the resultant applied torque solely arises from the surface and volume force densities which act on the subdomain. Thus, similar to the resultant applied force, the resultant applied torque can be split as

$$\mathbf{M}^0 = \mathbf{M}_a^0 + \mathbf{M}_v^0 \tag{4.16}$$

into a part

$$\mathbf{M}_a^0 = \int\limits_{\partial\mathcal{R}_t} \left(\mathbf{x} - \mathbf{x}^0\right) \times \mathbf{t}\,da \tag{4.17}$$

and into a part

$$\mathbf{M}_v^0 = \int\limits_{\mathcal{R}_t} \left(\mathbf{x} - \mathbf{x}^0\right) \times \mathbf{b}\,dm = \int\limits_{\mathcal{R}_t} \left(\mathbf{x} - \mathbf{x}^0\right) \times \mathbf{b}\,\rho\,dv \quad . \tag{4.18}$$

$\mathbf{M}_a^0$ results from the surface force densities $\mathbf{t}$ and $\mathbf{M}_v^0$ accounts for the volume force densities $\rho\,\mathbf{b}$. With the rate form of (4.14), the balance of angular momentum can then be written as

$$\int\limits_{\mathcal{R}_t} \left(\mathbf{x} - \mathbf{x}^0\right) \times \dot{\mathbf{v}}\,\rho\,dv = \int\limits_{\partial\mathcal{R}_t} \left(\mathbf{x} - \mathbf{x}^0\right) \times \mathbf{t}\,da + \int\limits_{\mathcal{R}_t} \left(\mathbf{x} - \mathbf{x}^0\right) \times \mathbf{b}\,\rho\,dv \quad . \tag{4.19}$$

Replacing $\dot{\mathbf{v}}\,\rho$ by Cauchy's first law of motion, substituting Cauchy's theorem for $\mathbf{t}$, and applying the divergence theorem thereafter yields

$$\int\limits_{\mathcal{R}_t} \mathbf{I} \times \boldsymbol{\sigma}\,dv = \mathbf{0} \quad . \tag{4.20}$$

On stipulating arbitrariness of $\mathcal{R}_t \subseteq \mathcal{B}_t$ and continuity of the integrand, the local form of the balance of angular momentum labeled *Cauchy's second law of motion* can be deduced as

$$\mathbf{I} \times \boldsymbol{\sigma} = \mathbf{0} \quad , \tag{4.21}$$

which can only be fulfilled in general if

$$\boldsymbol{\sigma} = \boldsymbol{\sigma}^{\mathrm{T}} \quad . \tag{4.22}$$

In other words, the balance of angular momentum together with Boltzmann's theorem impose the symmetry of the Cauchy stress tensor.

4.2.4   Balance of energy

The *total energy* $E(t)$ of subdomain $\mathcal{R}_t$ comprises an *internal energy* $U(t)$ as well as a *kinetic energy* $K(t)$ as

$$E = U + K \quad . \tag{4.23}$$

With the specific internal energy $u(\mathbf{x}, t)$, the internal energy becomes

$$U = \int_{\mathcal{R}_t} u \, dm = \int_{\mathcal{R}_t} u \, \rho \, dv \quad , \tag{4.24}$$

whereas the kinetic energy may be written in terms of the velocity as

$$K = \frac{1}{2} \int_{\mathcal{R}_t} \mathbf{v} \cdot \mathbf{v} \, dm = \frac{1}{2} \int_{\mathcal{R}_t} \mathbf{v} \cdot \mathbf{v} \, \rho \, dv \quad . \tag{4.25}$$

E is a conservative quantity in contrast to its components U and K. More precisely, U and K can be transformed into each other, i.e., they can be created or destroyed in this way that E remains constant.

In agreement with the global form of the *balance of total energy*, the total energy change of $\mathcal{R}_t$ equals the increments of heat and work exchanged between the subdomain and its environment during a given thermodynamic process. This is reflected by the rate equation

$$\dot{E} = P + Q \quad , \tag{4.26}$$

in which Q denotes the *heat power* and P expresses the *power of the generalized applied forces*. Note that the total energy is a *state variable* accounting for the thermodynamic state of $\mathcal{R}_t$, whereas heat and work are *process variables* (cf. Kuiken (1994)). The generalized applied forces may be attributed to electrical, magnetical, or mechanical forces. Among these, mechanical forces are usually subject to classical continuum mechanics. Therewith, and with respect to

Boltzmann's theorem stated in Section 4.2.2, the power of the applied forces becomes

$$P = \int_{\partial \mathcal{R}_t} \mathbf{v} \cdot \mathbf{t} \, da + \int_{\mathcal{R}_t} \mathbf{b} \cdot \mathbf{v}\rho \, dv = \int_{\mathcal{R}_t} [\nabla \cdot (\mathbf{v} \cdot \boldsymbol{\sigma}) + \mathbf{b} \cdot \mathbf{v}\rho] \, dv \quad . \quad (4.27)$$

In (4.27), Cauchy's theorem is used and the divergence theorem is applied to the surface integral thereafter. The exchange of heat represents an alternative form of energy transfer. More precisely, after an energy supply of the subdomain either as work or heat, the transferred energy is indistinguishable in its origin (cf. Callen (1960)). Accordingly, heat is like work divided within the theory of rational thermodynamics into surface and volume parts. This is schematically depicted in Figure 4.2, where the quantities $\bar{Q}_i$ exemplarily represent the heat supply through the surface of the body. The heat transfer across the boundaries of the subdomain is reflected by the heat flux $\mathbf{q}(\mathbf{x}, t)$, while the heat absorbed by each particle within the volume of the subdomain is represented by the heat source $r(\mathbf{x}, t)$ (see Truesdell & Toupin (1960) and Truesdell (1969)). The heat power supplied to the subdomain $\mathcal{R}_t$, thus, takes the form

$$Q = \int_{\partial \mathcal{R}_t} -\mathbf{q} \cdot \mathbf{n} \, da + \int_{\mathcal{R}_t} r \rho \, dv = \int_{\mathcal{R}_t} [-\nabla \cdot \mathbf{q} + r \rho] \, dv \quad . \quad (4.28)$$
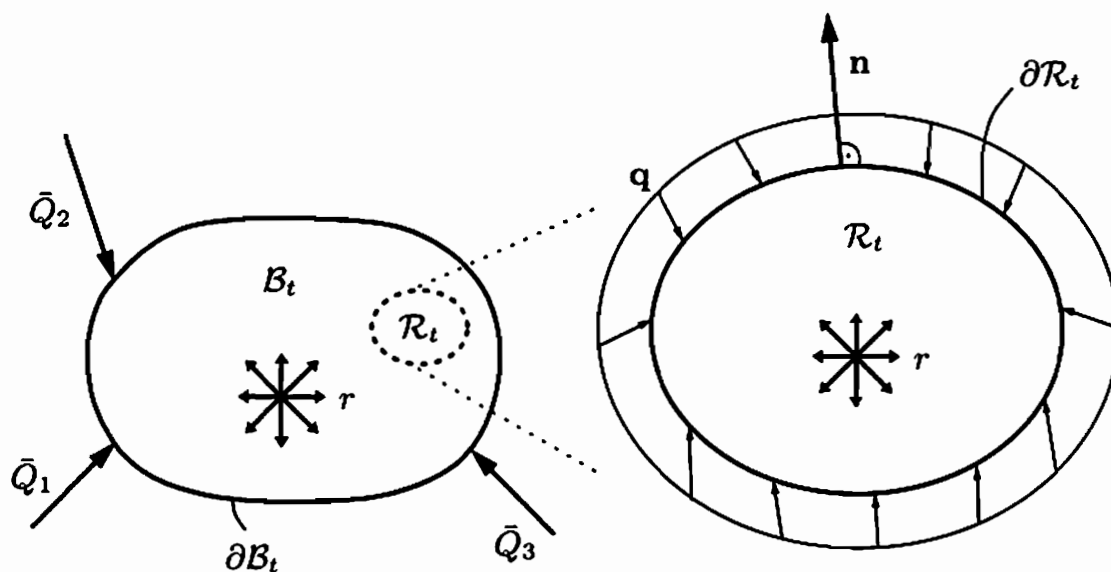

Figure 4.2: Heat supply of the current configuration $\mathcal{B}_t$ of the body B as well as of the (magnified) subdomain $\mathcal{R}_t \subseteq \mathcal{B}_t$

With the rate form of equations (4.23) to (4.25), together with (4.27) and (4.28), the balance of total energy (4.26) becomes

$$\int_{\mathcal{R}_t} [\dot{u} + \mathbf{v} \cdot \dot{\mathbf{v}}] \, \rho \, dv = \int_{\mathcal{R}_t} [\nabla \cdot (\mathbf{v} \cdot \boldsymbol{\sigma}) + \mathbf{b} \cdot \mathbf{v}\rho - \nabla \cdot \mathbf{q} + r\,\rho] \, dv \quad . \quad (4.29)$$

Hence, on stipulating arbitrariness of $\mathcal{R}_t$ and continuity of the integrands with respect to $\mathbf{x}$, the local form of the balance of total energy reads

$$[\dot{u} + \mathbf{v} \cdot \dot{\mathbf{v}}] \, \rho = \nabla \cdot (\mathbf{v} \cdot \boldsymbol{\sigma}) + \mathbf{b} \cdot \mathbf{v}\rho - \nabla \cdot \mathbf{q} + r\rho \quad . \quad (4.30)$$

The balance of energy is often termed *first law of thermodynamics*. Like the total energy, it can be split into an internal and an external balance, as subsequently demonstrated. However, the resulting balance equations do not represent conservation laws due to the non-conservative character of the internal energy U and the kinetic energy K.

Balance of internal energy

By expanding the term $\nabla \cdot (\mathbf{v} \cdot \boldsymbol{\sigma})$ and by using Cauchy's first law of motion, along with the relation $\mathbf{D} = 1/2 \, (\nabla\mathbf{v} + (\nabla\mathbf{v})^{\mathrm{T}})$, equation (4.29) can be recast into the global form of the *balance of internal energy*

$$\int_{\mathcal{R}_t} \dot{u} \, \rho \, dv = \int_{\mathcal{R}_t} [\boldsymbol{\sigma} : \mathbf{D} - \nabla \cdot \mathbf{q} + r\rho] \, dv \quad . \quad (4.31)$$

As this equation balances the internal energy rate, the term $\boldsymbol{\sigma} : \mathbf{D}$ may be considered as internal part of the specific power of the applied forces. In this sense, P may additively be decomposed as

$$P = P_{\mathrm{i}} + P_{\mathrm{e}} \quad (4.32)$$

into an internal part P_{i} and into a remaining, external part P_{e} with

$$P_{\mathrm{i}} = \int_{\mathcal{R}_t} \boldsymbol{\sigma} : \mathbf{D} \, dv \quad \text{and} \quad P_{\mathrm{e}} = \int_{\mathcal{R}_t} [\mathbf{v} \cdot (\nabla \cdot \boldsymbol{\sigma}) + \mathbf{b} \cdot \mathbf{v}\rho] \, dv \quad . \quad (4.33)$$

P_{i} expresses a production or destruction of internal energy and, thus, reflects that U is a non-conservative quantity (cf. Müller (1985b)). For a general thermodynamic process comprising reversible and irreversible deformations, it may additionally be split into a reversible part $P_{\mathrm{i}}^{\mathrm{rev}}$ and into an irreversible part $P_{\mathrm{i}}^{\mathrm{irr}}$ as

$$P_{\mathrm{i}} = P_{\mathrm{i}}^{\mathrm{rev}} + P_{\mathrm{i}}^{\mathrm{irr}} \quad (4.34)$$

(cf. Lehmann (1974, 1984)), with

$$P_i^{rev} = \int_{\mathcal{R}_t} \boldsymbol{\sigma} : \mathbf{D}^{rev}\, dv \quad \text{and} \quad P_i^{irr} = \int_{\mathcal{R}_t} \boldsymbol{\sigma} : \mathbf{D}^{irr}\, dv \quad . \tag{4.35}$$

It may further be assumed for an elastic-inelastic deformation process that the reversible stretching tensor $\mathbf{D}^{rev}$ and the irreversible stretching tensor $\mathbf{D}^{irr}$ arise from elastic and inelastic deformations, respectively. Then, on stipulating that $\mathbf{D}^{rev} = \mathbf{D}^{el}$ and $\mathbf{D}^{irr} = \mathbf{D}^{in}$, relations (4.34) and (4.35) furnish an additive decomposition of $\mathbf{D}$ as

$$\mathbf{D} = \mathbf{D}^{rev} + \mathbf{D}^{irr} = \mathbf{D}^{el} + \mathbf{D}^{in} \quad . \tag{4.36}$$

Finally, as $\mathcal{R}_t$ may arbitrarily be chosen, the corresponding local form of the balance of internal energy reads

$$\dot{u}\rho = \boldsymbol{\sigma} : \mathbf{D} - \nabla \cdot \mathbf{q} + r\rho \quad . \tag{4.37}$$

Balance of mechanical energy

Equation (4.26) balances all energetic quantities exchanged between the subdomain and its environment. On focusing only on *external* or *mechanical* quantities, the global form of the *balance of mechanical energy* becomes

$$\dot{K} = P_e \quad . \tag{4.38}$$

With the rate form of (4.25), together with (4.33$_2$), this leads to

$$\int_{\mathcal{R}_t} \mathbf{v} \cdot \dot{\mathbf{v}}\rho\, dv = \int_{\mathcal{R}_t} [\mathbf{v} \cdot (\nabla \cdot \boldsymbol{\sigma}) + \mathbf{b} \cdot \mathbf{v}\rho]\, dv \quad . \tag{4.39}$$

It may be inferred that the mechanical energy balance can alternatively be obtained by taking the difference between the total energy balance and the internal energy balance as in equations (4.29) and (4.31), as well as by multiplying Cauchy's first law of motion with the velocity $\mathbf{v}$ followed by an integration over $\mathcal{R}_t$. Relation (4.39) can be recast into the well-known form

$$\int_{\partial \mathcal{R}_t} \mathbf{v} \cdot \mathbf{t}\, da + \int_{\mathcal{R}_t} \mathbf{b} \cdot \mathbf{v}\rho\, dv = \int_{\mathcal{R}_t} \mathbf{v} \cdot \dot{\mathbf{v}}\rho\, dv + \int_{\mathcal{R}_t} \boldsymbol{\sigma} : \mathbf{D}\, dv \quad , \tag{4.40}$$

which balances the power of the applied forces with the rate of the kinetic energy and the power of the internal forces. Its corresponding local form may be written as

$$\nabla \cdot (\mathbf{v} \cdot \boldsymbol{\sigma}) + \mathbf{b} \cdot \mathbf{v}\rho = \mathbf{v} \cdot \dot{\mathbf{v}}\rho + \boldsymbol{\sigma} : \mathbf{D} \quad . \tag{4.41}$$

4.2.5 Balance of entropy

While the first law of thermodynamics expresses a general interconvertibility of total energy, work, and heat, natural processes show that the transformation direction of these quantities is restricted by a certain asymmetry. For instance, heat can only be transferred from warm to cold, whereas the reverse transformation is impossible without any compensation. Thus, in the sense of Section 4.1, the exchange of heat represents an irreversible process. The transformation asymmetry of energetic quantities and in turn the resulting irreversibility of natural processes is reflected by the *second law of thermodynamics*.

Fundamental work in the description of irreversible processes may be attributed to Clausius who studied the exchange of heat within Carnot cycles for thermodynamic systems with homogeneous temperature distributions (e.g., see Truesdell (1969) and Müller (1985b)). It turned out that for purely reversible processes the quotient between the heat power transferred into the thermodynamic system and the respective system temperature furnishes a new quantity that Clausius termed *entropy*.[14] Clausius extended his analysis to irreversible processes thereafter and stated that, in this case, the rate of entropy cannot be smaller than the rate of entropy transferred into the system by heat. Obviously, since the system temperature is supposed to be homogeneous, the approach of Clausius cannot account for irreversible effects due to heat conduction within the system. This deficiency is removed within the theory of rational thermodynamics in which the idea of Clausius is extended in this way, that a *local* entropy supply by heat is regarded (see Truesdell & Toupin (1960)). This leads to the inequality

$$\dot{S} \geq \int_{\partial \mathcal{R}_t} -\frac{\mathbf{q} \cdot \bar{\mathbf{n}}}{\Theta} \, da + \int_{\mathcal{R}_t} \frac{r}{\Theta} \rho \, dv \qquad (4.42)$$

which represents the global form of the *Clausius-Duhem inequality* (see Coleman & Noll (1963)). $S(t)$ and $\Theta(\mathbf{x}, t) \geq 0$ denote the entropy and the absolute (local) temperature. The definition of a non-negative temperature is sometimes referred to as *zeroth law of thermodynamics*. The Clausius-Duhem inequality reduces for a homogeneous temperature distribution to the *Clausius-Planck inequality* (cf. Truesdell & Noll (2004)). Moreover, for a reversible process, the Clausius-Duhem inequality yields the *Gibbs equation* known from thermostatics. Note that, although the transferred heat is a process variable, the entropy is a state variable being independent of the process path (cf. Müller (1985b)).

---

[14] The notion of entropy according to Clausius is based on the comparison of two equilibrium states at the beginning and at the end of a thermodynamic process. In this regard, the definition of the entropy rate as heat power divided by temperature is only valid close to equilibrium (e.g., see Müller (1985b, 1998) and Jou et al. (1993)).

By introducing the quantity $S^{\mathrm{rev}}(t)$ through

$$\dot{S}^{\mathrm{rev}} = \int_{\partial \mathcal{R}_t} -\frac{\mathbf{q} \cdot \bar{\mathbf{n}}}{\Theta} \, da + \int_{\mathcal{R}_t} \frac{r}{\Theta} \rho \, dv \tag{4.43}$$

together with the non-negative quantity $S^{\mathrm{irr}}(t)$ as

$$\dot{S}^{\mathrm{irr}} = \dot{S} - \dot{S}^{\mathrm{rev}} \geq 0 \quad , \tag{4.44}$$

the Clausius-Duhem inequality may be rewritten as the global form of the *balance of entropy*

$$\dot{S} = \dot{S}^{\mathrm{rev}} + \dot{S}^{\mathrm{irr}} \quad . \tag{4.45}$$

It shows that the rate of entropy is governed by two factors, i.e., by the exchange of entropy across the boundaries and into the interior of $\mathcal{R}_t$ expressed by $\dot{S}^{\mathrm{rev}}$, and by the production of entropy inside the system arising from irreversible processes reflected by $\dot{S}^{\mathrm{irr}}$. In this regard, the entropy is not a conservative quantity. Only in the case of pure reversibility for which $\dot{S}^{\mathrm{irr}}$ vanishes, S may be regarded as conservative.

With the introduction of the specific quantities $s(\mathbf{x}, t)$ and $s^{\mathrm{irr}}(\mathbf{x}, t)$, and after applying the divergence theorem and the continuity equation, the balance of entropy reads

$$\int_{\mathcal{R}_t} \dot{s} \rho \, dv = \int_{\mathcal{R}_t} \left[-\nabla \cdot \left(\frac{\mathbf{q}}{\Theta} \right) + \frac{r}{\Theta} \rho + \dot{s}^{\mathrm{irr}} \rho \right] dv \quad , \tag{4.46}$$

providing the local form

$$\dot{s} \rho = -\nabla \cdot \left(\frac{\mathbf{q}}{\Theta} \right) + \frac{r}{\Theta} \rho + \dot{s}^{\mathrm{irr}} \rho \quad . \tag{4.47}$$

Expanding the term $\nabla \cdot (\mathbf{q}/\Theta)$ and substituting the first law of thermodynamics (4.37) then yields

$$\Theta \dot{s} \rho = \frac{1}{\Theta} \mathbf{q} \cdot \nabla \Theta + \dot{u} \rho - \boldsymbol{\sigma} : \mathbf{D} + \Theta \dot{s}^{\mathrm{irr}} \rho \quad . \tag{4.48}$$

On this basis, the *dissipation function* $\mathcal{D}$ which reflects the uncompensated heat of irreversible processes can be defined as

$$\mathcal{D} = \Theta \dot{s}^{\mathrm{irr}} \rho \geq 0 \quad , \tag{4.49}$$

such that

$$\mathcal{D} = \boldsymbol{\sigma} : \mathbf{D} - \dot{u} \rho + \Theta \dot{s} \rho - \frac{1}{\Theta} \mathbf{q} \cdot \nabla \Theta \geq 0 \quad . \tag{4.50}$$

Equation (4.50) represents the local form of the Clausius-Duhem inequality. Accordingly, the local form of the Gibbs equation reads

$$\boldsymbol{\sigma} : \mathbf{D} - \dot{u}\rho + \Theta\dot{s}\rho = 0 \quad . \tag{4.51}$$

In line with Truesdell & Noll (2004) (see also Truesdell (1969)), a split of the local form of the Clausius-Duhem inequality may be postulated as

$$\mathcal{D} = \mathcal{D}_{\text{loc}} + \mathcal{D}_{\text{con}} \geq 0 \quad . \tag{4.52}$$

$\mathcal{D}_{\text{loc}}$ denotes the local form of the Clausius-Planck inequality expressing the local energy dissipation at constant temperature

$$\mathcal{D}_{\text{loc}} = \boldsymbol{\sigma} : \mathbf{D} - \dot{u}\rho + \Theta\dot{s}\rho \geq 0 \tag{4.53}$$

and $\mathcal{D}_{\text{con}}$ determines the local form of the *Fourier inequality* resulting from a convective energy dissipation in terms of thermal dissipations

$$\mathcal{D}_{\text{con}} = -\frac{1}{\Theta}\mathbf{q} \cdot \nabla\Theta \geq 0 \quad . \tag{4.54}$$

The latter inequality ensures the direction of the heat flow from warm to cold. The resolution above represents a stronger form of the Clausius-Duhem inequality. It is only valid if the local and convective dissipations are uncoupled (e.g., see Coleman & Gurtin (1967)).
It bears emphasis that the entropy cannot decrease for an adiabatic process for which a heat exchange between the thermodynamic system and its environment is inhibited, as it may be deduced from (4.42). In this case, the entropy is maximized in a state of equilibrium (see Müller (1985b)). Conversely, on rewriting (4.53)

$$\boldsymbol{\sigma} : \mathbf{D} + \Theta\dot{s}\rho \geq \dot{u}\rho \quad , \tag{4.55}$$

it may be inferred that the specific internal energy cannot increase for an isentropic process with constant entropy at constant deformations. In this context, the value of u in a state of equilibrium characterizes a minimum.

4.3   Stress power and conjugated work analysis

In Chapter 3, different measures of stress and strain are defined without relating these quantities to each other. With the results of Section 4.2.4, this is now complemented by adopting the formalism of the *conjugated work analysis* proposed by Hill (1968) (see also Macvean (1968) and Hill (1978)). An essential quantity therein is the *stress power* p_{i} defined as

$$p_{\text{i}} = \frac{1}{\rho}\boldsymbol{\sigma} : \mathbf{D} \quad . \tag{4.56}$$

It can be obtained from P_i introduced in (4.33$_1$) as

$$P_\mathrm{i} = \int\limits_{\mathcal{R}_t} \boldsymbol{\sigma} : \mathbf{D}\,\mathrm{d}v = \int\limits_{\mathcal{R}_t} p_\mathrm{i}\,\mathrm{d}m \quad . \tag{4.57}$$

Since $\boldsymbol{\sigma}$ and $\mathbf{D}$ constitute the stress power, the Cauchy stress tensor and the stretching tensor may be regarded as pair of energetically conjugated quantities. This assignment is, however, not unique, as the stress power may be formulated in different configurations (see Macvean (1968)). For instance, in regard of the stress tensors introduced in Section 3.3, p_i can be written as

$$p_\mathrm{i} = \frac{1}{\rho}\,\boldsymbol{\sigma} : \mathbf{D} = \frac{1}{\rho_0}\,\boldsymbol{\tau} : \mathbf{D} = \frac{1}{\rho_0}\,\mathbf{P} : \dot{\mathbf{F}} = \frac{1}{\rho_0}\,\mathbf{S} : \dot{\mathbf{E}} \quad , \tag{4.58}$$

providing additional pairs of conjugated quantities. Note that the conjugated stress of $\mathbf{D}$ may alternatively be $\boldsymbol{\sigma}$ or $\boldsymbol{\tau}$. This ambiguity can be resolved on substituting (4.58) into (4.57). It may be deduced that $\boldsymbol{\sigma}$ and $\mathbf{D}$ are conjugated with respect to an integration in the current configuration, while $\boldsymbol{\tau}$ and $\mathbf{D}$ form a conjugated pair for an integration in the reference configuration (cf. Malvern (1969)).

Kinematical tensors such as $\mathbf{D}$, $\dot{\mathbf{F}}$, or $\dot{\mathbf{E}}$ express the local shape change rate of the body. If one of these quantities equals the rate of a local deformation tensor, this tensor is said to be *work conjugated* to the respective conjugated stress tensor. Since a variety of objective rates within the Eulerian configuration exists, such an assignment may provide an additional unambiguity. For instance, the logarithmic rate of the Hencky strain tensor $\mathbf{h}$ as well as the Cotter-Rivlin rate of the Almansi-Eulerian strain tensor $\mathbf{e}$ equal the stretching tensor and, thus, $\mathbf{h}$ as well as $\mathbf{e}$ can be regarded as work conjugated to, both, $\boldsymbol{\tau}$ or $\boldsymbol{\sigma}$. In the Lagrangian configuration, however, for which the material time derivative is objective, the assignment of conjugated quantities is unique, such that $\mathbf{P}$ and $\mathbf{F}$ as well as $\mathbf{S}$ and $\mathbf{E}$ form conjugated pairs.

In what follows, in anticipation of the material model derived in Chapter 5, the Kirchhoff stress tensor $\boldsymbol{\tau}$ and its work conjugated Hencky strain tensor $\mathbf{h}$ are employed, along with the logarithmic rate as objective corotational time derivative. The balance equations of Section 4.2 are accordingly reformulated.

4.4 Thermodynamic consistency

The balance equations considered in Section 4.2 provide a general framework for the development of constitutive theories. Altogether, they basically require the following nine quantities to be specified for the description of a specific material behavior for each particle P of the body B at time t:[15]

---

[15] Note that the spatial position $\mathbf{x}$ renders the deformation gradient as well as the velocity gradient.

Spatial position	$\mathbf{x} = \mathbf{x}(P, t)$
Mass density	$\rho = \rho(P, t)$
Temperature	$\Theta = \Theta(P, t)$
Stress tensor	$\boldsymbol{\tau} = \boldsymbol{\tau}(P, t)$
Specific internal energy	$u = u(P, t)$
Specific entropy	$s = s(P, t)$
Force density	$\mathbf{b} = \mathbf{b}(P, t)$
Heat flux vector	$\mathbf{q} = \mathbf{q}(P, t)$
Heat source	$r = r(P, t)$

Such a specification is, however, not arbitrary as it has to ensure physical restrictions imposed by thermodynamics. A general procedure accounting for this essential aspect is provided by Coleman & Noll (1963). According to their formalism, a *thermodynamic process* is considered to be fully described by the above nine quantities, along with the balance equations of mass, momentum, and total energy.[16] This process is assumed to be driven by position $\mathbf{x}$ as well as entropy s as independent variables. Additionally, constitutive equations in form of *response functions* are introduced, specifying the four quantities temperature Θ, stress tensor $\boldsymbol{\tau}$, internal energy u, and heat flux vector $\mathbf{q}$. The remaining three quantities, i.e., density ρ, force density $\mathbf{b}$, and heat source r, are then uniquely determined by the continuity equation, Cauchy's first law of motion, and the first law of thermodynamics, as in relations (4.5), (4.13), and (4.37), respectively. The definitions of the constitutive equations for Θ, $\boldsymbol{\tau}$, $\mathbf{q}$, and u have to obey the following basic principles (e.g., see Wang & Truesdell (1973)):

1. Principle of determinism or alternatively principle of local action

2. Principle of equipresence

3. Principle of material frame indifference

The *principle of determinism* demands the response functions of a generic particle P at time t to depend on the current and past states of all particles defining the body during a process of deformation. This strict principle is usually replaced by the weaker *principle of local action*. It asserts that the constitutive equations for particle P at time t solely depend on the current and past states of the particles within the (local) neighborhood of P. A material body following the principle of local action is referred to as *simple body*. The *principle of equipresence* governs the independent variables of the constitutive equations. It states that the same independent variables should be present in all response functions, unless this does not lead to any contradiction with respect to material symmetry, material objectivity, or thermodynamic consistency (cf.

---

[16]Originally, Coleman & Noll do not consider the mass density as basic quantity.

Coleman & Noll (1964)). The *principle of material frame indifference* finally ensures the constitutive equations to be independent of the underlying frame of reference.

The dependence of the material behavior on the current and past thermodynamic states of the body may be interpreted as *memory*. This memory is said to be *fading* if the influence of past thermodynamic states decreases with increasing distance in time to the present thermodynamic state (see Coleman (1964) and Day (1972)). This particularly addresses internal relaxation processes which transfer the body from a non-equilibrium state to an equilibrium state (see Section 4.1), furnishing the theory of rational thermodynamics a non-equilibrium theory.

In Coleman & Gurtin (1967), the formalism above is extended by adding the following general set of tensorial variables to the thermodynamic framework:

$$\text{Set of internal variables} \quad \zeta = \zeta(P, t)$$

Its rate accounts for the change of the internal material structure during a deformation process. This may, for instance, result from the formation of dislocations due to plastic deformations, from viscosity, or from phase transformations. In contrast to quantities like density, temperature, or stress, the set of variables ζ can externally not be measured. In this sense, it is referred to as set of *internal variables*, whereas the former are termed *external variables* (cf. Lehmann (1989)).[17] Similar to the quantities Θ, τ, q, and u, a response function has to be defined for ζ.

A thermodynamic process is labeled *admissible* in agreement with Coleman & Noll (1963) if it is compatible with the constitutive equations for Θ, τ, q, and u, i.e., if it is reflected by the constitutive assumptions defining a specific material behavior. Then, by imposing the remaining entropy balance equation in form of the Clausius-Duhem inequality to hold true for all admissible thermodynamic processes, relations between the constitutive equations can be established. They show that the response functions are not independent of each other. This is considered next for two essential classes of materials.

Thermoelastic simple body

A widely used simple body material is a thermoelastic material. It may be defined in line with Coleman & Noll (1963) by the constitutive equations of the form:

$$
\begin{aligned}
u &= u\,(\mathbf{h}^{\text{el}}, s) \\
\tau &= \tau\,(\mathbf{h}^{\text{el}}, s) \\
\Theta &= \Theta(\mathbf{h}^{\text{el}}, s)
\end{aligned}
\tag{4.59}
$$

---

[17]Note that in classical thermodynamics *external state variables* are sometimes related to the external or mechanical state of the system as a whole, such as position in space or velocity, whereas *internal state variables* are associated with the internal or thermodynamical state of the system, e.g., density, temperature, or stress (see Kuiken (1994)).

In Coleman & Mizel (1964), this special kind of material is referred to as *perfect material* (see also Truesdell & Noll (2004)). $\mathbf{h}^{el}$ denotes the elastic Hencky strain tensor. It reflects that the total deformations of thermoelastic materials are purely elastic, i.e.,

$$\mathbf{h} = \mathbf{h}^{el} \quad . \tag{4.60}$$

As it may be inferred from equations (4.59), only the local deformation state and the local entropy affect the local response functions. This is in agreement with the principle of local action. The principle of equipresence is accounted for by selecting $\mathbf{h}^{el}$ and s as independent variables in all constitutive equations. The principle of material frame indifference may be satisfied by defining all response functions of the objective Eulerian second-order tensor $\mathbf{h}^{el}$ as isotropic tensor functions.[18]

The thermoelastic material defined by (4.59) does not include any memory, i.e., the state of each material particle is solely determined by the current state of this particle and its local neighborhood. Thus, in the sense of Section 4.1, a thermoelastic material is restricted to quasi-static processes for which it is in a state of equilibrium throughout the deformation process. Strictly speaking, internal relaxation processes transferring the material body from a non-equilibrium state to an equilibrium state proceed with unlimited velocity.

Application of the material time rate to the specific internal energy (4.59₁), along with the identity (3.89) between the logarithmic rate of the Hencky strain tensor and the stretching tensor, gives[19]

$$\dot{u} = \frac{\partial u}{\partial \mathbf{h}^{el}} : \mathbf{D}^{el} + \frac{\partial u}{\partial s} \dot{s} \quad . \tag{4.61}$$

Then, by replacing the Cauchy stress tensor with the Kirchhoff stress tensor, the local form of the Clausius-Duhem inequality (4.50) becomes

$$\mathcal{D} = \frac{\rho}{\rho_0} \left[\tau - \rho_0 \frac{\partial u}{\partial \mathbf{h}^{el}} \right] : \mathbf{D}^{el} + \rho \left[\Theta - \frac{\partial u}{\partial s} \right] \dot{s} \geq 0 \quad . \tag{4.62}$$

Since this inequality is assumed to hold true for all admissible processes, i.e., for all arbitrary admissible values of $\mathbf{h}^{el}$ and s as well as of $\mathbf{D}^{el}$ and $\dot{s}$, two equations of state can be deduced as

$$\tau = \rho_0 \frac{\partial u}{\partial \mathbf{h}^{el}} \quad \text{and} \quad \Theta = \frac{\partial u}{\partial s} \quad . \tag{4.63}$$

---

[18]A scalar-valued isotropic tensor function ϕ and a symmetric second-order tensor-valued isotropic tensor function $\boldsymbol{\phi}$, both depending on the objective Eulerian second-order tensor $\mathbf{A}$, possess the properties $\phi(\mathbf{Q} \star \mathbf{A}) = \phi(\mathbf{A})$ and $\boldsymbol{\phi}(\mathbf{Q} \star \mathbf{A}) = \mathbf{Q} \star \boldsymbol{\phi}(\mathbf{A})$, with $\mathbf{Q}$ denoting an arbitrary tensor of the special orthogonal group (e.g., see Wang (1970a)).

[19]This evaluation relies on the chain rule for scalar-valued isotropic tensor functions $\phi(\mathbf{A})$ of the form

$$\frac{d}{dt} \phi(\mathbf{A}) = \frac{d\phi}{d\mathbf{A}} : \dot{\mathbf{A}} = \frac{d\phi}{d\mathbf{A}} : \overset{\circ}{\mathbf{A}} \quad ,$$

which is holds true for arbitrary corotational rates $(\overset{\circ}{\cdot})$ (see Xiao et al. (1997a)).

They explicitly determine τ and Θ by the specific internal energy u. In this context, u is referred to as *thermodynamic potential.*

Substitution of equations (4.63) into the rate of the internal energy (4.61) reveals the Gibbs equation (4.51) in terms of the Kirchhoff stress tensor

$$\dot{u} = \frac{1}{\rho_0}\, \tau : \mathbf{D}^{\mathrm{el}} + \Theta\, \dot{s} \quad . \tag{4.64}$$

Hence, in addition to the observation that thermoelastic materials are restricted to quasi-static processes, these materials are also restricted to pure reversibility. This can also be observed by substituting relations (4.63) into the inequality (4.62), showing that the dissipation function vanishes. In this sense, the elastic stretching tensor in fact equals the reversible stretching tensor considered in (4.36).

In regard of the externally controllable variables within a thermodynamic process, the definition of other independent variables in relations (4.59) than $\mathbf{h}^{\mathrm{el}}$ and s may sometimes be convenient. Extending the right-hand side of (4.64) by the difference $1/\rho_0\, \mathbf{h}^{\mathrm{el}} : \overset{\circ}{\tau}{}^{\mathrm{Log}} - 1/\rho_0\, \mathbf{h}^{\mathrm{el}} : \overset{\circ}{\tau}{}^{\mathrm{Log}}$ yields after rearrangement[20]

$$\dot{h} = -\frac{1}{\rho_0}\, \mathbf{h}^{\mathrm{el}} : \overset{\circ}{\tau}{}^{\mathrm{Log}} + \Theta\, \dot{s} \quad , \tag{4.65}$$

with the thermodynamic potential

$$h(\tau,\, s) = u - \frac{1}{\rho_0}\, \tau : \mathbf{h}^{\mathrm{el}} \tag{4.66}$$

termed specific *enthalpy.* Then, with the internal energy and the enthalpy at hand, two additional potentials can be derived on replacing the entropy as independent variable by the temperature. Adding the difference $s\, \dot{\Theta} - s\, \dot{\Theta}$ to the right-hand side of relations (4.64) and (4.65) leads to

$$\dot{\psi} = \frac{1}{\rho_0}\, \tau : \mathbf{D}^{\mathrm{el}} - s\, \dot{\Theta} \tag{4.67}$$

and

$$\dot{g} = -\frac{1}{\rho_0}\, \mathbf{h}^{\mathrm{el}} : \overset{\circ}{\tau}{}^{\mathrm{Log}} - s\, \dot{\Theta} \quad , \tag{4.68}$$

with the specific *Helmholtz free energy*

$$\psi(\mathbf{h}^{\mathrm{el}},\, \Theta) = u - \Theta\, s \tag{4.69}$$

and the specific *Gibbs free energy*

$$g(\tau,\, \Theta) = h - \Theta\, s \quad . \tag{4.70}$$

---

[20]Note the identity $\dot{\tau} : \mathbf{h}^{\mathrm{el}} + \tau : \dot{\mathbf{h}}^{\mathrm{el}} = \overset{\circ}{\tau}{}^{\mathrm{Log}} : \mathbf{h}^{\mathrm{el}} + \tau : \overset{\circ}{\mathbf{h}}{}^{\mathrm{el\,Log}}$.

Thermodynamic potentials	Equations of state			
Internal energy $u(\mathbf{h}^{\mathrm{el}}, s)$	Θ	$= \dfrac{\partial u}{\partial s}$	τ	$= \rho_0 \dfrac{\partial u}{\partial \mathbf{h}^{\mathrm{el}}}$
Enthalpy $h(\tau, s)$	Θ	$= \dfrac{\partial h}{\partial s}$	$\mathbf{h}^{\mathrm{el}}$	$= -\rho_0 \dfrac{\partial h}{\partial \tau}$
Free energy $\psi(\mathbf{h}^{\mathrm{el}}, \Theta)$	s	$= -\dfrac{\partial \psi}{\partial \Theta}$	τ	$= \rho_0 \dfrac{\partial \psi}{\partial \mathbf{h}^{\mathrm{el}}}$
Free enthalpy $g(\tau, \Theta)$	s	$= -\dfrac{\partial g}{\partial \Theta}$	$\mathbf{h}^{\mathrm{el}}$	$= -\rho_0 \dfrac{\partial g}{\partial \tau}$

Table 4.1: Equations of state of the thermodynamic potentials

u, h, ψ, and g are equivalent representations of the stored energy in the material body. In this regard, equations (4.64), (4.65), (4.67), and (4.68) are equivalent representations of the Gibbs equation. Mathematically, the foregoing transformations are referred to as *Legendre transformations* (e.g., see Callen (1960)).

Equations of state for the additional thermodynamic potentials, namely the enthalpy, Helmholtz free energy, and Gibbs free energy, can be obtained by comparing the rates of these potentials with the respective forms of the Gibbs equation. The results are summarized in Table 4.1. For instance, matching the coefficients of the material time derivative of ψ

$$\dot{\psi} = \frac{\partial \psi}{\partial \mathbf{h}^{\mathrm{el}}} : \mathbf{D}^{\mathrm{el}} + \frac{\partial \psi}{\partial \Theta} \dot{\Theta} \tag{4.71}$$

with equation (4.67) gives

$$s = -\frac{\partial \psi}{\partial \Theta} \quad \text{and} \quad \tau = \rho_0 \frac{\partial \psi}{\partial \mathbf{h}^{\mathrm{el}}} \quad . \tag{4.72}$$

Furthermore, with the equations of state expressing the elastic strain or the stress, an explicit relation for the elastic stretching tensor may be derived. Taking the logarithmic rate of

$$\mathbf{h}^{\mathrm{el}} = -\rho_0 \frac{\partial g}{\partial \tau} \quad , \tag{4.73}$$

Thermodynamic potentials	Maxwell relations
Internal energy $u(\mathbf{h}^{el}, s)$	$\left.\dfrac{\partial \Theta}{\partial \mathbf{h}^{el}}\right|_{s} = \dfrac{1}{\rho_0}\left.\dfrac{\partial \tau}{\partial s}\right|_{\mathbf{h}^{el}}$
Enthalpy $h(\tau, s)$	$\left.\dfrac{\partial \Theta}{\partial \tau}\right|_{s} = -\dfrac{1}{\rho_0}\left.\dfrac{\partial \mathbf{h}^{el}}{\partial s}\right|_{\tau}$
Free energy $\psi(\mathbf{h}^{el}, \Theta)$	$-\left.\dfrac{\partial s}{\partial \mathbf{h}^{el}}\right|_{\Theta} = \dfrac{1}{\rho_0}\left.\dfrac{\partial \tau}{\partial \Theta}\right|_{\mathbf{h}^{el}}$
Free enthalpy $g(\tau, \Theta)$	$-\left.\dfrac{\partial s}{\partial \tau}\right|_{\Theta} = -\dfrac{1}{\rho_0}\left.\dfrac{\partial \mathbf{h}^{el}}{\partial \Theta}\right|_{\tau}$

Table 4.2: Maxwell relations of the thermodynamic potentials

together with relation (3.89), yields[21]

$$\mathbf{D}^{el} = \mathbb{D} : \overset{\circ}{\tau}{}^{\,\mathrm{Log}} + \boldsymbol{\alpha}\,\dot{\Theta} \quad . \tag{4.74}$$

$\mathbb{D}(\tau, \Theta)$ represents the elastic compliance tensor and $\boldsymbol{\alpha}(\tau, \Theta)$ denotes the tensor of thermal expansion coefficients, both defined as

$$\mathbb{D} = \left.\dfrac{\partial \mathbf{h}^{el}}{\partial \tau}\right|_{\Theta} \quad \text{and} \quad \boldsymbol{\alpha} = \left.\dfrac{\partial \mathbf{h}^{el}}{\partial \Theta}\right|_{\tau} \quad . \tag{4.75}$$

Adopting the preceding equations of state, four relations between the partial derivatives of the state variables named *Maxwell relations* can be derived on exploiting the identity of the mixed second derivatives of the thermodynamic potentials. They are listed in Table 4.2. For instance, the mixed second derivatives of the specific internal energy yield

$$\left.\dfrac{\partial \Theta}{\partial \mathbf{h}^{el}}\right|_{s} = \dfrac{\partial}{\partial \mathbf{h}^{el}}\left(\dfrac{\partial u}{\partial s}\right) = \dfrac{\partial}{\partial s}\left(\dfrac{\partial u}{\partial \mathbf{h}^{el}}\right) = \dfrac{1}{\rho_0}\left.\dfrac{\partial \tau}{\partial s}\right|_{\mathbf{h}^{el}} \quad . \tag{4.76}$$

---

[21] Use is made of the chain rule for symmetric second-order tensor-valued isotropic tensor functions $\phi(\mathbf{A})$ of the form

$$\dfrac{d}{dt}\,\phi(\mathbf{A}) = \dfrac{d\phi}{d\mathbf{A}} : \dot{\mathbf{A}} = \dfrac{d\phi}{d\mathbf{A}} : \overset{\circ}{\mathbf{A}} \quad ,$$

which is valid for arbitrary corotational rates $(\overset{\circ}{\cdot})$ (see Xiao et al. (1999)).

Thermoinelastic simple body with heat conduction

As the thermoelastic simple body material is restricted to pure reversibility, it cannot account for irreversible effects, such as plastic deformations, heat conduction, or phase transformations. Thus, with respect to the material model considered in Chapter 5, the thermoelastic simple body material has to be extended to irreversibility. In line with Coleman & Gurtin (1967), this may be achieved by defining internal variables and the heat flux as additional independent variables, such that the constitutive equations of a thermoinelastic simple body material with heat conduction become:[22]

$$
\begin{aligned}
\psi &= \psi(\mathbf{h}^{\text{el}}, \Theta, \zeta) \\
\tau &= \tau(\mathbf{h}^{\text{el}}, \Theta, \zeta) \\
s &= s(\mathbf{h}^{\text{el}}, \Theta, \zeta) \\
\mathbf{q} &= \mathbf{q}(\mathbf{h}^{\text{el}}, \Theta, \nabla\Theta, \zeta) \\
\zeta &= \zeta(\mathbf{h}^{\text{el}}, \Theta, \nabla\Theta, \zeta)
\end{aligned}
\tag{4.77}
$$

In anticipation of Chapter 5, the internal energy is replaced by the Helmholtz free energy, depending, in agreement with Lehmann (1984), on the purely elastic component of the total strain. This elastic strain may be understood as being directly related to the current stress (see Xiao et al. (2007)), e.g., for zero stress the elastic strain may vanish and vice versa. In this sense, stress, temperature, and elastic strain may be regarded as redundant quantities to some extent. A direct determination of the elastic strain from the total deformation, however, turns out to be cumbersome, if not even impossible, for an elastic-inelastic finite deformation process.[23] On this account, the elastic Hencky strain tensor in (4.77) is replaced by the Kirchhoff stress tensor, such that:

$$
\begin{aligned}
\psi &= \psi(\tau, \Theta, \zeta) \\
\mathbf{h} &= \mathbf{h}(\tau, \Theta, \zeta) \\
s &= s(\tau, \Theta, \zeta) \\
\mathbf{q} &= \mathbf{q}(\tau, \Theta, \nabla\Theta, \zeta) \\
\zeta &= \zeta(\tau, \Theta, \nabla\Theta, \zeta)
\end{aligned}
\tag{4.78}
$$

With this set of equations at hand, the Clausius-Duhem inequality can be exploited in the same way as for the thermoelastic material. On substituting the rate form of (4.69) and on replacing the Cauchy stress tensor with the Kirchhoff stress tensor thereafter, the local form of the Clausius-Duhem inequality (4.50) in terms of the Helmholtz free energy and the Kirchhoff stress tensor reads

$$
\mathcal{D} = \frac{\rho}{\rho_0}\,\tau : \mathbf{D} - \rho\left(\dot{\psi} + s\,\dot{\Theta}\right) - \frac{1}{\Theta}\,\mathbf{q}\cdot\nabla\Theta \geq 0 \quad .
\tag{4.79}
$$

---

[22] Alternatively to the introduction of internal variables, the entire deformation history of the body may be accounted for within the constitutive equations (see Coleman & Gurtin (1967)). This, however, may hardly be tractable for realistic purposes.

[23] See Xiao et al. (2006a) for a thorough discussion on this matter.

By virtue of the material time rate of (4.78_1)

$$\dot{\psi} = \frac{\partial \psi}{\partial \tau} : \overset{\circ}{\tau}^{\,\mathrm{Log}} + \frac{\partial \psi}{\partial \Theta} \dot{\Theta} + \frac{\partial \psi}{\partial \zeta} : \overset{\circ}{\zeta}^{\,\mathrm{Log}} \quad , \tag{4.80}$$

in conjunction with the additive decomposition of the stretching tensor as in (4.36) and the thermoelastic rate equation (4.74), equation (4.79) takes the form

$$\mathcal{D} = \frac{\rho}{\rho_0} \tau : \mathbf{D}^{\mathrm{in}} + \frac{\rho}{\rho_0} \left[\tau : \mathbb{D} - \rho_0 \frac{\partial \psi}{\partial \tau} \right] : \overset{\circ}{\tau}^{\,\mathrm{Log}}$$

$$- \rho \left[s + \frac{\partial \psi}{\partial \theta} - \frac{1}{\rho_0} \tau : \alpha \right] \dot{\Theta} - \rho \frac{\partial \psi}{\partial \zeta} : \overset{\circ}{\zeta}^{\,\mathrm{Log}} - \frac{1}{\Theta} \mathbf{q} \cdot \nabla \Theta \geq 0 \quad . \tag{4.81}$$

Assuming this inequality to hold true for all admissible processes then yields

$$\frac{\partial \psi}{\partial \Theta} = \frac{1}{\rho_0} \tau : \alpha - s \quad \text{and} \quad \frac{\partial \psi}{\partial \tau} = \frac{1}{\rho_0} \tau : \mathbb{D} \quad . \tag{4.82}$$

As a consequence, the Clausius-Duhem inequality reduces to

$$\mathcal{D} = \frac{\rho}{\rho_0} \tau : \mathbf{D}^{\mathrm{in}} - \rho \frac{\partial \psi}{\partial \zeta} : \overset{\circ}{\zeta}^{\,\mathrm{Log}} - \frac{1}{\Theta} \mathbf{q} \cdot \nabla \Theta \geq 0 \quad . \tag{4.83}$$

With respect to the split of the Clausius-Duhem inequality (4.83) as performed in Section 4.2.5, the Clausius-Planck inequality, thus, becomes

$$\mathcal{D}_{\mathrm{loc}} = \frac{\rho}{\rho_0} \tau : \mathbf{D}^{\mathrm{in}} - \rho \frac{\partial \psi}{\partial \zeta} : \overset{\circ}{\zeta}^{\,\mathrm{Log}} \geq 0 \tag{4.84}$$

and the Fourier inequality takes the form

$$\mathcal{D}_{\mathrm{con}} = -\frac{1}{\Theta} \mathbf{q} \cdot \nabla \Theta \geq 0 \quad . \tag{4.85}$$

It bears emphasis that, although irreversible effects are accounted for by ζ and $\mathbf{q}$, the thermoelastic material response of the considered thermoinelastic material is restricted to states close to a local equilibrium. This reflects the intrinsic character of the regarded thermoinelastic material as extended thermoelastic material.

4.5   Thermomechanical coupling

In general, elastic-inelastic processes of deformation are involved processes, being characterized by a strong coupling between mechanical and thermal effects. In this regard, the temperature evolution of a deforming body is governed by three factors, i.e., the heat conduction, the heat entering the body, and the heat generated within the body during processes of deformation. This

may be expressed by the energy conservation principle considered in Section 4.2 for the subdomain $\mathcal{R}_t$ with the focus on heat. It yields

$$\dot{U} = Q + Q_{\text{gen}} \quad , \tag{4.86}$$

where Q and Q_{gen} represent the power of heat transferred into and the power of heat generated within the subdomain, respectively (cf. Mills (1999)). The latter may be attributed to the thermomechanically coupled property of elastic-inelastic deformation processes. This quantity may be introduced as

$$Q_{\text{gen}} = \int\limits_{\mathcal{R}_t} q_{\text{gen}}\, \rho \, \mathrm{d}v \quad , \tag{4.87}$$

with q_{gen} expressing the specific generated heat power. Moreover, since only heat related processes are considered, $\dot{U}$ may be written in terms of

$$\dot{U} = \int\limits_{\mathcal{R}_t} \dot{u}\, \rho \, \mathrm{d}v = \int\limits_{\mathcal{R}_t} c_v\, \dot{\Theta}\, \rho \, \mathrm{d}v \quad . \tag{4.88}$$

The quantity c_v represents the *specific heat capacity at constant volume*. In general, it may not be confused with the quantity c_p denoting the *specific heat capacity at constant pressure*, which is subsequently used. For solid materials as considered in this treatise, however, for which the ratio between the thermal expansion coefficient and the compressibility coefficient is sufficiently small, c_v and c_p may be regarded as equivalent (e.g., see Honig (1999), Mills (1999), and Tian & Wu (2001)), i.e.,

$$c_v = c_p = c \quad . \tag{4.89}$$

Then, along with (4.28), relation (4.86) becomes

$$\int\limits_{\mathcal{R}_t} c\, \dot{\Theta}\, \rho \, \mathrm{d}v = \int\limits_{\mathcal{R}_t} [-\nabla \cdot \mathbf{q} + r\, \rho + q_{\text{gen}}\, \rho]\, \mathrm{d}v \quad , \tag{4.90}$$

providing the local form

$$c\, \dot{\Theta}\, \rho = -\nabla \cdot \mathbf{q} + r\, \rho + q_{\text{gen}}\, \rho \quad , \tag{4.91}$$

where arbitrariness of $\mathcal{R}_t$ and continuity of the integrands with respect to $\mathbf{x}$ are stipulated.

Next, the specific generated heat power q_{gen} is specified. In doing so, the definition of the heat capacity at constant pressure may be exploited (e.g., see Honig (1999)), which reads

$$c_p = \Theta \left. \frac{\partial s}{\partial \Theta} \right|_\tau \quad . \tag{4.92}$$

On rearranging equation of state (4.82_1)

$$s = \frac{1}{\rho_0} \boldsymbol{\tau} : \boldsymbol{\alpha} - \frac{\partial \psi}{\partial \Theta} \quad , \tag{4.93}$$

the partial derivative of s with respect to Θ at constant $\boldsymbol{\tau}$ becomes

$$\left. \frac{\partial s}{\partial \Theta} \right|_{\tau} = \frac{1}{\rho_0} \boldsymbol{\tau} : \frac{\partial \boldsymbol{\alpha}}{\partial \Theta} - \frac{\partial^2 \psi}{\partial \Theta^2} \quad . \tag{4.94}$$

Therewith, (4.92) can be rewritten in terms of the Helmholtz free energy

$$c = \frac{1}{\rho_0} \Theta \boldsymbol{\tau} : \frac{\partial \boldsymbol{\alpha}}{\partial \Theta} - \Theta \frac{\partial^2 \psi}{\partial \Theta^2} \quad , \tag{4.95}$$

where use is made of approximation (4.89). Moreover, rearranging the material time derivative of (4.93) and replacing the result into (4.95) gives a rate equation for the temperature

$$c \dot{\Theta} = \Theta \dot{s} - \frac{1}{\rho_0} \Theta \boldsymbol{\tau} : \left(\overset{\circ}{\boldsymbol{\alpha}}{}^{\mathrm{Log}} - \frac{\partial \boldsymbol{\alpha}}{\partial \Theta} \dot{\Theta} \right)$$

$$+ \Theta \left(\frac{\partial^2 \psi}{\partial \Theta \, \partial \boldsymbol{\tau}} - \frac{1}{\rho_0} \boldsymbol{\alpha} \right) : \overset{\circ}{\boldsymbol{\tau}}{}^{\mathrm{Log}} + \Theta \frac{\partial^2 \psi}{\partial \Theta \, \partial \boldsymbol{\zeta}} : \overset{\circ}{\boldsymbol{\zeta}}{}^{\mathrm{Log}} \quad . \tag{4.96}$$

Its evaluation, however, requires the specification of $\dot{s}$, which may be obtained on comparing the rate form of the Helmholtz free energy as in (4.69)

$$\dot{\psi} = \dot{u} - \dot{\Theta} s - \Theta \dot{s} = \frac{\partial \psi}{\partial \boldsymbol{\tau}} : \overset{\circ}{\boldsymbol{\tau}}{}^{\mathrm{Log}} + \frac{\partial \psi}{\partial \Theta} \dot{\Theta} + \frac{\partial \psi}{\partial \boldsymbol{\zeta}} : \overset{\circ}{\boldsymbol{\zeta}}{}^{\mathrm{Log}} \tag{4.97}$$

with relation (4.80). This leads, together with equations of state (4.82) and rate equation (4.74), to

$$\Theta \dot{s} = \dot{u} - \frac{1}{\rho_0} \boldsymbol{\tau} : \mathbf{D}^{\mathrm{el}} - \frac{\partial \psi}{\partial \boldsymbol{\zeta}} : \overset{\circ}{\boldsymbol{\zeta}}{}^{\mathrm{Log}} \quad . \tag{4.98}$$

Substituting the first law of thermodynamics (4.37) in form of the Kirchhoff stress tensor

$$\dot{u} \rho = \frac{\rho}{\rho_0} \boldsymbol{\tau} : \mathbf{D} - \nabla \cdot \mathbf{q} + r \rho \tag{4.99}$$

and the elastic-inelastic separation (4.36) of the stretching tensor then gives

$$\Theta \dot{s} = \frac{1}{\rho_0} \boldsymbol{\tau} : \mathbf{D}^{\mathrm{in}} - \frac{1}{\rho} \nabla \cdot \mathbf{q} + r - \frac{\partial \psi}{\partial \boldsymbol{\zeta}} : \overset{\circ}{\boldsymbol{\zeta}}{}^{\mathrm{Log}} \quad . \tag{4.100}$$

Thus, on replacing (4.100) in (4.96) and comparing the result with (4.91), the specific generated heat power can finally be identified as

$$
q_{\text{gen}} = \Theta \left(\frac{\partial^2 \psi}{\partial \Theta \, \partial \tau} - \frac{1}{\rho_0} \alpha \right) : \overset{\circ}{\tau}^{\text{Log}} + \left(\Theta \frac{\partial^2 \psi}{\partial \Theta \, \partial \zeta} - \frac{\partial \psi}{\partial \zeta} \right) : \overset{\circ}{\zeta}^{\text{Log}}
$$

$$
+ \frac{1}{\rho_0} \tau : \mathbf{D}^{\text{in}} - \frac{1}{\rho_0} \Theta \tau : \left(\overset{\circ}{\alpha}^{\text{Log}} - \frac{\partial \alpha}{\partial \Theta} \dot{\Theta} \right) \quad . \quad (4.101)
$$

5 Phenomenological model

This chapter is concerned with the derivation of constitutive equations for the description of the pseudoelastic shape memory effect at finite deformations. In line with the Eulerian rate formulation proposed by Xiao et al. (2007), the model is consistently formulated within a Eulerian framework based on the Kirchhoff stress tensor, the stretching tensor, and the logarithmic rate. This formulation is discussed in Section 5.1. Of paramount importance for the material model is the introduction of a non-convex Helmholtz free energy function in Section 5.2. It comprises phase specific energies of the single phases austenite and martensite and an additional term which accounts for phase interactions. Internal variables are defined for the overall mass fraction of martensite and the average orientation of the martensite variants. Therewith, a separation of the martensite into a (stress-induced) oriented part and a (temperature-induced) self-accommodated part, both treated as two distinct phases as postulated in the phase-diagram approaches (see Brinson (1993)), can be avoided.[24] Section 5.3 addresses the total stress tensor, the total temperature, and the total stretching tensor of the material. The relations of these quantities conceptually rely on the principle of local equilibrium considered in Section 4.4. Moreover, in contrast to the commonly adopted assumption of equivalent phase specific stresses, a degree of freedom is introduced which allows for deviating martensitic and austenitic stresses. The implications of the underlying principle of local equilibrium are then analyzed in detail in Section 5.4. Finally, constitutive equations ensuring thermodynamic consistency as regarded in Section 4.4 are formulated for the mass fraction of martensite, the average orientation of the martensite variants, and the generated heat related to the thermomechanically coupled material behavior.

5.1 Mechanical framework

The material model derived in this treatise relies on a Eulerian rate formulation in terms of the Kirchhoff stress tensor, the stretching tensor, and the logarithmic rate, which may principally be attributed to the works of Hencky, Truesdell, and Xiao, Bruhns & Meyers. Analyzing pure elasticity within principal stress and strain, Hencky (1928, 1929b, 1929a) states that the simplest physically reasonable material law for finite elastic deformations of continuous material bodies, connecting linearly a stress measure with a strain measure, is given by a mapping between the Kirchhoff stress tensor and the Hencky

---

[24]Since the physical and chemical properties of oriented and self-accommodated martensite do not differ, both types of martensite formations belong to the same kind of phase. Strictly speaking, during an experimental measurement, such as a resistivity measurement, it cannot be distinguished between oriented and self-accommodated martensite (see also Boyd & Lagoudas (1996a) for a discussion).

strain tensor.[25] Therewith, Hencky formulates a physically sound extension of Hooke's law of infinitesimal isotropic elasticity to finite deformations which is referred to as *Hencky's elasticity model*. Experimental validations of this model are carried out by Anand (1979, 1986) for a wide class of elastic materials such as metals and rubber under a variety of finite deformation modes. In these works, Hencky's elasticity model coincides well with the experimental data for moderate deformations and it provides better agreements than alternative extensions of Hooke's law including different work conjugated stress and strain measures. This finding is confirmed by Bruhns et al. (2000) who analyze finite torsion of cylindrical rods and tubes with free ends. The authors also demonstrate that Hencky's elasticity model can predict second-order effects like the change of length in the axial direction commonly referred to as *Poynting effect*.

Although the preceding works motivate from a physical point of view that the Kirchhoff stress tensor and the Hencky strain tensor provide sound mechanical quantities for material laws at finite deformations, a direct description of finite elastic-inelastic deformation processes by means of these quantities turns out to be cumbersome. This is due to the fact, that such a description requires the total strain to be separated into elastic and inelastic components. To overcome this difficulty, the *hypoelastic theory* introduced by Truesdell (1953) may be helpful. Conceptually, this theory considers a mapping between the *rates* of stress and deformation (see Truesdell (1955)) in contrast to a classical direct mapping between stress and deformation. More precisely, the hypoelastic theory establishes a linear, possibly stress-dependent relation between the stretching tensor and the objective rate of a conjugated stress tensor (see Truesdell & Noll (2004)). In this connection, Truesdell (1955) refers to the hypoelastic theory as *simplest rate theory*. It is particularly free of strain-like variables. In the view of Truesdell (1952), a theory based on a strain measure requires the introduction of a *natural state* for which the body at issue is unstressed. In general, however, this state is not known or even impossible without destroying the continuity of the body.[26] Although Truesdell addresses only elastic deformation processes in the course of his considerations, the hypoelastic theory is not restricted to pure elasticity. Finite elastic-inelastic deformation processes may be encountered by an additive split of the total stretching tensor into elastic and inelastic parts as considered in relation (4.36). In this sense, the hypoelastic theory is to be regarded as a general theory including elasticity, in particular hyperelasticity as a special case (see Noll (1955)).

---

[25] Actually, Hencky first uses the Cauchy stress tensor (see Hencky (1928)). Due to the fact that the Kirchhoff stress tensor is an *absolute tensor* in contrast to the Cauchy stress tensor being a *tensor density* (cf. Brillouin (1925), see also Kästner (1964)), he replaces the Cauchy stress tensor by the Kirchhoff stress tensor in a later work (see Hencky (1929b)).

[26] For an elaborated review on this matter also refer to Xiao et al. (2006a).

The advantages of the hypoelastic theory and the Eulerian framework in terms of the Kirchhoff stress tensor and the Hencky strain tensor may be combined by virtue of the logarithmic rate, as this rate relates the Hencky strain tensor with the stretching tensor. From this point of view, the logarithmic rate may be regarded as unique objective time derivative for the resulting hypoelastic framework based on the Kirchhoff stress tensor and the stretching tensor. The uniqueness of the logarithmic rate may also be inferred from physical criteria ensuring physical consistency, which restrict the set of all corotational and non-corotational time derivatives. One of these criteria is the *exact integrability criterion* also referred to as *self-consistency criterion* (see Xiao et al. (1999) and Bruhns et al. (1999), also Simo & Pister (1984)). It conceptually states that a hypoelastic relation intended to describe an elastic material behavior must be exactly integrable to define an elastic, in particular a hyperelastic relation for a process of pure elastic deformations. In this sense, an objective rate obeying the exact integrability criterion is referred to as *self-consistent*, otherwise it is called *self-inconsistent*. Adopting the self-consistency criterion, Xiao et al. (2005) prove that among a wide class of corotational and non-corotational rates only the logarithmic rate turns out to be self-consistent, restricting uniquely the set of objective rates to the logarithmic rate. Alternatively, the uniqueness of the logarithmic rate may also be deduced from the *yielding stationarity criterion*. It basically states that the yield function known from plasticity is stationary for vanishing rates of its arguments, such as stress, temperature, or internal variables. In this regard, assuming that the yield function is represented by a scalar-valued function of the invariants of an objective Eulerian second-order tensor, Xiao et al. (2000) demonstrate for a wide class of corotational and non-corotational rates that only the former rates can fulfill the yielding stationarity criterion. Then, on stipulating that the integrated stretching tensor is a Eulerian strain tensor, Xiao et al. (1997b, 1998a, 1998b) uniquely determine the logarithmic rate as only admissible objective rate.

5.2 Specific Helmholtz free energy

In the course of the proposed model, the energetical state of the material is described by a specific Helmholtz free energy ψ which is introduced in Section 4.4 in a general form as function of the Kirchhoff stress tensor τ, the temperature Θ, and a set of internal variables ζ. In this context, to account for the local composition of the two-phase solid material in terms of austenitic and martensitic phase fractions, the introduction of the scalar-valued variable ξ referred to as *mass fraction of martensite* proves to be valuable. This quantity may be defined as

$$\xi = \frac{dm^{\mathrm{M}}}{dm} \quad \text{with} \quad dm = dm^{\mathrm{A}} + dm^{\mathrm{M}} \quad , \tag{5.1}$$

where dm denotes the total mass of all particles within a generic material neighborhood and dm^A and dm^M express the masses of the corresponding austenitic and martensitic particles. Here and henceforth, quantities related to the phases austenite and martensite are labeled with the superscripts A and M or with γ representing A or M. Then, on considering ξ as internal variable and on expressing the set of the remaining internal variables by the quantity Ξ, ζ may be decomposed as

$$\zeta = \{\xi, \Xi\} \quad . \tag{5.2}$$

Note that the mass fraction instead of the volume fraction is used here as a characteristic measure for the amount of the single phases, as this quantity is independent of the deformation. Moreover, since the chemical composition of the material is invariant during the diffusionless martensitic phase transformation (see Otsuka & Wayman (1998a)), no internal variable has to be defined in this regard.

5.2.1   Specific Helmholtz free energy of a two-phase solid

In agreement with the thermodynamics of mixtures, an extensive specific quantity of a multiphase material can generally be written as weighted sum of the extensive specific quantities of the single phases plus an additional term expressing phase interactions (see Müller (2001) and Baehr (2002)). In particular, with respect to the two-phase solid material comprising austenitic and martensitic phases, the specific total Helmholtz free energy ψ may be expressed by

$$\psi(\tau, \Theta, \xi, \Xi) = (1 - \xi)\,\psi^A + \xi\,\psi^M + \Delta^{AM}\psi \quad . \tag{5.3}$$

Here, the mass fraction ξ is employed as weighting factor between the specific Helmholtz free energies of austenite and martensite ψ^A and ψ^M. $\Delta^{AM}\psi$ denotes the *specific Helmholtz free energy of internal interactions*. This energy proves crucial for the modeling of shape memory alloys, since it allows for the description of the hysteretic behavior observed for phase transformations in solid materials (cf. Müller (1989)). Accordingly, $\Delta^{AM}\psi$ vanishes in the absence of phase interactions, which is, for instance, the case for phase transformations in gases (cf. Müller (1985b)) or for single-phase materials.

Intrinsic specific Helmholtz free energy

It may be inferred from experimental data provided by Jacobus et al. (1996) and Orgéas & Favier (1998) for NiTi shape memory alloys that the material behavior of the single phases austenite and martensite is isotropic and linear-elastic in stress and strain. On this account, the phase specific, *intrinsic* energies of the single phases may be described by an isotropic thermoelastic

energy function of the form[27]

$$
\left[\psi(\mathbf{h}^{\mathrm{el}},\,\Theta)\right]^{\gamma} = \left[\frac{1}{2\rho_0}\,\mathbf{h}^{\mathrm{el}} : \mathbb{C} : \mathbf{h}^{\mathrm{el}} - (\Theta - \Theta_0)\,\frac{1}{\rho_0}\,\alpha : \mathbb{C} : \mathbf{h}^{\mathrm{el}}\right.
$$

$$
\left. + c_{\mathrm{v}}\left(\Theta - \Theta_0 - \Theta\ln\left(\frac{\Theta}{\Theta_0}\right)\right) + u_0 - s_0\,\Theta\right]^{\gamma} \quad . \qquad (5.4)
$$

Its derivation can be reviewed in the works of Raniecki & Bruhns (1991) and Oberste-Brandenburg (1999). Here, the phase specific quantities $\mathbb{C}^{\gamma}$ and α^{γ} express the *isotropic elasticity tensor* and the *isotropic tensor of thermal expansion coefficients*, the constants u_0^{γ} as well as s_0^{γ} denote energetical and entropical parameters, and Θ_0^{γ} represents a referential temperature. $\mathbb{C}^{\gamma}$ and α^{γ} are particularly defined as

$$
\mathbb{C}^{\gamma} = \lambda^{\gamma}\,\mathbf{I}\otimes\mathbf{I} + 2\,\mu^{\gamma}\,\mathbb{I} \quad \text{and} \quad \alpha^{\gamma} = \alpha^{\gamma}\,\mathbf{I} \quad , \qquad (5.5)
$$

with the *Lamé constants* λ^{γ} and μ^{γ} related to *Young's modulus* E^{γ} and *Poisson's ratio* μ^{γ} through

$$
\lambda^{\gamma} = \left[\frac{\nu E}{(1+\nu)(1-2\nu)}\right]^{\gamma} \quad \text{and} \quad \mu^{\gamma} = \left[\frac{E}{2(1+\nu)}\right]^{\gamma} \qquad (5.6)
$$

and with $\mathbb{I}$ denoting the symmetric fourth-order identity tensor. Equation (5.4) relies on the assumption of a constant specific heat capacity c_{v}^{γ} at constant volume, which may be regarded as being sufficiently fulfilled for the pseudoelastic temperature range of near equiatomic NiTi shape memory alloys (see Raniecki & Bruhns (1991)). Also, the elasticity tensor as well as the tensor of thermal expansion coefficients are supposed to be at most linear in temperature. Finally, since ψ^{γ} defined in (5.4) is an isotropic tensor function of the objective second-order tensor $\mathbf{h}^{\mathrm{el}\,\gamma}$, it identically fulfills the principle of material frame indifference stated in Section 4.4.

Equation (5.4) may be employed to derive a relation for the intrinsic elastic Hencky strain tensor. In doing so, equation of state (4.72_2) may be invoked for each single phase, i.e.,

$$
\tau^{\gamma} = \left[\rho_0\,\frac{\partial\psi}{\partial\mathbf{h}^{\mathrm{el}}}\right]^{\gamma} \quad , \qquad (5.7)
$$

so that $\mathbf{h}^{\mathrm{el}\,\gamma}$ becomes

$$
\mathbf{h}^{\mathrm{el}\,\gamma} = \left[\mathbb{C}^{-1} : \tau + \alpha\,(\Theta - \Theta_0)\right]^{\gamma} \quad . \qquad (5.8)
$$

---

[27] It should be noted that this assumption does not restrict the description of the frequently observed asymmetric deformation behavior of pseudoelastic NiTi shape memory alloys well-known as tension/compression asymmetry (see Jacobus et al. (1996), Lim & McDowell (1999), and Bouvet et al. (2004b) among others), as this effect may be ascribed to phase transformations (e.g., see Patoor et al. (1995), Saburi (1998), Gall & Sehitoglu (1999), and Lexcellent et al. (2006)).

Evidently, the intrinsic elastic Hencky strain tensor can only be quantified for given stress and temperature. Substituting relation (5.8) into (5.4) then gives the specific Helmholtz free energy in terms of the Kirchhoff stress tensor

$$[\psi(\tau, \Theta)]^\gamma = \left[\frac{1}{2\rho_0} \tau : \mathbb{C}^{-1} : \tau - \frac{1}{2\rho_0} (\Theta - \Theta_0)^2 \alpha : \mathbb{C} : \alpha\right.$$

$$\left. + c\left(\Theta - \Theta_0 - \Theta \ln\left(\frac{\Theta}{\Theta_0}\right)\right) + u_0 - s_0 \Theta\right]^\gamma \quad , \quad (5.9)$$

where use is made of approximation (4.89) for the specific heat capacity. For constant values of ψ^γ and Θ, equation (5.9) reflects a paraboloid within the principle stress space, being oriented into the $(1, 1, 1)$-direction. This finding is adopted in Figure 5.1 for a graphical representation of ψ^γ at constant temperature, which relies on the definition of a two-dimensional stress space perpendicular to the paraboloid orientation.
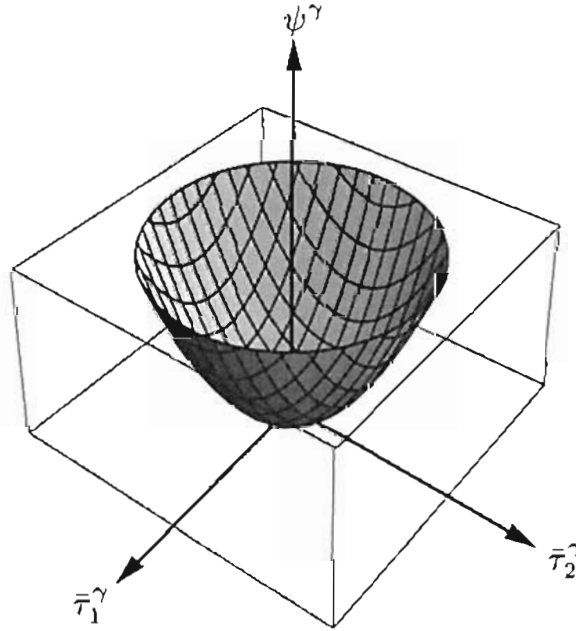
Figure 5.1: Representation of the specific Helmholtz free energy for constant temperature within a plane perpendicular to the $(1, 1, 1)$-direction in the principle stress space; $\bar\tau_1^\gamma$ and $\bar\tau_2^\gamma$ denote the stresses in this plane.

It should be noted that equation of state (5.7) is a stronger form of the principle of local equilibrium than it is stated by equation of state (4.72$_2$). More precisely, (5.7) imposes the principle of local equilibrium for every single phase within each material particle of the body B, while (4.72$_2$) demands the local equilibrium for each material particle as a whole.

In what follows, the thermoelastic properties of the single phases are assumed to be equal and constant, i.e.,

$$c^A = c^M = c \quad \text{and} \quad \rho_0^A = \rho_0^M = \rho_0 \quad , \tag{5.10}$$

as well as

$$\mathbb{C}^A = \mathbb{C}^M = \mathbb{C} \quad \text{and} \quad \alpha^A = \alpha^M = \alpha \quad . \tag{5.11}$$

The equality of the phase specific heat capacities and densities is in agreement with data provided by Hodgson & Brown (2000) and Tian & Wu (2001) for NiTi. Basically, the equality of the intrinsic densities relies on negligible volume changes during martensitic phase transformations as reported by Shimizu & Tadaki (1987). The equality of the phase specific elastic properties of NiTi may be inferred from in-situ ultrasonic experimental data obtained by Kaack (2002) and Šittner et al. (2006a), in which the phase specific Poisson's ratios as well as Young's moduli may be regarded as comparable. Within both works, however, the austenitic Poisson's ratio seems to be slightly higher than its martensitic counterpart and the specific Young's modulus for austenite is slightly lower than for martensite.

Specific Helmholtz free energy of internal interaction

In agreement with Müller (1989) and Müller & Xu (1991), the specific Helmholtz free energy of internal interactions $\Delta^{AM}\psi$ may be attributed to the interfacial energy between austenitic and martensitic domains within the solid material body. The latter reflects the energy necessary to form interfaces between austenitic and martensitic regions which specifically comprises the energy arising from distortions due to elastic misfits or elastic interactions of the phases. A micromechanical motivation of the interaction energy is given by Patoor et al. (1995), who relates this energy to the internal stress field which arises from coexisting phases (see also Gall & Sehitoglu (1999), Patoor et al. (2006), and Wang et al. (2008) among others). Based on the works of Müller (1989), Raniecki et al. (1992), and Müller & Seelecke (2001), $\Delta^{AM}\psi$ is introduced here as

$$\Delta^{AM}\psi(\Theta, \xi, \Xi) = \xi(1 - \xi) A \quad , \tag{5.12}$$

with the scalar-valued isotropic tensor function $A(\Theta, \Xi)$ denoting the *coherency coefficient*. In contrast to the aforementioned authors, the arguments of the coherency coefficient are amended by the independent set of internal variables Ξ, as A is related to the interaction of the phases and, thus, to the internal material structure. As outlined by Müller & Xu (1991), the coherency coefficient proves to be eminent for the description of the hysteresis observed for pseudoelasticity.

5.2.2 The essence of solid state phase transformations

Getting a deeper insight into phase stability criteria and equilibrium states is of fundamental importance for the understanding of phase transformation processes and, thus, for the modeling of shape memory alloys. It is pointed out in Section 4.2.5 that an equilibrium state is principally characterized by two factors, i.e., a minimum of the specific internal energy and a maximum of the specific entropy. Based on this finding, it may be inferred from (4.69) that the specific Helmholtz free energy tends towards a minimum for a general irreversible process of deformation on reaching an equilibrium state (cf. Müller (1985b)). This result may also be deduced from the local form of the Clausius-Planck inequality (4.53), which can be written in terms of the specific Helmholtz free energy and the Kirchhoff stress tensor as

$$\mathcal{D}_{\text{loc}} = \frac{\rho}{\rho_0}\,\boldsymbol{\tau} : \mathbf{D} - \rho\left(\dot{\psi} + s\,\dot{\Theta}\right) \geq 0 \quad . \tag{5.13}$$

Rearranging inequality (5.13) leads, along with (4.36) and (4.74), to

$$\frac{1}{\rho_0}\,\boldsymbol{\tau} : \mathbf{D}^{\text{in}} + \frac{1}{\rho_0}\,\boldsymbol{\tau} : \mathbb{D} : \overset{\circ}{\boldsymbol{\tau}}{}^{\text{Log}} - \left(\frac{1}{\rho_0}\,\boldsymbol{\tau} : \boldsymbol{\alpha} + s\right)\dot{\Theta} \geq \dot{\psi} \quad . \tag{5.14}$$

It shows that ψ cannot increase for an isothermal state with constant stress and constant inelastic deformation. This tendency of the specific Helmholtz free energy towards a minimum provides a first criterion for the onset of phase transformations in multiphase materials, i.e., an austenite to martensite transformation can only initiate if

$$\psi^{\text{A}} > \psi^{\text{M}} \quad , \tag{5.15}$$

whereas a martensite to austenite transformation requires

$$\psi^{\text{M}} > \psi^{\text{A}} \tag{5.16}$$

to hold true. In this regard, criteria (5.15) and (5.16) are necessary for the initiation of phase transformations. Phase transformations, however, do not instantaneously initiate if either of the criteria (5.15) and (5.16) is fulfilled. The difference between the specific intrinsic energies has merely to exceed a certain threshold value which represents the *driving force* for the phase nucleation (e.g., see Shimizu & Tadaki (1987)). This requirement furnishes a second and sufficient criterion for the onset of phase transformations.
The preceding considerations are schematically illustrated in Figure 5.2 for temperature-induced phase transformations at zero stress. In this figure, starting temperatures of phase transformations into martensite and austenite on cooling and on heating are represented by M_0^{s} and A_0^{s}, respectively. The equilibrium temperature $\bar{\Theta}$ reflects the arithmetic mean of these quantities as

$$\bar{\Theta} = \frac{1}{2}(M_0^{\text{s}} + A_0^{\text{s}}) \quad , \tag{5.17}$$
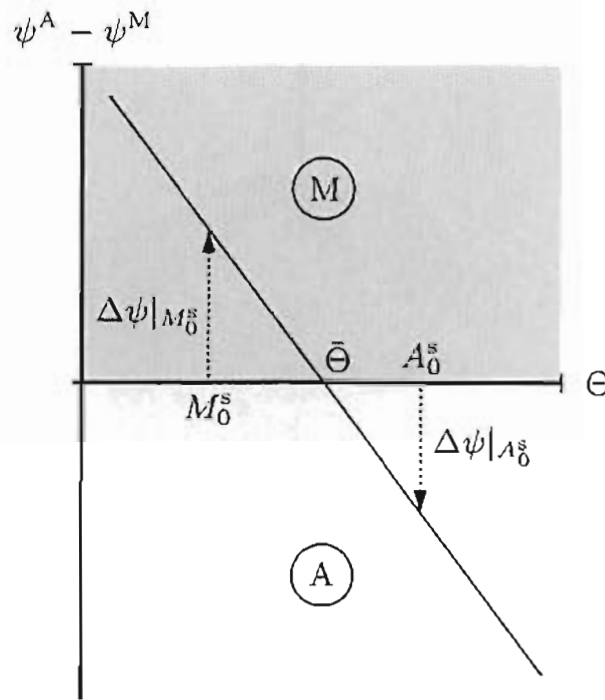
Figure 5.2: Temperature-induced phase transformations at zero stress; starting temperatures M_0^s and A_0^s for initiating phase transformations, driving forces $\Delta\psi|_{A_0^s}$ and $\Delta\psi|_{M_0^s}$, and equilibrium temperature $\bar{\Theta}$

at which the phase specific energies are identical (see Otsuka & Wayman (1998a)). The driving forces for the phase nucleation are expressed by the quantities $\Delta\psi|_{M_0^s}$ and $\Delta\psi|_{A_0^s}$. They are linked to the differences between M_0^s and $\bar{\Theta}$ and between A_0^s and $\bar{\Theta}$ by means of the degree of supercooling and superheating of the material. It bears emphasis that, according to Falk (1983), the difference between the specific intrinsic energy functions ψ^A and ψ^M is taken to be linear in temperature. This is in line with (5.9) if the referential temperatures Θ_0^A and Θ_0^M are assumed to be equal for both phases. Falk (1983) also attributes the stability of martensite and austenite at different temperature levels to the decomposition of ψ into energetic and entropic parts (see also Müller (1989)). In this context, as the influence of the entropic part on ψ increases with increasing temperature, the two phases austenite and martensite may be regarded as being stabilized by entropy and by internal energy, respectively.

The stabilization of martensite is, however, not restricted to low temperatures. At high temperatures, at which the austenite is stable in the unstressed state, the martensitic phase can also be stabilized by stress as it may be observed for pseudoelastic deformation processes (cf. Otsuka & Wayman (1998b)).
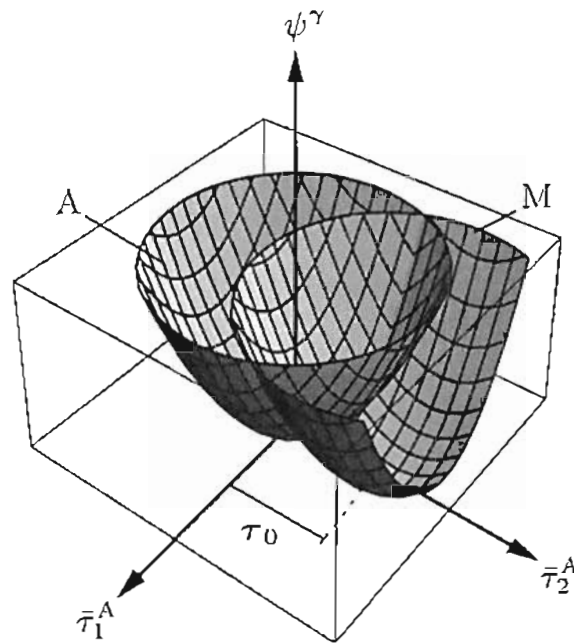
Figure 5.3: Specific Helmholtz free energies of martensite and austenite within the austenitic stress space $\bar{\tau}_1^A$ and $\bar{\tau}_2^A$ (see Figure 5.1)

Conceptual analysis of pseudoelastic phase transformations

A deeper insight into the martensitic stabilization by stress may be obtained on introducing an arbitrary but fixed reference stress space to render the specific intrinsic energy functions comparable. In particular, since austenite is the initial or *parent* phase for pseudoelasticity, it is convenient to define the austenitic stress space as a reference space. For the conceptual analysis, the stress is assumed to be externally controlled in this way that the material is exposed to a constant stress direction throughout the process of phase transformation. In this case, only a small number of martensite variants is preferably activated showing the most favorable orientation to the applied stress (see Šittner et al. (2006b)). Focus is specifically on one martensite variant nucleating during a stress-induced phase transformations. From the phase stability criteria considered above it may then be inferred for this variant that the minimum of its specific Helmholtz free energy, i.e., its potential well is shifted towards higher stresses compared to the potential well of the austenite.[28] This is indicated in Figure 5.3, where, in accord with (5.9), the specific intrinsic energy functions are represented by parabolas. Note that a vertical shift of the parabolas may also arise from different values of the material parameters u_0^γ and s_0^γ, reflecting the entropic stabilization of the austenitic phase in the unstressed state. The horizontal shift of the martensitic parabola provides a new essential tensorial

---

[28]Note that the potential well of the martensitic phase is commonly regarded as being shifted towards higher *strains* (e.g., see Falk (1983), Ball & James (1987), and Müller (1989)), despite the fact that martensite is *stress-induced*.

quantity τ_0 which furnishes a transformation rule for the martensitic stress into the austenitic stress space of the form

$$\tau^M = \tau^A - \tau_0 \quad . \tag{5.18}$$

In this sense, the second-order tensor τ_0 can be interpreted as the potential well position of the single martensite variant in the austenitic stress space. It bears emphasis that (5.18) is not to be confused with an approach for the intrinsic stresses. Up to this point, it only serves for the transformation of the specific martensitic Helmholtz free energy into the austenitic stress space.
For a further analysis of stress-induced phase transformation processes, the preceding conceptual analysis is extended in such a way, that the material is assumed to transform completely from austenite into martensite. In this case, the material in the martensitic state may be supposed to compensate the same load as in its austenitic state, such that the stresses of austenite and martensite before and after the phase transformation may be regarded as comparable. Moreover, on concentrating on purely mechanical properties, the temperatures before and after the phase transformation are considered to be equal. This may hold true after a sufficient time range for a non-adiabatic process. Then, with the purely thermoelastic relation (5.8), together with assumption (5.11$_1$), the intrinsic elastic strains become

$$\mathbf{h}^{\mathrm{el\,A}} = \mathbb{C}^{-1} : \tau^A \quad \text{and} \quad \mathbf{h}^{\mathrm{el\,M}} = \mathbb{C}^{-1} : \tau^M \quad . \tag{5.19}$$

Since the thermoelastic austenite is the parent phase for pseudoelasticity, the total strain $\mathbf{h}$ equals the total austenitic strain $\mathbf{h}^A$ before the phase transformation. It follows

$$\mathbf{h} = \mathbf{h}^A = \mathbf{h}^{\mathrm{el\,A}} = \mathbb{C}^{-1} : \tau^A \quad . \tag{5.20}$$

Consequently, τ^A vanishes for an unstrained material. In this case, if the reverse phase transformation from martensite to austenite is imaginarily inhibited, it may be deduced from (5.18) that the martensitic stress τ^M equals $-\tau_0$. Analogously to the austenitic state, $\mathbf{h}$ is equivalent to the total martensitic strain $\mathbf{h}^M$ after the completion of the phase transformation. Then, as the martensitic phase is purely thermoelastic, it follows that the total strain of the material after the phase transformation takes the form

$$\mathbf{h} = \mathbf{h}^M = \mathbb{C}^{-1} : (\tau^M + \tau_0) \quad . \tag{5.21}$$

In other words, $\mathbf{h}^M$ is linear-elastic in terms of the stress $\tau^M + \tau_0$. Relations (5.20) and (5.21) allow for an estimation of the total deformations before and after complete phase transformation processes with constant stress direction. From this, an essential property of τ_0 may be deduced, stating that this
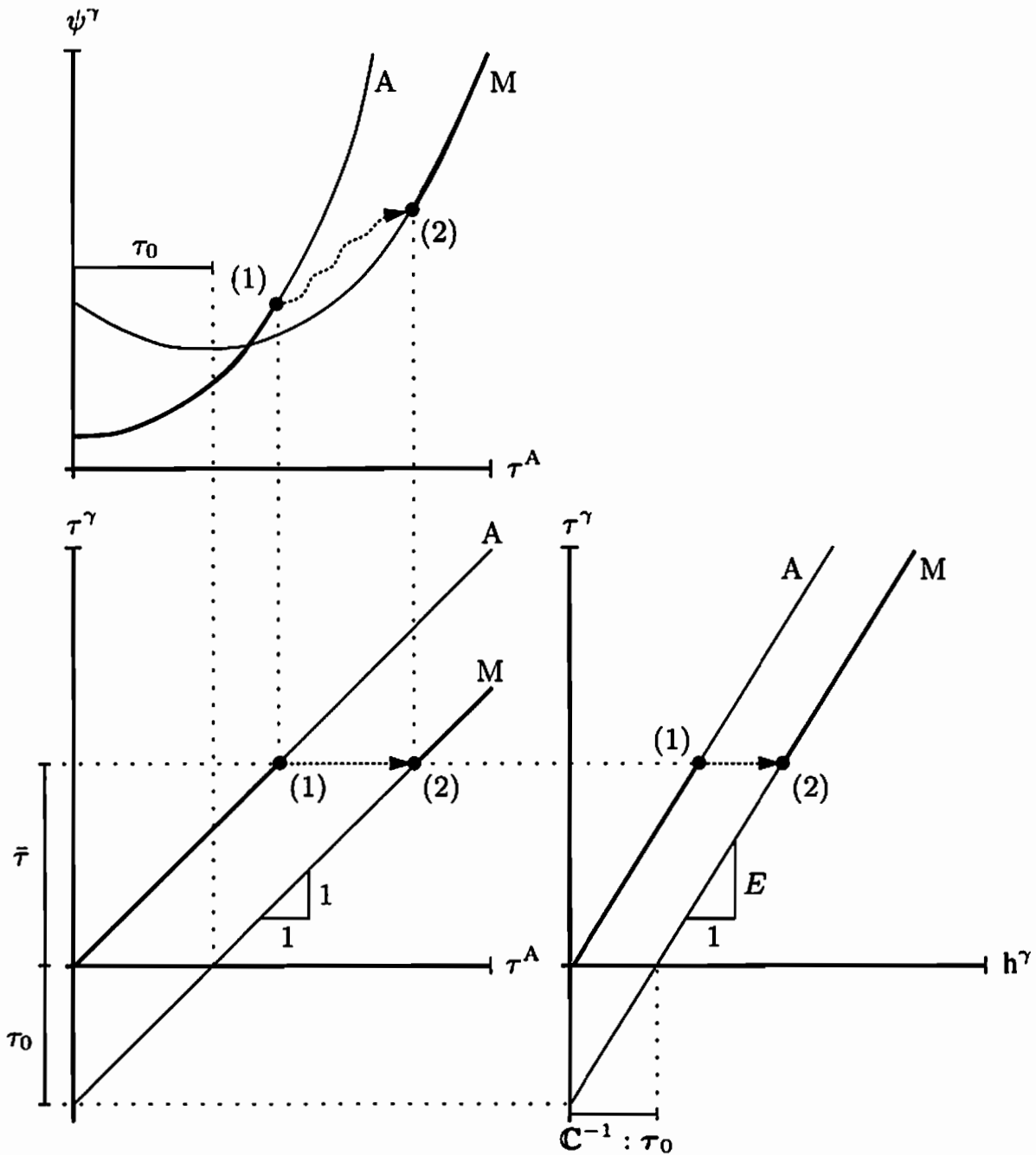
Figure 5.4: Process of phase transformation proceeding from point (1) to point (2); the upper-left diagram depicts the intrinsic energy functions, the lower-left diagram reflects the intrinsic stresses within the austenitic stress space, and the lower-right diagram expresses the intrinsic relations between stress and strain.

quantity is deviatoric. In particular, as the volume change of the material during phase transformation processes is negligible for NiTi shape memory alloys (see Shimizu & Tadaki (1987)), it follows that

$$\text{tr}\left(\mathbb{C}^{-1} : \bar{\tau}\right) \overset{!}{=} \text{tr}\left(\mathbb{C}^{-1} : (\bar{\tau} + \tau_0)\right) \quad \Rightarrow \quad \text{tr}\left(\mathbb{C}^{-1} : \tau_0\right) \overset{!}{=} 0 \tag{5.22}$$

and, hence,

$$\text{tr}\,(\tau_0) \stackrel{!}{=} 0 \quad . \tag{5.23}$$

The quantity $\bar{\tau}$ in relations (5.22) denotes the equivalent austenitic and martensitic stresses before and after the phase transformation process.

The preceding considerations are graphically illustrated in Figure 5.4. The upper-left diagram shows the specific Helmholtz free energy functions of the phases martensite and austenite. The phase transformation sets in at point (1) in the austenitic state and comes to a complete rest at point (2) in the martensitic state. The lower-left diagram depicts the intrinsic stresses within the austenitic stress space. This diagram particularly reflects relation (5.18). The lower-right diagram finally visualizes the intrinsic thermoelastic relations between strain and stress which are represented by (5.20) and (5.21). In all three diagrams, the transformation path is unknown. This is indicated by the dashed line between points (1) and (2).

Multivariant phase transformation processes

Up to this point, only one martensite variant which forms during a phase transformation process is considered. In this context, the deviatoric tensorial quantity τ_0 is introduced, describing the position of the martensitic potential well within the austenitic stress space. Generally, however, different martensite variants can be activated with differently distributed potential wells. In fact, up to 24 martensite variants with distinct orientations may nucleate in NiTi single crystals (cf. Miyazaki (1996)). Thus, motivated by the fact that a polycrystal consists of a manifold of differently oriented single crystals, the potential wells of all martensite variants may be considered as continuously distributed around the potential well of the austenite. This approximation may be regarded as fairly accurate for an untextured polycrystal within the context of a phenomenological theory. Hence, the possible locations τ_0 of all potential wells of the martensite variants may be approximated by

$$\tau_0 = \bar{\tau}_0 \, \frac{\tau^{A'}}{|\tau^{A'}|} \quad , \tag{5.24}$$

where $|\tau^{A'}|$ denotes the *Frobenius norm* of the austenitic stress deviator $\tau^{A'}$. Equation (5.24) describes a sphere with radius $\bar{\tau}_0$ in the austenitic stress space. It is schematically illustrated in Figure 5.5 within the two-dimensional stress space employed in Figure 5.3. Note that the radius $\bar{\tau}_0$ in this figure is taken as stress dependent with respect to a possibly asymmetric initiation of phase transformation processes.

In regard of the diversity of different martensite variants, the martensitic Helmholtz free energy function introduced by relation (5.9) is to be regarded as average energetical quantity of solely the *activated* martensite variants, as
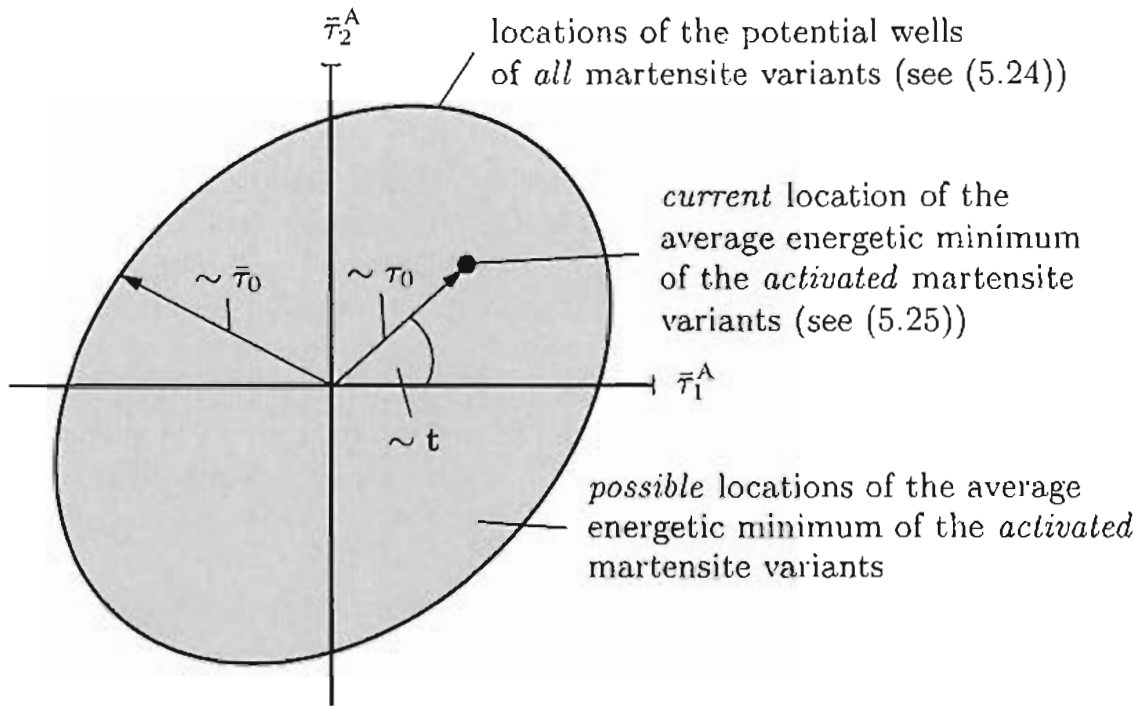
Figure 5.5: Potential well positions of the martensite variants within a plane perpendicular to the (1, 1, 1)-direction in the principle austenitic stress space and suggestive interpretation of the quantities $\bar{\tau}_0$, τ_0, and t

only these variants dominate the actual material behavior of shape memory alloys. Accordingly, the quantity τ_0 describes the location of the energetical minimum of the currently activated variants. In this sense and with respect to relation (5.24), it may multiplicatively be decomposed into the two average quantities t and τ_0 as

$$\tau_0 = \tau_0\, t \quad \text{with} \quad t:t = 1 \quad \text{and} \quad \tau_0 \in [0, \bar{\tau}_0] \quad , \tag{5.25}$$

where the deviatoric second-order tensor t and the scalar-valued variable τ_0 reflect the *average orientation* and the *average distortion of the activated martensite variants*. This decomposition may also be reviewed in Figure 5.5. Among both quantities t and τ_0, the former may directly be specified for proportional loadings with constant stress direction. In this case, the martensite orientation t and the stress direction s may be regarded as parallel, so that

$$t = s \quad \text{with} \quad s = \frac{\tau'}{|\tau'|} \quad . \tag{5.26}$$

It may, hence, be inferred that t changes on every variation of s which is in line with the observation that unfavorable martensite variants transform into favorable ones to accommodate the current stress. For a constant mass fraction of martensite this effect is referred to as *reorientation*. Nevertheless, although

it seems physically sound to describe reorientation by (5.26), this approach can only be regarded as rough estimation for general, non-proportional loadings (e.g., see Orgéas & Favier (1998)). This issue is addressed Section 5.5.3.

The two variables τ_0 and t may be employed as internal variables for the description of the internal material structure. In particular, these variables can be used to describe reoriented martensite during the pseudoelastic and the pseudoplastic effects. Thus, the set of internal variables ζ in (5.2) may be finalized as

$$\zeta = \{\xi, \tau_0, t\} \quad . \tag{5.27}$$

However, on restricting the subsequent derivations to pseudoelasticity, τ_0 is set equal to $\bar{\tau}_0$, such that only ξ and t are considered as internal variables. For the sake of simplicity, $\bar{\tau}_0$ is additionally set constant, i.e., invariant on the stress direction.

5.3   Stress, temperature, and stretching

By invoking the principle of local equilibrium, the temperatures of the phases austenite and martensite may locally assumed to be equal

$$\Theta^A = \Theta^M = \Theta \quad . \tag{5.28}$$

For the intrinsic, phase specific stresses, however, an equivalent relation need not necessarily hold true as there exist mechanical interactions between austenite and martensite even in the state of a local equilibrium. This is addressed in the first part of this section. Based on the findings therein, the second part is devoted to the total stretching tensor and the total stress tensor.

5.3.1   Intrinsic stress and intrinsic temperature

To review the mechanical interactions between the single phases austenite and martensite, consider an austenitic material that instantaneously and completely transforms into martensite under a given load. It may then be deduced from (5.18) that the material structure is weakened right after the transformation which leads to a *snap-through-like problem*. More precisely, if the material in the martensitic state is exposed to the same load as in the austenitic state, the material structure is in a non-equilibrium state directly after the phase transformation, so that stress and strain cannot explicitly be assigned to each other. This is graphically illustrated in Figure 5.6, in which the phase transformation proceeds from point (1) in the austenitic state to a certain point in the martensitic state. Ideally, point (2′) would directly be reached after the phase transformation. Since the material at point (2′) is, however, instantaneously exposed to the load $\bar{\tau}$, its state directly moves over to the stable point (2″), such that the material in point (2′) is in a strong non-equilibrium. Hence,
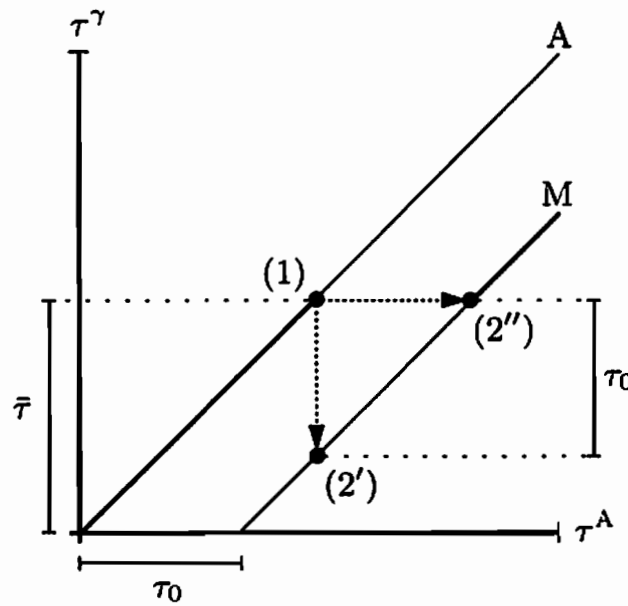
Figure 5.6: Process of phase transformation proceeding from point (1) to point (2″) at high transformation velocity, with point (2′) being in a strong non-equilibrium state

similar to the approach used for the intrinsic temperatures in equation (5.28), an approach of the form

$$\tau^A = \tau^M = \tau \tag{5.29}$$

seems to be reasonable for the phase specific stresses.

The snap-through-like problem is fully developed for high transformation velocities as motivated by the example above. Nevertheless, it represents a limiting case, as thermoelastic martensitic phase transformations proceed sequentially, i.e., the amount of the transformed material depends on the velocity of the externally controlled thermomechanical process. Hence, the transformed domain is generally embedded within a matrix consisting of austenite and martensite. This matrix provides a *supporting effect* which compensates the weakening of the transformed region to some extent. Due to this, the transformed domain after the phase transformation is not fully exposed to the same load as before the phase transformation. In this sense, point (2′) in Figure 5.6 may be regarded to be in a state of equilibrium if the transformed region is sufficiently small. This leads to the following limiting case for slow processes of phase transformation

$$\tau^M = \tau^A - \tau_0 \quad . \tag{5.30}$$

Altogether, relations (5.29) and (5.30) may be regarded as complementary limiting cases, representing upper and lower bounds for the intrinsic stresses.
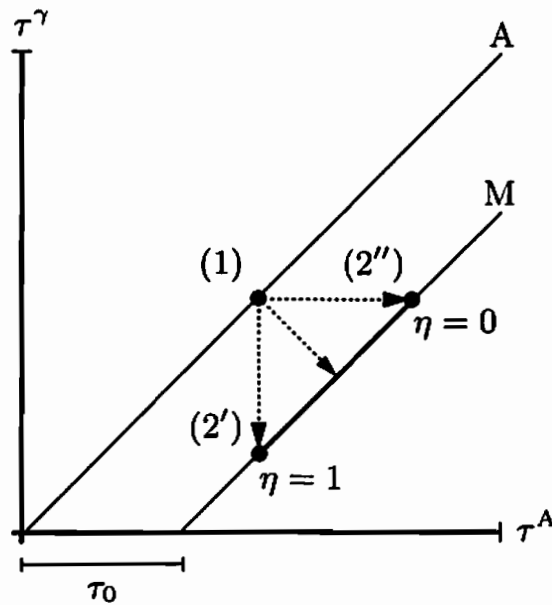
Figure 5.7: Martensitic stress directly after phase transformation from the austenitic phase

They may be combined in a simple manner on introducing a phenomenological scaling parameter $\eta \in [0, 1]$ through the linear mapping

$$\tau^{M} = \tau^{A} - \eta \tau_0 \quad , \tag{5.31}$$

in which η accounts for the internal stress field distribution and, thus, for the influence of the supporting effect. The selection $\eta = 0$ provides (5.29) for high transformation velocities, whereas the choice $\eta = 1$ yields (5.30) for slow transformation processes. This is indicated in Figure 5.7.

It bears emphasis, that the preceding considerations do not account for mechanical interactions of the single phases at the phase interfaces. Strictly speaking, the stresses in the vicinity of the phase interfaces may deviate from the *average* intrinsic stresses which are encountered by the generalized relation (5.31). This, however, is restricted by the fact that significant differences may cause additional phase transformations, which minimize the deviations between the stresses. Consequently, the limiting case $\eta = 1$ cannot be expected to be reached for realistic processes. As this can also not be expected for the limiting case $\eta = 0$ at unlimited transformation velocities, the selections $\eta = 0$ and $\eta = 1$ are to be excluded from the considerations, so that η is to be defined over the open set $]0, 1[$. It should also be noted that η generally depends on the material microstructure, although it is taken as constant here for the sake of simplicity.

The foregoing approaches are illustrated by a suggestive case study in terms of a numerical homogenization scheme. The example is based on the concept of a representative volume element (e.g., see Hill (1963)) for which a volume

element of the material at the microscale is assumed to represent statistically the material properties at the macroscale. The volume element is taken as rectangular in shape, being fully austenitic in its initial state. In its center, a small spherical domain is supposed to transform instantaneously into martensite. The distribution of the single phases after phase transformation is depicted in Figure 5.8. The calculations are restricted to infinitesimal deformations, so that the Hencky strain tensor and the Kirchhoff stress tensor are replaced by the tensors ε and σ denoting the respective nominal quantities of the geometrically linearized theory. Moreover, on concentrating on purely mechanical properties, the temperature is assumed to be constant throughout the process of phase transformation. With equations (5.20) and (5.21), the intrinsic strain-stress relations are then given by

$$\sigma^{A} = \mathbb{C} : \varepsilon^{A} \quad \text{and} \quad \sigma^{M} = \mathbb{C} : \varepsilon^{M} - \sigma_0 \quad . \tag{5.32}$$

In order to satisfy Hill's condition (e.g., see Hill (1963) or Zohdi & Wriggers (2005)) demanding the stress power at the microscale to be identical to the stress power at the macroscale, a linear displacement into the x-direction is prescribed at the boundary of the representative volume element. In this regard, it may be expected that the average orientation t of the martensite variants equals the loading direction. It is additionally assumed for simplicity that the phase transformation initiates if the austenitic stress exceeds a given threshold value.

The distribution of the local stress component σ^{γ}_{xx} after phase transformation is illustrated in Figure 5.9, whereas in Figure 5.10 the xx-, yy-, and zz-components of the stress tensor within the center of the transformed domain are plotted against the corresponding strains. Both figures show that the average magnitudes of the phase specific stresses cannot be regarded as comparable. In particular, the magnitude of the stress component into the loading direction, i.e., the x-direction, instantaneously decreases on the initiation of the phase transformation, instead of remaining constant. This reflects the support of the transformed domain by the surrounding structure. Nevertheless, a moderate inelastic deformation resulting from the instantaneous phase transformation can be observed, indicating the existence of a snap-through-like problem. Both results support the considerations above in which the two approaches (5.29) and (5.30) are regarded as limiting cases.

The strain-stress relations in Figure 5.10 may be predicted by the approaches for the intrinsic stresses considered so far. In doing so, the parameter η may be estimated and the inelastic strain arising from the phase transformation may be analyzed. On adopting (5.31)

$$\sigma^{M} = \sigma^{A} - \eta\,\sigma_0 \quad , \tag{5.33}$$

together with (5.32$_2$), the total martensitic strain is obtained as

$$\varepsilon^{M} = \mathbb{C}^{-1} : (\sigma^{A} + (1 - \eta)\,\sigma_0) \quad , \tag{5.34}$$
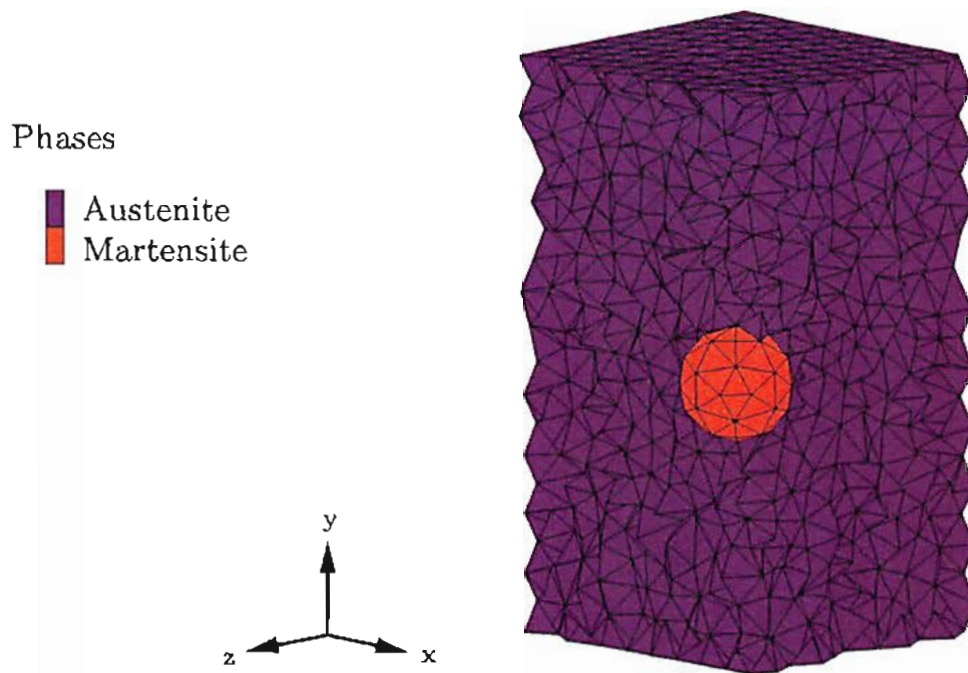
Figure 5.8: Phase distribution inside one-fourth of the representative volume element after phase transformation
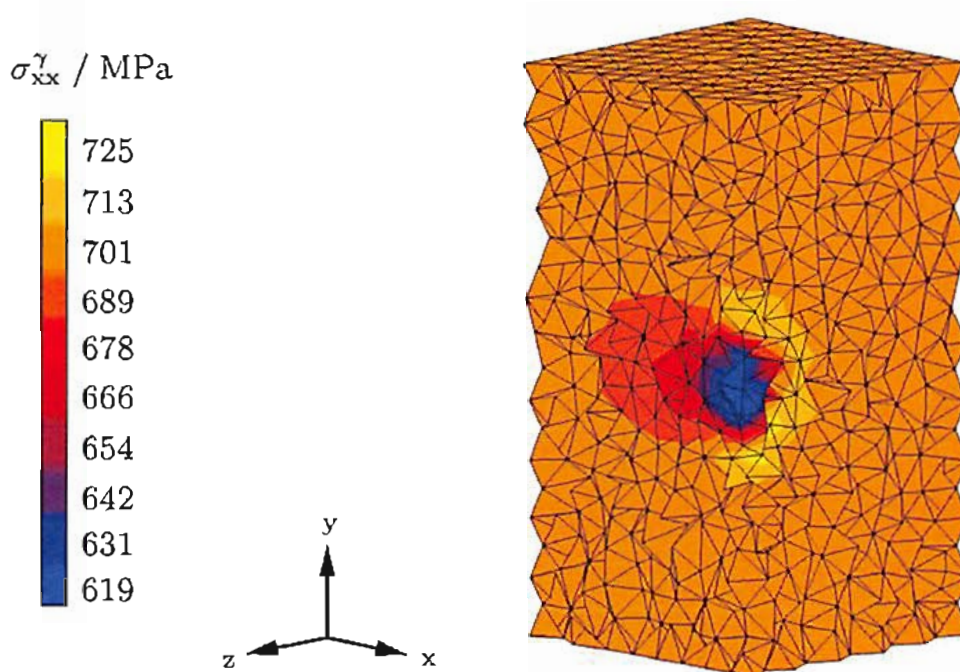
Figure 5.9: Distribution of the intrinsic stresses σ_{xx}^{γ} after phase transformation
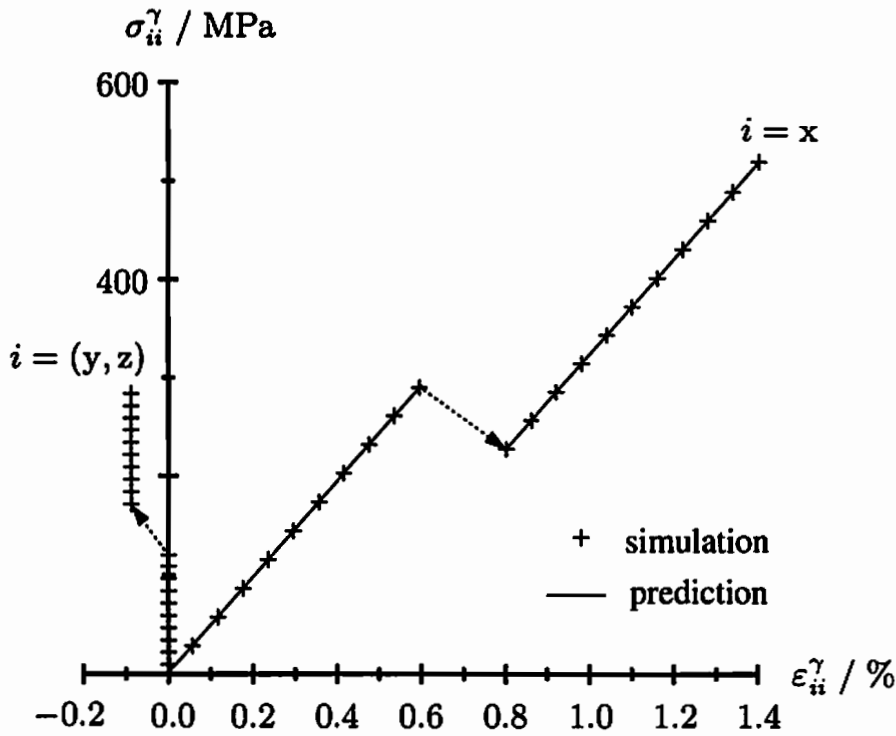
Figure 5.10: Strain-stress relations inside the transformation region for the directions $i = (x, y, z)$

such that σ^M and ε^M can be determined for given σ^A and σ_0. Analogously, with (5.32$_1$), the total austenitic strain in terms of σ^A reads

$$\varepsilon^A = \mathbb{C}^{-1} : \sigma^A \quad . \tag{5.35}$$

Among both quantities σ^A and σ_0, the latter may be set equivalent to the loading direction with the regard to the example considered above. Then, on noting that the austenitic stresses are, in average, unaffected by the phase transformation, the predicted results in Figure 5.10 may be obtained, for which η equals 0.6. Evidently, this value is just in-between the limiting cases $\eta = 0$ and $\eta = 1$. Also, the inelastic strain ε^{AM} of the snap-through-like problem can be quantified within the underlying geometrically linear framework as

$$\varepsilon^{AM} = \varepsilon^M - \varepsilon^A = (1 - \eta)\mathbb{C}^{-1} : \sigma_0 \quad . \tag{5.36}$$

This strain is illustrated in Figure 5.11. It may be inferred that for $\eta = 1$ the austenitic and martensitic strains are equivalent, which corresponds to the *Voigt bound* (e.g., see Doghri (2000)). Accordingly, $\eta = 0$ provides equivalent intrinsic stresses in analogy to the *Reuß bound*.

5.3.2   Total stretching

In order to derive a relation for the total stretching tensor, consider a representative volume element dv consisting of the two parts dv^A and dv^M of austenite
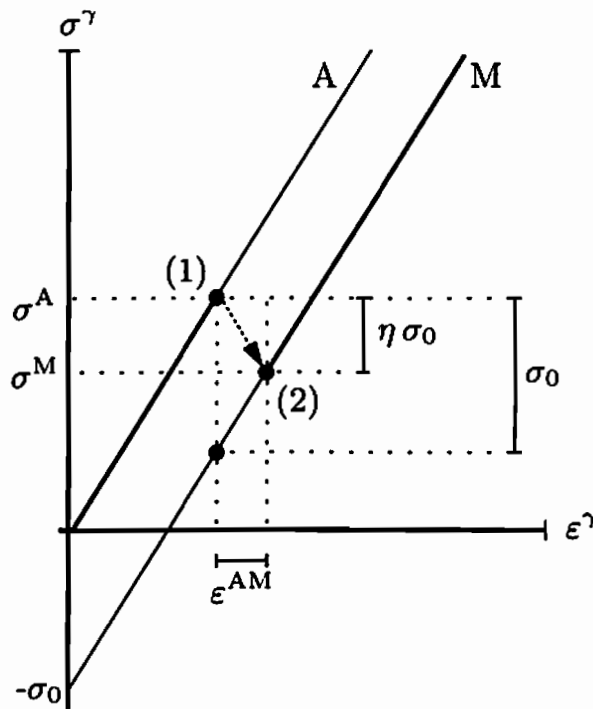
Figure 5.11: Material behavior of the single phases and phase transformation strain ε^{AM} arising from the snap-through-like problem due to the phase transformation from point (1) to point (2)

and martensite under a general deformation process. The rate of change of $\mathrm{d}v$ is then given by

$$(\mathrm{d}v)^{\cdot} = (\mathrm{d}v^{A})^{\cdot} + (\mathrm{d}v^{M})^{\cdot} \quad , \tag{5.37}$$

with $(\cdot)^{\cdot}$ denoting the material time derivative of $(\cdot)$. On adopting (3.24), (5.37) can be recast into

$$\mathrm{tr}\left(\mathrm{d}v\,\mathbf{D}\right) = \mathrm{tr}\left(\mathrm{d}v^{A}\,\mathbf{D}^{A} + \mathrm{d}v^{M}\,\mathbf{D}^{M}\right) \quad . \tag{5.38}$$

Motivated by this relation, it is convenient to define the total stretching tensor as weighted sum of the total intrinsic stretching tensors as

$$\mathbf{D} = \xi\,\mathbf{D}^{M} + (1 - \xi)\,\mathbf{D}^{A} \quad . \tag{5.39}$$

Here, the equality of the intrinsic densities is exploited, so that the volume fractions and mass fractions coincide. The intrinsic stretching tensors may be derived from the intrinsic Hencky strain tensors by virtue of the logarithmic rate. In this context, the total thermoelastic austenitic strain may be obtained from equations (5.8), (5.11), and (5.28) as

$$\mathbf{h}^{A} = \mathbb{C}^{-1} : \tau^{A} + \alpha\,(\Theta - \Theta_{0}) \quad . \tag{5.40}$$

Analogously, application of (5.21), (5.25), and (5.31) shows that

$$\mathbf{h}^{\mathrm{M}} = \mathbb{C}^{-1} : (\tau^{\mathrm{A}} + (1 - \eta)\,\tau_0\,\mathbf{t}) + \boldsymbol{\alpha}\,(\Theta - \Theta_0) \quad . \tag{5.41}$$

Taking the logarithmic rate of these quantities then gives

$$\mathbf{D}^{\mathrm{A}} = \mathbb{C}^{-1} : \overset{\circ}{\tau}{}^{\mathrm{A\,Log}} + \boldsymbol{\alpha}\,\dot{\Theta} \tag{5.42}$$

for austenite and

$$\mathbf{D}^{\mathrm{M}} = \mathbb{C}^{-1} : \overset{\circ}{\tau}{}^{\mathrm{A\,Log}} + \boldsymbol{\alpha}\,\dot{\Theta} + (1 - \eta)\,\tau_0\,\mathbb{C}^{-1} : \overset{\circ}{\mathbf{t}}{}^{\mathrm{Log}} \tag{5.43}$$

for martensite. Evidently, equation (5.42) can be replaced in (5.43), which provides a relation for $\mathbf{D}^{\mathrm{M}}$ in terms of $\mathbf{D}^{\mathrm{A}}$ as

$$\mathbf{D}^{\mathrm{M}} = \mathbf{D}^{\mathrm{A}} + (1 - \eta)\,\tau_0\,\mathbb{C}^{-1} : \overset{\circ}{\mathbf{t}}{}^{\mathrm{Log}} \quad . \tag{5.44}$$

It may be inferred that both intrinsic stretching tensors are equivalent for purely thermoelastic deformations. This is in accordance with experimental data provided by Šittner et al. (2006b) obtained during a neutron diffraction analysis. Since the austenitic phase is assumed to be purely thermoelastic, it follows for the elastic part of the martensitic stretching tensor that

$$\mathbf{D}^{\mathrm{el\,M}} = \mathbf{D}^{\mathrm{A}} \quad . \tag{5.45}$$

Up to this point, phase transformations are not included into the total stretching tensor. In this regard, equation (5.39) is amended by a term $\mathbf{D}^{\mathrm{tr}}$ to express transformational stretchings

$$\mathbf{D} = \xi\,\mathbf{D}^{\mathrm{M}} + (1 - \xi)\,\mathbf{D}^{\mathrm{A}} + \mathbf{D}^{\mathrm{tr}} \quad . \tag{5.46}$$

Motivated by the previous section, $\mathbf{D}^{\mathrm{tr}}$ is set proportional to the local inelastic deformations considered in (5.36), and it is related to the corresponding amount of martensite nucleating during the ongoing phase transformation as

$$\mathbf{D}^{\mathrm{tr}} = \dot{\xi}\,\left[(1 - \eta)\,\mathbb{C}^{-1} : \tau_0\right] \quad . \tag{5.47}$$

On substituting equations (5.44) and (5.47) into (5.46), the total stretching can then be recast into

$$\mathbf{D} = \mathbf{D}^{\mathrm{A}} + \xi\,(1 - \eta)\,\tau_0\,\mathbb{C}^{-1} : \overset{\circ}{\mathbf{t}}{}^{\mathrm{Log}} + (1 - \eta)\,\tau_0\,\mathbb{C}^{-1} : \mathbf{t}\,\dot{\xi} \quad . \tag{5.48}$$

The first term on the right-hand side expresses total thermoelastic deformations of the material, i.e.,

$$\mathbf{D}^{\mathrm{el}} = \mathbf{D}^{\mathrm{A}} \quad , \tag{5.49}$$

whereas the second and third terms account for deformations arising from reorientations of the martensite variants and from phase transformations, respectively. The latter terms describe inelastic deformations as

$$\mathbf{D}^{\text{in}} = \xi \left(1 - \eta\right) \tau_0 \, \mathbf{C}^{-1} : \overset{\circ}{\mathbf{t}}{}^{\text{Log}} + \left(1 - \eta\right) \tau_0 \, \mathbf{C}^{-1} : \mathbf{t} \, \dot{\xi} \quad . \tag{5.50}$$

Thus, $\mathbf{D}$ can additively be decomposed into

$$\mathbf{D} = \mathbf{D}^{\text{el}} + \mathbf{D}^{\text{in}} \quad . \tag{5.51}$$

It should be noted that the inelastic stretching tensor introduced here does not account for inelastic deformations resulting from damage or plasticity. Nevertheless, on defining an additional adequate stretching tensor which is added to (5.50), these deformations may be included. It also bears emphasis that the derivations leading to equations (5.42) and (5.43) underlie the assumption of identical logarithmic spin tensors for austenite and martensite. This may be justified on assigning both phases to the same material particle.

5.3.3   Total stress and total stress rate

The total stress tensor may be obtained from equation of state (4.82_2) as

$$\tau = \rho_0 \, \mathbb{C} : \frac{\partial \psi}{\partial \tau} \quad . \tag{5.52}$$

Replacing (5.3), (5.9), as well as (5.12), and noting (5.10) and (5.11) lead to

$$\tau = \left(1 - \xi\right) \tau^{\text{A}} : \frac{\partial \tau^{\text{A}}}{\partial \tau} + \xi \, \tau^{\text{M}} : \frac{\partial \tau^{\text{M}}}{\partial \tau} \quad . \tag{5.53}$$

Moreover, from the approach (5.31) for the martensitic stress follows that

$$\frac{\partial \tau^{\text{M}}}{\partial \tau} = \frac{\partial \tau^{\text{A}}}{\partial \tau} \quad \text{and} \quad \frac{\partial \tau^{\text{M}}}{\partial \tau^{\text{A}}} = \mathbb{I} \quad . \tag{5.54}$$

Substitution of (5.54_1) into (5.53) and differentiating the result with respect to τ^{A} thereafter then yields, along with (5.54_2), to

$$\frac{\partial \tau}{\partial \tau^{\text{A}}} = \frac{\partial \tau^{\text{A}}}{\partial \tau} \quad . \tag{5.55}$$

Here, use is made of the identity

$$\frac{\partial^2 \tau^{\text{A}}}{\partial \tau^{\text{A}} \, \partial \tau} = \frac{\partial}{\partial \tau} \left(\frac{\partial \tau^{\text{A}}}{\partial \tau^{\text{A}}} \right) = \mathbb{O} \quad , \tag{5.56}$$

with $\mathbb{O}$ denoting the fourth-order zero tensor. In addition, since $\mathbf{D}^{\text{el}} = \mathbf{D}^{\text{A}}$, it may be deduced that

$$\frac{\partial \tau}{\partial \tau^{\text{A}}} = \mathbb{I} \quad . \tag{5.57}$$

Accordingly, the following identities hold true

$$\frac{\partial \tau^{\mathrm{M}}}{\partial \tau} = \frac{\partial \tau^{\mathrm{A}}}{\partial \tau} = \mathbb{I} \quad . \tag{5.58}$$

Application of (5.53) then shows that the total stress equals the weighted phase specific stresses

$$\tau = (1 - \xi)\,\tau^{\mathrm{A}} + \xi\,\tau^{\mathrm{M}} \quad . \tag{5.59}$$

With (5.31), the austenitic stress becomes

$$\tau^{\mathrm{A}} = \tau + \eta\,\xi\,\tau_0\,\mathbf{t} \quad , \tag{5.60}$$

whereas the martensitic stress takes the form

$$\tau^{\mathrm{M}} = \tau - \eta\,(1 - \xi)\,\tau_0\,\mathbf{t} \quad . \tag{5.61}$$

In regard of the preceding findings, the total stress rate can be quantified. Taking the logarithmic rate of (5.60)

$$\overset{\circ}{\tau}{}^{\mathrm{Log}} = \overset{\circ}{\tau}{}^{\mathrm{A\,Log}} - \eta\,\dot{\xi}\,\tau_0\,\mathbf{t} - \eta\,\xi\,\tau_0\,\overset{\circ}{\mathbf{t}}{}^{\mathrm{Log}} \quad , \tag{5.62}$$

solving (5.42) for the austenitic stress rate, and substituting the result into (5.62) yields

$$\overset{\circ}{\tau}{}^{\mathrm{Log}} = \mathbb{C} : (\mathbf{D}^{\mathrm{A}} - \alpha\,\dot{\Theta}) - \eta\,\tau_0\,\mathbf{t}\,\dot{\xi} - \eta\,\xi\,\tau_0\,\overset{\circ}{\mathbf{t}}{}^{\mathrm{Log}} \quad . \tag{5.63}$$

This can be rewritten on employing (5.48) as

$$\overset{\circ}{\tau}{}^{\mathrm{Log}} = \mathbb{C} : \left(\mathbf{D} - \alpha\,\dot{\Theta}\right) - \tau_0\,\mathbf{t}\,\dot{\xi} - \xi\,\tau_0\,\overset{\circ}{\mathbf{t}}{}^{\mathrm{Log}} \quad . \tag{5.64}$$

Equation (5.64) expresses the total stress rate in terms of the total stretching tensor, the temperature rate, and the rates of the internal variables.

It bears emphasis that, with the relations for the total stretching tensor and the total stress tensor at hand, and in agreement with (4.32), the total stress power defined in (4.58) can additively be decomposed into an elastic part and an inelastic part according to

$$p_{\mathrm{i}} = \frac{1}{\rho_0}\,\tau : \mathbf{D} = \frac{1}{\rho_0}\,\left[(1 - \xi)\,\tau^{\mathrm{A}} + \xi\,\tau^{\mathrm{M}}\right] : \left[\mathbf{D}^{\mathrm{el}} + \mathbf{D}^{\mathrm{in}}\right]$$

$$= (1 - \xi)\,\frac{1}{\rho_0}\,\tau^{\mathrm{A}} : \mathbf{D}^{\mathrm{A}} + \xi\,\frac{1}{\rho_0}\,\tau^{\mathrm{M}} : \mathbf{D}^{\mathrm{el\,M}} + \frac{1}{\rho_0}\,\tau : \mathbf{D}^{\mathrm{in}} \tag{5.65}$$

$$= (1 - \xi)\,p_{\mathrm{i}}^{\mathrm{el\,A}} + \xi\,p_{\mathrm{i}}^{\mathrm{el\,M}} + p_{\mathrm{i}}^{\mathrm{in}} = p_{\mathrm{i}}^{\mathrm{el}} + p_{\mathrm{i}}^{\mathrm{in}} \quad .$$

Here, use is made of equations (5.45), (5.49), (5.51), and (5.59). $p_{\mathrm{i}}^{\mathrm{el}}$ and $p_{\mathrm{i}}^{\mathrm{in}}$ denote the elastic and inelastic stress power, respectively.

5.4   Equilibrium states

If the total stress is taken as externally controlled quantity, the minimum of the total specific Helmholtz free energy in a state of equilibrium is governed by the following constraint minimization problem (see (5.3) and (5.59))

$$(1 - \xi)\,\psi^{\mathrm{A}} + \xi\,\psi^{\mathrm{M}} + \xi\,(1 - \xi)\,A \to \min \quad , \tag{5.66}$$

subject to

$$\tau = (1 - \xi)\,\tau^{\mathrm{A}} + \xi\,\tau^{\mathrm{M}} \quad . \tag{5.67}$$

Therewith, the coherency coefficient A can be estimated. In this context, $A(\Theta, t)$ is replaced by the more general formulation $\bar{A}(\Theta, \tau^{\mathrm{A}}, \tau^{\mathrm{M}})$ which reflects that the elastic misfits and elastic interactions of the single phases affecting the interfacial energy are dominated by the local stress field. Then, on adopting the *method of Lagrange multipliers* in the same line as demonstrated in Müller (1989), the constraint minimization problem above can be recast into the relaxed minimization problem of the form

$$\mathcal{L}(\Theta, \tau^{\mathrm{A}}, \tau^{\mathrm{M}}, \xi) = (1 - \xi)\,\psi^{\mathrm{A}} + \xi\,\psi^{\mathrm{M}} + \xi\,(1 - \xi)\,\bar{A}$$

$$- \lambda : \left[(1 - \xi)\,\tau^{\mathrm{A}} + \xi\,\tau^{\mathrm{M}} - \tau\right] \to \min \quad . \tag{5.68}$$

The second-order tensor λ denotes the *Lagrange multiplier*. As the solution of problem (5.68) requires zero partial derivatives of $\mathcal{L}$, the derivatives with respect to the intrinsic stresses, expressing the mechanical equilibrium, give

$$\frac{\partial \mathcal{L}}{\partial \tau^{\mathrm{A}}} \overset{!}{=} 0 \quad \Rightarrow \quad \lambda = \frac{1}{\rho_0}\,\tau^{\mathrm{A}} : \mathbb{C}^{-1} + \xi\,\frac{\partial \bar{A}}{\partial \tau^{\mathrm{A}}}$$

$$\frac{\partial \mathcal{L}}{\partial \tau^{\mathrm{M}}} \overset{!}{=} 0 \quad \Rightarrow \quad \lambda = \frac{1}{\rho_0}\,\tau^{\mathrm{M}} : \mathbb{C}^{-1} + (1 - \xi)\,\frac{\partial \bar{A}}{\partial \tau^{\mathrm{M}}} \tag{5.69}$$

and equating both relations yields

$$(1 - \xi)\,\frac{\partial \bar{A}}{\partial \tau^{\mathrm{M}}} - \xi\,\frac{\partial \bar{A}}{\partial \tau^{\mathrm{A}}} = \frac{1}{\rho_0}\,(\tau^{\mathrm{A}} - \tau^{\mathrm{M}}) : \mathbb{C}^{-1} \quad . \tag{5.70}$$

It may be expected that, on the one hand, the intrinsic stresses affect the interfacial energy in a similar manner and that, on the other hand, their influences are governed by the internal material structure. In this vein the following equivalences may be assumed

$$\left|\frac{\partial A}{\partial t}\right| = \left|\frac{\partial \bar{A}}{\partial \tau^{\mathrm{M}}}\right| = \left|\frac{\partial \bar{A}}{\partial \tau^{\mathrm{A}}}\right| \quad . \tag{5.71}$$

They provide two approaches for the partial derivative $\partial A/\partial t$ which differ in the sign. Considering first the case

$$\frac{\partial A}{\partial t} = \frac{\partial \bar{A}}{\partial \tau^{\mathrm{M}}} = \frac{\partial \bar{A}}{\partial \tau^{\mathrm{A}}} \quad , \tag{5.72}$$

together with relations (5.25) and (5.31) for the martensitic stress, yields

$$\frac{\partial A}{\partial t} = \left[\frac{1}{\rho_0}\, \eta\, \tau_0\, \mathbf{t} : \mathbb{C}^{-1}\right] \frac{1}{1-2\xi} \quad . \tag{5.73}$$

The step between equations (5.70) and (5.73) may mathematically be regarded as substitution $(\tau^{\mathrm{A}}, \tau^{\mathrm{M}}) \rightarrow \mathbf{t}$. Obviously, the derivative $\partial A/\partial t$ is singular for $\xi = 0.5$ and it changes its sign in the vicinity of $\xi = 0.5$. Since this result may not be regarded as physically sound, (5.72) is replaced by the alternative approach for $\partial A/\partial t$ as

$$\frac{\partial A}{\partial t} = \frac{\partial \bar{A}}{\partial \tau^{\mathrm{M}}} = -\frac{\partial \bar{A}}{\partial \tau^{\mathrm{A}}} \tag{5.74}$$

which provides the constant expression in ξ

$$\frac{\partial A}{\partial t} = \frac{1}{\rho_0}\, \eta\, \tau_0\, \mathbf{t} : \mathbb{C}^{-1} \quad . \tag{5.75}$$

Integration of (5.75) with respect to $\mathbf{t}$ then gives

$$A = \frac{1}{2\,\rho_0}\, \eta\, \tau_0\, \mathbf{t} : \mathbb{C}^{-1} : \mathbf{t} + a_0 \quad , \tag{5.76}$$

with the integration constant $a_0(\Theta)$ possibly depending on the temperature. The dependence of A on τ_0 and $\mathbf{t}$ demonstrates the explicit property of the coherency coefficient as being directly related to the internal structure of the material. However, since $\mathbb{C}$ is isotropic and $\mathbf{t}$ is deviatoric and normalized, such that

$$\mathbb{C}^{-1} : \mathbf{t} = \frac{1}{2\,\mu}\, \mathbf{t} \quad \text{and} \quad \mathbf{t} : \mathbb{C}^{-1} : \mathbf{t} = \frac{1}{2\,\mu} \quad , \tag{5.77}$$

A turns out to be independent of $\mathbf{t}$. With respect to the temperature dependence of A it is then assumed, in line with Raniecki et al. (1992), that A is linear in Θ. Accordingly, the coherency coefficient takes the form

$$A = A_1 + A_2\, \Theta \quad , \tag{5.78}$$

with the material parameters A_1 and A_2.

The partial derivative of the minimization problem (5.68) with respect to ξ, reflecting phase equilibrium, reads

$$\frac{\partial \mathcal{L}}{\partial \xi} = 0 \quad \Rightarrow \quad \psi^{\mathrm{M}} - \psi^{\mathrm{A}} + (1-2\xi)\, A - \boldsymbol{\lambda} : (\tau^{\mathrm{M}} - \tau^{\mathrm{A}}) = 0 \quad . \tag{5.79}$$

From this equation, an explicit relation for the mass fraction of martensite can be formulated. Employing (5.69_2), along with (5.61), (5.74), and (5.75), gives the Lagrange multiplier λ as

$$\lambda = \frac{1}{\rho_0}\, \boldsymbol{\tau} : \mathbf{C}^{-1} \quad . \tag{5.80}$$

Then, with equation (5.31), (5.79) can be rearranged into

$$\xi = \frac{1}{2A} \left[\psi^{\mathrm{M}} - \psi^{\mathrm{A}} + \frac{\eta\, \tau_0}{\mu\, \rho_0}\, \boldsymbol{\tau} : \mathbf{t} + A \right] \quad . \tag{5.81}$$

It should be noted that (5.81) expresses the evolution of ξ if the material undergoes a sequence of equilibrium states. This, however, does not hold true for general processes of phase transformation as these processes are characterized by a sequence of meta-stable, in particular non-equilibrium states (cf. Müller & Xu (1991)).

5.5   Thermodynamic consistency

For the description of general deformation processes, the preceding relations have to be complemented by constitutive equations for the heat generation and conduction as well as for the internal variables, namely the mass fraction of martensite ξ and the average orientation of the martensite variants $\mathbf{t}$. In doing so, the restrictions imposed by thermodynamics have to be obeyed to ensure physical consistency as considered in Section 4.4. In this regard, the Clausius-Duhem inequality as crucial thermodynamic relation is first specified to the equations which have been derived in the preceding sections. Then, the transformation kinetics, the reorientation of the martensite variants, as well as the heat generation and conduction are considered. Throughout this section, the variables $\boldsymbol{\tau}$, Θ, ξ, and $\mathbf{t}$ are taken as independent in line with the principle of equipresence stated in Section 4.4.

5.5.1   Clausius-Duhem inequality

As ξ and $\mathbf{t}$ are the only internal variables within the general set ζ, the local form of the Clausius-Duhem inequality (4.83) reduces to

$$\mathcal{D} = \frac{\rho}{\rho_0}\, \boldsymbol{\tau} : \mathbf{D}^{\mathrm{in}} - \rho \left[\frac{\partial \psi}{\partial \xi}\, \dot{\xi} + \frac{\partial \psi}{\partial \mathbf{t}} : \overset{\circ}{\mathbf{t}}{}^{\mathrm{Log}} \right] - \frac{1}{\Theta}\, \mathbf{q} \cdot \nabla\Theta \geq 0 \quad . \tag{5.82}$$

With equations (5.3), (5.9), (5.12), and (5.78) the partial derivative of ψ with respect to ξ can be determined as

$$\frac{\partial \psi}{\partial \xi} = -\psi^{\mathrm{A}} + (1 - \xi) \frac{1}{\rho_0} \tau^{\mathrm{A}} : \mathbf{C}^{-1} : \frac{\partial \tau^{\mathrm{A}}}{\partial \xi}$$

$$+ \psi^{\mathrm{M}} + \xi \frac{1}{\rho_0} \tau^{\mathrm{M}} : \mathbf{C}^{-1} : \frac{\partial \tau^{\mathrm{M}}}{\partial \xi} + (1 - 2\xi) A \quad , \quad (5.83)$$

whereas the partial derivative of ψ with respect to t reads

$$\frac{\partial \psi}{\partial t} = (1 - \xi) \frac{1}{\rho_0} \tau^{\mathrm{A}} : \mathbf{C}^{-1} : \frac{\partial \tau^{\mathrm{A}}}{\partial t} + \xi \frac{1}{\rho_0} \tau^{\mathrm{M}} : \mathbf{C}^{-1} : \frac{\partial \tau^{\mathrm{M}}}{\partial t} \quad . \quad (5.84)$$

Adopting (5.60) and (5.61) yields

$$\frac{\partial \tau^{\mathrm{A}}}{\partial \xi} = \eta \, \tau_0 \, \mathbf{t} \quad \text{and} \quad \frac{\partial \tau^{\mathrm{M}}}{\partial \xi} = \eta \, \tau_0 \, \mathbf{t} \quad , \quad (5.85)$$

as well as

$$\frac{\partial \tau^{\mathrm{A}}}{\partial t} = \xi \, \eta \, \tau_0 \, \mathbb{I} \quad \text{and} \quad \frac{\partial \tau^{\mathrm{M}}}{\partial t} = -(1 - \xi) \, \eta \, \tau_0 \, \mathbb{I} \quad . \quad (5.86)$$

Therewith, together with the relations (5.31), (5.59), and (5.77$_1$), the partial derivatives of ψ can be recast into

$$\frac{\partial \psi}{\partial \xi} = \frac{\eta \, \tau_0}{2 \, \mu \, \rho_0} \tau : \mathbf{t} + \psi^{\mathrm{M}} - \psi^{\mathrm{A}} + (1 - 2\xi) A \quad (5.87)$$

and

$$\frac{\partial \psi}{\partial t} = \frac{\eta^2 \, \tau_0^2}{2 \, \mu \, \rho_0} \xi \, (1 - \xi) \, \mathbf{t} \quad . \quad (5.88)$$

Thus, substituting (5.50), (5.87), and (5.88) into the Clausius-Duhem inequality (5.82) and noting the identity

$$\mathbf{t} : \overset{\circ}{\mathbf{t}}{}^{\mathrm{Log}} = 0 \quad (5.89)$$

which directly follows from definition (5.25$_2$), give

$$\mathcal{D} = \frac{\rho}{\rho_0} \pi^\xi \, \dot{\xi} + \frac{\rho}{\rho_0} \pi^{\mathbf{t}} : \overset{\circ}{\mathbf{t}}{}^{\mathrm{Log}} - \frac{1}{\Theta} \mathbf{q} \cdot \nabla \Theta \geq 0 \quad . \quad (5.90)$$

$\pi^\xi(\tau, \Theta, \xi, \mathbf{t})$ and $\pi^{\mathbf{t}}(\tau, \Theta, \xi, \mathbf{t})$ denote thermodynamic forces driving phase transformations and reorientations of the martensite variants. They are defined as

$$\pi^\xi = \frac{(1 - 2\eta) \, \tau_0}{2 \, \mu} \tau : \mathbf{t} + \rho_0 \, (\psi^{\mathrm{A}} - \psi^{\mathrm{M}} - (1 - 2\xi) A) \quad (5.91)$$

and

$$\pi^t = \xi \, \frac{(1-\eta)\,\tau_0}{2\,\mu}\,\tau \quad . \tag{5.92}$$

On substituting (5.9) into (5.91), along with equations (5.31) and (5.60), π^ξ can further be specified to

$$\pi^\xi = \frac{(1-\eta)\,\tau_0}{2\,\mu}\,\tau : t - (1-2\xi)\left(\frac{\eta^2\,\tau_0^2}{4\,\mu} + \rho_0\,A\right) + \rho_0\,(\Delta u_0 - \Theta\,\Delta s_0) \quad , \tag{5.93}$$

with

$$\Delta u_0 = u_0^{A} - u_0^{M} \quad \text{and} \quad \Delta s_0 = s_0^{A} - s_0^{M} \quad . \tag{5.94}$$

To ensure physical consistency for the subsequently regarded constitutive equations, it is supposed that the Clausius-Duhem inequality may be written in a stronger form as

$$\mathcal{D} = \mathcal{D}^\xi_{\mathrm{loc}} + \mathcal{D}^t_{\mathrm{loc}} + \mathcal{D}_{\mathrm{con}} \geq 0 \quad , \tag{5.95}$$

with

$$\mathcal{D}^\xi_{\mathrm{loc}} = \frac{\rho}{\rho_0}\,\pi^\xi\,\dot{\xi} \qquad \geq 0$$

$$\mathcal{D}^t_{\mathrm{loc}} = \frac{\rho}{\rho_0}\,\pi^t : \overset{\circ}{t}{}^{\mathrm{Log}} \geq 0 \tag{5.96}$$

$$\mathcal{D}_{\mathrm{con}} = -\frac{1}{\Theta}\,\mathbf{q}\cdot\nabla\Theta \quad \geq 0 \quad .$$

This formulation practically uncouples the convective dissipation and the local dissipation arising from phase transformations and reorientations.

5.5.2 Processes of phase transformation

In agreement with the phase transformation formalism proposed by Raniecki et al. (1992), the thermodynamic driving force associated with phase transformations from austenite to martensite (A $\rightarrow$ M) and from martensite to austenite (M $\rightarrow$ A) is prescribed by two phenomenological functions $k^{A\rightarrow M}(\xi)$ and $k^{M\rightarrow A}(\xi)$ for each transformation process as

$$\pi^\xi \overset{!}{=} k^{A\rightarrow M} \quad \text{and} \quad \pi^\xi \overset{!}{=} k^{M\rightarrow A} \quad . \tag{5.97}$$

Both functions are to be defined in this way, that the rate of the entropy production during processes of phase transformation is non-negative. In doing

$A \to M$		$M \to A$	
$k^{A \to M}$	≥ 0	$k^{M \to A}$	≤ 0
$\displaystyle\lim_{\xi \to 1} k^{A \to M} = \infty$		$\displaystyle\lim_{\xi \to 0} k^{M \to A} = -\infty$	
$k^{A \to M}\big|_{\xi=0} = 0$		$k^{M \to A}\big|_{\xi=1} = 0$	
$\dfrac{\partial k^{A \to M}}{\partial \xi} > 0$		$\dfrac{\partial k^{M \to A}}{\partial \xi} > 0$	

Figure 5.12: Constraints for $k^{A \to M}(\xi)$ and $k^{M \to A}(\xi)$ over $\xi \in [0, 1]$

so, it may be inferred from inequality (5.96$_1$) that π^ξ is non-negative for the $A \to M$ phase transformation for which $\dot{\xi} > 0$, whereas it is non-positive for the $M \to A$ phase transformation with $\dot{\xi} < 0$. Together with relations (5.97), this requires that $k^{A \to M}$ and $k^{M \to A}$ are non-negative and non-positive, respectively. Also, as complete phase transformations do generally not occur for natural processes (see Miyazaki et al. (1981), Brinson et al. (2004), Schmahl et al. (2004)), the absolute value of the driving force for phase transformations may be regarded as large at the end the forward and reverse transformation processes. This can mathematically be realized on demanding the limiting values of $k^{A \to M}$ and $k^{M \to A}$ to reach infinity and minus infinity for $\xi \to 0$ and $\xi \to 1$, respectively. Additionally, formal constraints may be imposed on stipulating that π^ξ vanishes for initiating phase transformations and that $k^{A \to M}$ and $k^{M \to A}$ increase monotonically in ξ.

The preceding considerations lead to the set of constraints over $\xi \in [0, 1]$ summarized in Figure 5.12. They may be fulfilled by the following phenomenological functions

$$k^{A \to M}(\xi) = -a_1\, \xi^{b_1} \ln(1 - \xi) + c_1\, \xi \tag{5.98}$$

and

$$k^{M \to A}(\xi) = a_2\,(1 - \xi)^{b_2} \ln(\xi) - c_2\,(1 - \xi) \quad, \tag{5.99}$$

in which $a_i \geq 0$, $b_i \geq 0$ and $c_i \geq 0$ with $i = (0, 1)$ denote material parameters. These functions are exemplarily depicted in Figure 5.13.

Based on relations (5.97) and on also taking into account states beyond phase transformations, *phase transformation functions* $f^\beta(\pi^\xi, \xi)$ with β represent-
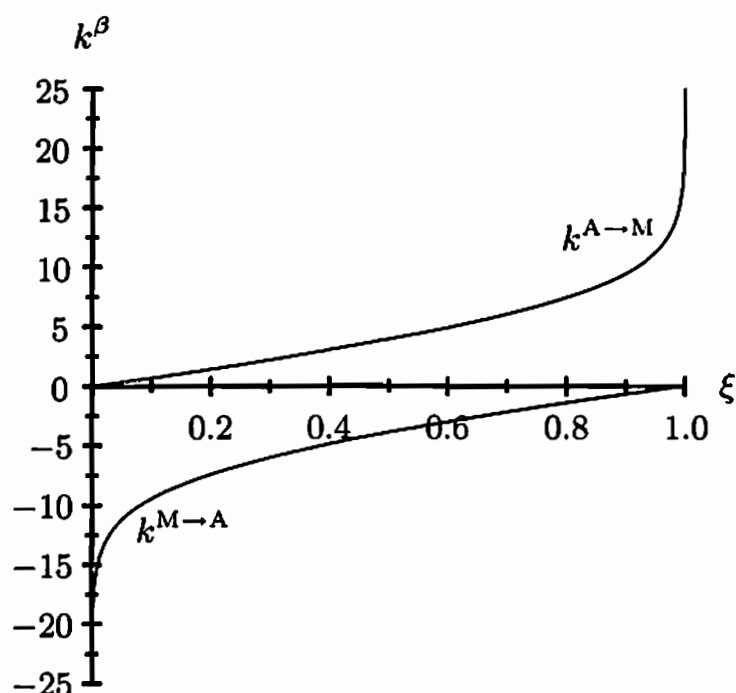
Figure 5.13: Phenomenological functions $k^{A \to M}$ and $k^{M \to A}$

ing $A \to M$ and $M \to A$ may be introduced as:

$$f^\beta = \begin{cases} \pi^\xi - k^{A \to M} \leq 0 & \text{for } A \to M \text{ transformation} \\[2mm] -\pi^\xi + k^{M \to A} \leq 0 & \text{for } M \to A \text{ transformation} \end{cases} \qquad (5.100)$$

These functions separate processes of phase transformation from all other processes such as thermoelastic or reorientation processes.[29] Thus, with (5.97), necessary criteria for the initiation of phase transformations read:

Transformation $A \to M$: $f^{A \to M} = 0$

Transformation $M \to A$: $f^{M \to A} = 0$

$$(5.101)$$

They prove particularly to be necessary but not sufficient, as they are restricted to a current material state and do not consider the current deformation process. Hence, the rates of the phase transformation functions are additionally to be analyzed. In this context, it follows from (5.101) during each process of phase transformation that

$$\dot{f}^\beta = 0 \quad , \qquad (5.102)$$

or, equivalently, that

$$\dot{\pi}^\xi = \dot{k}^\beta \quad , \qquad (5.103)$$

---

[29] Note the analogy to the classical theory of plasticity in which the phase transformation functions correspond to yield functions governing the initiation of plastic deformations.

i.e., f^β is stationary during phase transformations.[30] This finding may be employed to derive an evolution equation for the mass fraction of martensite. On quantifying $\dot{\pi}^\xi$ and $\dot{k}^\beta$ as

$$\dot{\pi}^\xi = \frac{\partial \pi^\xi}{\partial \tau} : \overset{\circ}{\tau}{}^{\text{Log}} + \frac{\partial \pi^\xi}{\partial \Theta} \dot{\Theta} + \frac{\partial \pi^\xi}{\partial t} : \overset{\circ}{t}{}^{\text{Log}} + \frac{\partial \pi^\xi}{\partial \xi} \dot{\xi} \tag{5.104}$$

and

$$\dot{k}^\beta = \frac{\mathrm{d}k^\beta}{\mathrm{d}\xi} \dot{\xi} \quad , \tag{5.105}$$

it turns out, however, that such a derivation requires the determination of an evolution equation for the average orientation of the martensite variants at first. In doing so, the analysis of the correction of t during processes of phase transformation may be helpful. More precisely, during a particular phase transformation process, only these martensite variants are activated which are consistent with the current stress direction (e.g., see Šittner et al. (2006b)). Then, if the stress direction changes during the process of phase transformation, the orientation of the newly activated martensite variants differs from the average orientation of the already existing variants, such that t has to be corrected by a new averaging procedure. In this context, consider a state of the material at time t for which the mass fraction of martensite and the average orientation of the martensite variants are given by $\xi|_t$ and $t|_t$. Assume that the material at time $t + \Delta t$ is loaded into a different direction than $t|_t$, leading to the nucleation of the mass fraction of martensite $\Delta \xi = \xi|_{t+\Delta t} - \xi|_t$ into the current stress direction $s|_{t+\Delta t}$ as regarded in (5.26). The average orientation of the martensite variants at time $t + \Delta t$ then becomes

$$t|_{t+\Delta t} = \frac{\xi|_t \, t|_t + \Delta \xi \, s|_{t+\Delta t}}{\xi|_{t+\Delta t}} \quad . \tag{5.106}$$

On taking the limit $\Delta t \to 0$, the total derivative of t with respect to ξ can be obtained as

$$\frac{\mathrm{d}t}{\mathrm{d}\xi} = \lim_{\Delta t \to 0} \frac{t|_{t+\Delta t} - t|_t}{\Delta \xi} = \frac{s - t}{\xi} \quad . \tag{5.107}$$

Thus, the correction of t during a process of phase transformation is accounted for by the evolution equation

$$\overset{\circ}{t}{}^{\text{Log}} = \frac{s - t}{\xi} \dot{\xi} \quad . \tag{5.108}$$

---

[30]In regard of the analogy to the theory of plasticity, (5.102) may be considered as *consistency criterion* during A → M and M → A phase transformations.

A correction of the average orientation of the martensite variants is only necessary if new martensite variants nucleate, i.e., during an A → M phase transformation. For the M → A phase transformation, however, t may be regarded as constant. Hence, the evolution equation for the average orientation of the martensite variants reads

$$\overset{\circ}{t}{}^{\mathrm{Log}} = \Lambda^\beta \, \dot\xi \quad , \tag{5.109}$$

with:

$$\Lambda^\beta = \begin{cases} \dfrac{s-t}{\xi} & \text{for A} \to \text{M transformation} \\[2mm] 0 & \text{for M} \to \text{A transformation} \end{cases} \tag{5.110}$$

With this finding, a rate equation for the mass fraction of martensite can now be quantified. On substituting (5.104), (5.105), and (5.109) into (5.103) this rate equation reads

$$\dot\xi = \frac{\left.\dot\pi^\xi\right|_{(\xi,\,t)}}{\dfrac{\mathrm{d}k^\beta}{\mathrm{d}\xi} - \dfrac{\partial\pi^\xi}{\partial\xi} - \dfrac{\partial\pi^\xi}{\partial t} : \Lambda^\beta} \quad , \tag{5.111}$$

with $\left.\dot\pi^\xi\right|_{(\xi,\,t)}$ denoting the rate of the driving force at constant ξ and constant t and being defined as

$$\left.\dot\pi^\xi\right|_{(\xi,\,t)} = \frac{\partial\pi^\xi}{\partial\tau} : \overset{\circ}{\tau}{}^{\mathrm{Log}} + \frac{\partial\pi^\xi}{\partial\Theta}\,\dot\Theta \quad . \tag{5.112}$$

The latter quantity particularly complements the criteria for the onset of phase transformations given by (5.101), as an ongoing phase transformation process requires $\left.\dot\pi^\xi\right|_{(\xi,\,t)}$ to be positive or negative for A → M or M → A phase transformations, respectively. Consequently, the complemented criteria (5.101) become:[31]

$$\text{Transformation A} \to \text{M:} \quad f^{\mathrm{A}\to\mathrm{M}} = 0 \quad \wedge \quad \left.\dot\pi^\xi\right|_{(\xi,\,t)} > 0$$
$$\text{Transformation M} \to \text{A:} \quad f^{\mathrm{M}\to\mathrm{A}} = 0 \quad \wedge \quad \left.\dot\pi^\xi\right|_{(\xi,\,t)} < 0 \tag{5.113}$$

To conclude the derivations of a constitutive equation for ξ, the derivatives necessary to quantify (5.111) are left to be evaluated. With respect to (5.78) and (5.93), the rate of the driving force at constant ξ and constant t takes the form

$$\left.\dot\pi^\xi\right|_{(\xi,\,t)} = \frac{(1-\eta)\,\tau_0}{2\,\mu}\, t : \overset{\circ}{\tau}{}^{\mathrm{Log}} - \rho_0 \left((1-2\xi)\,A_2 + \Delta s_0\right)\dot\Theta \tag{5.114}$$

---

[31] Within the context of the analogy to the theory of plasticity, the additional criteria may be regarded as *loading conditions*.

and the partial derivatives $\partial \pi^\xi / \partial \xi$ and $\partial \pi^\xi / \partial t$ become

$$\frac{\partial \pi^\xi}{\partial \xi} = \frac{\eta^2 \tau_0^2}{2\mu} + 2\rho_0 \left(A_1 + A_2 \Theta\right) \tag{5.115}$$

and

$$\frac{\partial \pi^\xi}{\partial t} = \frac{(1-\eta)\,\tau_0}{2\mu}\,\tau \quad . \tag{5.116}$$

Moreover, evaluating the derivatives of the phenomenological functions $k^{A \to M}$ and $k^{M \to A}$ with respect to ξ gives

$$\frac{dk^{A \to M}}{d\xi} = \frac{a_1\,\xi^{b_1}}{1-\xi} - a_1\,b_1\,\xi^{b_1-1}\ln\left(1-\xi\right) + c_1 \tag{5.117}$$

and

$$\frac{dk^{M \to A}}{d\xi} = \frac{a_2\,(1-\xi)^{b_2}}{\xi} - a_2\,b_2\,(1-\xi)^{b_2-1}\ln\left(\xi\right) + c_2 \quad . \tag{5.118}$$

The constitutive equations considered above satisfy the restrictions imposed by thermodynamics, i.e., they comply with the Clausius-Duhem inequality in terms of inequalities ($5.96_{1,2}$). In particular, with the restrictions of the phenomenological functions $k^{A \to M}$ and $k^{M \to A}$ stated in Figure 5.12, inequality (5.96_1) is identically fulfilled for the evolution of the martensitic mass fraction. Moreover, on recalling (5.92), inequality (5.96_2) becomes

$$\mathcal{D}_{\text{loc}}^{\text{t}} = \frac{\rho}{\rho_0}\,\xi\,\frac{(1-\eta)\,\tau_0}{2\mu}\,\tau : \overset{\circ}{\mathbf{t}}{}^{\text{Log}} \geq 0 \quad . \tag{5.119}$$

With the property of $\mathbf{t}$ being deviatoric, together with the definition of $\mathbf{s}$ in (5.26_2), this inequality can be recast into

$$\mathcal{D}_{\text{loc}}^{\text{t}} = \left(\frac{\rho}{\rho_0}\,\xi\,\frac{(1-\eta)\,\tau_0}{2\mu}\,|\tau'|\right)\mathbf{s} : \overset{\circ}{\mathbf{t}}{}^{\text{Log}} \geq 0 \quad . \tag{5.120}$$

The expression in the parentheses is non-negative in general. It is, thus, left to ensure that

$$\mathbf{s} : \overset{\circ}{\mathbf{t}}{}^{\text{Log}} \geq 0 \quad , \tag{5.121}$$

or, equivalently with (5.109), that

$$\mathbf{s} : \mathbf{\Lambda}^\beta\,\dot{\xi} \geq 0 \quad . \tag{5.122}$$

Along with (5.110), this inequality is identically fulfilled for the M $\to$ A phase transformation. For the A $\to$ M phase transformation, for which $\dot{\xi} \geq 0$, the proof of the thermodynamic consistency reduces to

$$\left(1 - \mathbf{s} : \mathbf{t}\right) \geq 0 \quad , \tag{5.123}$$

which is identically fulfilled as

$$-1 \leq s : t \leq 1 \quad . \tag{5.124}$$

For the particular loading case of radial loadings, relations for the initiation and conclusion of phase transformations in terms of the respective critical stresses τ_{eq}^{β} can explicitly be derived from (5.97). In doing so and on replacing relations (5.26) and (5.93) into (5.97), these critical stresses read

$$\tau_{eq}^{\beta} = \frac{2\,\mu\,\rho_0}{(1-\eta)\,\tau_0} \left[(1 - 2\,\xi) \left(\frac{\eta^2\,\tau_0^2}{4\,\mu\,\rho_0} + A \right) - \Delta u_0 + \Theta\,\Delta s_0 + k^{\beta} \right] \quad , \tag{5.125}$$

where the equivalent stress measure τ_{eq} is defined as

$$\tau_{eq} = |\tau'| \quad . \tag{5.126}$$

Then, with (5.78) and on noting that the functions k^{β} only depend on ξ, differentiation of (5.125) with respect to Θ gives

$$\frac{\partial \tau_{eq}^{\beta}}{\partial \Theta} = \frac{2\,\mu\,\rho_0}{(1-\eta)\,\tau_0} \left[(1 - 2\,\xi)\,A_2 + \Delta s_0 \right] \quad . \tag{5.127}$$

It may be deduced that, since (5.127) is constant in temperature, the stress necessary to induce phase transformations increases linearly with increasing temperature. This is in accord with the *Clausius-Clapeyron-like relation* considered, e.g., in Ortín & Planes (1989), Shaw & Kyriakides (1995), and Hayashi et al. (2004). Figure 5.14 exemplarily shows the stresses plotted against the temperature at the initiation and conclusion of A → M or M → A phase
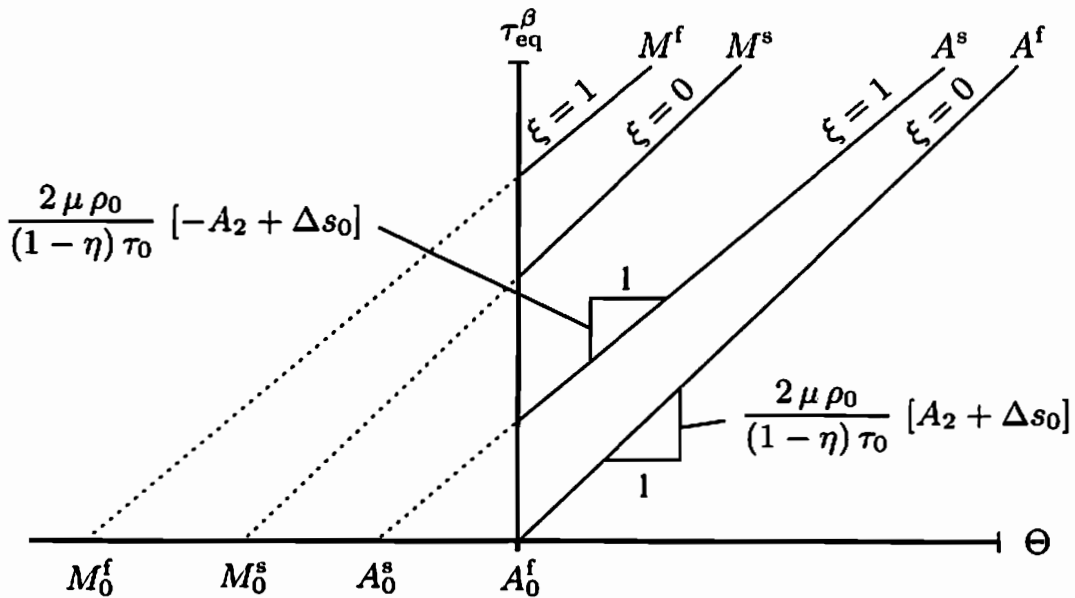
Figure 5.14: Transformation stresses plotted against the temperature

transformations, i.e., for $\xi = 0$ and $\xi = 1$.[32] These curves reflect the stress dependence of the transformation start and finish temperatures M^s and M^f for the A $\to$ M transformation and of the transformation start and finish temperatures A^s and A^f for the M $\to$ A transformation. M_0^s and A_0^s may directly be estimated from (5.125) in the absence of stress by setting τ_{eq}^β and k^β equal to zero. It should also be noted that, since the proposed constitutive model is concerned with pseudoelasticity, only temperatures above A_0^f are in the focus of the present considerations.

5.5.3 Processes of reorientation

In the preceding section, an evolution equation accounting for the correction of t during phase transformation processes is proposed. This relation, however, does not account for reorientations of formerly activated variants during general loadings, as it is based on a reconducted averaging procedure of t for newly activated variants. In this sense, the preceding considerations are complemented in this section by a constitutive relation for t in the case of reorientations of the martensite variants.

Raniecki et al. (1992) set the average orientation of the martensite variants parallel to the current direction of the stress deviator to provide a suggestive approach for t. This approach is essentially based on the experimental observation, that only these martensite variants are activated during radial loadings which are preferred by the respective loading direction. On changing the current stress direction, the approach also implies that the average orientation of the martensite variants changes accordingly, in particular instantaneously. In this case, both, the loading direction and the martensite orientation remain parallel throughout the processes of deformation. It may, however, be inferred from experiments concerned with biaxial loadings of polycrystalline NiTi shape memory alloys carried out, e.g., by Lim & McDowell (1999) and Grabe & Bruhns (2008) that the preceding assumption is to be regarded as rough approximation, i.e., the loading direction and the martensite orientation should not be assumed parallel for general loadings. In this regard, a circle-shaped test conducted by Grabe & Bruhns (2008) spanning all axial and torsional quadrants is exemplarily analyzed more in detail. The biaxial experiment is carried out at a strain controlled rate of $10^{-3}\,\mathrm{s}^{-1}$ under quasi-isothermal conditions. The results are shown in Figure 5.15 for the prescribed axial/torsional strains and in Figure 5.16 for the material response in terms of

---

[32]The microstructure at the end of the pseudoelastic hysteresis is generally not completely martensitic, as it is known from experiments (see Miyazaki et al. (1981), Brinson et al. (2004), Schmahl et al. (2004)). The exact determination of the actual mass fraction of martensite, however, requires sophisticated experimental methods such as neutron deflection or synchrotron radiations (see Bourke et al. (1996), Šittner et al. (2004), Sitepu et al. (2003)). In this sense, the assumption of a complete phase transformation, i.e., the selection $\xi = 1$, is to be regarded as limiting case, until reliable data are available.
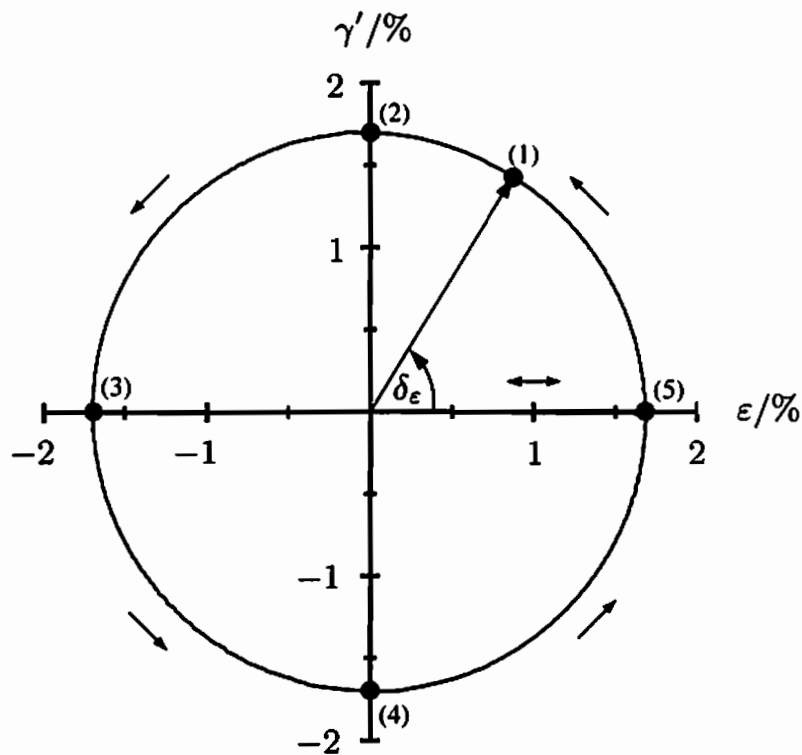
Figure 5.15: Combined circle test; prescribed axial/torsional strains
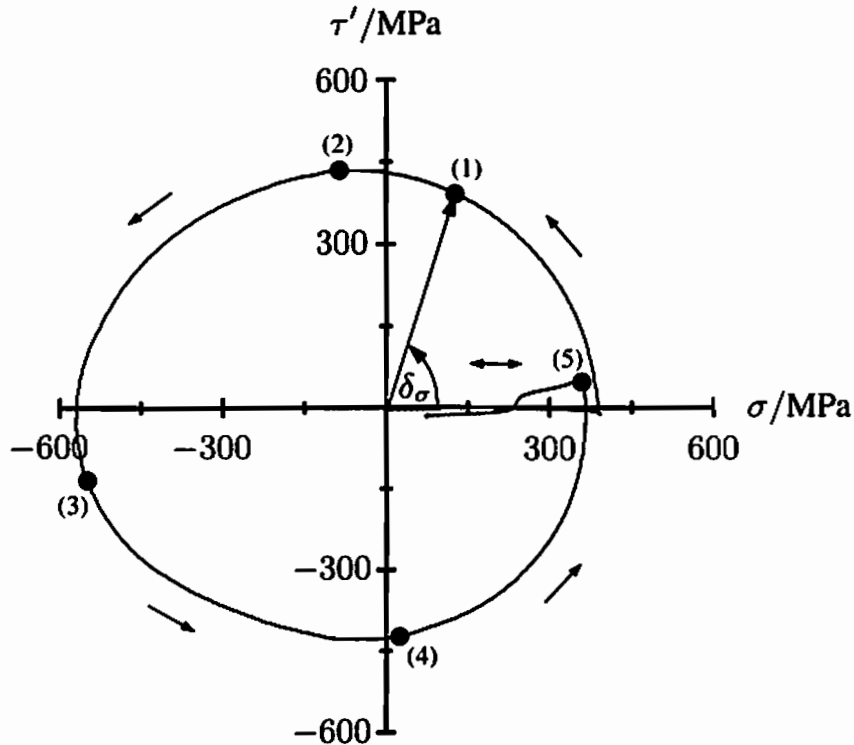
Figure 5.16: Combined circle test; results for axial/torsional stresses

the axial/torsional stresses. In both diagrams, the arrows indicate the loading path. ε and σ denote the tensile strain and the tensile stress, whereas γ' and τ' are defined as

$$\gamma' = \frac{\gamma}{\sqrt{3}} \quad \text{and} \quad \tau' = \sqrt{3}\tau \quad , \tag{5.128}$$

with γ and τ representing the measured shear strain and shear stress, respectively. Note the asymmetry of the axial/torsional stresses in Figure 5.16. It reflects the asymmetric transformation behavior of the material well-known as tension/compression asymmetry. Points (1) to (5) denote the loading sequence. They particularly represent same points in time within both diagrams and can, thus, directly be associated with each other. From this, Grabe & Bruhns (2008) infer that the stress-stress curve is somehow rotated with respect to the strain-strain curve. In other words, it seems that the stress-stress curve anticipates the prescribed strain-strain curve to some extent. The foregoing can also be observed in Figure 5.17 in which the angles δ_ε and δ_σ introduced in Figures 5.15 and 5.16 are plotted against the experimental runtime. It may be concluded from the foregoing that the average orientation of the martensite variants and the stress direction are not parallel, i.e., there exists a degree of freedom between t and s which may be encountered by the
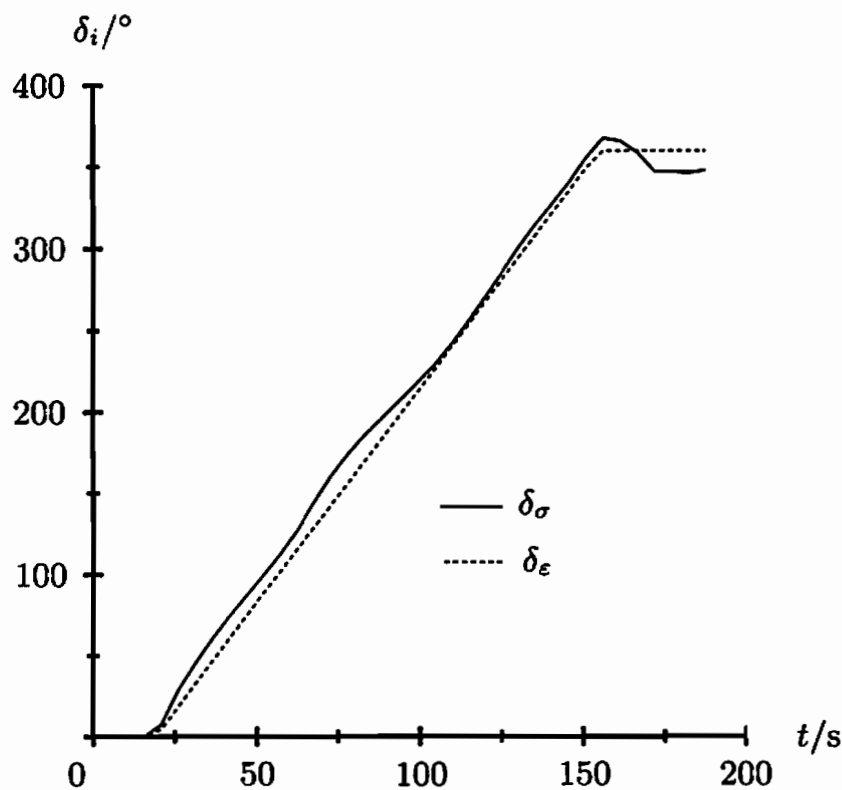
Figure 5.17: Angles δ_ε and δ_σ introduced in Figures 5.15 and 5.16 plotted against the experimental runtime

reorientation function $r(\mathbf{t}, \mathbf{s})$ of the form

$$r = \mathbf{t} : \mathbf{s} \geq \vartheta = \text{const} \quad . \tag{5.129}$$

Here, ϑ denotes a material parameter within the domain $|\vartheta| \leq 1$. The equality in relation (5.129) as limiting case states that the projection of $\mathbf{s}$ on $\mathbf{t}$ remains constant throughout a process of reorientation, such that the maximum admissible deviation between $\mathbf{s}$ and $\mathbf{t}$ is restricted by ϑ. In this sense, it may be inferred that for $\vartheta = 1$ the orientation of the martensite variants and the stress direction are parallel, in particular identical during all deformation processes, as it is assumed in the work of Raniecki et al. (1992).

With r at hand, a first criterion for the initiation of reorientations is given by

$$r = \mathbf{t} : \mathbf{s} = \vartheta \quad . \tag{5.130}$$

It represents a necessary criterion, as it solely reflects a current state of the material and not the current process of deformation. This criterion has, thus, to be amended by the evolution of r which takes the form[33]

$$\dot{r} = \mathbf{t} : \overset{\circ}{\mathbf{s}}{}^{\text{Log}} + \mathbf{s} : \overset{\circ}{\mathbf{t}}{}^{\text{Log}} \quad . \tag{5.131}$$

If reorientations are not initiated, the rate of $\mathbf{t}$ is governed by phase transformations expressed by (5.109). In this case, $\dot{r}$ reads

$$\dot{r} = \mathbf{t} : \overset{\circ}{\mathbf{s}}{}^{\text{Log}} + \mathbf{s} : \boldsymbol{\Lambda}^{\beta} \dot{\xi} \quad . \tag{5.132}$$

If (5.130) additionally holds and $\dot{r}$ as in (5.132) is negative, inequality (5.129) would be violated. This, however, is impeded by the initiation of reorientations. More precisely, $\mathbf{t}$ is adjusted through reorienting martensite variants in this way, that r remains stationary. Then, (5.130) holds throughout the process of deformation and, thus,

$$\dot{r} = \mathbf{t} : \overset{\circ}{\mathbf{s}}{}^{\text{Log}} + \mathbf{s} : \overset{\circ}{\mathbf{t}}{}^{\text{Log}} = 0 \quad . \tag{5.133}$$

Contrariwise, if (5.130) holds and $\dot{r}$ in (5.132) is positive, inequality (5.129) will be obeyed and reorientations do not initiate. Consequently, the criteria for the initiation of reorientations of the martensite variants take the form

$$r = \vartheta \quad \wedge \quad \mathbf{t} : \overset{\circ}{\mathbf{s}}{}^{\text{Log}} + \mathbf{s} : \boldsymbol{\Lambda}^{\beta} \dot{\xi} < 0 \quad . \tag{5.134}$$

An additional criterion results from the requirement of a sufficient stress magnitude to induce reorientations. In the case of pseudoelasticity, this is to be regarded as being implicitly fulfilled.

---

[33]Here, the identities $\mathbf{s} : \overset{\circ}{\mathbf{t}}{}^{\text{Log}} = \mathbf{s} : \dot{\mathbf{t}}$ and $\mathbf{t} : \overset{\circ}{\mathbf{s}}{}^{\text{Log}} = \mathbf{t} : \dot{\mathbf{s}}$ are used.

A formalism for exploiting inequality (5.129) may be obtained on expressing **t** and **s** in their spectral representations as

$$\mathbf{t} = \sum_{i=1}^{3} t_i \, \mathbf{T}_i \quad \text{and} \quad \mathbf{s} = \sum_{i=1}^{3} s_i \, \mathbf{S}_i \quad . \tag{5.135}$$

t_i and s_i denote the eigenvalues of **t** and **s**, and $\mathbf{T}_i$ and $\mathbf{S}_i$ are the respective eigenprojections. For distinct eigenvalues, the latter can be written in terms of the eigenvectors $\mathbf{t}_i$ and $\mathbf{s}_i$ as

$$\mathbf{T}_i = \mathbf{t}_i \otimes \mathbf{t}_i \quad \text{and} \quad \mathbf{S}_i = \mathbf{s}_i \otimes \mathbf{s}_i \quad . \tag{5.136}$$

Here and henceforth, the subscript i equals (1, 2, 3). The reorientation function then becomes

$$r = \sum_{i=1}^{3} t_i \, r_i \geq \vartheta \quad \text{with} \quad r_i = \mathbf{s} : \mathbf{T}_i \quad , \tag{5.137}$$

leading for a process of reorientation to

$$\mathbf{t} : \mathbf{s} = \vartheta \quad \Rightarrow \quad \sum_{i=1}^{3} t_i \, r_i = \vartheta \quad . \tag{5.138}$$

Also, the property of **t** being deviatoric gives

$$\text{tr}\,(\mathbf{t}) = 0 \quad \Rightarrow \quad \sum_{i=1}^{3} t_i = 0 \quad , \tag{5.139}$$

whereas the property of **t** being normalized yields

$$\mathbf{t} : \mathbf{t} = 1 \quad \Rightarrow \quad \sum_{i=1}^{3} t_i^2 = 1 \quad . \tag{5.140}$$

Consequently, for known eigenprojections $\mathbf{T}_i$, the eigenvalues t_i can explicitly be determined from equations (5.138) to (5.140) during a process of reorientation. A deeper insight into this solution may be obtained on adopting the relation

$$t_i = \sqrt{\frac{2}{3}} \, \sin \left(\frac{2\pi i}{3} - \alpha_t \right) \quad , \tag{5.141}$$

which identically fulfills (5.139) and (5.140). Therein, α_t represents an independent variable which uniquely governs all eigenvalues of **t**. In this context and on substituting relation (5.141) into (5.137) as

$$r = \sqrt{\frac{2}{3}} \, \sum_{i=1}^{3} \sin \left(\frac{2\pi i}{3} - \alpha_t \right) r_i \geq \vartheta \quad , \tag{5.142}$$

the reorientation function can graphically be illustrated in terms of α_t if the coefficients r_i are held constant. For the sake of simplicity, the case of **t** and **s** being coaxial is considered first. The coefficients r_i then reduce to s_i, such that the reorientation function becomes

$$r = \sqrt{\frac{2}{3}} \sum_{i=1}^{3} \sin\left(\frac{2\pi i}{3} - \alpha_t\right) s_i \geq \vartheta \quad . \tag{5.143}$$

For constant s_i, (5.143) is visualized in Figure 5.18. It may be inferred that
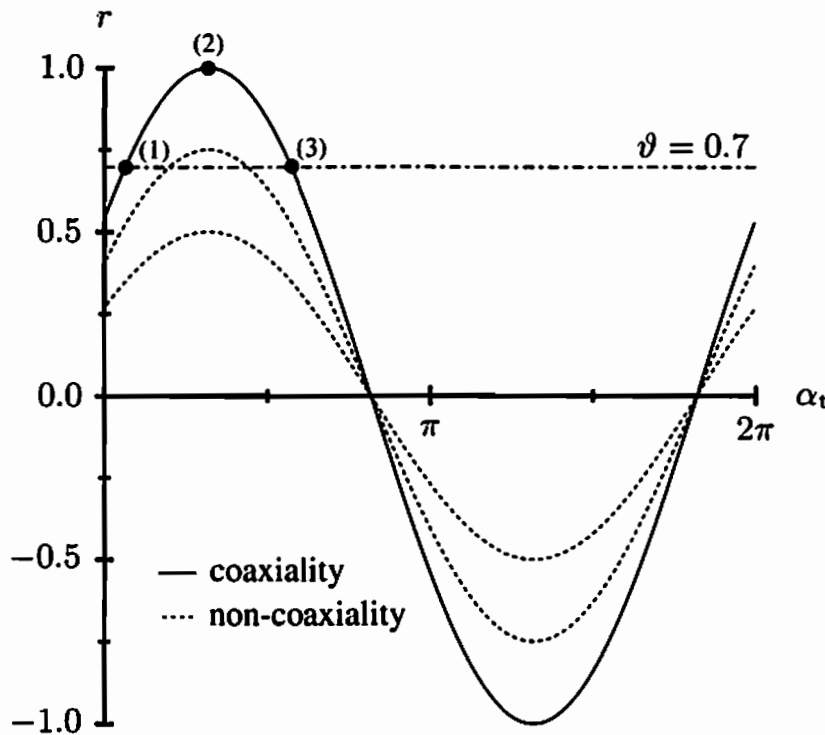
Figure 5.18: Reorientation function r for the cases of coaxiality and non-coaxiality of **t** and **s**; r is shown for two different sets of parameters r_i in the absence of coaxiality.

the solution of (5.138) for α_t is not unambiguous in general if $|\vartheta| < 1$, which is indicated by the points (1) and (3). This ambiguity may be resolved on ensuring the rotation direction between **t** and **s** to be maintained within the principle space during reorientation processes. It can also be observed that the maximum value of r equals 1 as indicated by point (2). In this case, the eigenvalues of **t** and **s** are equivalent and, thus, along with the coaxiality of **t** and **s**, both tensors are parallel, in particular identical. Analogously, the eigenvalues t_i and s_i deviate by their sign for $r = -1$.

Altogether, since $|\vartheta| \leq 1$, a solution of (5.138) always exists for coaxiality of **t** and **s**. This, however, is not the case in the absence of coaxiality. More precisely, if **t** and **s** are not coaxial, the maximum value of r is always smaller than 1, such that a solution of (5.138) is not necessarily guaranteed. This

fact has to be considered in deriving a constitutive equation for the eigenprojections of **t**. In the following, however, coaxiality of **t** and **s** is postulated for simplicity. It should be noted that this postulation implies the eigenprojections of **t** to change instantaneously on changing the eigenprojections of **s** during non-proportional loadings, even for the case of pure phase transformations as considered in the previous section. Although this behavior expresses a reorientation process of the martensite variants to some extent, the term *reorientation* is restricted in the following to the case in which the criteria (5.134) are fulfilled.

Along with equations (5.26_2) and (5.130), the thermodynamic force driving phase transformations given in (5.93) simplifies during reorientations to

$$\pi^{\xi} = \frac{(1-\eta)\,\tau_0\,\vartheta}{2\,\mu}\,|\tau'| - (1-2\,\xi)\left(\frac{\eta^2\,\tau_0^2}{4\,\mu} + \rho_0\,A\right) + \rho_0\,(\Delta u_0 - \Theta\,\Delta s_0) \quad.$$

$$(5.144)$$

On employing the same formalism as in the preceding section, the evolution equation for the mass fraction of martensite can then be derived as

$$\dot{\xi} = \frac{\dot{\pi}^{\xi}\big|_{\xi}}{\dfrac{dk^{\beta}}{d\xi} - \dfrac{\partial \pi^{\xi}}{\partial \xi}} \quad.$$

$$(5.145)$$

The derivatives of π^{ξ}, $k^{A \to M}$, and $k^{M \to A}$ with respect to ξ are given by equations (5.115), (5.117), and (5.118), whereas the rate of the driving force at constant ξ reads

$$\dot{\pi}^{\xi}\big|_{\xi} = \frac{\partial \pi^{\xi}}{\partial \tau} : \overset{\circ}{\tau}{}^{\mathrm{Log}} + \frac{\partial \pi^{\xi}}{\partial \Theta}\,\dot{\Theta}$$

$$(5.146)$$

$$= \frac{(1-\eta)\,\tau_0\,\vartheta}{2\,\mu}\,\mathbf{s} : \overset{\circ}{\tau}{}^{\mathrm{Log}} - \rho_0\left((1-2\,\xi)\,A_2 + \Delta s_0\right)\dot{\Theta} \quad.$$

It may, thus, be inferred that the criteria for the initiation of phase transformations in the case of reorientations take the form:

Transformation A $\to$ M: $\quad f^{A \to M} = 0 \quad \wedge \quad \dot{\pi}^{\xi}\big|_{\xi} > 0$

Transformation M $\to$ A: $\quad f^{M \to A} = 0 \quad \wedge \quad \dot{\pi}^{\xi}\big|_{\xi} < 0$

$$(5.147)$$

Finally, the thermodynamic consistency of the reorientation approach is left to be analyzed, i.e., the approach for **t** has to obey inequality (5.96_2) or, alternatively, the relation (see inequality (5.121))

$$\mathbf{s} : \overset{\circ}{\mathbf{t}}{}^{\mathrm{Log}} \geq 0 \quad.$$

$$(5.148)$$

In this context, equation (5.133) provides the identity

$$\mathbf{s} : \overset{\circ}{\mathbf{t}}{}^{\mathrm{Log}} = -\mathbf{t} : \overset{\circ}{\mathbf{s}}{}^{\mathrm{Log}} \tag{5.149}$$

which holds true during reorientation processes. In addition, the sufficient criterion (5.134_2) for the initiation of reorientations demands

$$\mathbf{t} : \overset{\circ}{\mathbf{s}}{}^{\mathrm{Log}} + \mathbf{s} : \Lambda^\beta \, \dot{\xi} < 0 \quad . \tag{5.150}$$

As the second term on the left-hand side of this inequality is non-negative (see inequality (5.122)), it follows that

$$\mathbf{t} : \overset{\circ}{\mathbf{s}}{}^{\mathrm{Log}} < 0 \quad . \tag{5.151}$$

Consequently, along with (5.149), inequality (5.148) is fulfilled in general, such that the approach for $\mathbf{t}$ considered in this section satisfies the criteria for thermodynamically consistency.

5.5.4 Processes of heat conduction and heat generation

Equations are introduced in Section 4.5 describing the thermomechanically coupled material behavior during processes of deformation in its general form, i.e., in terms of the heat conduction, the heat exchange, and the heat generation. In this regard, constitutive equations for the heat conduction and for the rate of heat generation are left to be defined.

Heat conduction

In the context of a phenomenological theory, the conduction of heat may be encountered by *Fourier's law of heat conduction* (cf. Mills (1999))

$$\mathbf{q} = -k \nabla \Theta \quad . \tag{5.152}$$

The material parameter k is referred to as *thermal conductivity*. For most materials, it may be taken as constant and positive. In this case, Fourier's law of heat conduction identically fulfills the dissipation inequality (5.96_3) as

$$\mathcal{D}_{\mathrm{con}} = -\frac{1}{\Theta} \, \mathbf{q} \cdot \nabla \Theta = \frac{1}{\Theta} \, k \nabla \Theta \cdot \nabla \Theta \geq 0 \quad , \tag{5.153}$$

and it, thus, can be regarded as thermodynamically consistent. (5.152) states that the transport of heat is linked with the steepest descent of the temperature field, i.e., heat can only be transferred from warm to cold. Substitution of (5.152) into (4.91) then leads to the *heat conduction equation* of the form

$$c \, \dot{\Theta} \, \rho = \nabla \cdot (k \nabla \Theta) + r \, \rho + q_{\mathrm{gen}} \, \rho \quad . \tag{5.154}$$

Heat generation

The term q_{gen} in equation (5.154) accounts for the specific heat generated during processes of deformation. It may be specified on adopting (4.101), with ξ and t being the only internal variables in the general set ζ. Then, noting that the tensor of thermal expansion coefficients given by equations (5.5$_2$) and (5.11$_2$), leads to

$$q_{\text{gen}} = \Theta \left(\frac{\partial^2 \psi}{\partial \Theta \, \partial \tau} - \frac{1}{\rho_0} \, \alpha \, \mathbf{I} \right) : \overset{\circ}{\tau}{}^{\text{Log}} + \left(\Theta \, \frac{\partial^2 \psi}{\partial \Theta \, \partial \xi} - \frac{\partial \psi}{\partial \xi} \right) \dot{\xi}$$

$$+ \left(\Theta \, \frac{\partial^2 \psi}{\partial \Theta \, \partial t} - \frac{\partial \psi}{\partial t} \right) : \overset{\circ}{t}{}^{\text{Log}} + \frac{1}{\rho_0} \, \tau : \mathbf{D}^{\text{in}} \quad . \quad (5.155)$$

The derivatives of ψ with respect to ξ and t are formulated in (5.87) and (5.88). In particular, with equations (5.9), (5.31), (5.60), and (5.78), the derivative (5.87) takes the form

$$\frac{\partial \psi}{\partial \xi} = \left(\frac{\eta^2 \, \tau_0^2}{4 \, \mu \, \rho_0} + (A_1 + A_2 \, \Theta) \right) (1 - 2\xi) - \Delta u_0 + \Theta \, \Delta s_0 \quad . \quad (5.156)$$

Therewith, the following mixed partial derivatives can be obtained

$$\frac{\partial^2 \psi}{\partial \Theta \, \partial \xi} = (1 - 2\,\xi) A_2 + \Delta s_0 \quad\quad\quad\quad (5.157)$$

and

$$\frac{\partial^2 \psi}{\partial \Theta \, \partial t} = \mathbf{0} \quad . \quad\quad\quad\quad (5.158)$$

Moreover, application of relations (4.82$_2$) and (5.11$_1$) shows that

$$\frac{\partial^2 \psi}{\partial \Theta \, \tau} = \mathbf{0} \quad . \quad\quad\quad\quad (5.159)$$

Consequently, on substituting equations (5.50), (5.88), and (5.156) to (5.159) into relation (5.155), and on recalling (5.77$_1$) and (5.89), the specific generated heat can be written as

$$q_{\text{gen}} = \bar{\mathbf{q}}_{\text{gen}}^{\tau} : \overset{\circ}{\tau}{}^{\text{Log}} + \bar{q}_{\text{gen}}^{\xi} \, \dot{\xi} + \bar{\mathbf{q}}_{\text{gen}}^{t} : \overset{\circ}{t}{}^{\text{Log}} \quad , \quad (5.160)$$

with

$$\bar{\mathbf{q}}_{\text{gen}}^{\tau} = -\frac{1}{\rho_0} \, \alpha \, \Theta \, \mathbf{I}$$

$$\bar{q}_{\text{gen}}^{\xi} = \frac{1 - \eta}{2 \, \mu \, \rho_0} \, \tau_0 \, \tau : t - \left(\frac{\eta^2 \, \tau_0^2}{4 \, \mu \, \rho_0} + A_1 \right) (1 - 2\xi) + \Delta u_0 \quad (5.161)$$

$$\bar{\mathbf{q}}_{\text{gen}}^{t} = \frac{1 - \eta}{2 \, \mu \, \rho_0} \, \tau_0 \, \xi \, \tau \quad .$$

The quantities $\bar{\mathbf{q}}_{\text{gen}}^{\tau}$, $\bar{q}_{\text{gen}}^{\xi}$, and $\bar{\mathbf{q}}_{\text{gen}}^{t}$ govern the specific generated heat related to stress, mass fraction of martensite, and reorientation of the martensite variants, respectively.

5.6 Summary of the material model

This section summarizes the essential relations of the proposed material model. Basic equations of the model, e.g., concerning the stress rate and the generation of heat are given in Figure 5.19. The constitutive equations for the internal variables as well as the criteria for phase transformations are reflected in Figure 5.20 for, both, in the absence of reorientations and under reorientations. The two cases are separated by the reorientation criteria listed in Figure 5.19.

- Stress rate:

$$\overset{\circ}{\tau}{}^{\text{Log}} = \mathbb{C} : \left(\mathbf{D} - \alpha\, \overset{\cdot}{\Theta} \right) - \tau_0\, \mathbf{t}\, \dot{\xi} - \xi\, \tau_0\, \overset{\circ}{\mathbf{t}}{}^{\text{Log}}$$

- Heat generation:

$$q_{\text{gen}} = \bar{\mathbf{q}}_{\text{gen}}^{\tau} : \overset{\circ}{\tau}{}^{\text{Log}} + \bar{q}_{\text{gen}}^{\xi}\, \dot{\xi} + \bar{\mathbf{q}}_{\text{gen}}^{t} : \overset{\circ}{\mathbf{t}}{}^{\text{Log}}$$

with:

$$\bar{\mathbf{q}}_{\text{gen}}^{\tau} = -\frac{1}{\rho_0}\, \alpha\, \Theta\, \mathbf{I}$$

$$\bar{q}_{\text{gen}}^{\xi} = \frac{1-\eta}{2\,\mu\,\rho_0}\, \tau_0\, \boldsymbol{\tau} : \mathbf{t} - \left(\frac{\eta^2\, \tau_0^2}{4\,\mu\,\rho_0} + A_1 \right) (1 - 2\,\xi) + \Delta u_0$$

$$\bar{\mathbf{q}}_{\text{gen}}^{t} = \frac{1-\eta}{2\,\mu\,\rho_0}\, \tau_0\, \xi\, \boldsymbol{\tau}$$

- Phenomenological functions driving phase transformations:

$$k^{\text{A}\rightarrow\text{M}}(\xi) = -a_1\, \xi^{b_1}\, \ln(1 - \xi) + c_1\, \xi$$

$$k^{\text{M}\rightarrow\text{A}}(\xi) = a_2\, (1 - \xi)^{b_2}\, \ln(\xi) - c_2\, (1 - \xi)$$

- Coherency coefficient:

$$A = A_1 + A_2\, \Theta$$

- Criteria for reorientations:

$$r = \vartheta \quad \wedge \quad \mathbf{t} : \overset{\circ}{\mathbf{s}}{}^{\text{Log}} + \mathbf{s} : \boldsymbol{\Lambda}^{\beta}\, \dot{\xi} < 0$$
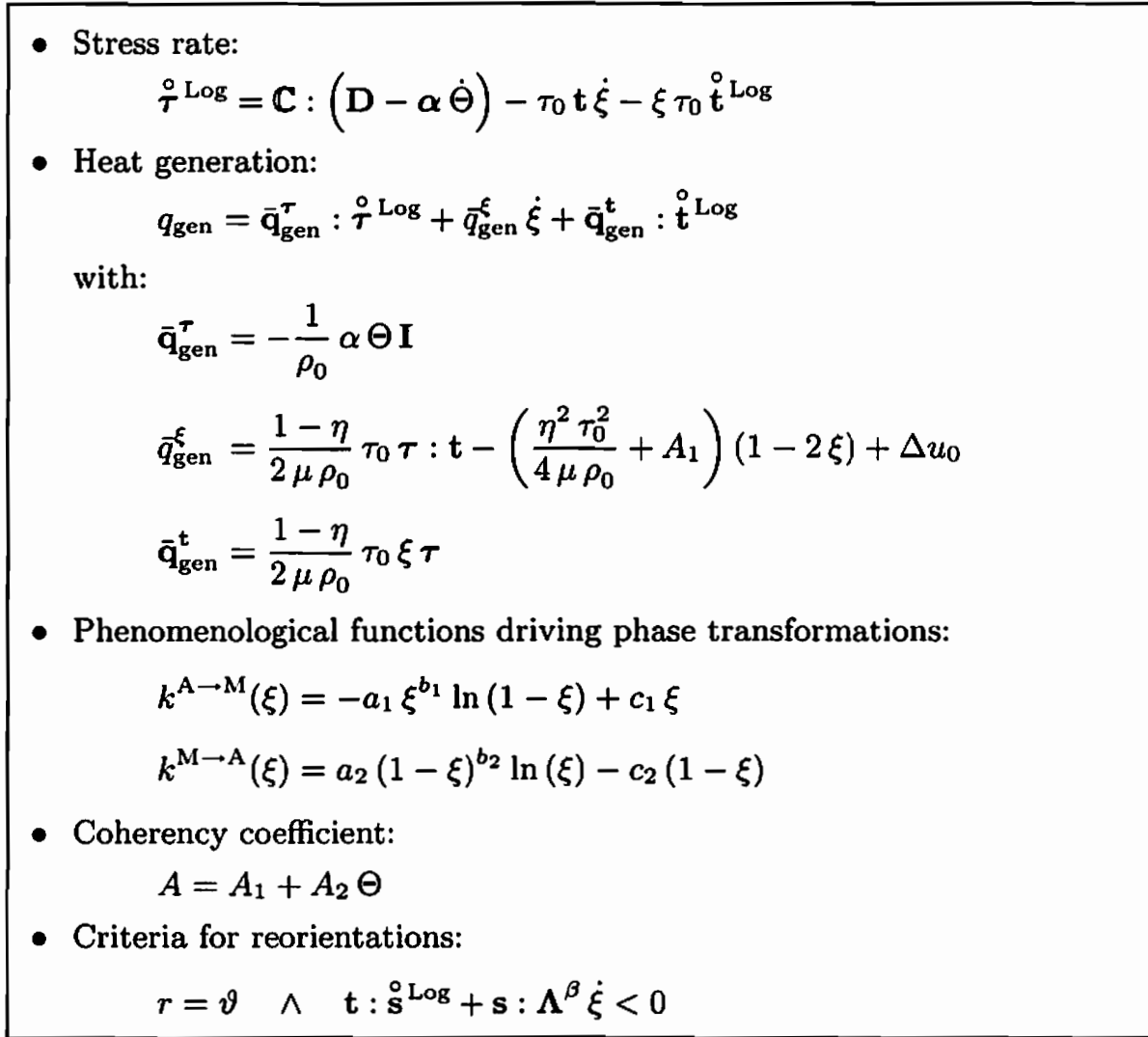
Figure 5.19: Summary of the material model

(a) Constitutive equations in the absence of reorientations

- Thermodynamic force driving phase transformations:

$$\pi^\xi = \frac{(1-\eta)\,\tau_0}{2\,\mu}\,\boldsymbol{\tau}:\mathbf{t} - (1-2\,\xi)\left(\frac{\eta^2\,\tau_0^2}{4\,\mu} + \rho_0 A\right) + \rho_0\,(\Delta u_0 - \Theta\,\Delta s_0)$$

- Criteria for phase transformations:

$$A \to M: \qquad \pi^\xi = k^{A\to M} \quad \wedge \quad \dot\pi^\xi\big|_{(\xi,\,t)} > 0$$

$$M \to A: \qquad \pi^\xi = k^{M\to A} \quad \wedge \quad \dot\pi^\xi\big|_{(\xi,\,t)} < 0$$

- Constitutive equations for the internal variables:

$$\dot\xi \;\; = \dot\pi^\xi\big|_{(\xi,\,t)}\left(\frac{\mathrm{d}k^\beta}{\mathrm{d}\xi} - \frac{\partial\pi^\xi}{\partial\xi} - \frac{\partial\pi^\xi}{\partial t}:\Lambda^\beta\right)^{-1}$$

$$\overset{\circ}{\mathbf{t}}{}^{\mathrm{Log}} = \Lambda^\beta\,\dot\xi$$

with:

$$\Lambda^\beta = \left\{\begin{array}{cc} (\mathbf{s}-\mathbf{t})\,\xi^{-1} & \text{for } A\to M \\ 0 & \text{for } M\to A \end{array}\right.$$

t and s coaxial

(b) Constitutive equations under reorientations

- Thermodynamic force driving phase transformations:

$$\pi^\xi = \frac{(1-\eta)\,\tau_0\,\vartheta}{2\,\mu}\,|\tau'| - (1-2\,\xi)\left(\frac{\eta^2\,\tau_0^2}{4\,\mu} + \rho_0 A\right) + \rho_0\,(\Delta u_0 - \Theta\,\Delta s_0)$$

- Criteria for phase transformations:

$$A \to M: \qquad \pi^\xi = k^{A\to M} \quad \wedge \quad \dot\pi^\xi\big|_\xi > 0$$

$$M \to A: \qquad \pi^\xi = k^{M\to A} \quad \wedge \quad \dot\pi^\xi\big|_\xi < 0$$

- Constitutive equations for the internal variables:

$$\dot\xi = \dot\pi^\xi\big|_\xi\left(\frac{\mathrm{d}k^\beta}{\mathrm{d}\xi} - \frac{\partial\pi^\xi}{\partial\xi}\right)^{-1}$$

$$\sum_{i=1}^{3} t_i\,s_i = \vartheta \qquad \sum_{i=1}^{3} t_i = 0 \qquad \sum_{i=1}^{3} t_i^2 = 1$$

t and s coaxial

Figure 5.20: Summary of the material model (cont'd)

6   Implementation

Some basic characteristics of the proposed material model are illustrated in this chapter. The aim is to asses the reliability of the constitutive assumptions for complex loadings and the applicability of the constitutive equations for structural simulations. In this context, the material model is implemented into the commercially available finite element environment MSC.Marc/Mentat whose basic properties are addressed in Section 6.1. Section 6.2 is concerned with a calibration of the material parameters and a comparison of numerical results with experimental measurements. As experimental data are generally given in terms of nominal quantities like nominal strain and nominal stress the calibration and implementation are restricted to a geometrically linear framework. Finite deformations are then regarded in Section 6.3 in which a fully thermomechanically coupled finite element analysis of a structural example in terms of a testing specimen for experimental measurements is conducted. Complementary to the geometrically linear framework, special attention is in this section on the incremental objectivity of the integration procedure to satisfy the principle of material frame indifference from a numerical point of view.

6.1   Introduction

Mathematically, the kinematic and static relations, the balance equations, the constitutive relations presented in the previous sections, and the initial and boundary conditions of the considered thermomechanical problem furnish a non-linear initial boundary value problem. For its numerical solution, the problem may be discretized in space and time within the framework of the finite element method. In doing so, the displacement and temperature fields can be computed by solving the discretized balance equation of linear momentum and the discretized heat equation for each time step. The material response is then obtained by evaluating, in particular integrating the local constitutive equations on the basis of the local deformation and the local temperature. This evaluation includes the determination of the local state variables, the local incremental heat generation, as well as the local algorithmic tangent moduli. Finally, on the grounds of the integrated material model, new displacement and temperature fields can be calculated, relaunching the above iterative solution procedure.

The foregoing formalism may be categorized into a global iteration in which the displacement and temperature fields are determined and into a local iteration computing the local material response. For the local iteration, the total initial boundary value problem reduces to an initial value problem, i.e., the local state of the material at initial time t_n is known and the increments of the local deformation as well as of the local temperature, driving the state of the material from time t_n to time $t_{n+1} = t_n + \Delta t_n$, are given. Here, Δt_n denotes the

time increment. The explicit set of differential equations representing the material response is, however, unknown, as the state of the material at time t_{n+1} is not specified. To circumvent this difficulty, an operator split method may be employed which uncouples the initial value problem by means of predictor and corrector steps (e.g., see Ortiz et al. (1983) and Pinsky et al. (1983)). For the predictor step, relaxed trial states may be computed on freezing the evolution of the internal variables. In this context, the corrector step is only mandatory if the predictor step does not meet physical constraints imposed by the material model. On adopting efficient numerical integration schemes such as single-step or multi-step algorithms (e.g., see Hairer & Wanner (2002)) the constitutive equations can then be integrated. In what follows, focus is on the local iteration and the underlying integration scheme. For an elaborated review on the finite element method, refer to the works of Hughes (2000), Belytschko et al. (2000), and Zienkiewicz & Taylor (2005).

In this treatise, the finite element environment MSC.Marc/Mentat is employed, which provides the subroutines hypela and hypela2 for the specification of user-defined material models. While the subroutine hypela is restricted to a geometrically linear framework, finite deformations can be encountered by the subroutine hypela2. Two aspects are noteworthy concerning the implementation into this environment. On the one hand, MSC.Marc/Mentat does not support the Eulerian framework comprising the Kirchhoff stress tensor, the stretching tensor, and the logarithmic rate as it is used in this treatise. Due to this, the respective quantities which are required to evaluate the material model have to be transformed from the mechanical framework of the subroutine hypela2, for example the Lagrangian framework including the second Piola-Kirchhoff stress tensor as well as the Green-Lagrangian strain tensor, to the adopted Eulerian framework. As a direct consequence, the local algorithmic tangent moduli being of fundamental importance for the convergence of the global iteration procedure during the determination of the displacement and temperature fields are computed numerically, based on a formalism proposed by Miehe (1996). On the other hand, MSC.Marc/Mentat does not account for a monolithic solution of the discretized balance equation of linear momentum and the discretized heat equation, i.e., these equations are solved sequentially. More precisely, the incremental heat generated during the incremental processes of deformation is computed during the solution of the balance equation of linear momentum and is then passed to the subsequent solution of the heat equation.

6.2   Basic characteristics of the material model

A major issue in the material modeling is to ensure consistency of the constitutive assumptions with experimental measurements. Only if the constitutive model complies with experiments, it can be expected to provide reliable results

for structural simulations. Experimental data are generally given in terms of nominal quantities, i.e., in nominal stress and nominal strain. The reason for this lies in the complexity of the determination of actual quantities which requires a sophisticated experimental setup. This determination may even render impossible for complex experiments as discussed in Grabe (2007). For instance, measuring the actual stress implies the determination of the actual cross section area of the specimen, which is not necessarily constant over the gauge length. This may particularly be cumbersome for tubular specimens which are commonly used for biaxial experiments. As a consequence, a material model formulated at finite deformations is enforcedly to be specified to a geometrically linear framework in the context of a calibration and a validation. In doing so, the respective integration strategy of the material model derived in Chapter 5 is presented in Section 6.2.1. The identification and the calibration of the material parameters are then addressed in Section 6.2.2. Section 6.2.3 is concerned with the validation of the material model with experimental results. In this context, the quality of the constitutive assumptions is estimated. Finally, some thermomechanical properties of the model are presented in Section 6.2.4.

6.2.1 Implementation within a geometrically linear theory

For the integration of the material model summarized in Figures 5.19 and 5.20, an implicit backward Euler scheme is used in the following. Although this integration algorithm is only first-order accurate, it features some noticeable properties. On the one hand, the implicit backward Euler scheme is unconditionally stable which especially proves crucial for the integration of stiff differential systems (cf. Hairer & Wanner (2002)). On the other hand, it inherits a good long-term accuracy for $\Delta t \rightarrow \infty$ which can even be superior to the long-term accuracies of alternative higher-order algorithms (cf. Simo (1998)). With respect to the operator split method considered above, two trial states are introduced capturing the processes of phase transformation and reorientation. The employed formalism principally follows the return-mapping algorithm regarded by Simo & Hughes (1998). Note, however, that only one trial state is considered by the authors in regard of a single physical constraint in terms of the yield condition of plasticity.

Adaptation of the implicit backward Euler scheme to the stress rate equation (5.64) yields the total stress at time t_{n+1} in the form

$$\sigma_{n+1} = \sigma_n + \mathbb{C} : (\Delta\varepsilon - \alpha\,\Delta\Theta_n)$$
$$- \sigma_0\,t_{n+1}\,(\xi_{n+1} - \xi_n) - \sigma_0\,\xi_{n+1}\,(t_{n+1} - t_n) \quad . \quad (6.1)$$

Here, as this section is devoted to a geometrically linear framework, the Kirchhoff stress tensor τ is replaced by the nominal stress tensor σ and τ_0 is substituted by σ_0, accordingly. $\Delta\varepsilon$ as well as $\Delta\Theta_n$ represent the nominal strain and

temperature increments, both corresponding to the time increment Δt_n. Certainly, the rate equation for the mass fraction of martensite given by (5.111) and (5.145) may be integrated in an analogous manner. As the thermodynamic force π^ξ, however, equals k^β during processes of phase transformation, ξ_{n+1} may alternatively be obtained on evaluating equations (5.93), (5.98), and (5.99), along with (5.97) at time t_{n+1}, i.e.,

$$\pi^\xi(\sigma_{n+1}, \Theta_{n+1}, \mathbf{t}_{n+1}, \xi_{n+1}) = k^\beta(\xi_{n+1}) \quad . \tag{6.2}$$

Note that no distinction between the driving forces in the presence and in the absence of reorientation processes is necessary for the iterative solution. Then, based on the current stress σ_{n+1} and the current mass fraction of martensite ξ_{n+1}, the actual average martensite variant orientation $\mathbf{t}_{n+1}$ can be quantified. In doing so, as the correction of $\mathbf{t}$ during phase transformations as discussed in Section 5.5.2 may be expected to show minor impacts on the computed pseudoelastic material behavior and as this chapter is devoted to some basic properties of the proposed material model, the correction of $\mathbf{t}$ during phase transformations is neglected, such that $\mathbf{t}_{n+1}$ is explicitly determined by the eigenvalues $(s_i)_{n+1}$ and eigenprojections $(\mathbf{S}_i)_{n+1}$ of the current stress direction $\mathbf{s}_{n+1}$. Thus, based on the definition

$$\mathbf{s}_{n+1} = \frac{\sigma'_{n+1}}{|\sigma'_{n+1}|} \quad , \tag{6.3}$$

$\mathbf{t}_{n+1}$ may be written as

$$\mathbf{t}_{n+1} = \sum_{i=1}^{3} (t_i)_{n+1} (\mathbf{S}_i)_{n+1} \tag{6.4}$$

in the presence of reorientation processes, whereas it may be recast into

$$\mathbf{t}_{n+1} = \sum_{i=1}^{3} (t_i)_n (\mathbf{S}_i)_{n+1} \tag{6.5}$$

in the absence of reorientation processes. The eigenvalues $(t_i)_{n+1}$ of $\mathbf{t}_{n+1}$ can be obtained from the following system of equations

$$\sum_{i=1}^{3} (t_i)_{n+1} (s_i)_{n+1} = \vartheta \qquad \sum_{i=1}^{3} (t_i)_{n+1} = 0 \qquad \sum_{i=1}^{3} (t_i)^2_{n+1} = 1 \tag{6.6}$$

on maintaining the rotation direction between $\mathbf{t}_n$ and $\mathbf{s}_n$ and between $\mathbf{t}_{n+1}$ and $\mathbf{s}_{n+1}$ within the principle space to ensure uniqueness of the solution.

Although the total stress state and the internal variables are specified by equations (6.1) to (6.6), their computation requires an estimation of the material state at time step t_{n+1}. This is due to the fact that the underlying constitutive equations for the determination of σ_{n+1}, ξ_{n+1}, and $\mathbf{t}_{n+1}$ rely on the

1. Given state t_n, $\Delta\varepsilon$ and $\Delta\Theta$, and $\Theta_{n+1} = \Theta_n + \Delta\Theta$

2. Compute trial state t^{ro}_{n+1} in the absence of reorientations

    i. Compute trial state t^{pt}_{n+1} in the absence of phase transformations

        solve for σ^{pt}_{n+1} and ξ^{pt}_{n+1}

$$\sigma^{pt}_{n+1} = \sigma_n + \mathbb{C} : (\Delta\varepsilon - \alpha\,\Delta\Theta_n) - \sigma_0\,\xi_n\,(t^{pt}_{n+1} - t_n)$$

$$\xi^{pt}_{n+1} = \xi_n$$

        with

$$\mathbf{t}^{pt}_{n+1} = \sum_{i=1}^{3} (t_i)_n\,(\mathbf{S}_i)^{pt}_{n+1}$$

    ii. Test for phase transformations

        $A \to M$: $\pi^\xi\big|^{pt}_{n+1} - k^{A \to M}\big|^{pt}_{n+1} > 0$

        $M \to A$: $-\pi^\xi\big|^{pt}_{n+1} + k^{M \to A}\big|^{pt}_{n+1} > 0$

        if not $(A \to M$ or $M \to A)$ then

            set $(\cdot)^{ro}_{n+1} = (\cdot)^{pt}_{n+1}$ and go to step 3

        end if

    iii. Compute trial state t^{ro}_{n+1} under phase transformations

        solve for σ^{ro}_{n+1} and ξ^{ro}_{n+1}

$$\sigma^{ro}_{n+1} = \sigma_n + \mathbb{C} : (\Delta\varepsilon - \alpha\,\Delta\Theta_n)$$
$$- \sigma_0\,\mathbf{t}^{ro}_{n+1}\,(\xi^{ro}_{n+1} - \xi_n) - \sigma_0\,\xi^{ro}_{n+1}\,(t^{ro}_{n+1} - t_n)$$

$$\pi^\xi(\sigma^{ro}_{n+1}, \Theta_{n+1}, \mathbf{t}^{ro}_{n+1}, \xi^{ro}_{n+1}) = k^\beta(\xi^{ro}_{n+1})$$

        with

$$\mathbf{t}^{ro}_{n+1} = \sum_{i=1}^{3} (t_i)_n\,(\mathbf{S}_i)^{ro}_{n+1}$$

3. Test for reorientations

    if $(\mathbf{s}^{ro}_{n+1} : \mathbf{t}^{ro}_{n+1} < \vartheta)$ then

        go to step 4.

    else

        set $(\cdot)_{n+1} = (\cdot)^{ro}_{n+1}$ and go to step 5

    end if

Figure 6.1: Extended return-mapping algorithm

4. Compute state t_{n+1} under reorientations

   i. Compute trial state t_{n+1}^{pt} in the absence of phase transformations

       solve for σ_{n+1}^{pt} and ξ_{n+1}^{pt}

$$\sigma_{n+1}^{\text{pt}} = \sigma_n + \mathbf{C} : (\Delta\varepsilon - \alpha\,\Delta\Theta_n) - \sigma_0\,\xi_n\,(t_{n+1}^{\text{pt}} - t_n)$$

$$\xi_{n+1}^{\text{pt}} = \xi_n$$

       with

$$t_{n+1}^{\text{pt}} = \sum_{i=1}^{3} (t_i)_{n+1}^{\text{pt}}\,(\mathbf{S}_i)_{n+1}^{\text{pt}}$$

$$(t_i)_{n+1}^{\text{pt}} = (t_i)_{n+1}^{\text{pt}}((s_j)_{n+1}^{\text{pt}})$$

  ii. Test for phase transformations

$$A \to M: \qquad \pi^\xi\big|_{n+1}^{\text{pt}} - k^{A\to M}\big|_{n+1}^{\text{pt}} > 0$$

$$M \to A: \qquad -\pi^\xi\big|_{n+1}^{\text{pt}} + k^{M\to A}\big|_{n+1}^{\text{pt}} > 0$$

       if not $(A \to M$ or $M \to A)$ then

          set $(\cdot)_{n+1} = (\cdot)_{n+1}^{\text{pt}}$ and go to step 5

       end if

 iii. Compute state t_{n+1} under phase transformations

       solve for σ_{n+1} and ξ_{n+1}

$$\sigma_{n+1} = \sigma_n + \mathbf{C} : (\Delta\varepsilon - \alpha\,\Delta\Theta_n)$$
$$- \sigma_0\,t_{n+1}\,(\xi_{n+1} - \xi_n) - \sigma_0\,\xi_{n+1}\,(t_{n+1} - t_n)$$

$$\pi^\xi(\sigma_{n+1}, \Theta_{n+1}, t_{n+1}, \xi_{n+1}) = k^\beta(\xi_{n+1})$$

       with

$$t_{n+1} = \sum_{i=1}^{3} (t_i)_{n+1}\,(\mathbf{S}_i)_{n+1}$$

$$(t_i)_{n+1} = (t_i)_{n+1}((s_j)_{n+1})$$

5. Compute incremental generation of heat

$$\Delta(q_{\text{gen}})_n = \bar{\mathbf{q}}_{\text{gen}}^\sigma\big|_{n+1} : (\sigma_{n+1} - \sigma_n) + \bar{q}_{\text{gen}}^\xi\big|_{n+1}(\xi_{n+1} - \xi_n)$$
$$+ \bar{\mathbf{q}}_{\text{gen}}^t\big|_{n+1} : (t_{n+1} - t_n)$$

Figure 6.2: Extended return-mapping algorithm (cont'd)

elastic-inelastic deformation processes driving the material state from time t_n to time t_{n+1}. In this context, the operator split method is employed for which the material state at time t_{n+1} is estimated by an predictor step and, if necessary, corrected by a subsequent corrector step. The resulting procedure is summarized in Figures 6.1 and 6.2. Note therein that the quantities σ_{n+1} and ξ_{n+1} are the only independent variables. They may be computed from equations (6.1) to (6.6) by a classical iterative solution procedure such as Newton's method or the BFGS method. It also bears emphasis that two trial states t_{n+1}^{pt} and t_{n+1}^{ro} are introduced in which phase transformation and reorientation processes are frozen, respectively.

The predictor-corrector iteration begins with a given material state at time t_n as well as given strain and temperature increments (step 1.). It is assumed as an initial guess that reorientations do not occur, i.e., the trial state t_{n+1}^{ro} in the absence of reorientations is computed first (step 2.). In this context, the trial state t_{n+1}^{pt} in the absence of phase transformations is quantified (step 2.i.). If this state does not meet the criteria for phase transformations, the trial state t_{n+1}^{ro} equals the trial state t_{n+1}^{pt} (step 2.ii.). Otherwise the trial state t_{n+1}^{ro} has to be recomputed on also including phase transformations (step 2.iii.). With the trial state t_{n+1}^{ro} at hand, the reorientation function can be checked (step 3.). If it is obeyed, the trial state t_{n+1}^{ro} equals the state of the material at time t_{n+1}. Otherwise, the state t_{n+1} has to be corrected by additionally considering reorientations (step 4.). The integration scheme is completed with the computation of the incrementally generated heat $\Delta(q_{\mathrm{gen}})_n$ (step 5.).

6.2.2 Calibration of the material parameters

The proposed constitutive model for NiTi shape memory alloys depends on a series of distinct material parameters which are briefly summarized in Table 6.1. Thereof, the first six parameters characterize the purely thermoelastic behavior of the material, whereas the pseudoelastic material behavior including phase transformations and reorientations is reflected by the remaining thirteen parameters. The parameter η accounts for mechanical interactions between the phases martensite and austenite. With respect to Section 5.3.1, it may be set equal to 0.5. As the parameter σ_0 expresses the average distortion of the martensite variants, it is directly related to the length of the pseudoelastic hysteresis. The level and the height of the hysteresis are determined by the parameters Δu, Δs, A_1, and A_2. More precisely, after replacing the equivalent stress τ_{eq} in (5.125) by the corresponding nominal quantity σ_{eq}, the critical stresses $\sigma_{\mathrm{eq}}^{\mathrm{A}\to\mathrm{M}}$ and $\sigma_{\mathrm{eq}}^{\mathrm{M}\to\mathrm{A}}$ at the initiation of phase transformations can be deduced as

$$\sigma_{\mathrm{eq}}^{\mathrm{A}\to\mathrm{M}} = \frac{2\,\mu\,\rho_0}{(1-\eta)\,\sigma_0}\left[\frac{\eta^2\,\sigma_0^2}{4\,\mu\,\rho_0} + A_1 - \Delta u_0 + \Theta\,(\Delta s_0 + A_2)\right] \qquad (6.7)$$

Symbol	Description
α	thermal expansion coefficient
ρ_0	density
c	heat capacity
k	thermal conductivity
μ	Lamé constant
λ	Lamé constant
η	degree of the mechanical interactions between the phases
σ_0	average distortion of martensite variants
Δu	internal energy difference of the unloaded phases
Δs	internal entropy difference of the unloaded phases
A_1	parameter of the coherency coefficient
A_2	parameter of the coherency coefficient
a_1	phenomenological parameter for A → M transformations
a_2	phenomenological parameter for M → A transformations
b_1	phenomenological parameter for A → M transformations
b_2	phenomenological parameter for M → A transformations
c_1	phenomenological parameter for A → M transformations
c_2	phenomenological parameter for M → A transformations
ϑ	deviation between stress direction/martensite orientation

Table 6.1: Summary of the material parameters

for the A → M phase transformation at $\xi = 0$ and as

$$\sigma_{eq}^{M \to A} = \frac{2\,\mu\,\rho_0}{(1-\eta)\,\sigma_0} \left[-\frac{\eta^2\,\sigma_0^2}{4\,\mu\,\rho_0} - A_1 - \Delta u_0 + \Theta\,(\Delta s_0 - A_2) \right] \qquad (6.8)$$

for the M → A phase transformation at $\xi = 1$.[34] Relations (6.7) and (6.8) characterize two opposite points within the hysteresis as schematically depicted in Figure 6.3. Therein, analogously to the equivalent stress σ_{eq}, the equivalent total strain ε_{eq} is defined by

$$\varepsilon_{eq} = |\varepsilon'| \quad , \qquad (6.9)$$

with ε' denoting the deviator of the nominal total strain tensor. Evidently, the height $\Delta\sigma_{eq}^{AM}$ of the hysteresis at constant temperature can be obtained from the difference between equations (6.7) and (6.8) as

$$\Delta\sigma_{eq}^{AM} = \frac{4\,\mu\,\rho_0}{(1-\eta)\,\sigma_0} \left[\frac{\eta^2\,\sigma_0^2}{4\,\mu\,\rho_0} + A_1 + \Theta\,A_2 \right] \quad , \qquad (6.10)$$

[34]See Footnote 32 on Page 102.
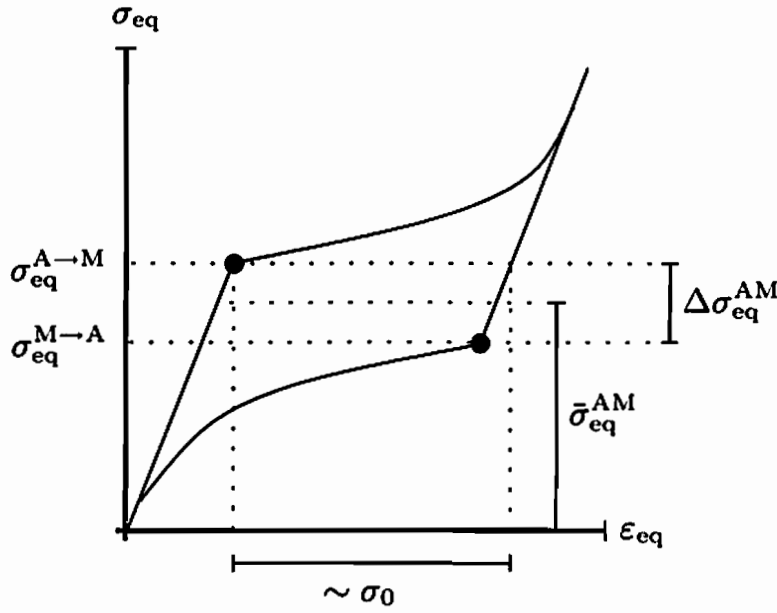
Figure 6.3: Influence of the material parameters Δu, Δs, A_1, A_2, and σ_0 on the pseudoelastic hysteresis

while the hysteresis level $\bar{\sigma}_{\mathrm{eq}}^{\mathrm{AM}}$ equals the arithmetic mean of (6.7) and (6.8)

$$\bar{\sigma}_{\mathrm{eq}}^{\mathrm{AM}} = \frac{2\,\mu\,\rho_0}{(1-\eta)\,\sigma_0}\,[-\Delta u_0 + \Theta\,\Delta s_0] \quad . \tag{6.11}$$

On stipulating that the thermoelastic parameters μ and ρ_0 are known and that η and σ_0 are given, evaluation of (6.7) and (6.8) or alternatively of (6.10) and (6.11) at two distinct temperatures provides a set of four equations for the determination of the parameters Δu, Δs, A_1, and A_2. In solving this set of equations, however, it has to be ensured that the Clausius-Clapeyron-like relation considered in Section 5.5.2 is obeyed. In particular, in line with experiments, e.g., in Miyazaki et al. (1981), Shaw & Kyriakides (1995), and Hayashi et al. (2004), the critical stresses for A → M and M → A phase transformations described by (6.7) and (6.8) feature positive slopes in Θ. This constraint is expressed by the two inequalities

$$\Delta s + A_2 \overset{!}{>} 0 \quad \text{and} \quad \Delta s - A_2 \overset{!}{>} 0 \quad . \tag{6.12}$$

Also, the critical stress for the A → M phase transformation always exceeds the critical stress for the M → A phase transformation. This furnishes the requirement

$$\frac{\eta^2\,\sigma_0^2}{4\,\mu\,\rho_0} + A_1 + \Theta\,A_2 \overset{!}{>} 0 \quad . \tag{6.13}$$

The parameters a_i, b_i, and c_i with $i = (1, 2)$ are purely phenomenological. They specify the particular shape of the hysteresis during phase transformations, such as slope and curvature. The parameter ϑ finally expresses the

maximum admissible deviation between the stress direction and the average orientation of the martensite variants.

The material model is calibrated to experimental data presented in the work of Grabe (2007) which is concerned with an extensive analysis of uniaxial and bi-axial experiments of NiTi shape memory alloys at different temperature levels. In this work, the thermoelastic parameters of the investigated alloy are already determined by the author and can directly be adopted. For the calibration of the phase transformation related parameters Δu, Δs, A_1, A_2, a_1, a_2, b_1, b_2, c_1, c_2, and σ_0, two isothermal tests in simple tension are considered, showing a maximum tensile strain of 5 % and being conducted at the testing temperatures of 10 °C and 27.5 °C. In this context, the microstructure is assumed to be completely martensitic at the maximum applied tensile strain in order to employ relations (6.7) and (6.8) or, alternatively, relations (6.10) and (6.11). The latter assumption is supported by the observation that the experiments cover the whole pseudoelastic hysteresis of the material.[35] The selection of the parameter ϑ is finally based on the non-proportional box-shaped test considered at the end of this section.

The calibrated material parameters are listed in Table 6.2 and the measured and computed simple tension tests can be reviewed in Figures 6.4 and 6.5. ε and σ denote the tensile strain and the tensile stress within the linearized theory. It bears emphasis that, although the material model seems to be well-adapted to the experiments, the presented calibration relies on an estimation of the material parameters. Specifically, rigorous calibration techniques should generally be employed based on a monolithic minimization of the error between the computed and the measured material responses, for example in terms of the least square error, considering the whole set of all relevant material parameters at once. The so-defined problem constitutes an *inverse problem* in which the model parameters are to be calculated from a known material response (cf. Tarantola (1987)). Due to its complexity, hard optimization techniques have to be utilized. For instance, neural networks and evolutionary algorithms are successfully adopted in the works of Helm (2005) and Grabe (2007) for the calibration of material models for shape memory alloys.

It should be noted that the material used in the work of Grabe (2007) exhibits the R-phase, as pointed out by the author.[36] Although this phase may have a strong influence on the material behavior, it is classically omitted in the course of the material modeling of NiTi shape memory alloys, i.e., it is commonly assumed that the B2-austenite directly transforms into the B19'-martensite. Phase transformations are supposed to occur only at the upper and lower bounds of the pseudoelastic hysteresis within the strain-stress diagram, while all other regions are regarded as purely thermoelastic. The reason

---

[35]See Footnote 32 on Page 102.

[36]For an introduction to R-phase related phenomena, the reader is referred to the works of Miyazaki & Otsuka (1986), Otsuka (1990), and Saburi (1998).

Symbol	Value	Unit
α	$8 \cdot 10^{-6}$	$1/\text{K}$
ρ_0	6500	kg/m^3
c	837.3	$\text{J}/\text{kg K}$
k	10	$\text{W}/\text{m K}$
μ	15598	MPa
λ	2289	MPa
η	0.50	–
σ_0	1540	MPa
Δu	6078	J/kg
Δs	23.55	$\text{J}/\text{kg K}$
A_1	-281.2	J/kg
A_2	-3.40	$\text{J}/\text{kg K}$
a_1	0.15	–
a_2	0.15	–
b_1	1.80	–
b_2	3.00	–
c_1	2.80	–
c_2	2.80	–
ϑ	0.65	–

Table 6.2: Calibrated material parameters

for this may be attributed to the fact that R-phase activities inherit comparatively small inelastic deformations (cf. Otsuka & Ren (1999)), so that their occurrence can often not be perceived on solely concentrating on the strain-stress diagram (see Šittner et al. (2006a)). On this account, the regions providing linear relations between strain and stress may mistakenly be interpreted as linear-elastic, although these regions may already be affected by the R-phase. A thorough analysis on this matter can be found in Šittner et al. (2006a,c). Also, the works of Raniecki et al. (1999), Oliferuk (1999), and Tanaka et al. (1999) are concerned with the thermomechanical behavior of the R-phase under tension/torsion tests. The influences of the R-phase on the material behavior can be manifold. For instance, R-phase transformations may lead to a severe generation of heat (cf. Oliferuk (1999)), which may also be observed in the *apparently* linear-elastic regions of the material. Moreover, the inelastic deformations resulting from R-phase transformations and/or reorientations of R-phase variants may lead to a significant decrease of the magnitude of the apparently linear-elastic material parameters such as the Lamé constants (see Šittner et al. (2006b)). Finally, the R-phase may
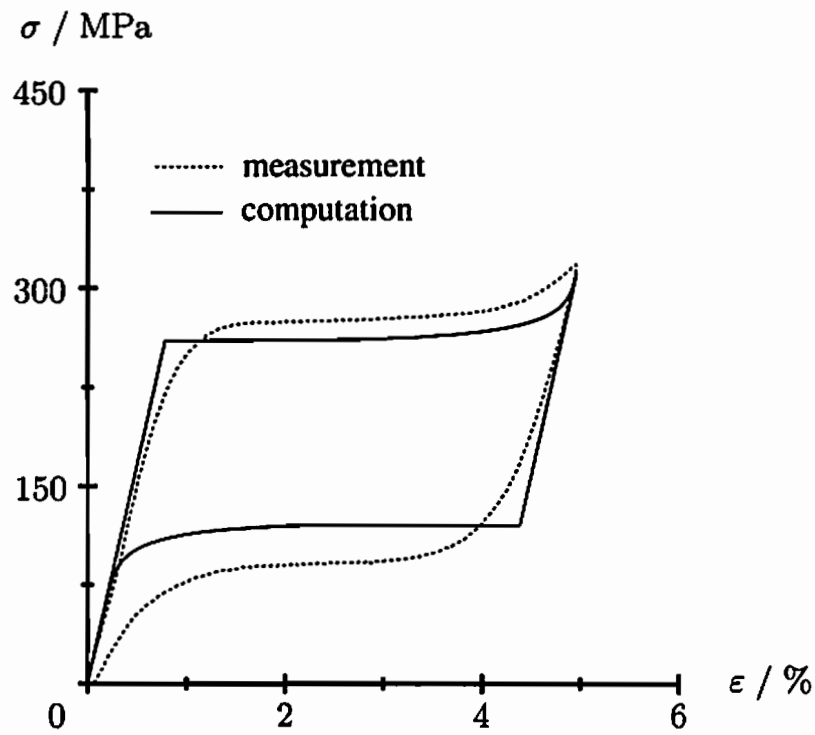
Figure 6.4: Simple tension test at 10 °C; experimental and numerical results
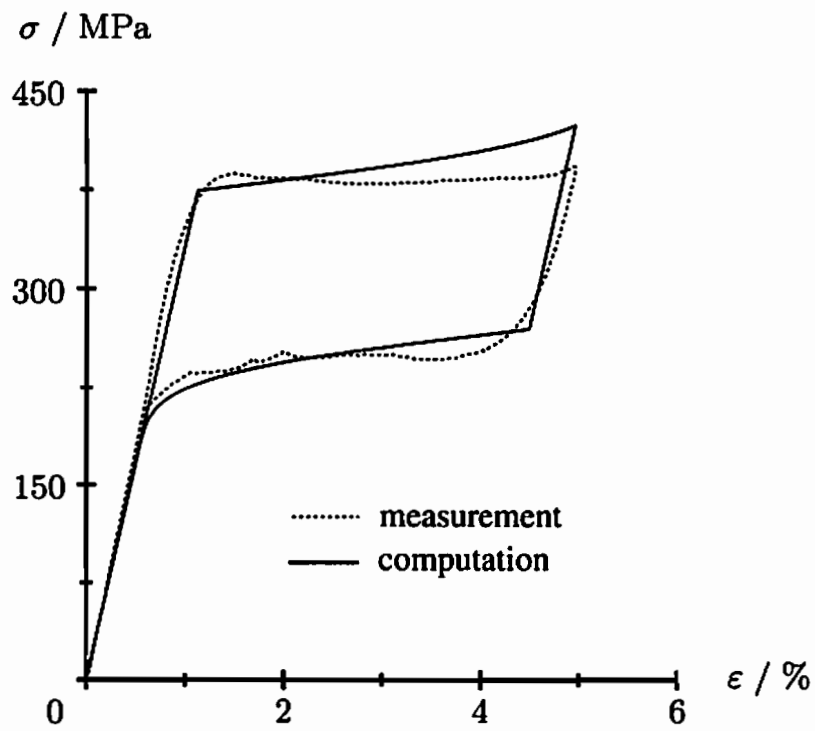
Figure 6.5: Simple tension test at 27.5 °C; experimental and numerical results

inherit an asymmetric transformation behavior contributing to the overall tension/compression asymmetry of NiTi shape memory alloys (cf. Šittner et al. (2006a) and Raniecki et al. (1999)). As reported in Luig et al. (2007), some of these effects can be observed for the investigated alloy.

6.2.3 Validation of the material model

Although the experiments in the work of Grabe (2007) are affected by the R-phase, they may be taken as reference for an estimation of some basic properties of the proposed constitutive model. This may be motivated by the fact that the inelastic deformations related to R-phase activities can be regarded as subordinate compared to the inelastic deformations arising from B2 → B19' phase transformations and from reorientations of B19' martensite variants (cf. Saburi (1998)).[37] In this context, the calibrated parameters listed in Table 6.2 are utilized for the computations. In order to reduce the impact of R-phase activities on the thermomechanical material behavior, the validation is restricted to isothermal tests. Moreover, all considered experiments are carried out strain-controlled. Throughout this section, ε and σ represent the tensile strain and the tensile stress. Additionally, following Grabe (2007), the quantities τ' and γ' are defined as

$$\gamma' = \frac{\gamma}{\sqrt{3}} \quad \text{and} \quad \tau' = \sqrt{3}\,\tau \quad , \tag{6.14}$$

with τ and γ denoting the measured shear stress and shear strain.

At first, two isothermal simple tests in torsion with a maximum shear strain of $\gamma' = 3.4\%$, both conducted at $10\,^\circ$C and $27.5\,^\circ$C, are considered. The experimental and numerical results are depicted in Figures 6.6 and 6.7. The observable deviations principally reflect the consequences of the asymmetric transformation behavior of NiTi shape memory alloys, i.e., the tension/compression asymmetry, which is not accounted for in the proposed material model. Nevertheless, as the calibrated material parameters stem from an adaptation to tensile tests, the predictions can be improved by a recalibration to shear tests. In this regard, it proves imperative to incorporate the tension/compression asymmetry into the material model to improve the accuracy of the predictions for complex loadings. Note, however, that the observable asymmetric transformation behavior of the material may also be attributed to existing R-phase activities, which may enlarge the effects of the tension/compression asymmetry to some extent.

Next, an isothermal box-shaped loading path in the first axial/torsional strain quadrant is considered. The experiment is carried out at the testing temperature of $27.5\,^\circ$C with, both, a maximum tensile strain ε and a maximum shear

---

[37] Maximum recoverable strains due to B2 → B19' and B2 → R phase transformations are the range of 8% and 1%, respectively (cf. Miyazaki (1996) and Otsuka & Ren (1999)).

$\tau' \ / \ \mathrm{MPa}$
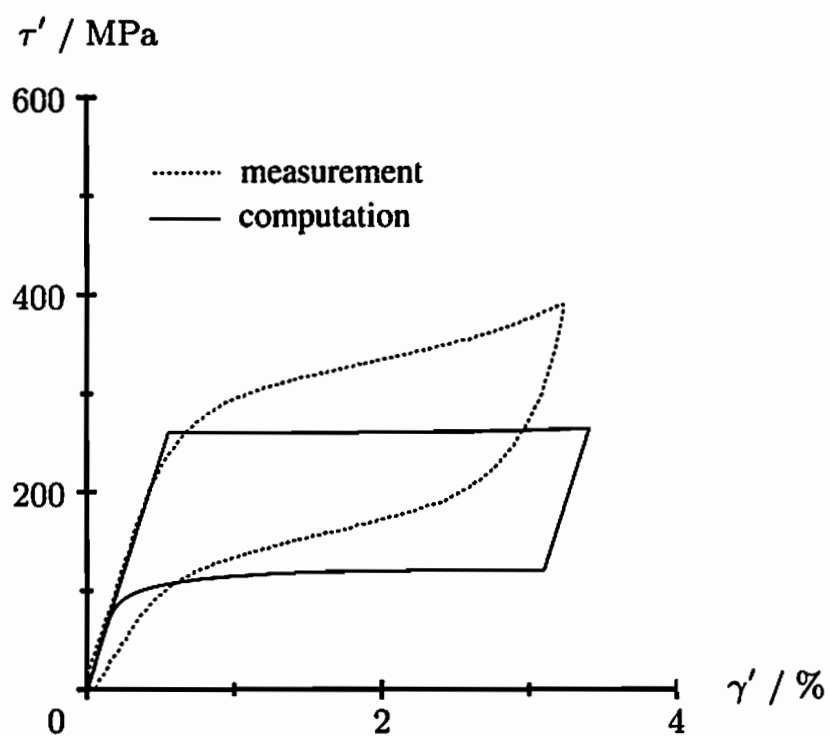
Figure 6.6: Simple torsion test at 10 °C; experimental and numerical results

$\tau' \ / \ \mathrm{MPa}$
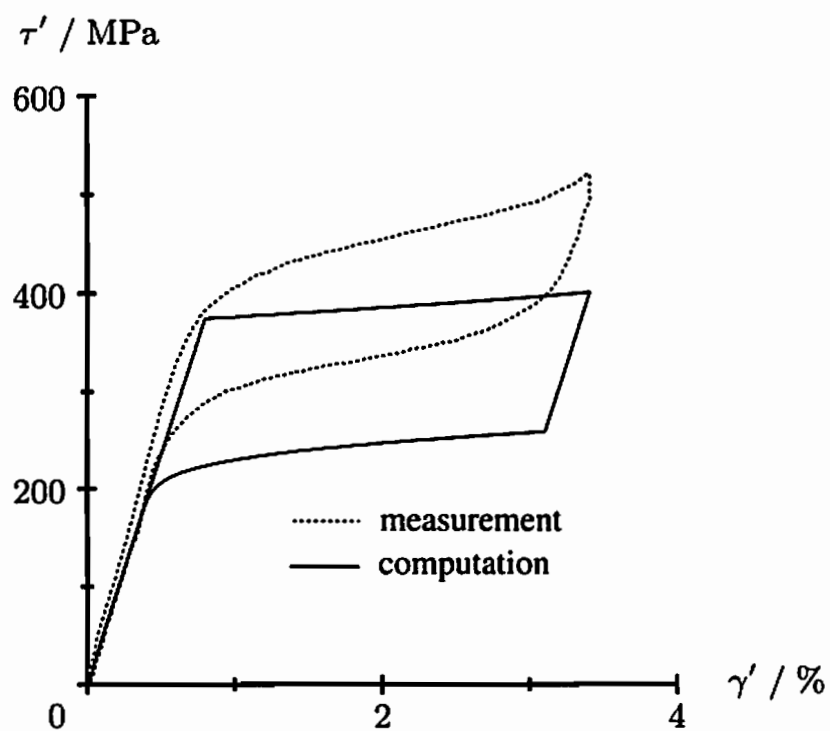
Figure 6.7: Simple torsion test at 27.5 °C; experimental and numerical results

strain γ' of 2 %. The loading sequence can be reviewed in Figure 6.8, being indicated by the points (1) to (4). First, the specimen is elongated into the axial direction and is then distorted at constant tensile strain. Thereafter, the axial displacement is reversed, followed by a release of the distortion. The stress response in terms of experimental and numerical results is graphically illustrated in Figures 6.9 to 6.11. The points (1) to (4) in all figures can directly be assigned to each other, as they denote same points in time. The material response in Figure 6.9 is qualitatively predicted by the computation. Especially, the introduced reorientation function expressing the deviation between the stress direction and the martensite orientation proves eminent for the description of the negative axial stress at zero tensile strain in point (4). In particular, on selecting $\vartheta = 1$, the strain and stress directions are parallel and, thus, this effect cannot be captured by the computation. The magnitude of the negative axial stress decreases on reversing the distortion, until it completely disappears between points (4) and (1). This originates from the fact that the unloading process induces a M $\rightarrow$ A phase transformation, leading to a vanishing contribution of the martensitic phase on the total deformation. The kink between points (3) and (4) indicates an initiating M $\rightarrow$ A phase transformation which provides an increase of the shear stress. The softening of the shear response starting in point (3) during the computation arises from the assumed coaxiality of the stress direction and the martensite orientation. To some extent, this coaxiality expresses a reorientation process of the martensite variants during the non-proportional loading section. Figures 6.10 and 6.11 show the extracted results for the axial and torsional directions. The material response into the axial direction is well-predicted, whereas the predictions into the torsional direction are in a qualitative agreement with the experiment.

Principally, the deviations between the computed and measured results may be attributed to three factors. Firstly, they may originate from the occurrence of the R-phase. Certainly, as the R-phase is not accounted for in the material model, inelastic deformations resulting from R-phase activities cannot be reflected by the computation. These deformations, however, can be regarded to be small compared the total deformations. Secondly, the deviations may arise from the tension/compression asymmetry of the material which is not considered in the constitutive model. This is supported by the observation that the predictions of the material response are in good accord with the experiment for the axial direction, which is not the case for the torsional direction. Thirdly, the deviations may result from the assumed coaxiality of the stress direction and the average orientation of the martensite variants. As discussed above for the loading sequence starting in point (3) in Figure 6.9, this assumption may particularly lead to a weakening of the predicted material response.

In order to gain a deeper insight into the deviations between the computed and measured results, an isothermal butterfly-shaped loading path in the first axial/torsional strain quadrant is regarded next. The testing temperatures
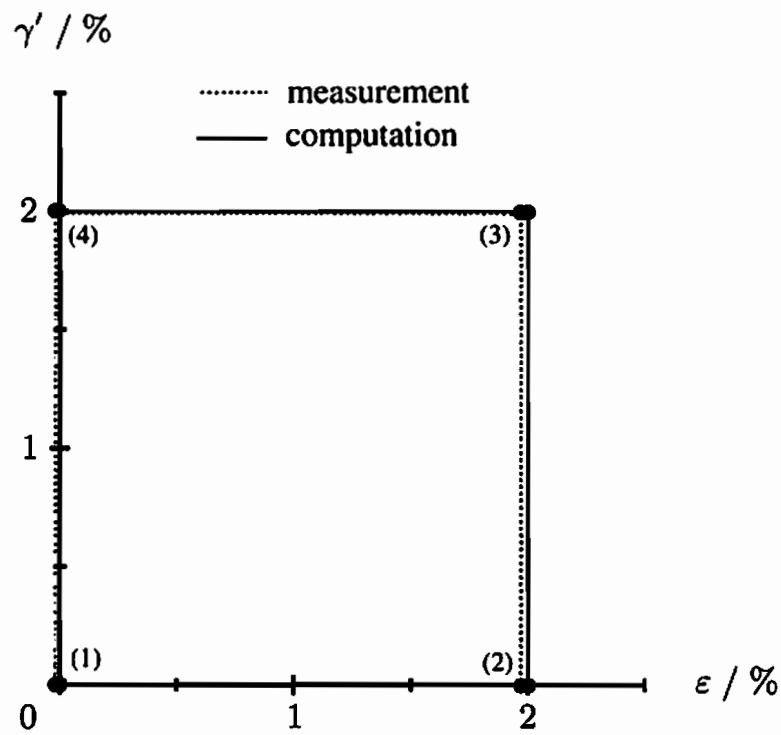
Figure 6.8: Combined box test; prescribed axial/torsional strains
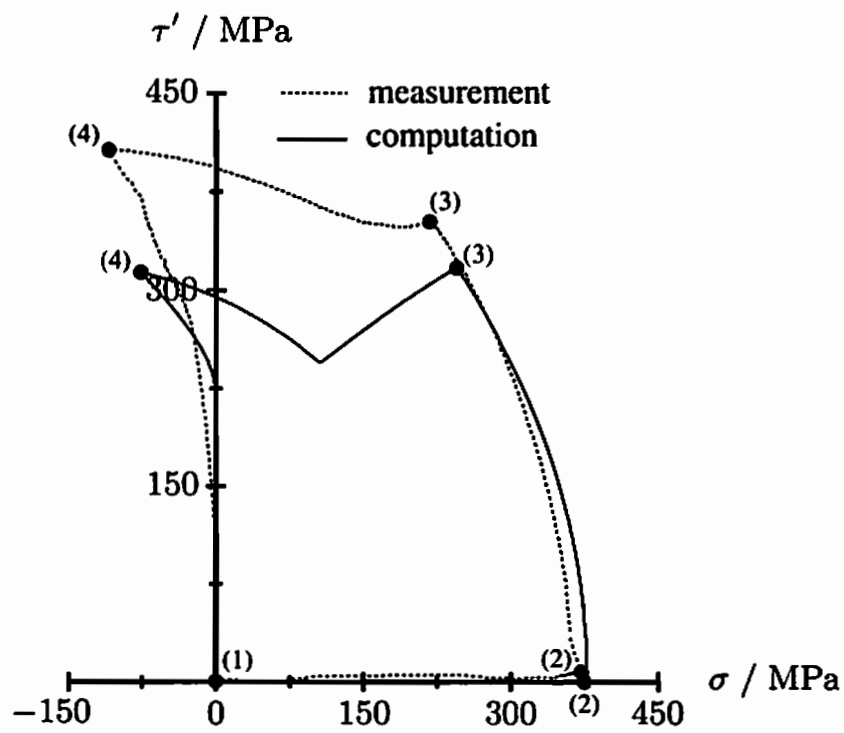
Figure 6.9: Combined box test; results for axial/torsional stresses
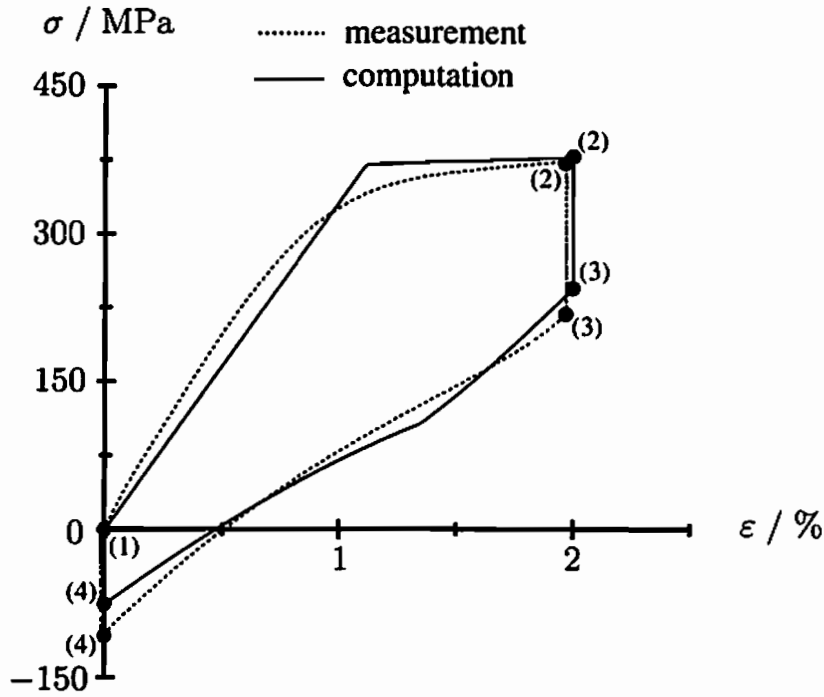
Figure 6.10: Combined box test; results for axial strain-stress
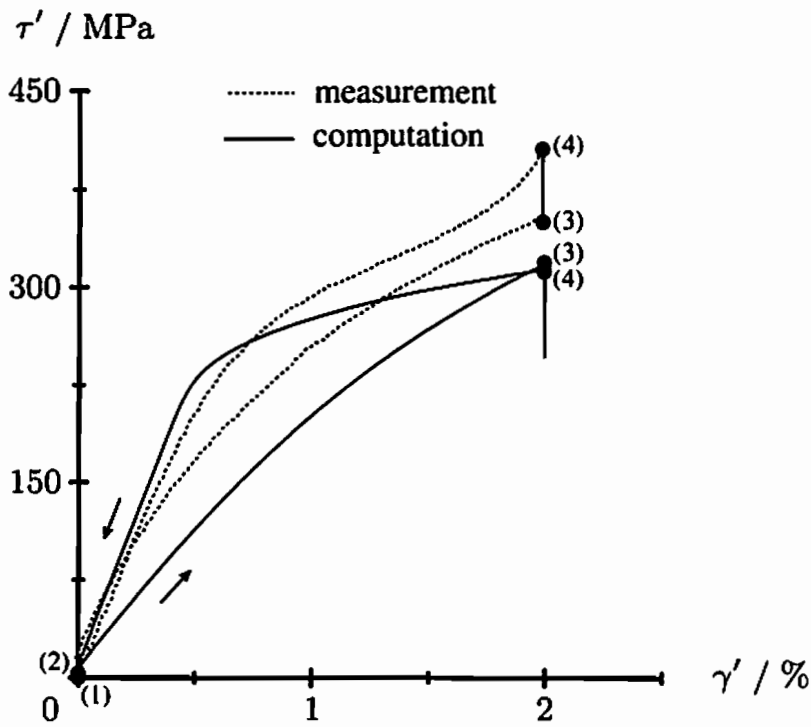
Figure 6.11: Combined box test; results for torsional strain-stress
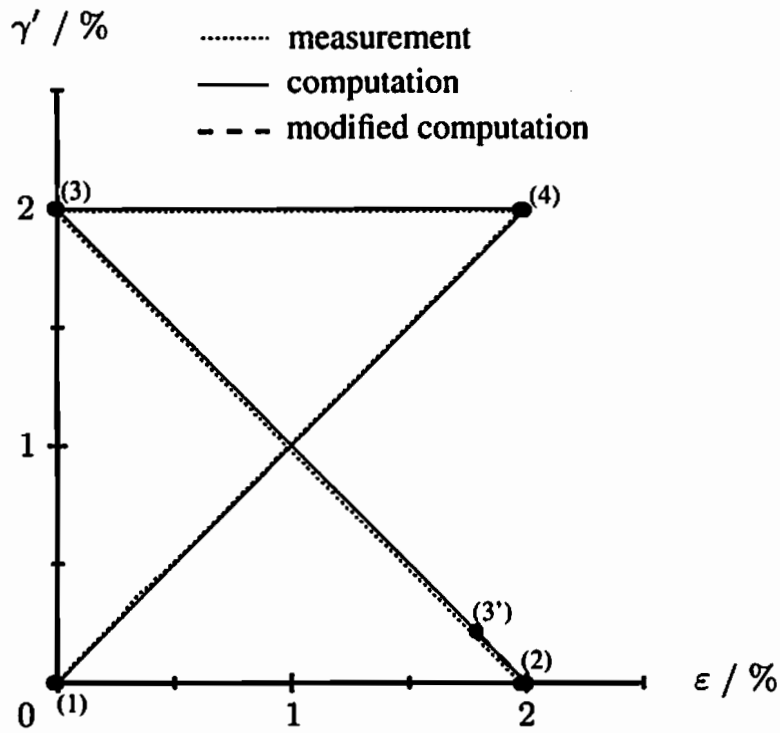
Figure 6.12: Combined butterfly test; prescribed axial/torsional strains
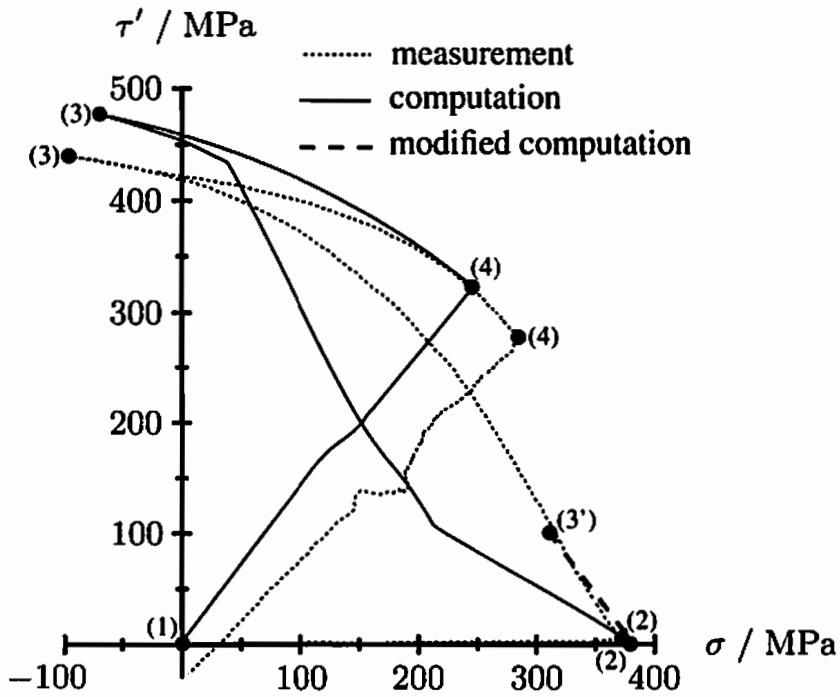
Figure 6.13: Combined butterfly test; results for axial/torsional stresses
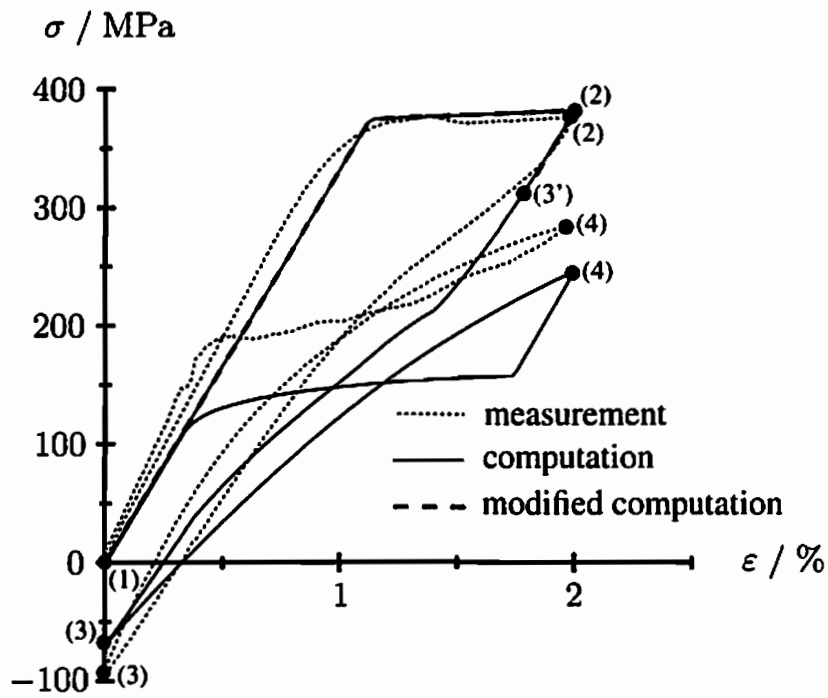
Figure 6.14: Combined butterfly test; results for axial strain-stress
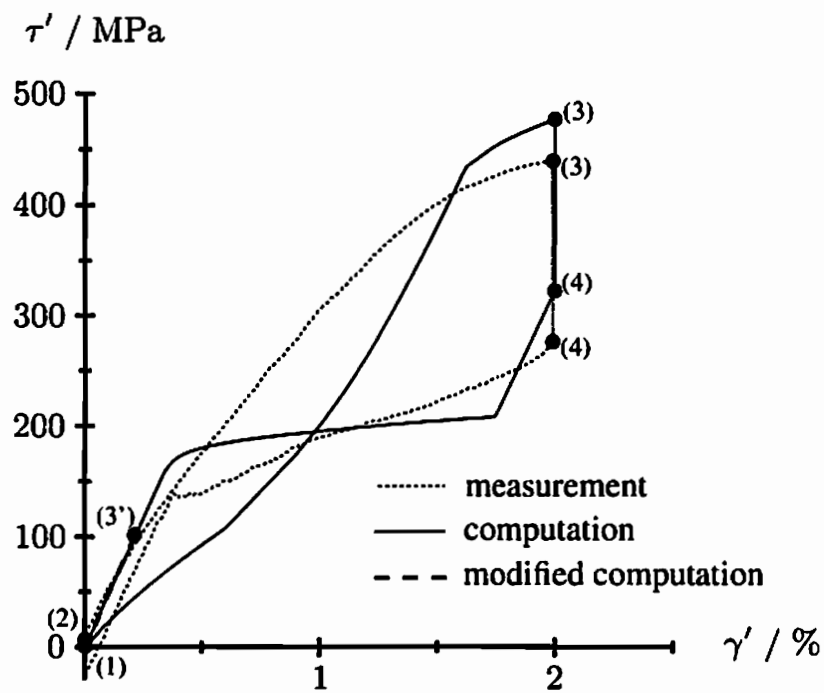
Figure 6.15: Combined butterfly test; results for torsional strain-stress

and the maximum prescribed strains are the same as for the box-shaped experiment. The loading sequence is depicted in Figure 6.12. The specimen is strained into the axial direction, followed by an increasing distortion and a proportional release of the axial displacement. Then, at constant shear, the specimen is again elongated into the axial direction. Finally, the axial and torsional deformations are proportionally reversed. The corresponding computed and measured stress responses are given in Figures 6.13 to 6.15. Like for the box-shape loading path, the predicted material response visualized in Figure 6.13 is in a fairly good agreement with the measured response. Again, the negative tensile stress at zero tensile strain in point (3) can be reproduced. However, the predicted response of the loading section starting in point (2) and proceeding to point (3) in Figures 6.13 and 6.15 is well-below the measured response. The two observable kinks in this section result from initiating phase transformations. Specifically, the phase transformations starting at the kink near point (2) stop soon after their initiation. Moreover, the criteria for reorientations are not fulfilled between point (2) and the first kink. Hence, the computed material response for this section of the loading sequence is solely dominated by the assumed coaxiality of the stress direction and the average orientation of the martensite variants. A deeper insight into this finding may be gained from a modified computation in which the coaxiality assumption is removed. It is specifically assumed that the material behavior for the loading section starting in point (2) is purely elastic. The results of this computation are accordingly represented by the dashed lines in Figures 6.12 to 6.15. The computation is arbitrarily interrupted in point (3'), as the analysis concentrates on the predicted material behavior for a changing loading direction. Apparently, the computed predictions may significantly be enhanced by the modification. This suggests that reorientations do not instantaneously initiate on changing the loading direction during non-proportional loadings. Along with the analysis of the box-shaped experiment, it may, thus, be concluded that the assumed coaxiality between the stress direction and the average martensite variant orientation leads to a weak predicted material response for complex loadings.

6.2.4 Thermomechanical characteristics

In this section, the foregoing isothermal analyses are complemented by a presentation of some thermomechanical characteristics. Again, the computations are based on the calibrated material parameters listed in Table 6.2.

A comparison between the stress responses for isothermal and adiabatic simple tension tests is graphically illustrated in Figure 6.16. The temperature of the isothermal test as well as the initial temperature of the adiabatic test are $10\,^{\circ}$C. Conceptually, the results reflect the exothermic and endothermic properties of $A \rightarrow M$ and $M \rightarrow A$ phase transformations. As heat is generated for the

σ / MPa

450

    .... adiabatic
    ———— isothermal

300

150

0   2   4   6   ε / %
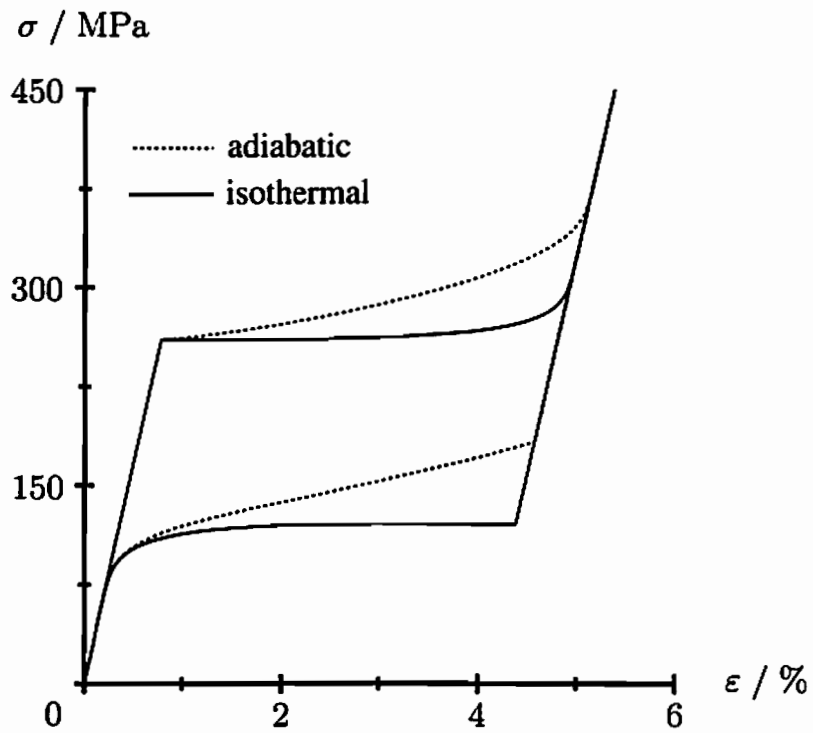
Figure 6.16: Isothermal and adiabatic simple tension tests; stress response for prescribed strain

σ / MPa

450   ●(4)

300   ●(2)

150   ●(3)

    (1)
0   2   4   6   ε / %
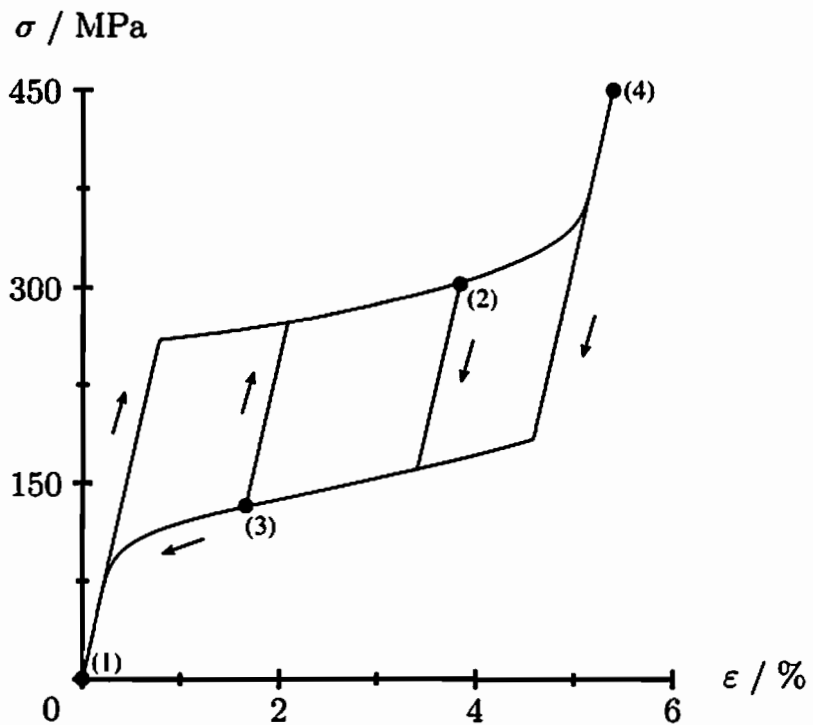
Figure 6.17: Adiabatic simple tension test with one internal cycle; stress response for prescribed strain
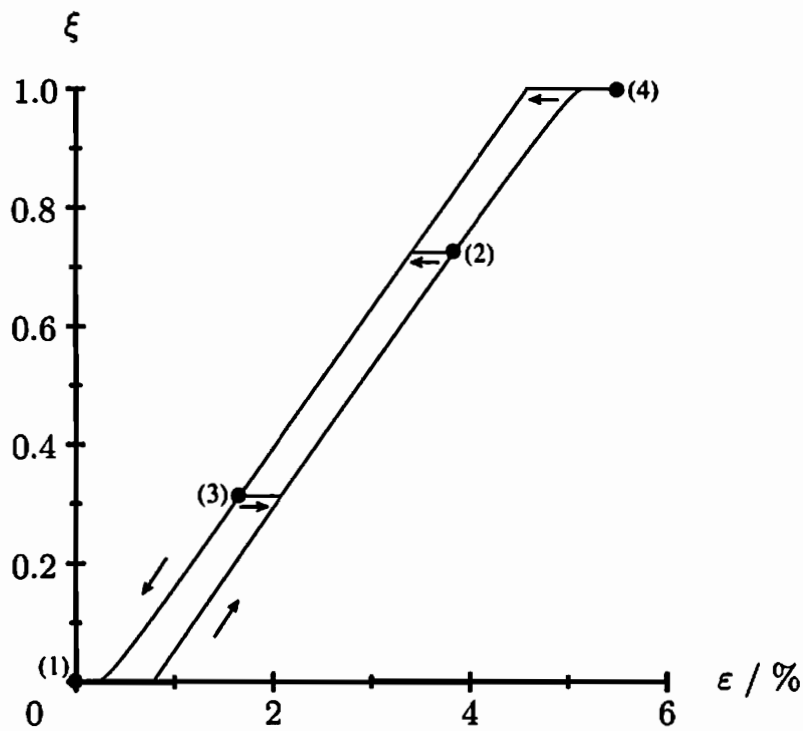
Figure 6.18: Adiabatic simple tension test with one internal cycle; martensite evolution for prescribed strain
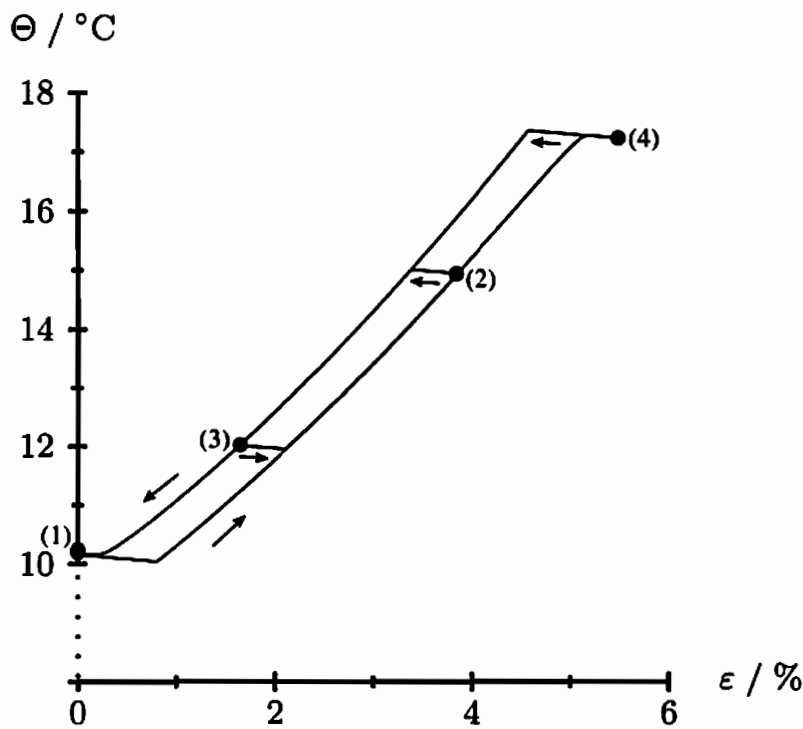
Figure 6.19: Adiabatic simple tension test with one internal cycle; temperature evolution for prescribed strain

exothermic A → M phase transformation, the temperature increases in the adiabatic case. Along with the Clausius-Clapeyron-like relation considered in Section 5.5.2, this results in an increase of the critical transformation stresses. For the endothermic M → A phase transformation, however, the temperature and in turn the critical transformation stresses decrease, such that the stresses in the isothermal and in the adiabatic cases nearly coincide at the end of the unloading process.

Figure 6.17 depicts the stress response of an adiabatic tension test with one internal cycle. Therein, points (1) to (4) represent the loading sequence, while the arrows indicate the loading direction. The initial temperature of this test is again 10 °C. It may be inferred that phase transformations only initiate at the upper and lower bounds of the pseudoelastic hysteresis. This behavior can experimentally be observed for NiTi in Tanaka et al. (1995), Helm (2001), or Tobushi et al. (2003). Figures 6.18 and 6.19 show the corresponding evolutions of the martensitic mass fraction and of the temperature, both plotted against the tensile strain. The linear relation between the mass fraction of martensite and the strain is consistent with in-situ neutron diffraction analyses obtained by Vaidyanathan et al. (1999) and the temperature evolution clearly reflects the exothermic and endothermic characteristics of the A → M and M → A phase transformations discussed above. Particularly, the piezocaloric effect can be observed in the strain-temperature diagram leading to a temperature change for elastic, volumetric deformations. This effect may, however, be regarded as subordinate compared to the temperature change arising from phase transformations. Note that the temperature at the end of the unloading process is slightly above the initial temperature.

6.2.5 Concluding remarks

As demonstrated in Section 6.2.3, the introduction of the tensorial internal variable **t** is essential for the prediction of the material response in the case of complex loadings. Particularly, the degree of freedom expressing the deviation between the stress direction and the martensite orientation in terms of the re-orientation function proves valuable for the description of the experimentally observed negative axial stress at zero tensile strain. The comparisons between the computed and measured material responses reveal, however, some deviations which may principally be ascribed to the asymmetric transformation behavior of NiTi shape memory alloys as well as to the assumed coaxiality of the stress direction and the martensite orientation. As considered in Section 6.2.3, the tension/compression asymmetry may not be neglected and should, thus, be incorporated into the constitutive model. Further analyses on this matter can be found, e.g., in Bouvet et al. (2004a) and Lexcellent et al. (2006). Moreover, although the assumed coaxiality of the stress direction and the martensite orientation leads to a straightforward formalism for the com-

putation of the tensorial internal variable t, this approach seems to provide a weak material response for complex loadings. It may specifically be inferred from the modified computation performed at the end of Section 6.2.3 that the material behavior is purely elastic directly on changing the loading direction within an intermediate austenitic-martensitic state. This finding motivates that t and s can neither be taken as coaxial nor as parallel as assumed by Raniecki et al. (1992). In this regard, the existing approach for the tensorial internal variable t has to be modified. For instance, the coaxiality assumption may be removed by introducing a constitutive equation for the eigenprojections of t in which they rotate into the direction of the eigenprojections of s after reaching a certain threshold value. In this context, it has to be guaranteed that a solution of the reorientation function for the eigenvalues of t unconditionally exists as discussed in Section 5.5.3, which requires the maximum value of the reorientation function to exceed the parameter ϑ. This provides, on the one hand, a criterion for the initiation of the eigenprojection rotation of t and, on the other hand, an equation for the respective rotation angle. Alternatively to this approach, the reorientation function may be exploited on adopting the formalism for the correction of t during processes of phase transformation as regarded in Section 5.5.2. The underlying idea follows the observation that, during reorientations, martensite variants being inconsistent with the current stress direction are to be replaced by new, favored variants. Then, on satisfying the reorientation function, the amount of the exchanged martensitic mass fraction may be determined, which provides an evolution equation for t in the same line as in Section 5.5.2.

6.3   Finite element analysis

This section addresses the numerical implementation of the proposed constitutive model at finite deformations. Since these deformations may exhibit superimposed rigid body motions, the implementation considered in Section 6.2.1 cannot be adopted here. Instead, integration algorithms have to be employed ensuring the integrated discretized constitutive equations to be consistent with the principle of material frame indifference and, thus, to be *incrementally objective* (cf. Simo & Hughes (1998)). This aspect is addressed in Section 6.3.1 in deriving a general framework for the incrementally objective time integration. In Section 6.3.2, the resulting formalism is specified to the proposed material model. Throughout the implementation, the coaxiality assumption between the stress direction and the martensite orientation is removed and the reorientation approach for the martensite variants is not taken into account. Focus is particularly on phase transformations including the correction of the average orientation of the martensite variants discussed in Section 5.5.2. A fully thermomechanically coupled structural example in terms of a testing specimen for experimental measurements is then presented in Section 6.3.3.

6.3.1   Incrementally objective time integration

Incrementally objective time integration algorithms require proper objective approximations of the relevant kinematical quantities. In this regard, suppose that the motions χ_n and χ_{n+1} of each material particle of the body at issue at time t_n and time t_{n+1} are given. Then, any intermediate motion $\chi_{n+\alpha}$ at time $t_{n+\alpha}$ may be approximated by

$$\chi_{n+\alpha} = (1 - \alpha)\,\chi_n + \alpha\,\chi_{n+1} \quad , \tag{6.15}$$

where α represents a scalar parameter with $\alpha \in [0,1]$ and $t_{n+\alpha}$ denotes an intermediate time between t_n and t_{n+1}, accordingly. Using this approximation, along with relation (3.5), provides the intermediate deformation gradient

$$\mathbf{F}_{n+\alpha} = (1 - \alpha)\,\mathbf{F}_n + \alpha\,\mathbf{F}_{n+1} \quad . \tag{6.16}$$

Therewith, the intermediate *incremental deformation gradient* $\mathbf{f}_{n+\alpha}$ may be introduced as

$$\mathbf{f}_{n+\alpha} = \mathbf{F}_{n+\alpha} \cdot \mathbf{F}_n^{-1} \quad . \tag{6.17}$$

It reflects the incremental mapping between the line elements $\mathrm{d}\mathbf{x}_n$ and $\mathrm{d}\mathbf{x}_{n+\alpha}$ at times t_n and $t_{n+\alpha}$ as

$$\mathrm{d}\mathbf{x}_{n+\alpha} = \mathbf{f}_{n+\alpha} \cdot \mathrm{d}\mathbf{x}_n \quad . \tag{6.18}$$

The intermediate incremental deformation gradient especially proves helpful for the determination of the properly discretized stretching tensor $\mathbf{D}_{n+\alpha}$ and vorticity tensor $\mathbf{W}_{n+\alpha}$. According to Simo & Hughes (1998), objective approximations of these quantities read

$$\mathbf{D}_{n+\alpha} = \frac{1}{2\,\Delta t}\,\mathbf{f}_{n+\alpha}^{-T} \cdot \left(\mathbf{f}_{n+1}^{T} \cdot \mathbf{f}_{n+1} - \mathbf{I} \right) \cdot \mathbf{f}_{n+\alpha}^{-1} \tag{6.19}$$

and

$$\mathbf{W}_{n+\alpha} = \frac{1}{2\,\Delta t}\,\left((\mathbf{f}_{n+1} - \mathbf{I}) \cdot \mathbf{f}_{n+\alpha}^{-1} - \mathbf{f}_{n+\alpha}^{-T} \cdot (\mathbf{f}_{n+1}^{T} - \mathbf{I}) \right) \quad . \tag{6.20}$$

Moreover, with the deformation gradient $\mathbf{F}_{n+\alpha}$ together with equation (3.17$_2$), the intermediate left Cauchy-Green tensor $\mathbf{B}_{n+\alpha}$ becomes

$$\mathbf{B}_{n+\alpha} = \mathbf{F}_{n+\alpha} \cdot \mathbf{F}_{n+\alpha}^{T} \quad . \tag{6.21}$$

Altogether, the objective approximations of the stretching tensor, the vorticity tensor, as well as the left Cauchy-Green tensor furnish the properly discretized logarithmic spin tensor $\mathbf{\Omega}_{n+\alpha}^{\mathrm{Log}}$ considered in Section 3.5.2. A formalism for its computation can be found in Xiao et al. (1998a). Then, with $\mathbf{\Omega}_{n+\alpha}^{\mathrm{Log}}$ at hand, the logarithmic rotation tensor $\mathbf{R}_{n+\alpha}^{\mathrm{Log}}$ defining the logarithmic corotational

frame can be quantified by solving the incremental form of the initial value problem (3.90). As the state of the material at time t_n is given, the latter can be rewritten as

$$\dot{\mathbf{R}}^{\mathrm{Log}} = -\mathbf{R}^{\mathrm{Log}} \cdot \Omega^{\mathrm{Log}} \quad \text{with} \quad \mathbf{R}^{\mathrm{Log}}|_{t=t_n} = \mathbf{R}_n^{\mathrm{Log}} \quad . \tag{6.22}$$

Its solution

$$\mathbf{R}_{n+\alpha}^{\mathrm{Log}} = \mathbf{R}_n^{\mathrm{Log}} \cdot (\exp(\alpha \, \Delta t \, \Omega_{n+\alpha}^{\mathrm{Log}}))^{\mathrm{T}} \tag{6.23}$$

is presented in the work of Simo & Hughes (1998), in which a procedure for the evaluation of the *exponential map* can additionally be reviewed (see also Belytschko et al. (2000)).

On the basis of the preceding incrementally objective quantities, the corotational time integration regarded in Section 3.5.2 can be employed. As this procedure conceptually relies on the correspondence between the corotational rate of the arbitrary objective Eulerian second-order tensor $\mathbf{A}$ and the material rate of the transformed tensor $\mathbf{A}^*$ in the corotating frame, the implicit backward Euler scheme may directly be adopted to equation (3.74). Along with transformation rule (3.43$_3$), and on focusing on the logarithmic rate, this leads to the relation

$$\mathbf{A}_{n+1}^* = \mathbf{A}_n^* + \Delta t \, \dot{\mathbf{A}}_{n+1}^* = \mathbf{R}_n^{\mathrm{Log}} \star \mathbf{A}_n + \Delta t \, \mathbf{R}_{n+1}^{\mathrm{Log}} \star \overset{\circ}{\mathbf{A}}{}_{n+1}^{\mathrm{Log}} \quad , \tag{6.24}$$

where equations (3.43$_3$) and (3.74) are evaluated at time t_n and at time t_{n+1}, respectively. The tensor $\mathbf{A}_{n+1}$ at time t_{n+1} can then be obtained from a backward rotation of (6.24) into the Eulerian frame as

$$\mathbf{A}_{n+1} = (\mathbf{R}_{n+1}^{\mathrm{Log}})^{\mathrm{T}} \star \mathbf{A}_{n+1}^* = \mathbf{r}_{n+1}^{\mathrm{Log}} \star \mathbf{A}_n + \Delta t \, \overset{\circ}{\mathbf{A}}{}_{n+1}^{\mathrm{Log}} \quad , \tag{6.25}$$

with

$$\mathbf{r}_{n+1}^{\mathrm{Log}} = (\mathbf{R}_{n+1}^{\mathrm{Log}})^{\mathrm{T}} \cdot \mathbf{R}_n^{\mathrm{Log}} = \exp(\Delta t \, \Omega_{n+1}^{\mathrm{Log}}) \tag{6.26}$$

representing the *incremental logarithmic rotation tensor*.

6.3.2 Implementation within a geometrically non-linear theory

Concentrating on processes of phase transformation, the subsequent implementation is carried out on the basis of the relations summarized in Figures 5.19 and 5.20 (a). Although the assumption of coaxiality between $\mathbf{t}$ and $\mathbf{s}$ is removed throughout this section, the correction of $\mathbf{t}$ during phase transformation processes is particularly taken into account.

Adaptation of the implicit backward Euler scheme as in equation (6.25) to the rate form of the Kirchoff stress tensor yields

$$\tau_{n+1} = \mathbf{r}_{n+1}^{\mathrm{Log}} \star \tau_n + \Delta t \, \overset{\circ}{\tau}{}_{n+1}^{\mathrm{Log}} \quad , \tag{6.27}$$

along with the discretized stress rate

$$\Delta t \, \overset{\circ}{\tau} \, \overset{\text{Log}}{_{n+1}} = \mathbb{C} : (\Delta t \, \mathbf{D}_{n+1} - \alpha \, \Delta\Theta) - \tau_0 \, \mathbf{t}_{n+1} \, (\xi_{n+1} - \xi_n)$$
$$- \tau_0 \, \xi_{n+1} \, (\mathbf{t}_{n+1} - \mathbf{r}^{\text{Log}}_{n+1} \star \mathbf{t}_n) \quad . \quad (6.28)$$

Here, the rate of $\mathbf{t}$ is consistently approximated by a differential quotient derived from (6.25). Thus, the Kirchhoff stress τ_{n+1} takes the form

$$\tau_{n+1} = \mathbf{r}^{\text{Log}}_{n+1} \star (\tau_n + \tau_0 \, \xi_{n+1} \, \mathbf{t}_n) + \mathbb{C} : (\Delta t \, \mathbf{D}_{n+1} - \alpha \, \Delta\Theta)$$
$$- \tau_0 \, \mathbf{t}_{n+1} \, (2 \, \xi_{n+1} - \xi_n) \quad . \quad (6.29)$$

As outlined in Section 6.2.1, the mass fraction of martensite ξ_{n+1} may be obtained by evaluating the thermodynamic force driving phase transformations as well as the functions k^β at time t_{n+1} as

$$\pi^\xi(\tau_{n+1}, \Theta_{n+1}, \mathbf{t}_{n+1}, \xi_{n+1}) = k^\beta(\xi_{n+1}) \quad . \quad (6.30)$$

Finally, adopting (6.25) to the rate equation for $\mathbf{t}$ in Figure 5.20 (a) gives:

$$\mathbf{t}_{n+1} = \begin{cases} \mathbf{r}^{\text{Log}}_{n+1} \star \mathbf{t}_n + \dfrac{1}{\xi_{n+1}} \, (\mathbf{s}_{n+1} - \mathbf{t}_{n+1}) \, (\xi_{n+1} - \xi_n) & \text{for A} \to \text{M} \\[2ex] \mathbf{r}^{\text{Log}}_{n+1} \star \mathbf{t}_n & \text{for M} \to \text{A} \end{cases} \quad (6.31)$$

For the solution of the unknown quantities τ_{n+1}, ξ_{n+1}, and $\mathbf{t}_{n+1}$ in equations (6.29) to (6.31), a similar strategy as in Section 6.2.1 based on an operator split method may be employed. In contrast to the foregoing strategy, however, only the trial state t^{pt}_{n+1} accounting for phase transformations is required here, as processes of reorientation are excluded. The resulting formalism is summarized in Figure 6.20. It is assumed that all relevant quantities at time t_n as well as the increments Δt and $\Delta\Theta$ are given. From this, along with the deformation gradient at time t_{n+1}, the input variables Θ_{n+1}, $\mathbf{D}_{n+1}$, and $\mathbf{r}^{\text{Log}}_{n+1}$ are to be specified (step 1). Then, the trial state t^{pt}_{n+1} is computed on assuming that phase transformations do not occur in the next time step (step 2). If the criteria for phase transformations are not fulfilled, this state equals the actual state at t_{n+1}. Otherwise, the state at t_{n+1} has to be recomputed on also taking phase transformations into account (step 4). The incrementally generated heat is finally evaluated at the end of the integration procedure (step 5).

6.3.3 Structural example

Based on the implementation in the preceding section, a fully thermomechanically coupled finite element simulation of a specimen used in the work of Heckmann (2003) for tensile tests is presented in this section. The experimental apparatus, the specimen geometry, and the corresponding finite element

1. Given state t_n, Δt and $\Delta\Theta$, $\Theta_{n+1} = \Theta_n + \Delta\Theta$, $\mathbf{D}_{n+1}$, and $\mathbf{r}_{n+1}^{\mathrm{Log}}$

2. Compute trial state t_{n+1}^{pt} in the absence of phase transformations

   solve for τ_{n+1}^{pt}, $\mathbf{t}_{n+1}^{\mathrm{pt}}$, and ξ_{n+1}^{pt}

   $$\tau_{n+1}^{\mathrm{pt}} = \mathbf{r}_{n+1}^{\mathrm{Log}} \star (\tau_n + \tau_0\,\xi_n\,\mathbf{t}_n) + \mathbb{C} : (\Delta t\,\mathbf{D}_{n+1} - \alpha\,\Delta\Theta)$$

   $$\mathbf{t}_{n+1}^{\mathrm{pt}} = \mathbf{r}_{n+1}^{\mathrm{Log}} \star \mathbf{t}_n$$

   $$\xi_{n+1}^{\mathrm{pt}} = \xi_n$$

3. Test for phase transformations

   $$\mathrm{A} \to \mathrm{M}: \qquad \pi^\xi\big|_{n+1}^{\mathrm{pt}} - k^{\mathrm{A}\to\mathrm{M}}\big|_{n+1}^{\mathrm{pt}} > 0$$

   $$\mathrm{M} \to \mathrm{A}: \qquad -\pi^\xi\big|_{n+1}^{\mathrm{pt}} + k^{\mathrm{M}\to\mathrm{A}}\big|_{n+1}^{\mathrm{pt}} > 0$$

   if not $(\mathrm{A} \to \mathrm{M}$ or $\mathrm{M} \to \mathrm{A})$ then

   set $(\cdot)_{n+1} = (\cdot)_{n+1}^{\mathrm{pt}}$ and go to step 5

   end if

4. Compute state t_{n+1} under phase transformations

   solve for τ_{n+1}, $\mathbf{t}_{n+1}$, and ξ_{n+1}

   $$\tau_{n+1} = \mathbf{r}_{n+1}^{\mathrm{Log}} \star (\tau_n + \tau_0\,\xi_{n+1}\,\mathbf{t}_n) + \mathbb{C} : (\Delta t\,\mathbf{D}_{n+1} - \alpha\,\Delta\Theta)$$

   $$\qquad\qquad - \tau_0\,\mathbf{t}_{n+1}\,(2\,\xi_{n+1} - \xi_n)$$

   $$\mathbf{t}_{n+1} = \begin{cases} \mathbf{r}_{n+1}^{\mathrm{Log}} \star \mathbf{t}_n + \dfrac{1}{\xi_{n+1}}\,(\mathbf{s}_{n+1} - \mathbf{t}_{n+1})\,(\xi_{n+1} - \xi_n) & \mathrm{A} \to \mathrm{M} \\[4mm] \mathbf{r}_{n+1}^{\mathrm{Log}} \star \mathbf{t}_n & \mathrm{M} \to \mathrm{A} \end{cases}$$

   $$\pi^\xi(\tau_{n+1}, \Theta_{n+1}, \mathbf{t}_{n+1}, \xi_{n+1}) = k^\beta(\xi_{n+1})$$

5. Compute incremental generation of heat

   $$\Delta(q_{\mathrm{gen}})_n = \bar{\mathbf{q}}_{\mathrm{gen}}^\tau\big|_{n+1} : (\tau_{n+1} - \tau_n) + \bar{q}_{\mathrm{gen}}^\xi\big|_{n+1}\,(\xi_{n+1} - \xi_n)$$

   $$\qquad\qquad + \bar{\mathbf{q}}_{\mathrm{gen}}^t\big|_{n+1} : (\mathbf{t}_{n+1} - \mathbf{t}_n)$$

Figure 6.20: Extended return-mapping algorithm at finite deformations

model exploiting the symmetry of the specimen are depicted in Figure 6.21. Altogether, the finite element model consists of 242 hexagonal elements including 456 nodes.
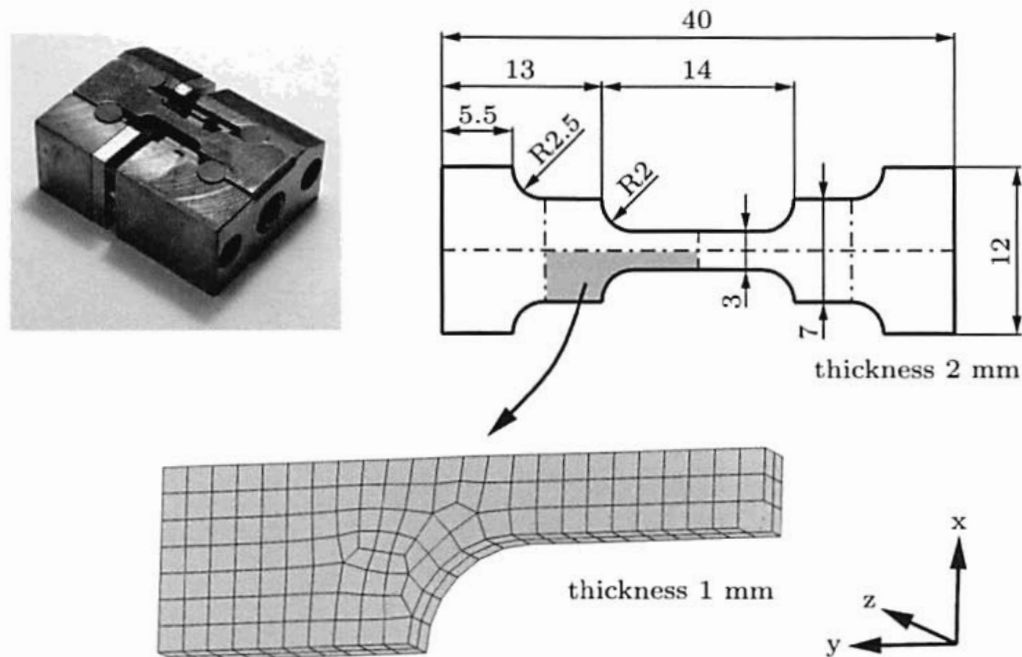
Figure 6.21: Experimental apparatus used in Heckmann (2003) (upper left),
           sample geometry (upper right), and finite element model of the
           sample; measures are in mm.

During the simulation, one loading-unloading cycle of the specimen into its
axial direction is considered. As the material exhibits a strong thermomechan-
ically coupled behavior, the specimen is simultaneously exposed to mechanical
and thermal loads, such that adequate initial and boundary conditions are
to be specified. At the beginning of the deformation process, the specimen
temperature is assumed to be equal to the ambient temperature of 10 °C. In
this stage, the initial structure of the material is considered to be completely
austenitic. The process of deformation is realized by a uniformly distributed
axial displacement of the left end of the model for 20 s with a constant velocity
of 0.02 $^{mm}/_{s}$ for, both, the loading and the unloading process, whereas the axial
position on the right end of the model is held constant. To account for the heat
exchange between the specimen and its environment, a convective heat flux
is applied to the outer surface of the specimen on assuming the heat transfer
coefficient to be 20 $^{W}/_{mm^2}$ K. The inner surfaces of the model resulting from
the exploited symmetry of the specimen, are taken as adiabatic. Moreover,
on stipulating that the temperature of the clamping is unaffected by thermal
effects, the surface temperature on the right end of the model is held constant
throughout the process of deformation. The simulation is carried out on the
basis of the material parameters identified in Section 6.2.2.
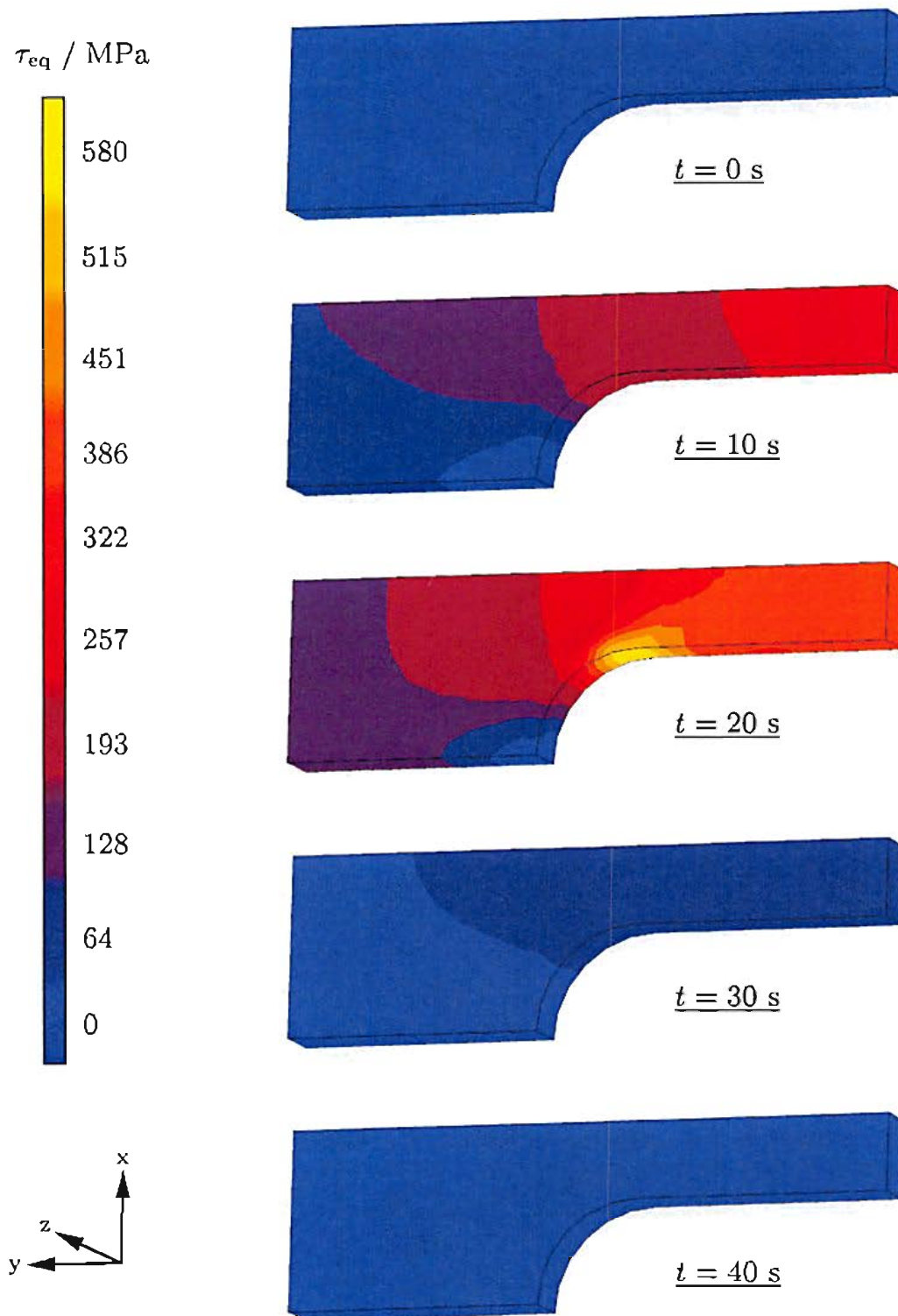
Figure 6.22: Evolution of the equivalent stress
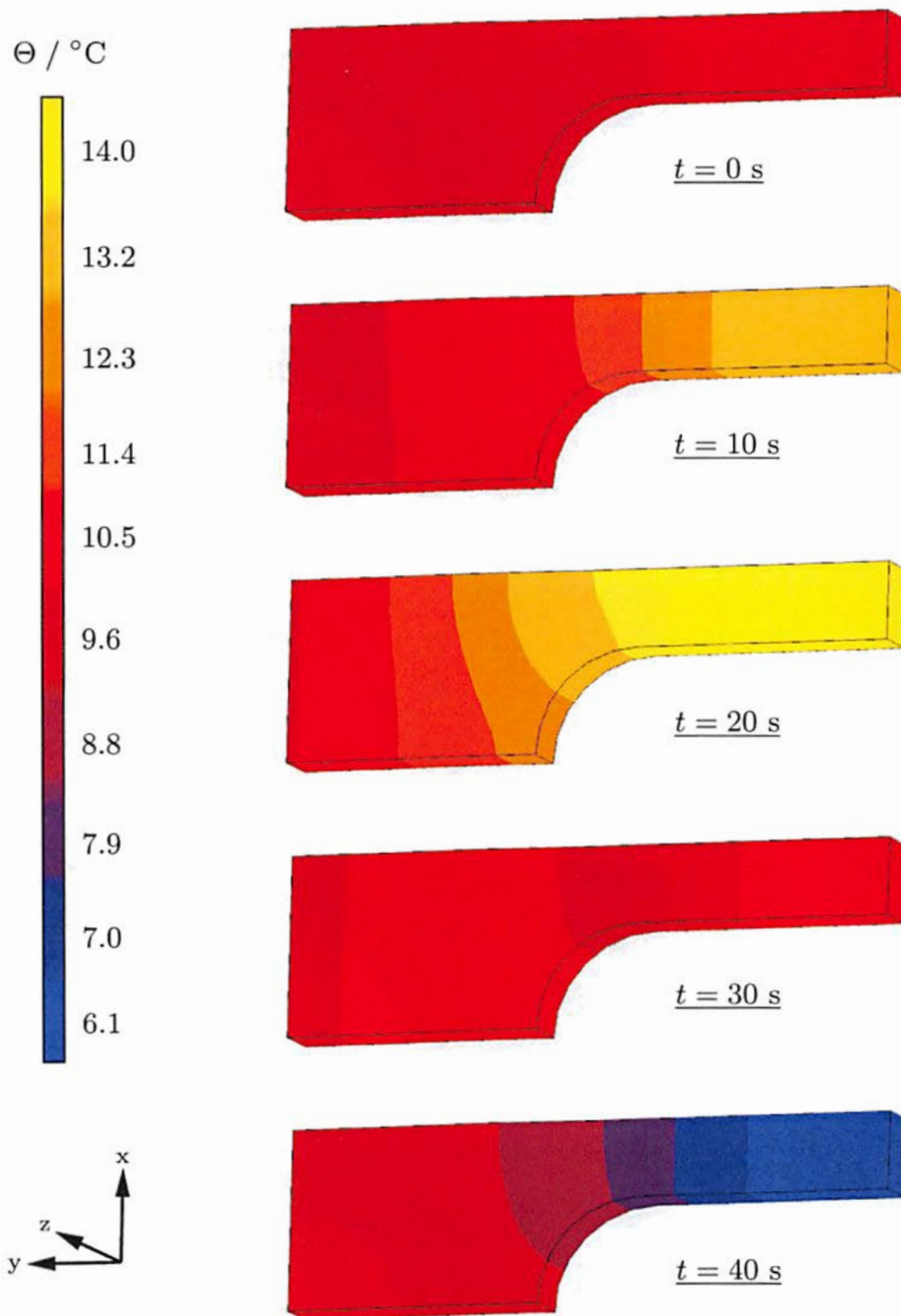
Figure 6.23: Evolution of the temperature
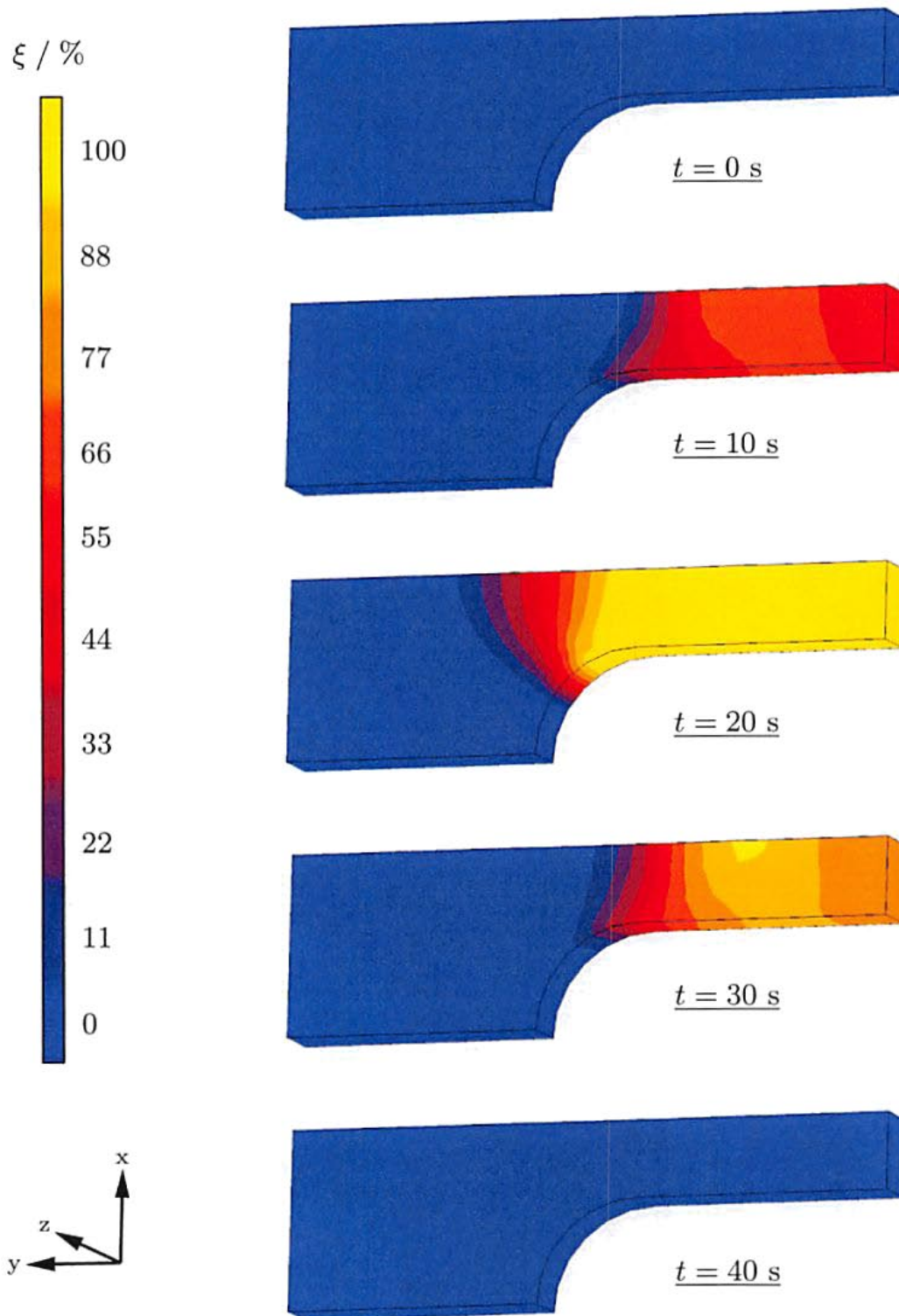
Figure 6.24: Evolution of the mass fraction of martensite
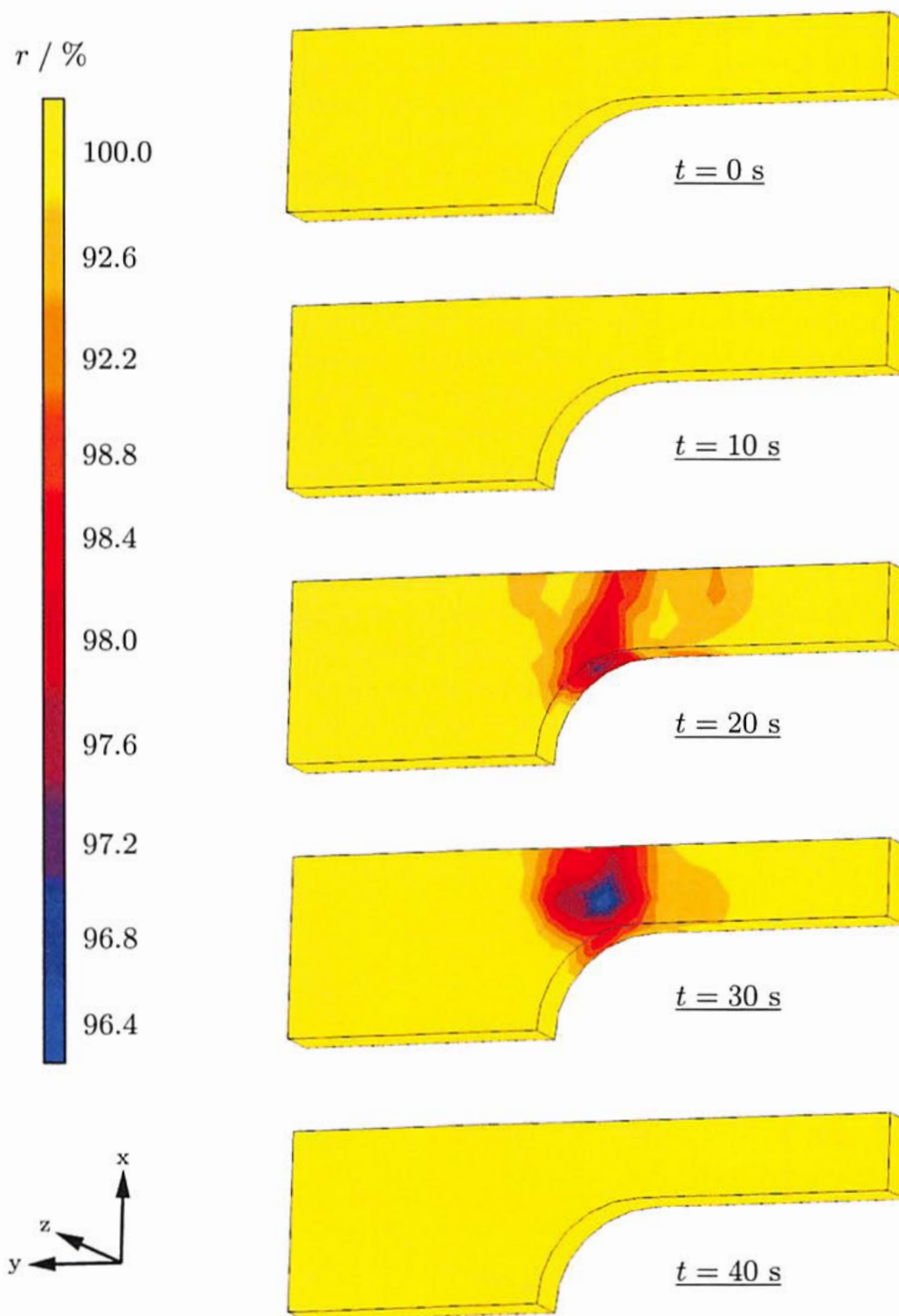
Figure 6.25: Evolution of the reorientation function

Figures 6.22 to 6.25 show the distribution of the equivalent Kirchhoff stress, the temperature, the mass fraction of martensite, and the reorientation function for selected time steps. Therein, the thermomechanically coupled deformation process can readily be observed. During the loading process, the specimen temperature increases due to the exothermic A → M phase transformation. Its maximum value of 14 °C is reached in the gauge length of the specimen at $t = 20$ s, which is not surprising as the phase transformation activities are merely restricted to this region. Accordingly, the specimen temperature decreases for the endothermic M → A phase transformation during the un-loading process, such that its minimum value of 6 °C is again reached in the gauge length at the end of the deformation process. The difference between this temperature and the initial temperature of 10 °C principally arises from the heat conduction within the specimen and the heat exchange between the specimen and its environment. In fact, the specimen would recover its initial temperature for a sufficiently long time range after the deformation. From the distribution of the reorientation function it may be inferred that the deviation between the stress direction and the martensite orientation can be regarded as small. In this context, a process of reorientation would possibly not initiate for the considered experiment. Beyond this finding, it can also be deduced that a pure radial loading path for which the stress direction remains constant can generally not be realized for elastic-inelastic deformation processes even in the case of constant external loads. This underlines the necessity of constitutive
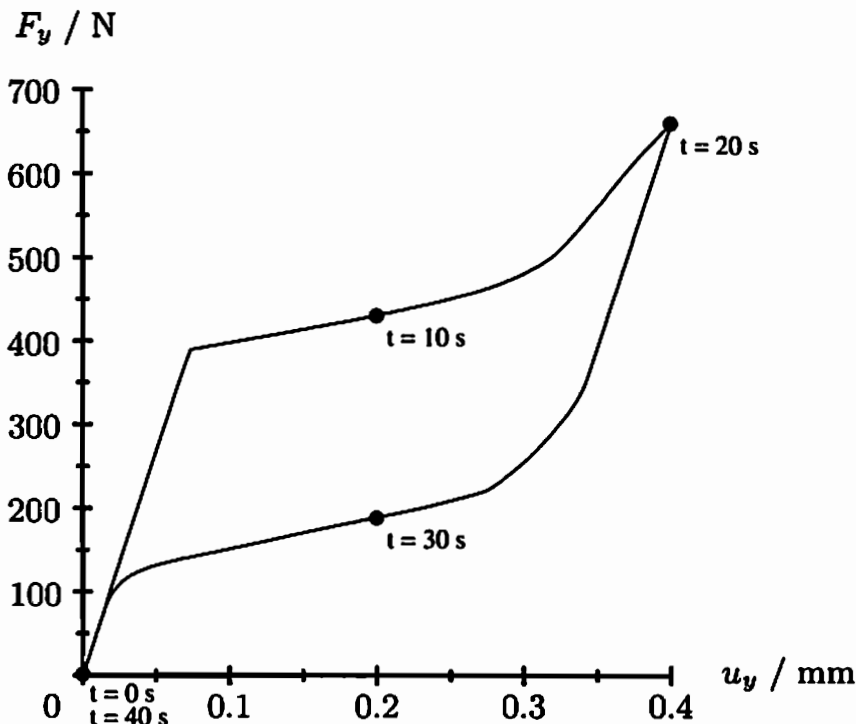
Figure 6.26: Applied total force for prescribed total displacement

models for shape memory alloys to account for non-proportional loadings in order to provide reliable results for a realistic simulation of complex structures.

Figure 6.26 depicts the total axial force plotted against the total axial displacement. The observable plateau can be ascribed to uniformly distributed phase transformations within the gauge length of the specimen. These transformations are completed at the end of the plateau, such that the slope of the displacement-force curve increases. The phase transformations are, however, not completed, as there exist ongoing phase transformation activities between the clamping region and the gauge length on additional loadings. As these activities are interrupted during unloading, the slopes for the loading and the unloading processes at the end of the plateau differ. In fact, the structural response on unloading characterizes a purely thermoelastic material behavior until the critical stress for the phase transformation into the austenite is reached.

7 Summary and outlook

This treatise addresses the formulation of a three-dimensional constitutive model for pseudoelastic NiTi shape memory alloys at finite deformations. The model is embedded into a hypoelastic theory in terms of the Kirchhoff stress tensor, the stretching tensor, and the logarithmic rate. It is consistently formulated in a general framework of continuum thermodynamics for solid state transformations between the two phases austenite and martensite, taking into account the irreversibility of the transformation processes.

The energetic state of the material is characterized by a non-convex specific Helmholtz free energy function which comprises the phase specific energies of austenite and martensite as well as an energetic term accounting for phase interactions. This energy is particularly formulated in terms of stress, temperature, and internal variables. The dependence on the stress does not contradict the classical formulation of the Helmholtz free energy in which the purely elastic component of the total strain is employed, as the elastic strain may be regarded as redundant quantity of the stress. The determination of the elastic strain may, however, be considered as cumbersome within the framework of finite deformations. On the basis of this formulation, the potential wells of the martensite variants are assumed to be continuously distributed around the single potential well of the austenite within the austenitic stress space. This consideration may ideally be regarded as fulfilled for untextured polycrystals. It accounts for the observation that martensite is stabilized by stress in the course of the pseudoelastic shape memory effect and that, thus, the potential wells of the single martensite variants are shifted towards higher stresses. The energetic state of the overall martensitic phase is then represented by an average specific Helmholtz free energy function.

A set of three internal variables is introduced. Two scalar-valued internal variables describe the overall mass fraction and average distortion of the martensitic phase. The average orientation of the martensite variants is accounted for by a tensorial internal variable. Together, the average distortion and the average orientation of the martensite characterize the position of the average martensitic energy minimum within the austenitic stress space. On this account, the unphysical decomposition of the mass fraction of martensite into self-accommodated and oriented parts as employed by phase diagram approaches can be avoided. Instead, the martensitic phase is described by averaged quantities. In restricting to pseudoelasticity, the average distortion of the martensite is then set constant.

An analysis of the mechanical interactions between martensitic and austenitic domains reveals an approach for the intrinsic, phase specific stresses. It turns out that snap through-like processes of phase transformation can neither exclusively be presumed nor can they be ignored. Application of the principle of local equilibrium then provides relations for the total stretching tensor and

the total stress tensor. In this regard, local mechanical and thermal equilibria are postulated, whereas a phase equilibrium is not assumed. In ensuring thermodynamic consistency in terms of the Clausius-Duhem inequality, thermodynamic forces driving the processes of phase transformation and reorientation of the martensite variants are identified. By virtue of the former, an evolution equation for the martensitic mass fraction is derived. The evolution equation for the average orientation of the martensite variants is formulated on the basis of experimental data obtained from biaxial test. These data specifically exhibit that the stress and strain directions, and in turn the average orientation of the martensite variants, generally deviate from each other for complex loadings. A constitutive equation accounting for this finding is accordingly proposed. Finally, exploitation of the first law of thermodynamics, along with the adopted specific Helmholtz free energy function, provides a relation for the heat generated during deformation processes, which particularly includes the generated heat arising from phase transformations.

The model is implemented into the finite element method by employing a straightforward extension of the classical return-mapping algorithm. The focus is first on a geometrically linear implementation in the course of a validation of the material model with experimental results. A calibration of the material parameters and a subsequent comparison between simulated and measured material responses during biaxial tests demonstrate the appropriateness of the constitutive assumptions. Thereafter, the numerical implementation is extended to finite deformations. Special attention is on the incremental objectivity in order to ensure an objective time integration of the Eulerian rate model. On the basis of this implementation, a thermomechanically coupled simulation of a shape memory structure is presented showing the applicability of the model for structural simulations.

Although the current formulation of the proposed constitutive model focuses on the pseudoelastic shape memory effect, an extension to the pseudoplastic effect and in turn to the one-way shape memory effect is possible. It can be achieved by specifying a constitutive equation for the average distortion of the martensite which is set constant in the course of pseudoelasticity. In doing so and in conjunction with the average orientation of the martensite variants, the position of the average energetic minimum of the martensitic phase within the austenitic stress space can be well-described, accounting for oriented and self-accommodated martensite through averaged quantities. For the specification of a respective thermodynamically consistent constitutive equation, a similar formalism as applied for the martensitic mass fraction ξ may be adopted. This methodology is based on the observation, that τ_0 and ξ exhibit similar structures, i.e., τ_0 and ξ are scalar-valued and underlie the restrictions $\tau_0 \in [0, \bar{\tau}_0]$ and $\xi \in [0, 1]$, where $\bar{\tau}_0$ is the maximum admissible distortion of the martensite. Thus, an evolution equation for τ_0 may accordingly be obtained from the Clausius-Duhem inequality.

As discussed during the validation of the constitutive model, the prediction of the pseudoelastic material response may be refined by accounting for the asymmetric transformation behavior which is often exhibited by NiTi alloys and by removing the coaxiality assumption between the stress direction and the martensite orientation. An valuable quantity for the former may be the third invariant of the average martensite orientation which basically inherits a directional information. Therewith, the maximum admissible martensitic distortion $\bar{\tau}_0$ and the functions k^β prescribing the evolution of the thermodynamic driving force for phase transformations may be defined as orientation-dependent isotropic tensor functions. Removing the coaxiality assumption between the stress direction and the average martensite orientation may require additional evolution equations for the respective eigenprojections in the case of reorientation processes. In this regard, it has to be ensured that a solution for the eigenvalues of the martensite orientation always exists. It may, for instance, be assumed that the eigenprojections of the martensite orientation rotate into the directions of the eigenprojections of the current stress direction. This approach may, however, lead to a high computational effort. Alternatively, the correction procedure of the martensite orientation during phase transformation processes may be adopted for reorientations. This idea is based on the observation, that favorably oriented variants grow during reorientations on the expense of unfavorably oriented variants. The amount of the reoriented mass fraction of martensite may then be obtained from the reorientation function.

References

ACHENBACH, M. (1989): *A model for an alloy with shape memory*, in: Int. J. Plast., Volume 5, 371–395.

ACHENBACH, M. & MÜLLER, I. (1985): *Simulation of material behaviour of alloys with shape memory*, in: Arch. Mech., Volume 37, 573–585.

ADKINS, C. J. (Ed.) (1983): *Equilibrium thermodynamics*, 3rd Edition, Cambridge University Press 1983.

ANAND, L. (1979): *On H. Hencky's approximate strain-energy function for moderate deformations*, in: J. Appl. Mech., Volume 46, 78–82.

ANAND, L. (1986): *Moderate deformations in extension-torsion of incompressible isotropic elastic materials*, in: J. Mech. Phys. Solids, Volume 34, 3, 293–304.

AURICCHIO, F. (1995): *Shape-memory alloys: applications, micromechanics, macromodelling and numerical simulations* 1995, Dissertation, University of California at Berkeley.

AURICCHIO, F. & TAYLOR, R. L. (1997): *Shape-memory alloys: modelling and numerical simulations of the finite-strain superelastic behavior*, in: Comput. Methods Appl. Mech. Engrg., Volume 143, 175–194.

AURICCHIO, F., TAYLOR, R. L. & LUBLINER, J. (1997): *Shape-memory alloys: macromodelling and numerical simulations of the superelastic behavior*, in: Comput. Methods Appl. Mech. Engrg., Volume 146, 281–312.

BAEHR, H. D. (2002): *Thermodynamik*, 11th Edition, Springer Verlag 2002.

BALL, J. M. & JAMES, R. D. (1987): *Fine phase mixtures as minimizers of energy*, in: Arch. Ration. Mech. An., Volume 100, 1, 13–52.

BELYTSCHKO, T., LIU, W. K. & MORAN, B. (2000): *Nonlinear finite elements for continua and structures*, John Wiley & Sons, Ltd. 2000.

BERTRAM, A. (1982): *Thermo-mechanical constitutive equations for the description of shape memory effects in alloys*, in: Nucl. Eng. Des., Volume 74, 173–182.

BO, Z. & LAGOUDAS, D. C. (1999a): *Thermomechanical modeling of polycrystalline SMAs under cyclic loading, part I: theoretical derivations*, in: Int. J. Engng. Sci., Volume 37, 1089–1140.

BO, Z. & LAGOUDAS, D. C. (1999b): *Thermomechanical modeling of polycrystalline SMAs under cyclic loading, part III: evolution of plastic strains and twoway shape memory effect*, in: Int. J. Engng. Sci., Volume 37, 1141–1173.

BO, Z. & LAGOUDAS, D. C. (1999c): *Thermomechanical modeling of polycrystalline SMAs under cyclic loading, part IV: modeling of minor hysteresis loops*, in: Int. J. Engng. Sci., Volume 37, 1174–1204.

BOURKE, M. A. M., VAIDYANATHAN, R. & DUNAND, D. C. (1996): *Neutron diffraction measurement of stress-induced transformation in superelastic NiTi*, in: Appl. Phys. Lett., Volume 69, 17, 2477–2479.

BOUVET, C., CALLOCH, S. & LEXCELLENT, C. (2004a): *A phenomenological model for pseudoelasticity of shape memory alloys under multiaxial proportional and nonproportional loadings*, in: Eur. J. Mech. A-Solid, Volume 23, 37–61.

BOUVET, C., CALLOCH, S., TAILLARD, K. & LEXCELLENT, C. (2004b): *Experimental determination of initial surface of phase transformation of SMA*, in: J. Phys. IV, Volume 115, 29–36.

BOYD, J. G. & LAGOUDAS, D. C. (1996a): *A thermodynamical constitutive model for shape memory materials. Part I. The monolithic shape memory alloy*, in: Int. J. Plast., Volume 12, 6, 805–842.

BOYD, J. G. & LAGOUDAS, D. C. (1996b): *A thermodynamical constitutive model for shape memory materials. Part II. The SMA composite material*, in: Int. J. Plast., Volume 12, 7, 843–873.

BRILLOUIN, L. (1925): *Les lois de l'élasticité sous forme tensorielle valable pour des coordonnées quelconques*, in: Ann. Phys., Volume 3, 10, 251–298.

BRINSON, L. C. (1993): *One-dimensional constitutive behavior of shape memory alloys: thermomechanical derivation with non-constant material functions and redefined martensite internal variable*, in: J. Intel. Mat. Syst. Str., Volume 4, 229–242.

BRINSON, L. C., SCHMIDT, I. & LAMMERING, R. (2004): *Stress-induced transformation behavior of a polycrystalline TiNi shape memory alloy: micro and macromechanical investigations via in situ optical microscopy*, in: J. Mech. Phys. Solids, Volume 52, 1549–1571.

BRUHNS, O. T., MEYERS, A. & XIAO, H. (2004): *On non-corotational rates of Oldroyd's type and relevant issues in rate constitutive formulations*, in: P. Roy. Soc. A, Volume 460, 909–928.

BRUHNS, O. T., XIAO, H. & MEYERS, A. (1999): *Self-consistent Eulerian rate type elasto-plasticity models based upon the logarithmic stress rate*, in: Int. J. Plast., Volume 15, 479–520.

BRUHNS, O. T., XIAO, H. & MEYERS, A. (2000): *Hencky's elasticity model with the logarithmic strain measure: a study on Poynting effect and stress response in torsion of tubes and rods*, in: Arch. Mech., Volume 52, 4-5, 489–509.

CALLEN, H. B. (1960): *Thermodynamics: an introduction to the physical theories of equilibrium thermostatics and irreversible thermodynamics*, John Wiley & Sons, Inc., New York 1960.

CHADWICK, P. (1976): *Continuum mechanics: Concise theory and problems*, Dover Publications, Inc., Mineola, New York 1976.

CHRIST, D., REESE, S. & NEUKING, K. (2004): *A new finite element technology for shape memory alloy composites*, in: Mat. Sci. Eng. A, Volume 5, 300–306.

COHEN, E. R. & GIACOMO, P. (1987): *Symbols, units, nomenclature and fundamental constants in physics*, International Union of Pure and Applied Physics (IUPAP) 1987.

COLEMAN, B. D. (1964): *Thermodynamics of materials with memory*, in: Arch. Ration. Mech. An., Volume 17, 1–46.

COLEMAN, B. D. & GURTIN, M. E. (1967): *Thermodynamics with internal state variables*, in: J. Chem. Phys., Volume 47, 2, 597–613.

COLEMAN, B. D. & MIZEL, V. (1964): *Existence of caloric equations of state in thermodynamics*, in: J. Chem. Phys., Volume 40, 4, 1116–1125.

COLEMAN, B. D. & NOLL, W. (1963): *The thermodynamics of elastic materials with heat conduction and viscosity*, in: Arch. Ration. Mech. An., Volume 13, 167–178.

COLEMAN, B. D. & NOLL, W. (1964): *Thermodynamics of materials with memory*, in: Arch. Ration. Mech. An., Volume 15, 87–111.

COTTER, B. A. & RIVLIN, R. S. (1955): *Tensors associated with time-dependent stress*, in: Q. Appl. Math., Volume 13, 177–182.

DAY, W. A. (1972): *The thermodynamics of simple materials with fading memory*, 1st Edition, Springer Verlag 1972.

DE GROOT, S. R. & MAZUR, P. (1963): *Non-equilibrium thermodynamics*, 1st Edition, North- Holland Publishing 1963.

DELOBELLE, P. & LEXCELLENT, C. (1996): *A phenomenological three dimensional model for pseudoelastic behavior of shape memory alloys*, in: J. Phys. IV, Volume 6, C1-293 – C1-300.

DIENES, J. K. (1979): *On the analysis of rotation and stress rate in deforming bodies*, in: Acta Mech., Volume 32, 217-232.

DOGHRI, I. (2000): *Mechanics of deformable solids: linear, nonlinear, analytical and computational aspects*, 1st Edition, Springer Verlag 2000.

DOYLE, T. C. & ERICKSEN, J. L. (1956): *Nonlinear elasticity*, in: Adv. Appl. Mech., Volume 4, 53-115.

DUERIG, T. W., MELTON, K. N., STÖCKEL, D. & WAYMAN, C. M. (1990): *Engineering aspects of shape memory alloys*, 1st Edition, Butterworth-Heinemann 1990.

ENTCHEV, P. B. & LAGOUDAS, D. C. (2004): *Modeling of transformation-induced plasticity and its effect on the behavior of porous shape memory alloys. Part II: porous SMA response*, in: Mech. Mater., Volume 36, 893-913.

FALK, F. (1983): *One-dimensional model of shape memory alloys*, in: Arch. Mech., Volume 35, 1, 63-84.

FUNAKUBO, H. (Ed.) (1987): *Shape Memory Alloys*, Gordon and Breach Science Publishers 1987.

GALL, K. & SEHITOGLU, H. (1999): *The role of texture in tension-compression asymmetry in polycrystalline NiTi*, in: Int. J. Plast., Volume 15, 69-92.

GAO, X., HUANG, M. & BRINSON, L. C. (2000): *A multivariant micromechanical model for SMAs Part 1. Crystallographic issues for single crystal model*, in: Int. J. Plast., Volume 16, 10-11, 1345-1369.

GOVINDJEE, S. & HALL, G. J. (2000): *A computational model for shape memory alloys*, in: Int. J. Solids Struct., Volume 37, 735-760.

GOVINDJEE, S. & MIEHE, C. (2001): *A multi-variant martensitic phase transformation model: formulation and numerical implementation*, in: Comp. Method. Appl. M., Volume 191, 3-5, 215-238.

GOVINDJEE, S., MIELKE, A. & HALL, G. J. (2003): *The free energy of mixing for n-variant martensitic phase transformations using quasi-convex analysis*, in: J. Mech. Phys. Solids, Volume 51, 4, 1-26.

GRABE, C. (2007): *Experimental testing and parameter identification of the multidimensional material behavior of shape memory alloys* 2007, Mitteilungen aus dem Institut für Mechanik, Ruhr-Universität Bochum.

GRABE, C. & BRUHNS, O. T. (2008): *Path dependence and multiaxial behavior of a polycristalline NiTi alloy within the pseudoelastic and pseudoplastic temperature regimes*, in: Int. J. Plast., Volume doi:10.1016/j.ijplas.2008.03.002.

GRAESSER, E. J. & COZZARELLI, F. A. (1994): *A proposed three-dimensional constitutive model for shape memory alloys*, in: J. Intel. Mat. Syst. Str., Volume 5, 78–89.

GREEN, A. E. & MCINNIS, B. C. (1967): *Generalized hypoelasticity*, in: P. Roy. Soc. A, Volume 57, 220–230.

GREEN, A. E. & NAGHDI, P. M. (1965): *A general theory of an elasto-plastic continuum*, in: Arch. Ration. Mech. An., Volume 18, 251–281.

GURTIN, M. E. (1981): *An introduction to continuum mechanics*, 1st Edition, Academic Press 1981.

HACKL, K. & HEINEN, R. (2008): *A micromechanical model for pretextured polycrystalline shape-memory alloys including elastic anisotropy*, in: Continuum Mech. Therm., Volume 19, 8, 499–510.

HAIRER, E. & WANNER, G. (2002): *Solving ordinary differential equations II*, 2nd Edition, Springer Verlag 2002.

HALL, G. J. & GOVINDJEE, S. (2002): *Application of a partially relaxed shape memory free energy function to estimate the phase diagram and predict global microstructure evolution*, in: J. Mech. Phys. Solids, Volume 50, 3, 501–530.

HAUPT, P. (Ed.) (2000): *Continuum mechanics and theory of materials*, Springer Verlag 2000.

HAYASHI, A., TOKUDA, M., INABA, T. & HASHIMOTO, K. (2004): *Experimental research on mechanical properties of a new NiTi shape memory alloy*, in: Key Eng. Mat., Volume 274-276, 1089–1094.

HECKMANN, A. (2003): *Mikrostruktur und Ermüdung von NiTi-Formgedächtnislegierung* 2003, VDI-Verlag, Ruhr-Universität Bochum.

HEINTZE, O. & SEELECKE, S. (2008): *A coupled thermomechanical model for shape memory alloys – from single crystal to polycrystal*, in: Mat. Sci. Eng. A, Volume 481, 389–394.

HELM, D. (2001): *Formgedächtnislegierungen - Experimentelle Unter-suchung, phänomenologische Modellierung und numerische Simulation der thermomechanischen Materialeigenschaften* 2001, Dissertation, Universität Gesamthochschule Kassel.

HELM, D. (2003): *Shape memory behaviour: modelling within continuum ther-momechanics*, in: Int. J. Solids Struct., Volume 40, 827–849.

HELM, D. (2005): *Pseudoelastic behavior of shape memory alloys: constitutive theorie and identification of the material parameters using neural networks*, in: Technische Mechanik, Volume 25, 1, 39–58.

HELM, D. (2007a): *Numerical simulation of martensitic phase transitons in shape memory alloys using an improved integration algorithm*, in: Int. J. Numer. Meth. Eng., Volume 69, 1997–2035.

HELM, D. (2007b): *Thermomechanics of martensitic phase transitions in shape memory alloys I. constitutive theories for small and large deforma-tions*, in: Int. J. Solids Struct., Volume 2, 1, 87–112.

HENCKY, H. (1928): *Über die Form des Elastizitätsgesetzes bei ideal elastis-chen Stoffen*, in: Z. Techn. Phys., Volume 9, 215–223.

HENCKY, H. (1929a): *Das Superpositionsgesetz eines endlich deformierten re-laxationsfähigen elastischen Kontinuums und seine Bedeutung für eine ex-akte Ableitung der Gleichungen für die zähe Flüssigkeit in der Eulerschen Form*, in: Ann. Phys., Volume 5, 617–630.

HENCKY, H. (1929b): *Welche Umstände bedingen die Verfestigung bei der bild-samen Verformung von festen isotropen Körpern?*, in: Z. Phys., Volume 55, 145–155.

HILL, R. (1963): *Elastic properties of reinforced solids: some theoretical prin-ciples*, in: J. Mech. Phys. Solids, Volume 11, 357–372.

HILL, R. (1968): *On constitutive inequalities for simple materials - I*, in: J. Mech. Phys. Solids, Volume 16, 229–242.

HILL, R. (1970): *Constitutive inequalities for isotropic elastic solids under finite strain*, in: P. Roy. Soc. A, Volume 314, 457–472.

HILL, R. (1978): *Aspects of invariance in solid mechanics*, in: Adv. Appl. Mech., Volume 18, 1–75.

HODGSON, D. E. & BROWN, J. W. (2000): *Using Nitinol Alloys*, Technical report, Shape Memory Applications, Inc., San Jose, CA, USA, 2000.

HONIG, J. M. (Ed.) (1999): *Thermodynamics*, 2nd Edition, Academic Press 1999.

HORNBOGEN, E. (1987): *Legierungen mit Formgedächtnis - Neue Werkstoffe für die Technik der Zukunft?*, in: Metall, Volume 41, 5, 488–493.

HORNBOGEN, E. (1995): *On the term "pseudo-elasticity"*, in: Z. Metallkd., Volume 86, 5, 341–344.

HUANG, M. & BRINSON, L. C. (1998): *A Multivariant model for single crystal shape memory alloy behavior*, in: J. Mech. Phys. Solids, Volume 46, 8, 1379–1409.

HUANG, M., GAO, X. & BRINSON, L. C. (2000): *A multivariant micromechanical model for SMAs Part 2. Polycrystal model*, in: Int. J. Plast., Volume 16, 1371–1390.

HUDSON, J. B. (1996): *Thermodynamics of materials*, 1st Edition, John Wiley & Sons, Inc. 1996.

HUGHES, T. J. R. (2000): *The finite element method*, Dover Publications, Inc., Mineola, New York 2000.

JACOBUS, K., SEHITOGLU, H. & BALZER, M. (1996): *Effect of stress state on the stress-induced martensitic transformation in polycrystalline Ni-Ti alloy*, in: Metall. Mat. Trans. A, Volume 27, 3066–3073.

JAUMANN, G. (1911): *Geschlossenes System physikalischer und chemischer Differentialgesetze*, in: Akad. Wiss. Wien Sitzber. (IIa), Volume 120, 385–530.

JOU, D., CASAS-VÁZQUEZ, J. & LEBON, G. (1993): *Extended irreversible thermodynamics*, 1st Edition, Springer Verlag 1993.

JUHÁSZ, L., SCHNACK, E., HESEBECK, O. & ANDRÄ, H. (2002): *Macroscopic modeling of shape memory alloys under non-proportional thermo-mechanical loadings*, in: J. Intel. Mat. Syst. Str., Volume 13, 825–836.

JUNG, Y., PAPADOPOULOS, P. & RITCHIE, R. (2004): *Constitutive modelling and numerical simulation of multivariant phase transformations in superelastic shape-memory alloys*, in: Int. J. Numer. Meth. Eng., Volume 60, 429–460.

KAACK, M. (2002): *Elastische Eigenschaften von NiTi-Formgedächtnis-Legierungen* 2002, Dissertation, Ruhr-Universität Bochum.

KÄSTNER, S. (1964): *Vektoren, Tensoren, Spinoren: eine Einführung in den Tensorkalkül unter Berücksichtigung der physikalischen Anwendung*, 2nd Edition, Akadademie Verlag 1964.

KHAN, A. S. & HUANG, S. (1995): *Continuum theory of plasticity*, John Wiley & Sons, Inc. 1995.

KIM, J.-S. & SEELECKE, S. (2007): *A rate-dependent three-dimensional free energy model for ferroelectic single crystals*, in: Int. J. Solids Struct., Volume 44, 1196–1209.

KUIKEN, G. D. C. (1994): *Thermodynamics of irreversible processes*, 1st Edition, John Wiley & Sons 1994.

LAGOUDAS, D. C. & BO, Z. (1999): *Thermomechanical modeling of polycrystalline SMAs under cyclic loading, part II: material characterization and experimental results for a stable transformation cycle*, in: Int. J. Engng. Sci., Volume 37, 1205–1249.

LAGOUDAS, D. C. & ENTCHEV, P. B. (2004): *Modeling of transformation-induced plasticity and its effect on the behavior of porous shape memory alloys. Part I: constitutive model for fully dense SMAs*, in: Mech. Mater., Volume 36, 865–892.

LAGOUDAS, D. C. & SHU, S. G. (1999): *Residual deformation of active structures with SMA actuators*, in: Int. J. Mech. Sci., Volume 41, 595–619.

LECLERCQ, S. & LEXCELLENT, C. (1996): *A general macroscopic description of the thermomechanical behavior of shape memory alloys*, in: J. Mech. Phys. Solids, Volume 44, 6, 953–980.

LEHMANN, T. (1972): *Einige Bemerkungen zu einer allgemeinen Klasse von Stoffgesetzen für große elasto-plastische Formänderungen*, in: Ing. Arch., Volume 41, 297–310.

LEHMANN, T. (1974): *Einige Betrachtungen zur Thermodynamik großer elasto-plastischer Formänderungen*, in: Acta Mech., Volume 20, 187–207.

LEHMANN, T. (1984): *General frame for the definition of constitutive laws for large non-isothermic elastic-plastic and elastic-visco-plastic deformations*, in: LEHMANN, T. (Ed.): *Constitutive law in thermoplasticity*, Springer Verlag 1984, pp. 379–463.

LEHMANN, T. (1989): *Some thermodynamical considerations on inelastic deformations including damage processes*, in: Acta Mech., Volume 79, 1–24.

LEHMANN, T., GUO, Z.-H. & LIANG, H. (1991): *The conjugacy between Cauchy stress and logarithm of the left stretch tensor*, in: Eur. J. Mech. A-Solid, Volume 10, 4, 395–404.

LEXCELLENT, C., BOUBAKAR, M. L., BOUVET, C. & CALLOCH, S. (2006): *About modelling the shape memory alloy behaviour based on the phase transformation surface identification under proportional loading and anisothermal conditions*, in: Int. J. Solids Struct., Volume 43, 613–626.

LEXCELLENT, C., LECLERCQ, S., GABRY, B. & BOURBON, G. (2000): *The two way shape memory effect of shape memory alloys: an experimental study and a phenomenological model*, in: Int. J. Plast., Volume 16, 1155–1168.

LEXCELLENT, C., ROGUEDA, C. & BOURBON, G. (1994a): *Parameter determination for thermodynamical models of the pseudoelastic behaviour of shape memory alloy by resistivity measurements and infrared thermography*, in: Continuum Mech. Therm., Volume 6, 273–290.

LEXCELLENT, C., TOBUSHI, H., ZIOLKOWSKI, A. & TANAKA, K. (1994b): *Thermodynamical model of reversible R-phase transformation in TiNi shape memory alloy*, in: Int. J. Pres. Ves. and Pip., Volume 58, 51–57.

LEXCELLENT, C., VIVET, A., BOUVET, C., CALLOCH, S. & BLANC, P. (2002): *Experimental and numerical determinations of the initial surface of phase transformation under biaxial loading in some polycrystralline shape-memory alloys*, in: J. Mech. Phys. Solids, Volume 50, 2717–2735.

LIM, T. J. & MCDOWELL, D. L. (1999): *Mechanical behavior of an TiNi shape memory alloy under axial-torsional proportional and nonproportional loading*, in: J. Eng. Mater.-T. ASME, Volume 121, 9–18.

LU, Z. K. & WENG, G. J. (1997): *Martensitic transformation and stress-strain relations of shape-memory alloys*, in: J. Mech. Phys. Solids, Volume 45, 11-12, 1905–1828.

LUBLINER, J. & AURICCHIO, F. (1996): *Generalized plasticity and shape-memory alloys*, in: Int. J. Solids Struct., Volume 33, 7, 991–1003.

LUIG, P. & BRUHNS, O. T. (2005): *Phenomenological and numerical simulation of shape memory alloys at finite strains*, in: PAMM, Volume 5, 431–432.

LUIG, P. & BRUHNS, O. T. (2007): *Consistent Eulerian rate model for finite pseudoelasticity of polycrystalline TiNi shape memory alloys*, in: BRUHNS, O. T. & MEYERS, A. (Eds.): *IMPLAST 2007*, IMPLAST, The University Press Bochum 2007, pp. 361–369.

LUIG, P. & BRUHNS, O. T. (2008a): *Eulerian rate model for pseudoelastic NiTi shape memory alloys*, in: PAMM, in press.

LUIG, P. & BRUHNS, O. T. (2008b): *On the modeling of shape memory alloys using tensorial internal variables*, in: Mat. Sci. Eng. A, Volume 481-482, 379–383.

LUIG, P., GRABE, C. & BRUHNS, O. T. (2007): *Thermomechanical behavior of pseudoelastic NiTi shape memory alloys*, in: PAMM, Volume 7, in press.

LUIG, P., KNOPIK, A., OBERSTE-BRANDENBURG, C., GRABE, C., BRUHNS, O. T. & PREDKI, W. (2006): *Damping couplings with elements of pseudoelastic TiNi shape memory alloys*, in: Arch. Appl. Mech, Volume 76, 75–87.

MACVEAN, D. B. (1968): *Die Elementararbeit in einem Kontinuum und die Zuordnung von Spannungs- und Verzerrungstensoren*, in: Z. Angew. Math. Phys., Volume 19, 157–185.

MALVERN, L. E. (1969): *Introduction to the mechanics of a continuous medium*, Prentice-Hall, Inc., Englewood Cliffs, New Jersey 1969.

MARSDEN, J. E. & HUGHES, T. J. R. (1983): *Mathematical formulations of elasticity*, Dover Publications, Inc., Mineola, New York 1983.

MIEHE, C. (1996): *Numerical computation of algorithmic (consistent) tangent moduli in large-strain computational inelasticity*, in: Comp. Method. Appl. M., Volume 134, 223–240.

MILLS, A. F. (1999): *Heat transfer*, 2nd Edition, Prentice Hall 1999.

MIYAZAKI, S. (1996): *Development and characterization of shape memory alloys*, in: KALISZKY, S., SAYIR, M., SCHNEIDER, W., BIANCHI, G. & TASSO, C. (Eds.): *Shape Memory Alloys*, International Centre for Mechanical Sciences 1996, Number 351 in CISM Courses and Lectures.

MIYAZAKI, S. & OTSUKA, K. (1986): *Deformation and transition behavior associated with the R-phase in Ti-Ni alloys*, in: Metall. Mat. Trans. A, Volume 17A, 53–63.

MIYAZAKI, S., OTSUKA, K. & SUZUKI, Y. (1981): *Transformation pseudoelasticity and deformation behavior in a Ti-50.6at%Ni alloy*, in: Scr. Metall., Volume 15, 287–292.

MÜLLER, C. (2003): *Thermodynamic modeling of polycrystalline shape memory alloys at finite strains* 2003, Mitteilungen aus dem Institut für Mechanik, Ruhr-Universität Bochum.

MÜLLER, C., LUIG, P., OBERSTE-BRANDENBURG, C. & BRUHNS, O. T. (2006): *On the thermomechanically coupled simulation of shape memory alloys*, in: MERTMANN, M. (Ed.): *SMST-2004*, SMST, ASM International 2006, pp. 165–170.

MÜLLER, I. (1985a): *Pseudoelasticity in shape memory alloys - an extreme case of thermoelasticity*, in: *IMA Preprint*, 1985, Volume 1.

MÜLLER, I. (1985b): *Thermodynamics*, 1st Edition, Pitman Publishing 1985.

MÜLLER, I. (1989): *On the size of the hysteresis in pseudelasticity*, in: Continuum Mech. Therm., Volume 1, 125–142.

MÜLLER, I. (2001): *Grundzüge der Thermodynamik*, 3rd Edition, Springer Verlag 2001.

MÜLLER, I. & RUGGERI, T. (1998): *Rational extended thermodynamics*, 2nd Edition, Springer Verlag 1998.

MÜLLER, I. & SEELECKE, S. (2001): *Thermodynamic aspects of shape memory alloys*, in: Math. Comp. Model., Volume 34, 1307–1355.

MÜLLER, I. & XU, H. (1991): *On the pseudoelastic hysteresis*, in: Acta Metall. Mater., Volume 39, 3, 263–271.

NICLAEYS, C., ZINEB, T. B., ARBAB-CHIRANI, S. & PATOOR, E. (2002): *Determination of the interaction energy in the martensitic state*, in: Int. J. Plast., Volume 18, 1619–1647.

NOLL, W. (1955): *On the continuity of the solid and fluid states*, in: J. Ration. Mech. Anal., Volume 4, 3–81.

OBERSTE-BRANDENBURG, C. (1999): *Ein Materialmodell zur Beschreibung der Austenit-Martensit Phasentransformation unter Berücksichtigung der transformationsinduzierten Plastizität* 1999, Mitteilungen aus dem Institut für Mechanik, Ruhr-Universität Bochum.

OGDEN, R. W. (1984): *Non-linear elastic deformations*, Dover Publications, Inc. Mineola, New York 1984.

OLDROYD, J. G. (1950): *On the formulation of the rheological equations of state*, in: P. Roy. Soc. A, Volume 200, 523–541.

OLIFERUK, W. (1999): *Experimental investigations of the thermomechanical couplings in TiNi shape memory alloy during a torsion-tension (compression) test*, in: Arch. Mech., Volume 51, 6, 717–726.

ORGÉAS, L. & FAVIER, D. (1998): *Stress-induced martensitic transformation of a NiTi alloy in isothermal shear, tension and compression*, in: Acta Mater., Volume 46, 15, 5579–5591.

ORTÍN, J. & PLANES, A. (1989): *Thermodynamics of thermoelastic martensitic transformations*, in: Acta Metall., Volume 37, 5, 1433–1441.

ORTIZ, M., PINSKY, P. M. & TAYLOR, R. L. (1983): *Operator split methods for the numerical solution of the elastoplastic dynamic problem*, in: Comp. Method. Appl. M., Volume 39, 2, 137–157.

OTSUKA, K. (1990): *Introduction to the R-phase transition*, in: DUERIG, T. W., MELTON, K. N., STÖCKEL, D. & WAYMAN, C. M. (Eds.): *Engineering aspects of shape memory alloys*, Butterworth-Heinemann 1990, pp. 36–45.

OTSUKA, K. & REN, X. (1999): *Recent developments in the research of shape memory alloys*, in: Intermetallics, Volume 7, 511–528.

OTSUKA, K. & WAYMAN, C. M. (1998a): *Introduction*, in: OTSUKA, K. & WAYMAN, C. M. (Eds.): *Shape memory materials*, Cambridge University Press 1998, pp. 1–26.

OTSUKA, K. & WAYMAN, C. M. (1998b): *Mechanism of shape memory effect and superelasticity*, in: OTSUKA, K. & WAYMAN, C. M. (Eds.): *Shape memory materials*, Cambridge University Press 1998, pp. 27–48.

OTSUKA, K. & WAYMAN, C. M. (1998c): *Shape memory materials*, Cambridge University Press 1998.

PANICO, M. & BRINSON, L. C. (2007): *A three-dimensional phenomenological model for martensite reorientation in shape memory alloys*, in: J. Mech. Phys. Solids, Volume 55, 11, 2491–2511.

PATOOR, E., EBERHARDT, A. & BERVEILLER, M. (1996): *Micromechanical modelling of superelasticity in shape memory alloys*, in: J. Phys. IV, Volume 6, C1-277 – C1-292.

PATOOR, E., EL AMRANI, M., EBERHARDT, A. & BERVEILLER, M. (1995): *Determination of the origin for the dissymmetry observed between tensile and compression tests on shape memory alloys*, in: J. Phys. IV, Volume 5, 2, 495–500.

PATOOR, E., LAGOUDAS, D. C., ENTCHEV, P. B., BRINSON, L. C. & GAO, X. (2006): *Shape memory alloys - part I: general properties and modeling of single crystals*, in: Mech. Mater., Volume 38, 5-6, 391–429.

PERZYNA, P. (1963): *The constitutive equations for rate sensitive plastic materials*, in: Q. Appl. Math., Volume 20, 5-6, 321–332.

PEULTIER, B., BEN ZINEB, T. & PATOOR, E. (2006): *Macroscopic constitutive law of shape memory alloy thermomechanical behaviour. Application to structure computation by FEM*, in: Mech. Mater., Volume 38, 510–524.

PINSKY, P. M., ORTIZ, M. & TAYLOR, R. L. (1983): *Operator split methods in the numerical solution of the finite deformation elastoplastic dynamic problem*, in: Comput. struc., Volume 17, 3, 45–359.

PLANCK, M. (1897): *Thermodynamik*, 1st Edition, Walter de Gruyter & Co. 1897.

POPE, M. I. & JUDD, M. D. (1977): *Differential thermal analysis*, 1st Edition, Heyden & Son 1977.

POPOV, P. & LAGOUDAS, D. C. (2007): *A 3-D constitutive model for shape memory alloys incorporating pseudoelasticity and detwinning of self-accommodated martensite*, in: Int. J. Plast., Volume 23, 1679–1720.

QIDWAI, M. A. & LAGOUDAS, D. C. (2000a): *Numerical implementation of a shape memory alloy thermomechanical constitutive model using return mapping algorithms*, in: Int. J. Numer. Meth. Eng., Volume 47, 1123–1168.

QIDWAI, M. A. & LAGOUDAS, D. C. (2000b): *On thermomechanics and transformation surfaces of polycrystalline NiTi shape memory alloy material*, in: Int. J. Plast., Volume 16, 1309–1343.

RANIECKI, B. & BRUHNS, O. T. (1991): *Thermodynamic reference model for elastic-plastic solids undergoing phase transformations*, in: Arch. Mech., Volume 43, 2-3, 343–376.

RANIECKI, B., DIETRICH, L., KOWALEWSKI, Z. L., SOCHA, G., MIYAZAKI, S., TANAKA, K. & ZIOLKOWSKI, A. (1999): *Experimental methodology for TiNi shape memory alloy testing under complex stress state*, in: Arch. Mech., Volume 51, 727–744.

RANIECKI, B. & LEXCELLENT, C. (1994): *R_L-models of pseudoelasticity and their specification for some shape memory solids*, in: Eur. J. Mech. A - Solid, Volume 13, 1, 21–50.

RANIECKI, B. & LEXCELLENT, C. (1998): *Thermodynamics of isotropic pseudoelasticity in shape memory alloys*, in: Eur. J. Mech. A - Solid, Volume 17, 2, 185–205.

RANIECKI, B., LEXCELLENT, C. & TANAKA, K. (1992): *Thermodynamic models of pseudoelastic behaviour of shape memory alloys*, in: Arch. Mech., Volume 44, 3, 261–284.

REESE, S. & CHRIST, D. (2008): *Finite deformation pseudo-elasticity of shape memory alloys - constitutive modelling and finite element implementation*, in: Int. J. Plast., Volume 24, 455–482.

REINHARDT, W. D. & DUBEY, R. N. (1995): *Eulerian strain-rate as a rate of logarithmic strain*, in: Mech. Res. Commun., Volume 22, 2, 165–170.

REINHARDT, W. D. & DUBEY, R. N. (1996): *Coordinate-independent representation of spins in continuum mechanics*, in: J. Elasticity, Volume 42, 133–144.

SABURI, T. (1998): *Ti-Ni shape memory alloys*, in: OTSUKA, K. & WAYMAN, C. M. (Eds.): *Shape memory materials*, Cambridge University Press 1998, pp. 49–96.

SCHMAHL, W. W., KHALIL-ALLAFI, J., HASSE, B., WAGNER, M., HECKMANN, A. & SOMSEN, C. (2004): *Investigation of the phase evolution in a super-elastic NiTi shape memory alloy (50.7 at.%Ni) under extensional load with synchrotron radiation*, in: Mat. Sci. Eng. A, Volume 378, 81–85.

SEELECKE, S. (1997): *Torsional vibration of a shape memory alloy wire*, in: Continuum Mech. Therm., Volume 9, 165–173.

SEELECKE, S. (2002): *Modeling the dynamic behavior of shape memory alloy alloys*, in: Int. J. Nonlinear Mech., Volume 37, 1363–1374.

SEELECKE, S., KIM, J.-S., BALL, B. L. & SMITH, R. C. (2005): *A rate-dependent two-dimensional free energy model for ferroelectic single crystals*, in: Continuum Mech. Therm., Volume 17, 4, 337–350.

SEELECKE, S. & MÜLLER, I. (2004): *Shape memory alloy actuators in smart structures: modeling and simulation*, in: Appl. Mech. Rev., Volume 57, 1, 23–46.

SETH, B. R. (1964): *Generalized strain measure with applications to physical problems*, in: REINER, M. & ABIR, D. (Eds.): *Second-order effects in elasticity, plasticity and fluid dynamics*, Pergamon Press 1964, pp. 162–172.

SHAW, J. A. & KYRIAKIDES, S. (1995): *Thermomechanical aspects of NiTi*, in: J. Mech. Phys. Solids, Volume 43, 8, 1243–1281.

SHIMIZU, K. & TADAKI, T. (1987): *Introduction*, in: FUNAKUBO, H. (Ed.): *Shape memory alloys*, Gordon and Breach Science Publishers 1987, pp. 1–60.

ŠILHAVÝ, M. (1997): *The mechanics and thermodynamics of continuous media*, Springer Verlag 1997.

SIMO, J. C. (1998): *Numerical analysis and simulation of plasticity*, in: CIARLET, P. G. & LIONS, J. L. (Eds.): *Handbook of numerical analysis*, Elsevier Science 1998, Volume IV.

SIMO, J. C. & HUGHES, T. J. R. (1998): *Computational inelasticity*, Springer Verlag 1998.

SIMO, J. C. & PISTER, K. S. (1984): *Remarks on rate constitutive equations for finite deformation problems: computational implications*, in: Comput. Method. Appl. M., Volume 46, 201–215.

SIREDEY, N., PATOOR, E., BERVEILLER, M. & EBERHARDT, A. (1999): *Constitutive equations for polycrystalline thermoelastic shape memory alloys. Part I. Intragranular interactions and behavior of the grain*, in: Int. J. Solids Struct., Volume 36, 28, 4289–4315.

SITEPU, H., SCHMAHL, W. W., EGGELER, G., KHALIL-ALLAFI, J. & TÖBBENS, D. M. (2003): *A neutron diffraction study of the martensitic transformations in aged Ni-rich NiTi alloys*, in: J. Phys. IV, Volume 112, 643–646.

ŠITTNER, P., LANDA, M., LUKÁS, P. & NOVÁK, V. (2006a): *R-phase transformation phenomena in thermomechanically loaded NiTi polycrystals*, in: Mech. Mater., Volume 38, 475–492.

ŠITTNER, P., LUKÁS, P., NOVÁK, V., DAYMOND, M. R. & SWALLOWE, G. M. (2004): *In situ neutron diffraction studies of martensitic transformations in NiTi polycrystals under tension and compression stress*, in: Mat. Sci. Eng. A, Volume 378, 97–104.

ŠITTNER, P., NOVÁK, V., LUKÁS, P. & LANDA, M. (2006b): *Stress-strain-temperature behavior due to B2-R-B19' transformation in NiTi polycrystals*, in: J. Eng. Mater.-T. ASME, Volume 128, 268–278.

ŠITTNER, P., SEDLÁK, P., LANDA, M., NOVÁK, V. & LUKÁS, P. (2006c): *In situ experimental evidence on R-phase related deformation processes in activated NiTi wires*, in: Mat. Sci. Eng. A, Volume 438-440, 579–584.

STEIN, E. & BARTHOLD, F.-J. (1996): *Elastizitätstheorie*, in: MEHLHORN, G. (Ed.): *Der Ingenieurbau, Grundwissen: Werkstoffe, Elastizitätstheorie*, Ernst & Sohn, Berlin 1996, ISBN 3-433-01570-8, pp. 165–428.

STEIN, E. & SAGER, G. (2008): *Theory and finite element computation of cyclic martensitic phase transformation at finite strain*, in: Int. J. Numer. Meth. Eng., Volume 74, 1, 1–31.

TANAKA, K., KITAMURA, K. & MIYAZAKI, S. (1999): *Shape memory alloy preparation for multiaxial tests and identification of fundamental alloy performance*, in: Arch. Mech., Volume 51, 6, 785–803.

TANAKA, K., NISHIMURA, F. & TOBUSHI, H. (1995): *Transformation start lines in TiNi and Fe-based shape memory alloys after incomplete transformations induced by mechanical and/or thermal loads*, in: Mech. Mater., Volume 19, 271–280.

TARANTOLA, A. (1987): *Inverse problem theory: methods for data fitting and model parameter estimation*, Elsevier Science 1987.

TIAN, Q. & WU, J. (2001): *A thermal perspective of NiTi alloy under non-isothermal conditions*, in: Mater. Trans., Volume 42, 11, 2446–2451.

TOBUSHI, H., ENDO, M., IKAWA, T. & SHIMADA, D. (2003): *Pseudoviscoelastic behavior of NiTi shape memory alloys under stress-controlled subloop loadings*, in: Arch. Mech., Volume 55, 5-6, 519–530.

TOBUSHI, H., SHIMENO, Y., HACHISUKA, T. & TANAKA, K. (1998): *Influence of strain rate on superelastic properties of NiTi shape memory alloy*, in: Arch. Mech., Volume 30, 141–150.

TROCHU, F. & QIAN, Y.-Y. (1997): *Nonlinear finite element simulation of superelastic shape memory alloy parts*, in: Comput. Struct., Volume 62, 5, 799–810.

TRUESDELL, C. (1952): *The mechanical foundations of elasticity and fluid dynamics*, in: J. Ration. Mech. Anal., Volume 1, 125–300.

TRUESDELL, C. (1953): *Corrections and additions to 'The mechanical foundations of elasticity and fluid dynamics'*, in: J. Ration. Mech. Anal., Volume 2, 593–616.

TRUESDELL, C. (1955): *The simplest rate theory of pure elasticity*, in: Comm. pur. appl. math., Volume 8, 123–132.

TRUESDELL, C. (1969): *Rational thermodynamics*, 1st Edition, Springer Verlag 1969.

TRUESDELL, C. & NOLL, W. (2004): *The non-linear field theories of mechanics*, 3rd Edition, Springer Verlag 2004.

TRUESDELL, C. & TOUPIN, R. A. (1960): *The classical field theories*, in: FLÜGGE, S. (Ed.): *Handbuch der Physik*, Springer Verlag 1960, Volume III/1.

VAIDYANATHAN, R., BOURKE, M. A. M. & DUNAND, D. C. (1999): *Analysis of neutron diffraction spectra acquired in situ during stress-induced transformations in superelastic NiTi*, in: J. Appl. Phys., Volume 86, 6, 3020–3029.

VIVET, A. & LEXCELLENT, C. (1998): *Micromechanical modelling for tension-compression pseudoelastic behavior of AuCd single crystals*, in: Eur. Phys. J. Appl. Phys., Volume 4, 2, 125–132.

WANG, C.-C. (1970a): *A new representation theorem for isotropic functions: An answer to Professor G. F. Smith's criticism of my papers on representions for isotropic functions: Part 1. Scalar-valued isotropic functions*, in: Arch. Ration. Mech. An., Volume 36, 166–197.

WANG, C.-C. (1970b): *A new representation theorem for isotropic functions: An answer to Professor G. F. Smith's criticism of my papers on representions for isotropic functions: Part 2. Vector-valued isotropic functions, symmetric tensor-valued isotropic functions and skew-symmetric tensor-valued isotropic functions*, in: Arch. Ration. Mech. An., Volume 36, 198–223.

WANG, C.-C. & TRUESDELL, C. (1973): *Introduction to rational elasticity*, 1st Edition, Noordhoff International Publishing 1973.

WANG, X. M., XU, B. X. & YUE, Z. F. (2008): *Micromechanical modelling of the effect of plastic deformation on the mechanical behaviour in pseudoelastic shape memory alloys*, in: Int. J. Plast., Volume 24, 1307–1332.

WAYMAN, C. M. & DUERIG, T. W. (1990): *An introduction to martensite and shape memory*, in: DUERIG, T. W., MELTON, K. N., STÖCKEL, D. & WAYMAN, C. M. (Eds.): *Engineering aspects of shape memory alloys*, Butterworth-Heinemann 1990, pp. 3–20.

XIAO, H., BRUHNS, O. T. & MEYERS, A. (1997a): *Hypo-elasticity model based upon the logarithmic stress rate*, in: J. Elasticity, Volume 47, 51–68.

XIAO, H., BRUHNS, O. T. & MEYERS, A. (1997b): *Logarithmic strain, logarithmic spin and logarithmic rate*, in: Acta Mech., Volume 124, 89–105.

XIAO, H., BRUHNS, O. T. & MEYERS, A. (1998a): *On objective corotational rates and their defining spin tensors*, in: Int. J. Solids Structures, Volume 35, 30, 4001–4014.

XIAO, H., BRUHNS, O. T. & MEYERS, A. (1998b): *Strain rates and material spins*, in: J. Elasticity, Volume 52, 1–41.

XIAO, H., BRUHNS, O. T. & MEYERS, A. (1999): *Existence and uniqueness of the integrable-exactly hypoelastic equation* $\overset{\circ}{\tau}{}^* = \lambda(trD)I + 2\mu D$ *and its significance to finite inelasticity*, in: Acta Mech., Volume 138, 31–50.

XIAO, H., BRUHNS, O. T. & MEYERS, A. (2000): *The choice of objective rates in finite elastoplasticity: general results on the uniqueness of the logarithmic rate*, in: P. Roy. Soc. A, Volume 456, 1865–1882.

XIAO, H., BRUHNS, O. T. & MEYERS, A. (2005): *Objective stress rates, path-dependence properties and non-integrability problems*, in: Acta Mech., Volume 176, 135–151.

XIAO, H., BRUHNS, O. T. & MEYERS, A. (2006a): *Elastoplasticity beyond small deformations*, in: Acta Mech., Volume 182, 31–111.

XIAO, H., BRUHNS, O. T. & MEYERS, A. (2006b): *Objective stress rates, cyclic deformation paths, and residual stress accumulation*, in: ZAMM · Z. Angew. Math. Me., Volume 86, 11, 843–855.

XIAO, H., BRUHNS, O. T. & MEYERS, A. (2007): *Thermodynamic laws and consistent Eulerian formulation of finite elastoplasticity with thermal effects*, in: J. Mech. Phys. Solids, Volume 55, 338–365.

ZAREMBA, S. (1903): *Sur une forme perfectionée de la théorie de la relaxation*, in: Bull. Intern. Acad. Sci. Cracovie, , 594–614.

ZIENKIEWICZ, O. & TAYLOR, R. (2005): *The finite element method*, 6th Edition, Butterworth-Heinemann 2005.

ZIÓLKOWSKI, A. (2007): *Three-dimensional phenomenological thermodynamic model of pseudoelasticity of shape memory alloys at finite strains*, in: Continuum Mech. Therm., Volume 19, 379–398.

ZOHDI, T. I. & WRIGGERS, P. (2005): *Introduction to computational micromechanics*, 1st Edition, Springer Verlag 2005.

Mitteilungen aus dem Institut für Mechanik

Nr. 1 Theodor Lehmann:
Große elasto-plastische Formänderungen (Dezember 1976)

Nr. 2 Bogdan Raniecki/Klaus Thermann:
Infinitesimal Thermoplasticity and Kinematics of Finite Elastic-Plastic Deformations. Basic Concepts (Juni 1978)

Nr. 3 Wolfgang Krings:
Beitrag zur Finiten Element Methode bei linearem, viskoelastischem Stoffverhalten (Januar 1976)

Nr. 4 Burkhard Lücke:
Theoretische und experimentelle Untersuchung der zyklischen elasto-plastischen Blechbiegung bei endlichen Verzerrungen (Januar 1976)

Nr. 5 Knut Schwarze:
Einfluß von Querschnittsverformungen bei dünnwandigen Stäben mit stetig gekrümmter Profilmittellinie (Februar 1976)

Nr. 6 Hubert Sommer:
Ein Beitrag zur Theorie des ebenen elastischen Verzerrungszustandes bei endlichen Formänderungen (Januar 1977)

Nr. 7 H. Stumpf/F. J. Biehl:
Die Methode der orthogonalen Projektionen und ihre Anwendung zur Berechnung orthotroper Platten (März 1977)

Nr. 8 Albert Meyers:
Ein Beitrag zum optimalen Entwurf von schnellaufenden Zentrifugenschalen (April 1977)

Nr. 9 Berend Fischer:
Zur zyklischen, elastoplastischen Beanspruchung eines dickwandigen Zylinders bei endlichen Verzerrungen (April 1977)

Nr. 10 Wojciech Pietraszkiewicz:
Introduction to the Non-Linear Theory of Shells (Mai 1977)

Nr. 11 Wilfried Ullenboom:
Optimierung von Stäben unter nichtperiodischer dynamischer Belastung (Juni 1977)

Nr. 12 Jürgen Güldenpfennig:
Anwendung eines Modells der Vielkristallplastizität auf ein Problem gekoppelter elastoplastischer Wellen (Juli 1977)

Nr. 57 Andreas Pape:
Zur Beschreibung des transienten und stationären Verfestigungsverhaltens von Stahl mit Hilfe eines nichtlinearen Grenzflächenmodells (Mai 1988)

Nr. 58 Johannes Groß-Weege:
Zum Einspielverhalten von Flächentragwerken (Juni 1988)

Nr. 59 Peihua Liu:
Optimierung von Kreisplatten unter dynamischer nicht rotationssymmetrischer Last (Juli 1988)

Nr. 60 Reinhard Schmidt:
Die Anwendung von Zustandsbeobachtern zur Schwingungsüberwachung und Schadensfrüherkennung auf mechanische Konstruktionen (August 1988)

Nr. 61 Martin Pitzer:
Vergleich einiger FE-Formulierungen auf der Basis eines inelastischen Stoffgesetzes (Juli 1988)

Nr. 62 Jerzy Makowski/Helmut Stumpf:
Geometric structure of fully nonlinear and linearized Cosserat type shell theory (Dezember 1988)

Nr. 63 O. T. Bruhns:
Große plastische Formänderungen – Bad Honnef 1988 (Januar 1989)

Nr. 64 Khanh Chau Le/Helmut Stumpf/Dieter Weichert:
Variational principles of fracture mechanics (Juli 1989)

Nr. 65 Guido Obermüller:
Ein Beitrag zur Strukturoptimierung unter stochastischen Lasten (Juni 1989)

Nr. 66 Herbert Diehl:
Ein Materialmodell zur Berechnung von Hochgeschwindigkeitsdeformationen metallischer Werkstoffe unter besonderer Berücksichtigung der Schädigung durch Scherbänder (Juni 1989)

Nr. 67 Michael Geis:
Zur Berechnung ebener, elastodynamischer Rißprobleme mit der Randelementmethode (November 1989)

Nr. 68 Günter Renker:
Zur Identifikation nichtlinearer strukturmechanischer Systeme (November 1989)

Nr. 80   J. Chroscielewski/J. Makowski/H. Stumpf:
Computational Analysis of Shells Undergoing Large Elastic Deformation Part II: Finite Element Implementation

Nr. 81   R. H. Frania/H. Waller:
Entwicklung und Anwendung spezieller finiter Elemente für Kerbspannungsprobleme im Maschinenbau (Mai 1992)

Nr. 82   B. Bischoff-Beiermann:
Zur selbstkonsistenten Berechnung von Eigenspannungen in polykristallinem Eis unter Berücksichtigung der Monokristallanisotropie (Juli 1992)

Nr. 83   J. Pohé:
Ein Beitrag zur Stoffgesetzentwicklung für polykristallines Eis (Februar 1993)

Nr. 84   U. Kikillus:
Ein Beitrag zum zyklischen Kiechverhalten von Ck 15 (Mai 1993)

Nr. 85   T. Guo:
Untersuchung des singulären Rißspitzenfeldes bei stationärem Rißwachstum in verfestigendem Material (Juni 1993)

Nr. 86   Achim Menne:
Identifikation der dynamischen Eigenschaften von hydrodynamischen Wandlern (Januar 1994)

Nr. 87   Uwe Folchert:
Identifikation der dynamischen Eigenschaften hydrodynamischer Kupplungen (Januar 1994)

Nr. 88   Jörg Körber:
Ein verallgemeinertes Finite-Element-Verfahren mit asymptotischer Stabilisierung angewendet auf viskoplastische Materialmodelle (April 1994)

Nr. 89   Peer Schieße:
Ein Beitag zur Berechnung des Deformationsverhaltens anisotrop geschädigter Kontinua unter Berücksichtigung der thermoplastischen Kopplung (April 1994)

Nr. 90   Egbert Schopphoff:
Dreidimensionale mechanische Analyse der menschlichen Wirbelsäule (Juli 1994)

Nr. 91   Christoph Beerens:
          Zur Modellierung nichtlinearer Dämpfungsphänomene in der Struk-
          turmechanik (Juli 1994)

Nr. 92   K. C. Le/H. Stumpf:
          Finte elastoplasticity with microstructure (November 1994)

Nr. 93   O. T. Bruhns:
          Große plastische Formänderungen – Bad Honnef 1994 (Dezember
          1994)

Nr. 94   Armin Lenzen:
          Untersuchung von dynamischen Systemen mit der Singulärwertzer-
          legung – Erfassung von Strukturveränderungen (Dezember 1994)

Nr. 95   J. Makowski/H. Stumpf:
          Mechanics of Irregular Shell Structures (Dezember 1994)

Nr. 96   J. Chroscielewski/J. Makowski/H. Stumpf:
          Finte Elements for Irregular Nonlinear Shells (Dezember 1994)

Nr. 97   W. Krings/A. Lenzen/u. a.:
          Festschrift zum 60. Geburtstag von Heinz Waller (Februar 1995)

Nr. 98   Ralf Podleschny:
          Untersuchung zum Instabilitätsverhalten scherbeanspruchter Risse
          (April 1995)

Nr. 99   Bernd Westerhoff:
          Eine Untersuchung zum geschwindigkeitsabhängigen Verhalten von
          Stahl (Juli 1995)

Nr. 100   Marc Mittelbach:
          Simulation des Deformations- und Schädigungsverhaltens beim Stoß-
          versuch mit einem Kontinuums-Damage-Modell (Dezember 1995)

Nr. 101   Ulrich Hoppe:
          Über grundlegende Konzepte der nichtlinearen Kontinuumsmechanik
          und Schalentheorie (Mai 1996)

Nr. 102   Marcus Otto:
          Erweiterung des Kaustikenverfahrens zur Analyse räumlicher Span-
          nungskonzentrationen (Juni 1996)

Nr. 103   Horst Lanzerath:
          Zur Modalanalyse unter Verwendung der Randelementemethode (Juli
          1996)

Nr. 116 Thomas Pandorf:
Experimentelle und numerische Untersuchungen zur Kerbspitzenbeanspruchung bei schlagbelasteten Biegeproben (August 1998)

Nr. 117 Claus Oberste-Brandenburg:
Ein Materialmodell zur Beschreibung der Austenit-Martensit Phasentransformation unter Berücksichtigung der transformationsinduzierten Plastizität (Juni 1999)

Nr. 118 Michael Märtens:
Regelung mechanischer Strukturen mit Hilfe piezokeramischer Stapelaktoren (Dezember 1999)

Nr. 119 Dirk Kamarys:
Detektion von Strukturveränderungen durch neue Identifikationsverfahren in der experimentellen Modalanalyse (Dezember 1999)

Nr. 120 Wolfgang Hiese:
Gültigkeitskriterien zur Bestimmung von Scherbruchzähigkeiten (Januar 2000)

Nr. 121 Peter Jaschke:
Mathematische Modellierung des Betriebsverhaltens hydrodynamischer Kupplungen mit hybriden Modellansätzen (Februar 2000)

Nr. 122 Stefan Müller:
Zum Einsatz von semi-aktiven Aktoren zur optimalen Schwingungsreduktion in Tragwerken (Februar 2000)

Nr. 123 Dirk Eichel:
Zur Kondensation strukturdynamischer Aufgaben mit Hilfe von Polynommatrizen (Juni 2000)

Nr. 124 Andreas Bürgel:
Bruchmechanische Kennwerte beim Wechsel im Versagensverhalten dynamisch scherbeanspruchter Risse (August 2000)

Nr. 125 Daniela Lürding:
Modellierung großer Deformationen in orthotropen, hyperelastischen Schalenstrukturen (März 2001)

Nr. 126 Thorsten Quent:
Ein mikromechanisch begründetes Modell zur Beschreibung des duktilen Verhaltens metallischer Werkstoffe bei endlichen Deformationen unter Berücksichtigung von Porenschädigung (Mai 2001)